

# **An Investigation of Transcriptional Regulation of Wall Ingrowth Formation in Plant Transfer Cells**

by

**Kiruba Shankari Arun Chinnappa**  
**B.Tech (Agri. Biotech), M.Tech (Biotech)**

Thesis submitted for the Degree of Doctor of Philosophy in  
Discipline of Biological Sciences  
School of Environmental and Life Sciences  
The University of Newcastle  
New South Wales, Australia

April, 2016

# DECLARATIONS

## Statement of Originality

This thesis contains no material which has been accepted for the award of any other degree or diploma in any university or other tertiary institution and, to the best of my knowledge and belief, contains no material previously published or written by another person, except where due reference has been made in the text. I give consent to this copy of my thesis, when deposited in the University Library, being made available for loan and photocopying subject to the provisions of the Copyright Act 1968.

.....  
Kiruba Shankari Arun Chinnappa

## Statement of Authorship

I hereby certify that work embodied in this thesis contains published papers of which I am a joint author. I have included as part of the thesis a written statement, endorsed by my supervisor, attesting to my contribution to the joint publications.

.....  
Kiruba Shankari Arun Chinnappa

.....  
A/Prof. David W. McCurdy

## ACKNOWLEDGEMENTS

First and foremost, I would like to express my gratitude to my supervisor Assoc/Prof. David McCurdy for his inspiration, support, motivation and supervision throughout my PhD. I have always enjoyed discussing science with David and the amount of knowledge and skills I have gained is tremendous. I highly appreciate his efforts, and patience in grooming me as a better researcher and person than I was five years ago. I would like to express my sincere gratitude for his mentoring and guidance during PhD and writing this thesis. I also would like to thank my co-supervisor Assoc/Prof. Yong-Ling Ruan for his continuous encouragement and valuable comments to extend my research from various angle.

I would like to thank my mentor late Dr. Michael Sheahan, who as a good friend, was always willing to help and give his best suggestions. I will always look upon him as an inspiration and his passion for research is contagious. I would also like to extend my thanks to all academics in Centre for Plant Science for their, advice, support and encouragement.

I like to thank my fellow lab members Suong, Thomas and Jessie for their extra-ordinary support and motivation throughout my PhD journey. A very special thanks to Suong for all the valuable discussions, insight and prayers for my wellbeing. Many thanks to Dr. Yuhong Song, Anthony and Chris for assisting me with qPCR and FTIR experiments. I would like to specially thank Selina and Kate for their technical support in the lab. It's a great opportunity to work with and share lab with my fellow research students, Kim, Lei, Xia, Hui-Ming, Ricky, William, Fiona, Priyanka, Teighan, Terence, Youmin, Astija, Yonghua, Sheng, Simon. I have got a much more enjoyable experience and life time memories. I am thankful to all the technical staffs especially Joe Enright for helping me grow and maintain plants.

I would like to extend my thanks to The School of Environmental and Life Sciences and The University of Newcastle for providing me the support, equipment and research facilities without their support my research would not have been possible. And also for funding me via UNIPRS and UNRSC.

My sincere thanks also goes to Centre for Crop Health, The University of Southern Queensland (USQ) especially Prof. Mark Sutherland and Dr. Anke Martin and all my USQ colleagues and friends for supporting me to write this thesis.

My sincere thanks to all my friends particularly Sam, Faizan, Neelam, Akash, Krina, Aamir, Shai, Dipen and Suneel for their continued support and care throughout my study. I wish to thank my parents, sister Ranjani and brother Rahu for supporting me throughout my life and encouraging with their best wishes. Finally, I would like to thank my husband Karthik, without whom my dream to do PhD wouldn't have come true. My heartfelt thanks to him for believing in me, continuously supporting me and for all the sacrifices he made for me to complete this thesis. It wouldn't be possible to complete this thesis without his support.

# PUBLICATIONS

## Peer-Reviewed Research Papers

**Arun Chinnappa KS**, Nguyen TTS, Hou J, Wu Y and McCurdy DW (2013) Phloem parenchyma TCs in Arabidopsis – an experimental system to identify transcriptional regulators of wall ingrowth formation. *Front. Plant Sci.* **4**:102. doi: 10.3389/fpls.2013.00102

**Arun-Chinnappa KS** and McCurdy DW (2015) *De novo* assembly of a genome-wide transcriptome map of *V. faba* (L.) for transfer cell research. *Front. Plant Sci.* **6**:217. doi: 10.3389/fpls.2015.00217

**Arun-Chinnappa KS** and McCurdy DW (2015) Identification of candidate transcriptional regulators of epidermal transfer cell development in *V. faba* cotyledons. *Front. Plant Sci.* – manuscript submitted on December 20, 2015 and under review as on April 03, 2016.

## Conference Poster Presentations

**Arun Chinnappa KS**, Hou J, Wu Y, Sheahan MB and McCurdy DW. “Identification of two MYB-related transcription factors, At4g09450 and At2g38090, as putative regulators of wall ingrowth deposition in phloem parenchyma transfer cells” ICAR 2013 - 24th International Conference on Arabidopsis Research (2013), Sydney, NSW.

Wu Y, Hou J, **Arun Chinnappa KS**, Sheahan MB and McCurdy DW. “Investigating roles for At3g04420 & At1g33060, two NAC-domain transcription factors, as master regulators of transfer cell development in *Arabidopsis thaliana*” ICAR 2013 - 24th International Conference on Arabidopsis Research (2013), Sydney, NSW.

McCurdy DW, Hou J, Wu Y, **Arun Chinnappa KS** and Sheahan MB. “Genetic regulation of phloem parenchyma transfer cell development in Arabidopsis,” Presented and published at Plant Biology 2012 – Annual Meeting of the American Society of Plant Biologists (2012) and COMBIO 2012 – Australian Society for Biochemistry and Molecular Biology (2012).

# TABLE OF CONTENTS

|   |           |
|---|-----------|
| DECLARATIONS .....  | i         |
| ACKNOWLEDGEMENTS .....  | ii        |
| PUBLICATIONS .....  | iv        |
| TABLE OF CONTENTS .....   | v         |
| ABSTRACT.....   | 1         |
| CHAPTER 1 .....   | 5         |
| <b>1.1 INTRODUCTION .....</b>   | <b>6</b>  |
| <b>1.2 LONG AND SHORT DISTANCE NUTRIENT TRANSPORT.....</b>  | <b>7</b>  |
| 1.2.1 Transport of nutrients in plants.....   | 7         |
| 1.2.2 Phloem - Structurally specialized tissue for transporting photoassimilates                            | 7         |
| 1.2.3 Phloem loading is the first step in transport of photo-assimilates .....                              | 8         |
| 1.2.4 Phloem unloading in sink tissues.....   | 10        |
| <b>1.3 TRANSFER CELLS ARE SPECIALISED FOR NUTRIENT EXCHANGE</b><br>.....                                    | <b>11</b> |
| 1.3.1 Wall ingrowth deposition in TCs.....  | 12        |
| 1.3.1.1 Reticulate and Flange Morphologies .....  | 12        |
| 1.3.1.2 Reticulate wall ingrowths represent an example of localised wall deposition<br>in plant cells. .... | 13        |
| 1.3.1.3 Composition of wall ingrowths in TCs .....  | 15        |
| <b>1.4 REGULATION OF TRANSFER CELL <i>TRANS</i>-DIFFERENTIATION ..</b>                                      | <b>15</b> |
| 1.4.1 Signals inducing <i>trans</i> -differentiation of TCs .....   | 15        |
| 1.4.2 Transcriptional regulation of <i>trans</i> -differentiation of TCs.....                               | 17        |
| 1.4.3 Transcription factors regulating TC development.....  | 19        |
| <b>1.5 SECONDARY WALL DEPOSITION AS A TRANSCRIPTIONAL<br/>    MODEL FOR TRANSFER CELL DEVELOPMENT .....</b> | <b>20</b> |
| <b>1.6 EXPERIMENTAL MODELS TO EXAMINE TRANSFER CELLS THAT<br/>    BUILD RETICULATE WALL INGROWTHS .....</b> | <b>21</b> |
| 1.6.1 Adaxial epidermal transfer cell development in <i>Vicia faba</i> cotyledons ...                       | 21        |
| 1.6.2 Phloem parenchyma transfer cell development in minor veins of<br>Arabidopsis.....                     | 22        |

|  |            |
|--|------------|
| 1.7 AIMS AND HYPOTHESES .....  | 26         |
| <b>CHAPTER 2 .....</b>   | <b>29</b>  |
| <b>2.1 OVERVIEW.....</b>   | <b>30</b>  |
| <i>De novo</i> assembly of a genome-wide transcriptome map of <i>Vicia faba</i> (L.) for transfer cell research .....                      | 31         |
| <b>CHAPTER 3.....</b>  | <b>56</b>  |
| <b>3.1 OVERVIEW.....</b>   | <b>57</b>  |
| <b>Identification of Candidate Transcriptional Regulators of Epidermal Transfer Cell Development in <i>Vicia faba</i> Cotyledons .....</b> | <b>58</b>  |
| <b>CHAPTER 4.....</b>  | <b>86</b>  |
| <b>4.1 INTRODUCTION .....</b>  | <b>87</b>  |
| <b>4.2 MATERIALS AND METHODS .....</b>   | <b>89</b>  |
| 4.2.1 Plant growth conditions .....  | 89         |
| 4.2.2 Preparation of agar plates .....   | 89         |
| 4.2.3 Seed sterilisation and plating.....  | 89         |
| 4.2.4 Extraction of genomic DNA for genotyping.....  | 90         |
| 4.2.5 Genotyping of Arabidopsis mutants .....  | 90         |
| 4.2.6 Semi-quantitative RT-PCR.....  | 91         |
| 4.2.7 Generation of double mutants.....  | 92         |
| 4.2.8 Phenotyping of T-DNA insertional mutants.....  | 93         |
| <b>4.3 RESULTS .....</b>   | <b>94</b>  |
| 4.3.1 Genotyping of T-DNA insertional mutants .....  | 94         |
| 4.3.2 Analysis of T-DNA insertions on candidate gene expression.....   | 95         |
| 4.3.3 Generation of homozygous double mutants .....  | 97         |
| 4.3.4 Phenotypic analysis of T-DNA insertional double mutants .....  | 98         |
| <b>4.4 DISCUSSION.....</b>   | <b>102</b> |
| <b>CHAPTER 5.....</b>  | <b>115</b> |
| <b>5.1 INTRODUCTION .....</b>  | <b>116</b> |
| <b>5.2 TRANSCRIPTIONAL REGULATION OF <i>V. faba</i> TRANSFER CELLS .....</b>   | <b>117</b> |
| 5.2.1 <i>De novo</i> assembly of genome-wide transcriptome map of <i>V. faba</i> for TC research (Chapter 2) .....                         | 117        |
| 5.2.2 Putative roles of identified transcription factors in <i>V. faba</i> TCs (Chapter 3) .....   | 119        |

|  |            |
|--|------------|
| <b>5.3 IS ARABIDOPSIS A GOOD MODEL TO TEST ORTHOLOGS OF <i>V. faba</i>? (Chapter 4)</b> .....              | <b>122</b> |
| 5.3.1 Functional characterization of <i>V. faba</i> transcription factors using Arabidopsis orthologs..... | 122        |
| 5.3.2 Arabidopsis as a model to test <i>V. faba</i> orthologs .....  | 124        |
| <b>5.4 FUTURE DIRECTIONS</b> .....   | <b>124</b> |
| <b>5.5 CONCLUSIONS</b> .....   | <b>127</b> |
| <br>   |            |
| <b>APPENDICES</b> .....  | <b>129</b> |
| APPENDIX 1: Chapter 1 Supplementary Data .....   | 130        |
| APPENDIX 2: Chapter 2 Supplementary Data .....   | 145        |
| APPENDIX 3: Chapter 3 Supplementary Data .....   | 151        |
| APPENDIX 4: Chapter 4 Supplementary Data .....   | 166        |
| <br>   |            |
| <b>REFERENCES</b> .....  | <b>184</b> |

# ABBREVIATIONS

|                               |  |   |   |
|-------------------------------|--|---|---|
| ABA                           | Abscisic acid                                    | mRNA  | messenger RNA   |
| ABC                           | ATP-binding cassette                             | MS  | Murashige Skoog   |
| ABRC                          | Arabidopsis Biological Research Centre           | Na <sub>2</sub> S <sub>2</sub> O <sub>5</sub> | Sodium Metabisulphite                                     |
| ACC                           | 1-AminoCyclopropane-1-Carboxylic acid            | NaCl  | Sodium Chloride   |
| ACO                           | ACC Oxidase                                      | NADPH   | Nicotinamide Adenine Dinucleotide Phosphate Hydrogenase   |
| ACS                           | ACC Synthase                                     | NASC  | Nottingham Arabidopsis Stock Centre                       |
| ADP                           | Adenosine Di Phosphate                           | NGM   | Next Generation Mapping                                   |
| AFLP                          | Amplified Fragment Length Polymorphism           | NGS   | Next Generation Sequencing                                |
| AGP                           | ArabinoGalactan Proteins                         | NOX   | NADPH Oxidase   |
| AP2                           | APETELA2   | NST   | NAC Secondary wall thickening                             |
| ARF                           | Auxin Response Factor                            | PCIB  | p-Chlorophenoxy IsoButyricacid                            |
| At                            | <i>Arabidopsis thaliana</i>                      | PCR   | Polymerase Chain Reaction                                 |
| ATP                           | Adenosine Tri Phosphate                          | PP  | Phloem Parenchyma   |
| AVG                           | AminoethoxyVinylGlycine                          | RACE  | Rapid Amplification of cDNA Ends                          |
| BETC                          | Basal ETCs                                       | RBOH  | Respiratory Burst Oxidase Homolog                         |
| BETL                          | Basal Endosperm Transfer cell Layer              | RFOs  | Raffinose Family Oligosaccharides                         |
| BLAST                         | Basic Local alignment Search Tool                | RNA   | RiboNucleic Acid  |
| CaMV35S                       | Cauliflower Mosaic Virus 35S                     | RNA-Seq                                       | RNA sequencing  |
| CCs                           | Companion Cells                                  | ROS   | Reactive Oxygen Species                                   |
| cDNA                          | complement DeoxyriboNucleic Acid Coding Sequence | RP  | Right Primer  |
| CDS                           | Coding Sequence                                  | RPKM  | Reads Per Kilobase of transcript per Million mapped reads |
| CESA                          | Cellulose Synthase A                             | RT-PCR  | Reverse Transcription PCR                                 |
| DAP                           | Days After Pollination                           | S   | Sucrose   |
| DDC                           | DiethylDithioCarbamate                           | SDS   | Sodium Dodecyl Sulphate                                   |
| DNA                           | DeoxyriboNucleic Acid                            | SE/CC   | Sieve element/companion cell complex                      |
| DPI                           | Days Post Infection                              | SEs   | Sieve Elements  |
| EDTA                          | Ethylene Diamine Tetra Acetic acid               | SP  | Storage Parenchyma  |
| ENOD                          | Early NODulin-like protein                       | SND   | Secondary wall associated NAC Domain Spectroscopy         |
| EP                            | Epidermal Peel                                   | St  | Stachyose   |
| EREBP                         | Ethylene-Responsive Element Binding Protein      | TCRR  | TC specific type –A Response Regulator                    |
| ERF                           | Ethylene Response Factor                         | TCs   | Transfer Cells  |
| ETCs                          | Endosperm Transfer Cells                         | TCS   | Two Component Signaling                                   |
| FTIR                          | Fourier Transform Infrared Spectroscopy          | T-DNA   | Transfer DNA  |
| GFP                           | Green Fluorescent Protein                        | TEM   | Transmission Electron Microscopy                          |
| <i>GI</i>                     | <i>GIGANTEA</i>                                  | Tm  | Melting temperature                                       |
| GO                            | Gene Ontology                                    | UDP   | Uridine Diphosphate                                       |
| H <sub>2</sub> O <sub>2</sub> | Hydrogen Peroxide                                | UTR   | UnTranslated Region                                       |
| HCL                           | Hydrochloric Acid                                | UV  | Ultraviolet   |
| KOH                           | Potassium Hydroxide                              | VND   | Vascular related NAC Domain                               |
| LBP                           | Left Border Primer                               | WT  | Wild Type   |
| LP                            | Left primer                                      |   |   |
| LRR                           | Leucine Rich Repeat                              |   |   |
| Meg                           | Maternally expressed gene                        |   |   |
| mPS-PI                        | modified Pseudo-Schiff Propidium Iodide          |   |   |
| MQ                            | Milli Q  |   |   |

|              |                   |     |                   |
|--------------|-------------------|-----|-------------------|
| Xe           | Xylem element     | Gb  | Giga bases        |
| Zm           | <i>Zea Mays</i>   | h   | hour              |
| <b>Units</b> |                   | m   | metre             |
|              |                   | min | minute            |
| μl           | micro Litre       | ml  | milli litre       |
| μm           | micro metre       | mM  | milli Molar       |
| μmol         | micro mole        | N   | Normality         |
| bp           | base pair         | °C  | degree Celcius    |
| cm           | centi metre       | s   | second            |
| cv           | cultivar          | V   | Volt              |
| g            | centrifugal force | v/v | volume for volume |
| g            | gram              | w/v | weight for volume |

## ABSTRACT

Transfer cells (TCs) form wall ingrowths as an anatomical adaption to increase plasma membrane surface area to achieve enhanced rates of nutrient transport at apoplasmic-symplasmic bottlenecks in nutrient transport pathways in plants. TC formation occurs widely across the plant kingdom and also in algae and fungi. TCs can form as a consequence of normal development processes in plants or can be induced to form by biotic or abiotic stress. Various signaling pathways involving auxin, ethylene and reactive oxygen species are known to induce the formation of wall ingrowths in TCs, and abiotic factors such as cold and high light, the latter acting through jasmonic acid signaling, are reported to influence wall ingrowth deposition. Transcript profiling studies have shown that hundreds of genes are likely involved in regulating the biosynthesis of wall ingrowths, however, despite the importance of this process to nutrient transport in plants, little is known of the genetic regulation of wall ingrowth deposition. Hence, in this thesis, a combination of approaches were used in an attempt to identify transcription factors regulating wall ingrowth formation in TCs. First, a non-targeted strategy employing RNA sequencing (RNA-Seq) of epidermal TCs in cotyledons of *Vicia faba* was used to identify transcription factors and other cohorts of genes that showed extensive transcriptional regulation in epidermal cells undergoing *trans*-differentiation to become TCs. A role for selected *V. faba* transcription factors in regulating wall ingrowth deposition was then investigated by examining T-DNA insertional mutants of orthologous genes in *Arabidopsis thaliana*.

*V. faba* is a cool season grain-legume crop used extensively for human nutrition and livestock fodder and also as a model to study aspects of plant physiology, including epidermal TC development in cotyledons. Despite its agricultural importance, however, very limited genomic information is available for this species, in part due to its extreme genome size of approximately 13 Gb. Therefore, to provide a reference map for subsequent RNA-Seq, a genome-wide *de novo* assembly was generated by Next Generation Sequencing. Total RNA pooled from different vegetative and reproductive tissues at different stages of development, along with cultured cotyledons induced to form adaxial epidermal TCs, was subjected to deep sequencing using the Illumina Hi-Seq 2000 platform. Sixty five million reads were generated from 100-bp paired-end sequencing and *de novo* assembly was undertaken from this read set using CLC Genomics Workbench.

An optimum assembly using word size (*K*-mer) 47 and bubble size 300 was obtained which yielded 21,297 transcripts, of which 80.6% (17,160 contigs) were functionally annotated with GO terms. The assembly was validated by comparing against sequenced *V. faba* mRNAs from NCBI which also included transcripts known to have role in TC development, as well as sequenced *CesA* genes. This transcriptome map identified 726 transcription factors representing 31 of the 58 families of known plant transcription factors.

For RNA-Seq analysis of epidermal TC development, total RNA obtained from pooled epidermal and storage parenchyma tissues of cotyledons cultured for 0, 3, 9 and 24 h was subjected to 100-bp paired-end sequencing which yielded 368 million reads in total (42-48 million reads per sample). Log<sub>2</sub> fold-changes in RPKM values were calculated for both epidermal and storage parenchyma samples. Using stringent thresholds of Log<sub>2</sub> fold-change differences in epidermal and storage parenchyma samples, differentially expressed transcripts specific to epidermal TCs were identified. This analysis identified 444 transcripts that were up-regulated specifically in epidermal TCs, of which 22 were annotated as transcription factors. Prominent amongst this list were members of the MYB and ERF families, along with a trihelix GT-3B transcription factor which ranked as the highest fold-change transcript in epidermal cells undergoing *trans*-differentiation to become epidermal TCs. A similar analysis was carried out to identify 172 epidermal-specific down-regulated transcripts, of which 10 were annotated as transcription factors. This cohort included homeobox leucine zipper proteins, MADS-box and zinc finger CCCH-domain transcription factors. In addition to the categories of epidermal-specific up- or down-regulated genes, a third class of transcripts defined as “epidermal-enhanced” were identified. In this category, 198 transcripts, 20 of which were transcription factors, showed a  $\geq 25$ -times higher fold-change in epidermal tissue compared to storage parenchyma across cotyledon culture. Of the 20 transcription factors defined as “epidermal-enhanced”, almost half were members of the WRKY family, consistent with the induction of epidermal TCs in *V. faba* cotyledons representing a stress response. A manuscript describing this RNA-Seq study has been submitted to *Frontiers in Plant Science* and Chapter 3 of this thesis comprises the submitted manuscript plus additional unpublished material.

Since no transformation system is available for *V. faba*, to test the role of transcription factors identified from the RNA-Seq study, a strategy involving analysis of orthologous

genes in *Arabidopsis thaliana* (*Arabidopsis*) was adopted. Phloem parenchyma (PP) cells in minor veins of *Arabidopsis* leaves *trans*-differentiate to become PP TCs, and wall ingrowth deposition in these TCs can be visualised by confocal microscopy following pseudo-Schiff staining using propidium iodide. This development enabled phenotypic screening of wall ingrowth deposition in PP TCs in T-DNA insertional mutants of *Arabidopsis* genes orthologous to those identified in *V. faba*. *Arabidopsis* orthologs of MYB (*AtMYB20*), WRKY (*AtWRKY33*, *AtWRKY41*, *AtWRKY48*) and trihelix transcription factors (*AtGT-3B*) were identified along with each paralog (*AtMYB43*, *AtWRKY44*, *AtWRKY53*, *AtWRKY57* and *AtGT-3A*), respectively. Double mutants were created for all pairs except the trihelix transcription factors and then scored for wall ingrowth deposition in PP TCs by confocal microscopy of propidium iodide-stained leaves. However, no detectable change in the extent of wall ingrowth deposition was seen in any of the four double mutants analysed by this approach. Similarly, no change was seen in any of the *WRKY* double mutants exposed to low temperature, a growth condition reported to induce wall ingrowth deposition in PP TCs of minor veins. Single T-DNA insertional mutants in either *AtGT-3B* or *AtGT-3A* also failed to show any phenotype associated with wall ingrowth deposition in PP TCs as revealed by confocal microscopy. *AtMYB20*, and its closest paralog, *AtMYB43*, are known components of the transcriptional cascade required for secondary wall formation in *Arabidopsis*. Therefore the *atmyb20/atmyb43* double mutant generated in this study was also examined for general effects on secondary wall deposition in *Arabidopsis*. While Fourier transform infrared (FTIR) spectroscopy revealed quantitative differences in carbohydrate profiles of stem and leaf extracts from wild type and the double mutant, and phloroglucinol staining of stem sections revealed somewhat reduced levels of secondary wall deposition in the double mutant, surprisingly, no visible phenotype was detected in tracheary elements adjacent to PP TCs in leaf minor veins. This preliminary analysis of the *atmyb20/atmyb43* double mutant therefore suggests differences in secondary wall biogenesis in vascular tissue between stem and minor veins. The phenotypic analysis in *Arabidopsis* of orthologous transcription factors discovered by the RNA-Seq study, as well as the more detailed analysis of the *atmyb20/atmyb43* double mutant is reported in Chapter 4 of this thesis.

In summary, this study generated a genome-wide *de novo* transcriptome map of *V. faba* which not only enriches the genetic resources available for this important grain legume,

but also served as a template for subsequent transcript profiling by RNA-Seq. Analysis of epidermal TC development in cotyledons of *V. faba* by RNA-Seq identified cohorts of transcription factors, amongst other genes, that showed strong epidermal-specific or epidermal-enhanced transcriptional regulation across epidermal TC development, thus suggesting regulatory roles for these transcription factors in this process. However, a genetic analysis of orthologous genes in *Arabidopsis*, including genes known to regulate secondary wall deposition, failed to establish a role for these transcription factors in regulating TC development. A discussion of the strengths and limitations of the approach used in this study to identify putative transcriptional regulators of TC development is presented in Chapter 4. While this approach was ultimately unsuccessful, the study nonetheless identified numerous transcription factors in *V. faba* that warrant further investigation as putative regulators of the transcriptional cascades required for wall ingrowth building in TCs. Development of a robust transformation protocol for *V. faba* or disruption of gene activity by amiRNA constructs delivered by biolistic bombardment into cotyledons may offer a way forward to achieve this goal.

**CHAPTER 1**  
**GENERAL INTRODUCTION**

## 1.1 INTRODUCTION

Transfer cells (TCs) are specialised nutrient transport cells in plants. These cells are characterised by invaginated wall ingrowths with amplified plasma membrane surface area to achieve high densities of transporter proteins that facilitate nutrient transfer. TCs are formed by *trans*-differentiation from differentiated cells across apoplasmic/symplasmic boundaries of nutrient transport (Gunning et al., 1968; Harrington et al., 1997; Talbot et al., 2002). This *trans*-differentiation occurs at bottlenecks in nutrient transport throughout the plant, such as the maternal/filial interface, gametophyte-sporophyte interface, the rhizobium root nodule interface and plant parasite interactions (Offler et al., 2003). TCs have been studied experimentally in numerous species such as *Vicia faba*, *Arabidopsis thaliana* (*Arabidopsis*), *Zea mays* (maize), *Triticum sativum* (wheat) and *Hordeum vulgare* (barley) (Offler et al., 2003). Two different types of wall ingrowth morphologies in TCs are known; “reticulate” and “flange” (Talbot et al., 2002). Reticulate wall ingrowths are characterised by papillate projections which can form complex fenestrated labyrinths, whereas flange ingrowths form as parallel ridges of wall material (McCurdy et al., 2008). The *trans*-differentiation process is induced by various signaling factors like auxin, ethylene and ROS (Andriunas et al., 2013) and wall ingrowth formation is achieved by differential expression of a large number of genes which is hypothesized to be regulated by a small set of unidentified transcriptional regulators (Thiel et al., 2008; Dibley et al., 2009; Thiel et al., 2012a, 2012b; Arun-Chinnappa et al., 2013). So far, the only known transcription factor which regulates TC formation is ZmMRP-1, a MYB-like transcription factor expressed specifically in maize basal endosperm TCs (Gómez et al., 2002, 2009).

This research project focuses on discovering key transcriptional switch (es) proposed to be involved in TC formation. To undertake this task, several different experimental strategies were pursued. RNA-Seq was employed to identify potential transcription factors that were differentially expressed during wall ingrowth deposition using *in vitro* culture to induce epidermal TC development in *V. faba* cotyledons. In addition, targeted reverse genetics in *Arabidopsis* was used to test the involvement of transcription factors orthologous to those identified in *V. faba* as putative transcriptional regulators of TC development.

## **1.2 LONG AND SHORT DISTANCE NUTRIENT TRANSPORT**

### **1.2.1 Transport of nutrients in plants**

The evolution of land plants resulted in development of vascular tissues for transport functions (Pires and Dolan, 2012). The development of vascular tissue provided an integrated mechanism to connect and coordinate functioning of specialized tissues such as roots for nutrient mining from the soil and transport to aerial parts of the plant, shoots for providing not only mechanical support but also a long-distance route for transport of nutrients, and leaves for photosynthesis (Schulz and Thompson, 2009; Lucas et al., 2013). Xylem and phloem constitute the transport pipelines of vascular tissue. Xylem conducts water and mineral nutrients, whereas phloem transports photo-assimilates from source tissue (net exporters of assimilates) where it is synthesised (e.g., leaves), to sink tissues (net importers of assimilates) where it is utilized (e.g., root, flower and fruits) (Taiz and Zeiger, 2002; Schulz and Thompson, 2009). In xylem, transport is facilitated by bulk flow driven by negative pressure created due to evaporation of water from leaves (Lalonde et al., 2003). In tracheary elements, loading and unloading of resources exclusively follows an apoplasmic route (Taiz and Zeiger, 2002). However, transport of sugars and amino acids through phloem to adjacent sink tissues can follow either symplasmic or apoplasmic routes (Lalonde et al., 2003).

### **1.2.2 Phloem - Structurally specialized tissue for transporting photoassimilates**

Phloem tissue constitutes phloem parenchyma (PP), sieve elements (SEs) and companion cells (CCs) (Van Bel, 2003). SEs are specialised for performing low resistance but long distance transport of nutrients. These SEs are connected end-to-end through sieve plates that have pores, which allow materials to flow through them (Sjolund, 1997). Low resistance transport in SEs is achieved by limiting the cytoplasmic contents, as SEs are devoid of organelles like golgi, ribosomes and also the nucleus. Smooth endoplasmic reticulum forms fenestrated cisternae immediately below the plasma membrane in SEs and creates a space to trap and prevent enzymes, metabolites and other important molecules required for the functioning of SEs from being carried along with the assimilates (Schulz and Thompson, 2009). SEs form a functional complex with CCs, the so-called SE/CC complex, however the latter have dense cytoplasm with large numbers of mitochondria and ribosomes, hence, increased metabolic activity. Thus, it is

hypothesised that CCs play a critical role in enduring the life of SEs, and this is achieved in large part by numerous plasmodesmata which create symplastic connections between SEs with CCs. Hence SEs function along with CCs as part of the SE/CC complex in transporting assimilates from source to sink tissues (Taiz and Zeiger, 2002). In phloem, the mechanism of long-distance transport is bulk flow driven by pressure difference generated by a concentration gradient of sugars between source and sink (Thompson et al., 2001).

### **1.2.3 Phloem loading is the first step in transport of photo-assimilates**

Photo-assimilates are mostly transported in the form of sucrose. The first step in this process is loading of phloem (Slewinski and Braun, 2010), followed by translocation of the photo-assimilates and finally phloem unloading. Phloem loading collectively is the process of transporting photo-assimilates from the site of production in mesophyll cells to the SE/CC complex of minor veins driven by a concentration gradient. Sucrose initially moves from mesophyll cells to phloem cells through symplasmic pathway (Figure 1.1A; Beebe and Russin, 1999; Schulz and Thompson, 2009). Phloem loading in higher plants is achieved by two strategies, namely apoplastic loading (Roberts and Oparka, 2003; Gamalei, 2007; Sauer, 2007; Braun and Slewinski, 2009) or symplasmic loading (Patrick, 1997; Oparka and Turgeon, 1999).

Apoplastic loading occurs when the SE/CC complex is symplasmically isolated with less or no plasmodesmatal connections between them and the surrounding cells (Gamelei, 1989). Sucrose is transported from mesophyll cells to PP via a symplastic pathway and then is unloaded into the apoplastic space adjacent to cells of the SE/CC complex (Amiard et al., 2005). Initially, mechanisms like carrier-mediated membrane transport were observed to be involved in the efflux of sucrose into the apoplasm. For example, *Arabidopsis thaliana* sucrose transporter, AtSUC3 and *Saccharum hybridum* sucrose transporter, ShSUT1, in sugarcane, were localised in PP of leaf minor veins and functioned to efflux sucrose into the vein apoplasm through reversing sucrose/H<sup>+</sup> influx (Meyer et al., 2000; Rae et al., 2005; Kühn and Grof, 2010). Unloading of sucrose from PP into the apoplasm in *Arabidopsis* was recently identified to be achieved by members of the AtSWEET family of sugar transporters (Chen et al., 2012). Apoplastic sucrose is then transported into SE/CC complex via the action of plasma membrane sucrose/H<sup>+</sup> co-transporters (Figure 1.1A; Lalonde et al., 2004; Schulz and Thompson, 2009).

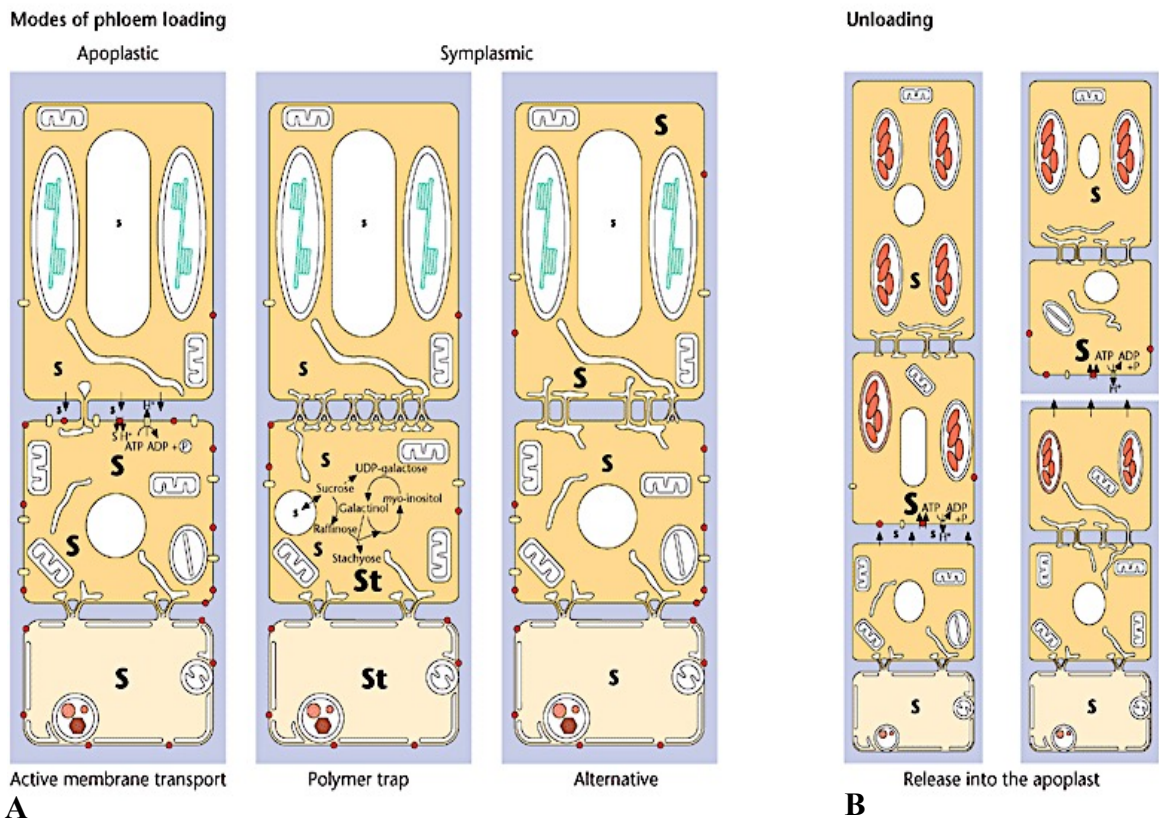


**Figure 1.1. Pathways of phloem loading and unloading in plants.**

Two modes of phloem loading strategies, (A) apoplastic loading and (B) symplasmic loading are illustrated. **(A)** Active membrane transport takes place in apoplastic loading, where sucrose (S) is transported from mesophyll cells to PP (top cell) symplasmically and effluxed into the apoplast where it is co-transported with protons into the SE/CC complex (Middle and bottom cell). In the polymer trap mechanism, sucrose is symplasmically transported into intermediary cell (CC, middle cell), where polymeric sugars like raffinose and stachyose (St) are synthesised and transported symplasmically to SEs (bottom cell) where backflow of the sugar polymers is prevented by the small orifice of connecting branched plasmodesmata. Alternative, or passive, symplasmic loading is where transport of sucrose into SEs is driven via a concentration gradient. **(B)** Sucrose unloading is mostly symplasmic as it follows concentration gradient. In some cases, where the SE/CC complex is symplasmically isolated, an active step including apoplastic unloading takes place where sucrose is retrieved (left image). This is mostly observed in maternal/filial interface where assimilates leave from maternal symplasm and are uptaken by filial tissue (right image). Adapted from Schulz and Thompson (2009).

Membrane-bound  $H^+$ -ATPase in the plasma membrane of the SE/CC complex hydrolyses ATP to ADP and generates a proton gradient to power the co-transport process. The stoichiometric ratio of sucrose transported relative to  $H^+$  is 1:1 (Bush, 1993; Schulz and Thompson, 2009).

Plants that load symplasmically have more plasmodesmata connecting the SE/CC complex to surrounding cells. The driving force for symplasmic loading is the pressure

differences between source and sink tissues created due to high concentration of sucrose in the SE/CC complex of source than in sink tissues (Holthaus and Schmitz, 1991; Beebe and Turgeon, 1992; Buchi et al., 1998). Some symplasmic loaders have a special type of CC called intermediary cells where bundle sheath cells are connected to CCs and not to PP. Plasmodesmata connecting the bundle sheath to intermediary cells are typically branched towards the CC side and have narrow orifices. Intermediary cells translocate raffinose family oligosaccharides (RFOs) along with or without sucrose. These intermediary cells load phloem through a so-called “Polymer Trap” mechanism in which raffinose and stachyose are synthesised from the translocated sucrose in intermediary cells (Figure 1.1A). These polymers are then too large to diffuse back into the bundle sheath cells through the narrow plasmodesmata channels connecting intermediary cells and bundle sheath cells, thus increasing concentration of sugars in intermediary cells and thus developing a concentration gradient that drives the phloem loading of sugars (Turgeon and Hepler, 1989; Turgeon et al., 1993; Schulz and Thompson, 2009; Turgeon and Wolf, 2009).

#### **1.2.4 Phloem unloading in sink tissues**

Nutrients exported from the source tissue through the SE/CC complex conduit are imported at various sink tissues along this conduit for their utilization. This process is called phloem unloading and can be either apoplasmic or symplasmic, or a combination of both (Oparka, 1990). In symplasmic unloading mechanisms, photo-assimilates in the SE/CC complex are unloaded into vascular parenchyma of sink tissue through connecting plasmodesmata. Most of the non-phloem tissues in sinks are symplasmically connected to SE/CC complexes through plasmodesmata in storage organs. In sink tissues which are symplasmically isolated, i.e., no continuity in plasmodesmatal connections with the SE/CC complex, the contents are effluxed into the apoplasm and then transported into the sink tissue by plasma membrane transporter proteins (Figure 1.1B; Patrick, 1997; Schulz and Thompson, 2009). For example, in developing seeds, maternal/filial tissues are symplasmically isolated and an apoplasmic step of unloading is involved in the parenchyma cells (Figure 1.1B; Patrick and Offler, 2001, Lalonde et al., 2003). Sucrose is unloaded into seed apoplasm through simple diffusion, facilitated diffusion and energy-coupled transport. Sucrose effluxed into the sink apoplasm may be broken down into glucose and fructose by cell wall-bound invertase or may be taken as such by sucrose

transporters in sink tissue (Kühn and Grof, 2010). In some cases, sucrose transporters (SUTs) were found to be facilitating efflux, for example in tomato (*Lycopersicon esculentum*; Hackel et al., 2006) and seed coats at developing stage (*Pisum sativum* (pea); Tegeder et al., 1999; *V. faba*; Zhou et al., 2007). Nutrients are retrieved from sink apoplast into developing seeds through a proton symport mechanism (Patrick and Offler, 2001).

### **1.3 TRANSFER CELLS ARE SPECIALISED FOR NUTRIENT EXCHANGE**

TCs are formed at bottleneck sites of nutrient transport across apoplastic/symplasmic boundaries in phloem loading and unloading regions (Pate and Gunning, 1972). In 1884, Fisher reported the presence of densely stained cells in leaf minor veins, and called these cells “uebergangszellen”. In 1968, Gunning, Pate and Briarty re-defined this term as “Transfer cells” (Gunning et al., 1968). They reported that TCs are anatomically specialised for solute transport, whereby they contain invaginated wall ingrowths polarized to the direction of solute flow (Gunning et al., 1974). They speculated that the increased plasma membrane surface area resulting from the extensive wall ingrowths provided a means for localised increase in membrane transporter proteins and thus increased capacity for plasma membrane transport of nutrients (Gunning and Pate, 1969). TCs are ubiquitous and found in all plant taxonomic groups as well as in algae and fungi (Gunning, 1977). TCs *trans*-differentiate from differentiated cells at regions where there is high demand for nutrient flow, and the TCs are polarised towards solute flow (Offler et al., 2003). In *Arabidopsis*, they are formed at loading sites of leaf minor veins to facilitate the nutrient exchange across membranes (Haritatos et al., 2000). TCs are formed at maternal/filial interfaces in seeds to facilitate apoplastic uptake of nutrients into filial tissue such as *V. faba* cotyledons (Offler et al., 1989), pea (Hardham, 1976), wheat (*Triticum turgidum*; Wang et al., 1995) and barley (Cochrane and Duffus, 1980). In *V. faba*, epidermal TCs of cotyledons were utilised to prove the function of TCs in solute transport (McDonald et al., 1996). Sucrose was demonstrated to be the major assimilate transported through these cells and a sucrose/H<sup>+</sup> transporter *V. faba* sucrose transporter-1 (*VfSUT1*) was found to be co-localised with H<sup>+</sup>-ATPase and found at high densities in these TCs (Weber et al., 2000; Harrington et al., 1997). Apart from such locations, TCs are also found at gametophyte/sporophyte nutrient exchange regions (Ligrone and Gambardella, 1988), sites of nematode infection (Jones and Gunning, 1976; Golinowski

et al., 1996) and mycorrhizal associations (Allaway et al., 1985), and at sites of plant and parasite interactions (Mims et al., 2001; Offler et al., 2003; McCurdy et al., 2008). TCs are also known to play a vital role in increasing yield and biomass in developing seeds (cotton: Pugh et al., 2010; pea: Zhang et al., 2015). Hence, TCs are crucial for nutrient transport in plants and identifying the regulatory networks inducing TCs may lead to increases in agricultural productivity.

### **1.3.1 Wall ingrowth deposition in TCs**

#### **1.3.1.1 Reticulate and Flange Morphologies**

Wall ingrowth deposition seen in TCs can be categorized into two major morphologies - reticulate wall ingrowths and flange wall ingrowths. Both morphologies are found in a variety of TC types. Reticulate wall ingrowths are initiated as small papillate wall ingrowths deposited at discrete loci across the parent cell wall. These ingrowths then branch and/or fuse to form a fenestrated layer. This layer acts as a platform for subsequent deposition of new papillate, which branch and fuse to create a second layer, a process which can be repeated to build a multi-layered fenestrated network of wall ingrowth material (Figure 1.2A; McCurdy et al., 2008). Reticulate wall ingrowths are seen in diverse TC types (e.g., epidermal cells, nodal xylem parenchyma cells, nucellar projection cells, phloem and xylem parenchyma cells) across a broad range of plant species, including both monocots and dicots (Offler et al., 2003). In *Arabidopsis*, PP TCs of leaf minor veins and epidermal TCs of *V. faba* cotyledons have reticulate wall ingrowth morphology (Talbot et al., 2002; Maeda et al., 2008; Edwards et al., 2010).

Flange wall ingrowths in contrast are deposited as curvilinear ribs of parallel strands or ridges of wall material, and these ribs broaden and can be cross-linked with each other to form a meshwork-like structure as seen in maize, wheat (*Triticum aestivum*), *Oryza sativa* (rice) and barley (Figure 1.2B; McCurdy et al., 2008; Offler et al., 2003; Talbot et al., 2002). The morphology of flange wall ingrowths resembles secondary wall thickenings in many cases (McCurdy et al., 2008). In some cases, both reticulate and flange wall ingrowths can be deposited in the same TC, for example in developing cotton seeds (Pugh et al., 2010).

### 1.3.1.2 Reticulate wall ingrowths represent an example of localised wall deposition in plant cells.

The reticulate wall ingrowth morphology is the most common morphology seen in TCs across the plant kingdom (Talbot et al., 2002; Offler et al., 2003). Reticulate wall ingrowths represent a novel example of localized wall deposition, and unlike secondary walls they are not strongly lignified (Vaughn et al., 2007, but see Rocha et al., 2014). A good example for reticulate wall ingrowth morphology that has been studied extensively are epidermal TCs in *V. faba* cotyledons. *In planta*, abaxial epidermal TCs in *V. faba* cotyledons exhibit localized deposition of reticulate wall ingrowths which facilitates spatially defined nutrient transport between maternal (seed coat) and filial (cotyledon) interfaces (Talbot et al., 2002). The mechanism of localised deposition of reticulate wall ingrowth formation is not very well understood.

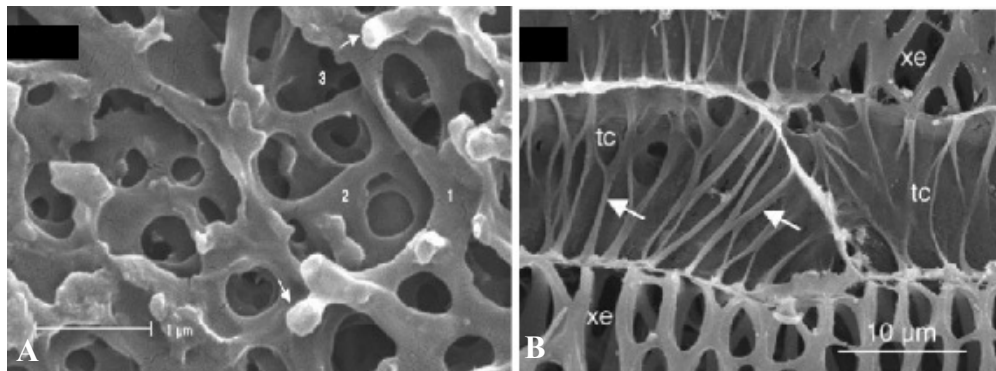


**Figure 1.2. SEM images of different morphologies of wall ingrowth deposition in TCs.**

**A)** Reticulate wall ingrowth network in epidermal TCs of *V. faba* cotyledons. A multi-layered fenestrated network is seen, with numbers indicating each layer. New papillate wall ingrowths emerging from the youngest layer are indicated by arrows. **B)** Flange wall ingrowths in xylem parenchyma TCs (tc) of *Triticum aestivum*. Ribs of mostly parallel wall ingrowths (arrows) are seen in each TC. The flange wall ingrowths are roughly parallel to secondary wall thickenings in underlying xylem elements (xe). Images adapted from McCurdy et al. (2008).

The initiation of wall ingrowth construction starts with the deposition of a uniform wall layer deposited across the parent cell wall (Talbot et al., 2007b). In epidermal TCs of *V. faba* cotyledons, the deposition of this uniform wall is highly polarized to the outer periclinal face of the cell.

Recent studies have shown that the polarized deposition of this uniform wall is directed by extracellular H<sub>2</sub>O<sub>2</sub> (Andriunas et al., 2012; Xia et al., 2012). However, the highly localized deposition of papillate wall ingrowths occurs at discrete but apparently random

loci across the surface of the uniform wall layer (Talbot et al., 2007b; Andriunas et al., 2012). Zhang et al. (2015a,c) reported that these random loci for deposition of wall ingrowth papillate are defined by so-called  $\text{Ca}^{2+}$  plumes generated by activities of clusters of plasma membrane  $\text{Ca}^{2+}$ -permeable channels surrounded by  $\text{Ca}^{2+}$ -ATPases that work in a co-ordinate manner. Cellulose microfibrils in the uniform wall are deposited as parallel arrays (Talbot et al., 2007b), presumably directed by cortical microtubules (Talbot et al., 2007a), but cellulose microfibrils which initiate papillate wall ingrowth deposition are laid down as raised patches of tangled and thickened “microfibrils” (Talbot et al., 2007b). The role of cortical microtubules in directing this type of highly localized cellulose deposition remained unknown (McCurdy et al., 2008), however, any role for microtubules in this process seems to be quite distinct from other examples of localized wall deposition such as that in xylem elements (Roberts et al., 2004). Zhang et al. (2015d) also reported that  $\text{Ca}^{2+}$  depletion zones are formed within the randomized cortical microtubule array that coincides with the spatio-temporal occurrence of papillate wall ingrowths in adaxial epidermal TCs of *V. faba* cotyledons. However, cortical microtubules do not appear to regulate papillate wall ingrowth deposition as this process continues apparently unaffected when cotyledons are cultured in the presence of the microtubule inhibitors oryzalin or taxol (Zhang et al., 2015d). Localized papillate wall deposition may be either due to reduced rates of cellulose production causing non-crystalline microfibril production, or possibly due to rosette complexes being restricted to discrete loci (McCurdy et al., 2008). Rosette complexes require different combinations of cellulose synthase (CesA) components to function (Persson et al., 2007) and absence of any of these components results in aberrant cellulose biosynthesis (Desprez et al., 2007; Persson et al., 2007). For example, in the Arabidopsis double mutant lacking both *CESA2* and *CESA6* (*Cellulose Synthase A*; *cesa2/cesa6*), cellulose biosynthesis was randomized and abnormal (Persson et al., 2007). A similar situation may be causing randomized microfibril deposition as the mechanism driving papillate wall ingrowth formation (McCurdy et al., 2008). In Arabidopsis, PP TCs contain reticulate wall ingrowths (Haritatos et al., 2000; Amiard et al., 2007; Edwards et al., 2010) and deposition of wall ingrowths is localized to the vicinity of neighbouring SE/CC complexes, presumably to facilitate highly localized unloading of sugars into the apoplasmic space immediately adjacent to cells of the SE/CC complex (Haritatos et al., 2000; Chen et al., 2012).

### **1.3.1.3 Composition of wall ingrowths in TCs**

Transmission electron microscopy (TEM) showed that reticulate wall ingrowths in epidermal TCs of *V. faba* cotyledons are composed of an inner, electron opaque region and an outer electron translucent region, and the ingrowth structure is deposited on a uniform wall layer deposited over the original primary wall (Talbot et al., 2001; Talbot et al., 2007b). Immunogold and affinity probe studies established that wall ingrowths and the uniform wall layer are composed of cellulose, hemi-celluloses and high levels of unesterified pectins (Vaughn et al., 2007). These authors therefore described wall ingrowths as “modified primary walls”. The electron translucent outer region of wall ingrowths contains callose, and the plasma membrane-wall interface in this region is rich in arabinogalactan proteins (AGPs; Vaughn et al., 2007). The function of these AGPs at the plasma membrane wall-interface might be to co-ordinate the incorporation of hemi-celluloses and pectins into the wall ingrowths. Inhibition of AGP function by  $\beta$ -D glucosyl Yariv reagent resulted in significant reduction of papillate wall ingrowth deposition (Talbot et al., 2007b). The callose present in the outer, electron translucent, regions of the wall ingrowths is thought to provide malleability to the wall ingrowths as they penetrate and spread into the cytoplasmic volume of the cell (McCurdy et al., 2008; Vaughn et al., 2007). Previous studies using phloroglucinol staining suggest that lignin is not found in wall ingrowths of TCs in *V. faba*, (Vaughn et al., 2007). However, recent studies in maize endosperm TCs using two different staining techniques, potassium permanganate in association with TEM-EDS (TEM-Energy Dispersive X-ray Spectrometry) and acriflavine in association with confocal laser scanning microscopy (CLSM) have suggested presence of lignin in developing TCs. TEM-EDS analysis revealed the presence of lignin in both reticulate and flange wall ingrowths in maize TCs, with flange wall ingrowths containing more lignin than the so-called reticulate wall ingrowths (Rocha et al., 2014). Acriflavine fluorescence as a marker of lignin increased as wall ingrowth development in the endosperm TCs progressed (Rocha et al., 2014).

## **1.4 REGULATION OF TRANSFER CELL *TRANS*-DIFFERENTIATION**

### **1.4.1 Signals inducing *trans*-differentiation of TCs**

TCs *trans*-differentiate from differentiated cells to form wall ingrowths as a consequence

of normal developmental pathways, such as when abaxial epidermal cells of *V. faba* cotyledons form epidermal TCs (McCurdy et al., 2008) and PP TCs of Arabidopsis, or they form in response to biotic and/or abiotic stresses, such as nematode attack (Jones and Gunning, 1976; Golinowski et al., 1996) or iron and phosphorus deficiency (Schikora and Schmidt, 2001, 2002). Various signaling pathways has been identified to be involved in different TC types.

Auxin acts as an inductive signal for *trans*-differentiation of *V. faba* cotyledon epidermal TCs, as inhibiting auxin action with *p*-chlorophenoxy-isobutyric acid (PCIB) reduced wall ingrowth formation in these TCs (Dibley et al., 2009). In tomato, high levels of auxin enhanced TC development in root rhizodermal cells (Schikora and Schmidt, 2001). Many AUX/IAA genes (and auxin responsive factors -ARFs, were induced in giant cells of nematode-infected roots in Arabidopsis after 3 and 5 days post infection (Cabrera et al., 2014). Ethylene, a major stress hormone in plant biology, has been demonstrated to play a clear role in inducing TC differentiation. In *V. faba* cotyledons, *trans*-differentiation is induced by a rapid burst of ethylene caused due to mechanical stress of expanding cotyledons inside seed coat. This hypothesis has been tested and shown that *V. faba AminoCyclopropane-1-Carboxylic-acid Synthase 2 (VfACS2)* and *V. faba 1-AminoCyclopropane-1-Carboxylic-acid Oxidase 2 (VfACO2)*, two genes involved in ethylene biosynthesis, were up-regulated when cultured cotyledons were induced to form adaxial epidermal TCs (Zhou et al., 2010). In addition, expression of *V. faba Ethylene Insensitive 3-1 (VfEIN3-1)* and *V. faba Ethylene Response Factor 1 and 3 (VfERF1 and 3)*, two ethylene-regulated transcription factors, were up-regulated concomitantly during epidermal TC development. Decreasing and increasing ethylene production by exposing cultured cotyledons to aminoethoxyvinylglycine (AVG) and 1-aminocyclopropane-1-carboxylic acid (ACC), decreased or increased, respectively, papillate wall ingrowth formation in these epidermal TCs. Furthermore, experimental evidences showed that auxin acts upstream of an ethylene signaling pathway which regulates wall ingrowth deposition in epidermal TCs of *V. faba* cotyledons (Zhou et al., 2010). In addition to these studies, it was noted that ethylene genes responsible for perception, transduction and responses, were up-regulated in nematode feeding cells at 3 and 5 days post infection in

Arabidopsis (Cabrera et al., 2014). Ethylene signaling components were also highly up-regulated across differentiation of endosperm transfer cells (ETCs) in barley (Thiel et al., 2012b).

In addition to auxin and ethylene, reactive oxygen species (ROS) have also been found to function as a regulatory signal for wall ingrowth deposition. Blocking action of NADPH oxidase (NOX), a plasma membrane-bound enzyme complex that generates ROS, by diethyldithiocarbamate (DDC) treatment decreased wall ingrowth deposition in epidermal TCs of *V. faba* cotyledons, which in turn was recovered by exposing DDC-treated cotyledons to H<sub>2</sub>O<sub>2</sub>, indicating that this is the ROS directly involved as the inductive signal (Andriunas et al., 2012). The polarized deposition of wall ingrowths is also governed through ROS signaling and it was hypothesised from preliminary experiments that ROS may act downstream of ethylene (Andriunas et al., 2012). Subsequently, Xia et al. (2012) reported that extra cellular H<sub>2</sub>O<sub>2</sub> regulates wall ingrowth deposition in TCs of *V. faba*. Abiotic stresses such as high light and low temperature also enhances wall ingrowth deposition in PP TCs adjacent to SEs in Arabidopsis (Amiard et al., 2007). In barley endosperm TCs (ETCs), abscissic acid (ABA) signaling pathways involving members of the two component signaling (TCS) system have been reported to play major roles in signal transduction pathways inducing ETC development (Thiel et al., 2012a). In plants, TCS pathways use phospho-relays to transmit signals from membrane to nucleus (Schaller et al., 2008). In maize basal ETCs, TCS phospho-relays are presumed to have a role in the differentiation process. Specific accumulation of *Z. mays* transfer cell-specific type-A response regulator transcripts (*ZmTCRR1* and *ZmTCRR2*), components of TCS pathways, were observed in basal ETC layer, and a physical interaction between these two proteins was observed with the phospho-intermediate ZmHP2, evidencing potential role of TCS phosphorelays in maize basal ETC differentiation (Muniz et al., 2006, 2010).

#### **1.4.2 Transcriptional regulation of *trans*-differentiation of TCs**

Genes specifically expressed in TCs, have, so far, only been reported in maize. In maize, *basal endosperm transfer cell layer 1* (*BETL1*, Hueros et al., 1995) and *maternally expressed gene 1* (*meg-1*, Gutierrez-Marcos et al., 2004) have been identified as being

expressed specifically in basal ETCs. *In situ* hybridization studies showed that *BETL1* expression was specifically restricted to the basal region of the endosperm corresponding to basal ETCs and also expressed only in developing maize endosperm (Hueros et al., 1995). *BETL1* promoter-reporter studies also indicated expression in ETC regions of maize kernels (Hueros et al., 1999). Promoter-reporter studies demonstrated that *Meg-1*, with parent-of-origin expression pattern, is exclusively expressed in ETCs in maize kernels. Immunolocalization indicated that MEG-1 protein is localized in the labyrinth wall ingrowths of TCs (Gutierrez-Marcos et al., 2004). Two TCS component genes *ZmTCRR1* and *ZmTCRR2* in maize were identified to be expressed specifically in ETC layer 8-14 days after pollination (DAP). These two genes encode type-A RR of TCS family, which are responsible for phospho-transfer-based signal transduction (Muniz et al., 2006, 2010). In barley, soluble invertase HvSF6FT1 is expressed in different tissues after pollination, at 3DAP in maternal pericarp, 4 DAP in vertical pericarp, but at 6 DAP it becomes limited to ETC layers (Weschke et al., 2003). HvSTP, a hexose transporter was highly expressed in barley ETC 3 days after fertilization in syncytial endosperm and at very low levels in pericarp (Weschke et al., 2003).

Extensive studies have been conducted to identify the cohort of genes involved in wall ingrowth deposition in TCs using different biological systems and experimental techniques. Laser micro dissection and macro array transcriptome analysis of ETCs in barley have shown that genes encoding transcription factors APETELA2/ ethylene-responsive element binding proteins (AP2/EREBP) involved in ethylene metabolism are up-regulated, indicating that ethylene may act as a regulatory signal in ETC development (Thiel et al., 2008). Transcript profiling of barley ETCs by Agilent microarrays showed that genes involved in cell wall biosynthesis (hemicelluloses, glucuronoxylans, arabinoxylans and callose) were differentially expressed during ETC formation. Furthermore, genes involved in amino acid catabolism, carbohydrate oxidation and starch degradation were up-regulated to meet the energy demands of ETC development (Thiel et al., 2012b). *De novo* transcriptome sequencing of laser capture microdissection of ETCs in barley revealed participation of TCS systems in differentiation of barley ETCs. TCS system works on the principle of phosphorylation of Asp and His residues of proteins. In plants, three components, namely membrane bound histidine kinase,

phosphotransfer protein and response regulators form the signaling system (Schaller et al., 2008). In total, 40 genes encoding for various components including transcripts of three subgroups of histidine kinases, histidine phosphotransfer proteins and response regulators, were detected to be up-regulated during differentiation of ETCs in barley, suggesting that they may have a role as a regulator of ETC development (Thiel et al., 2012a).

cDNA-AFLP analysis of epidermal TCs in *V. faba* cotyledons estimated approximately 650 genes are differentially expressed during wall ingrowth formation. Sequence identity of a limited number of these genes identified predicted functions involved in signaling, metabolism, cell wall biosynthesis and vesicle trafficking (Dibley et al., 2009). All these studies indicate that large numbers of genes are differentially expressed during the *trans*-differentiation of TCs. However, it is hypothesized that only a relatively small number of transcription factors might be required to act as regulatory switches to co-ordinate this transcriptional response to TC differentiation (Arun-Chinnappa et al., 2013).

### **1.4.3 Transcription factors regulating TC development**

It is hypothesized that transcription factor(s), operating downstream of and in response to signaling cascades, are switched on to co-ordinate downstream cascades of gene expression required for wall ingrowth deposition. However, knowledge on transcription factor(s) that act as key regulatory switches for TC development is very limited. *ZmMRP-1*, a MYB-related transcription factor in maize (*Z. mays*), is currently the only known transcriptional regulator to be specifically expressed in TCs, namely basal ETCs in maize kernels (Gómez et al., 2002). Over-expression of *ZmMRP-1* induces abgerminal cells of the endosperm aleurone layer, which normally do not form TCs, to develop wall ingrowths structurally similar to those that form in basal ETCs (Gómez et al., 2009). Interestingly, continued over-expression of *ZmMRP-1* was required to sustain the TC morphology of these abgerminal aleurone layer cells (Gómez et al. 2009). In addition, many other genes known to be specifically expressed in maize basal ETCs, such as *BETL1* and *BETL2* (Gómez et al., 2002), *Meg-1* (Gutierrez-Marcos et al., 2004) and *transfer cell response regulator 1* (*TCRRI*, Muniz et al., 2006), are transcriptionally regulated by *ZmMRP-1* (Gómez et al., 2009), thus providing strong evidence that *ZmMRP-1* functions as a transcriptional regulator of TC development in maize. Apart from *ZmMRP-1*, two

proteins ZmMRP-1 interactors 1 and 2 (ZmMRPI-1, ZmMRPI-2) were found to be interacting with full length ZmMRP-1 in a yeast two-hybrid screen. These proteins belong to the C<sub>2</sub>H<sub>2</sub> Zinc finger family and found to be modulating activity of ZmMRP-1 in binding to transfer cell specific promoters (Royo et al., 2009). However, ZmMRP-1 is the only identified transcription factor known to regulate flange-type wall ingrowths in maize (Gómez et al., 2009). To this date, no known transcription factors regulating reticulate wall ingrowth deposition have been identified. This thesis focusses on identifying the transcriptional switch(es) regulating reticulate wall ingrowth deposition.

### **1.5 SECONDARY WALL DEPOSITION AS A TRANSCRIPTIONAL MODEL FOR TRANSFER CELL DEVELOPMENT**

Some types of secondary wall formation, for example wall thickenings deposited during xylogenesis (Raven et al., 1999), represent examples of highly localized wall deposition in plant cells. In these cases, it is known that members of the MYB and NAC-domain families of transcription factors act as master switches in the cascade of gene expression required to build these secondary walls (Zhong et al., 2008). NST1 and NST2 (NAC Secondary wall Thickening promoting factor) act as master transcriptional switches and regulate secondary wall deposition in endothecium of anthers (Yang et al., 2007). Similarly, VND6 and VND7 (vascular related NAC domains), homologs of SND1, are master regulators of transcriptional cascades required for secondary wall deposition in protoxylem and metaxylem tissue in stems (Kubo et al., 2005). SND1 (secondary wall associated NAC domain protein) functions redundantly with NST1 to activate biosynthesis of secondary wall in fibers (Zhong et al., 2006; Mitsuda et al., 2007; Zhong et al., 2007). All the above master transcriptional switches up-regulate a similar cohort of second-tier transcription factors that in turn initiate expression of the biosynthetic genes required for secondary wall deposition (Mitsuda et al., 2005; Zhong et al., 2008). Collectively, from the viewpoint of wall ingrowth formation representing an example of localized wall deposition, these observations lead to the hypothesis that members of the MYB and NAC-domain gene families, possibly novel members of these large families, may also be operating as transcriptional switches for TC development. Aspects of this PhD thesis have tested this hypothesis (MYB gene family).

## 1.6 EXPERIMENTAL MODELS TO EXAMINE TRANSFER CELLS THAT BUILD RETICULATE WALL INGROWTHS

### 1.6.1 Adaxial epidermal transfer cell development in *Vicia faba* cotyledons

*V. faba* L. is a legume belonging to the family fabaceae (Duc, 1997). *V. faba* has been extensively used as a model system to study the guard cell biology (Schroeder et al., 1987, Song et al., 2006) and also to study TC biology (Offler et al., 1997, 2003; Wardini et al., 2007b; Andriunas et al., 2013). The abaxial epidermal cells and sub-epidermal cells of *V. faba* cotyledons form TC *in vivo* to facilitate nutrient transport at the maternal/filial interface of the seed (Offler et al., 1997). The abaxial epidermal TCs are formed just prior to seed fill as a consequence of mechanical stress caused by crushing against inner seed coat cells. These TCs are formed only on the abaxial surface of the cotyledon (Zhou et al., 2010). These abaxial TCs account for 80% of the sucrose accumulated in the cotyledons from seed apoplasm and thus they play a major role in nutrient transport during seed fill (McDonald 1996). Adaxial epidermal cells of *V. faba* cotyledons, however, can be induced to form TCs in culture (Figure 1.3; Offler et al., 2003; McCurdy et al., 2008). Furthermore, removal of cotyledons from the seed coat is straightforward without causing damage to cotyledons. These TCs are morphologically and functionally similar to abaxial epidermal TCs that form *in planta* during normal cotyledon development (Farley et al., 2000), and thus represent an excellent model system to study TC development. Extensive studies have established that the time course of adaxial epidermal TC development is reasonably synchronous across a time period of 15 h (Figure 1.4; Wardini et al., 2007b). After excision of cotyledons and culturing, by 2 h a new uniform wall is deposited over the outer periclinal surface of the primary wall. By 3 h, about 10% of the cells develop papillate wall ingrowths deposited over the surface of the newly formed uniform wall, and by 15 h about 90% of the epidermal cells show papillate wall ingrowth deposition (Figure 1.4; Wardini et al., 2007b). At 15 h, the papillate wall ingrowths show signs of branching and bifurcation (see Talbot et al., 2001), and by 24 h the wall ingrowths have initiated the development of fenestrated layers of wall ingrowth material (Figure 1.2, Figure 1.4; Wardini et al., 2007b). The study by Wardini et al. (2007b) also demonstrated that induction and continuous gene expression is required for wall ingrowth deposition, as evidenced by culturing cotyledons in the presence of 6-methyl purine, an RNA-synthesis inhibitor (Wardini et al., 2007b). The development of a TC identity upon cotyledon culture occurs exclusively in epidermal and

sub-epidermal cells of the cotyledons, but importantly from an experimental perspective, not in cells of the neighboring storage parenchyma tissue (Farley et al., 2000; Talbot et al., 2001; Wardini et al., 2007b).

Using the temporal profile established by Wardini et al. (2007b), a study employing cDNA-AFLP analysis of adaxial epidermal TC development in *V. faba* cotyledons revealed extensive transcriptional regulation of up to 650 genes (Dibley et al., 2009). Various classes of genes were induced specifically in adaxial epidermal TCs, including signaling pathways involving auxin and ethylene, cell division, metabolism, vesicle trafficking and cell wall biosynthesis (Dibley et al., 2009). This study indicated that TC *trans*-differentiation development corresponds with numerous cellular and genetic changes associated with de-differentiation of epidermal cell identity, re-entry into the cell cycle, and mitochondrial biogenesis to provide the energy required for wall ingrowth deposition. (Dibley et al., 2009). This study demonstrated that the *trans*-differentiation of epidermal TCs and associated wall ingrowth deposition is accompanied by substantial and rapid cell-specific transcriptional changes. Similar to the transcriptional cascades driving localized secondary wall formation, it is hypothesized that the extensive epidermal-specific gene expression to co-ordinate wall ingrowth formation presumably is regulated by a suite of transcription factors acting as master switches for the *trans*-differentiation process. These regulatory transcription factors are predicted to be responding to the auxin, ethylene and ROS signaling pathways demonstrated in the cotyledon culture system to be signaling the induction of wall ingrowth deposition in these cells (Dibley et al., 2009; Zhou et al., 2010; Andriunas et al., 2012). Thus, the available information and experimental system documenting TC development in *V. faba* cotyledons provides a strong platform to discover these transcriptional switches regulating the *trans*-differentiation process by using RNA-Seq as the most appropriate tool for transcript profiling in biological systems.

**1.6.2 Phloem parenchyma transfer cell development in minor veins of *Arabidopsis thaliana***, a flowering plant from family brassicaceae, is the most widely used genetic model in plant biology. PP cells in leaf minor veins *trans*-differentiate to form PP TCs (Figure 1.5, Haritatos et al., 2000). PP TCs are also present in major veins of the leaf (Edwards et al., 2010), consistent with the conclusion by Haritatos et al. (2000)

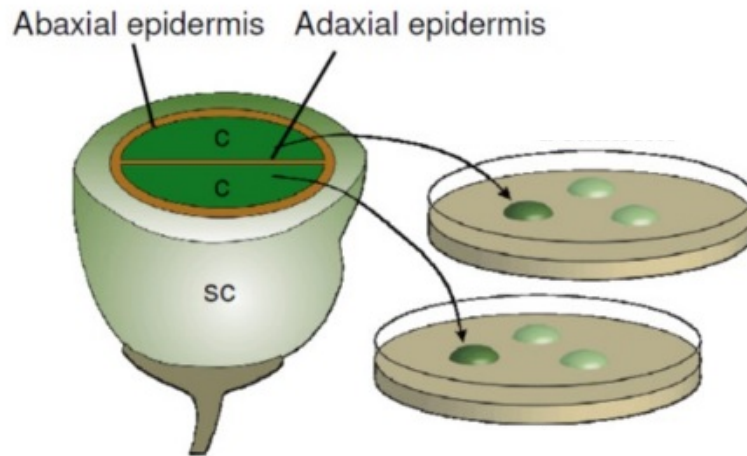


**Figure 1.3: Schematic representation of *V. faba* cotyledon culture system.**

Abaxial epidermal cells of cotyledons develop TCs *in planta* and adaxial epidermal cells do not. However, adaxial epidermal cells can be induced to form TCs in culture. Sister cotyledons from seeds coat can be extracted and used for culture system. c, cotyledons, sc, seed coat. Image adapted and modified from Andriunas 2011.

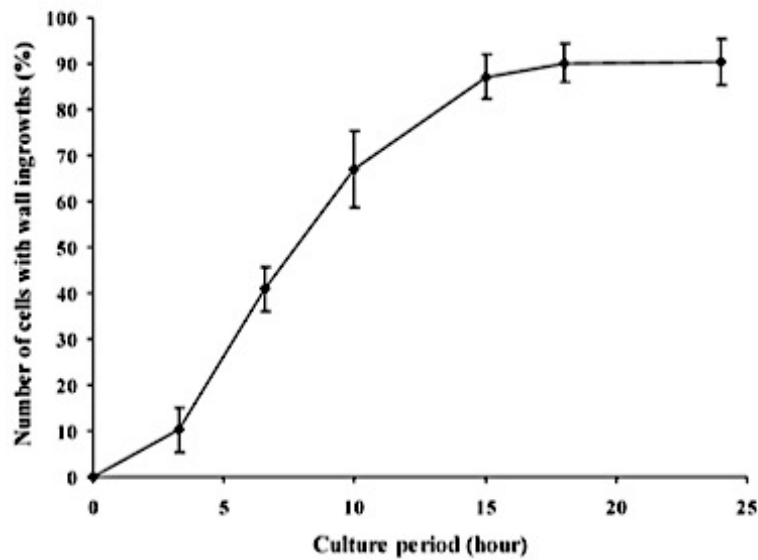


**Figure 1.4: Time course of wall ingrowth formation in adaxial epidermal cells of cultured *V. faba* cotyledons.**

This graph shows the synchronous development of TCs in adaxial epidermis of cultured cotyledons. After 3 h, 10% of the cells contain papillate wall ingrowths; by 15h, 90% of the cells have wall ingrowth papillate at different stages of development. Diagram adapted from Wardini et al. (2007b).

that these veins could also be physiologically defined as “minor” due to their close spatial relationship to mesophyll cells which is required for phloem loading.

PP TCs form reticulate wall ingrowths via deposition of papillate wall ingrowths which subsequently can develop into a fenestrated network (Maeda et al., 2008; Edwards et al., 2010). Highly localized wall ingrowth deposition occurs towards the flow of nutrient transport adjacent to neighbouring cells of the SE/CC complex (Figure 1.5B, Haritatos et al., 2000; Amiard et al., 2007). In *Arabidopsis* leaves, sucrose is transported from mesophyll cells to bundle sheath cells and then to PP via symplasmic transport through plasmodesmata. Sucrose is then effluxed from PP into the apoplasm via AtSWEET sucrose effluxers (Chen et al., 2012), and then is imported into the SE/CC complex via uptake by AtSUC2 on the plasma membrane of CCs (Gottwald et al., 2000). The availability of a complete annotated genome sequence, a huge collection of T-DNA insertion mutants, and databases derived from microarray and now RNA-Seq databases, provides valuable tools for molecular and genetic analysis of biological processes occurring in plants (Meinke et al., 1998; *Arabidopsis* Genome, 2000; Koornneef and Meinke, 2010). The development of PP TCs is responsive to abiotic stresses like high light and low temperature (Maeda et al., 2006; Amiard et al., 2007; Maeda et al., 2008), thus enabling bioinformatics approaches to be used to identify cohorts of genes showing differential expression in leaf tissue under these conditions. This approach was used to identify the flowering gene *GIGANTEA* (*GI*) as one of 46 genes up-regulated in leaves under the various biotic and abiotic stresses known to cause increased wall ingrowth deposition in PP TCs (Edwards et al., 2010). Among these, *GI* was the only mutant to show reduced levels of wall ingrowth deposition in PP TCs when stained with Calcofluor White. *GI* does not have a recognized DNA binding motif (Fowler et al., 1999) and is therefore not considered to be a direct transcriptional regulator of wall ingrowth deposition. However, *gi* mutants have increased antioxidant capacity due to increased levels of superoxide dismutase and ascorbate peroxidase, prompting Edwards et al. (2010) to speculate that this antioxidant capacity may suppress ROS levels in response to abiotic stress leading to reduced levels of wall ingrowth deposition.

An initial disadvantage in studying PP TC development in *Arabidopsis* was the necessity to use TEM to observe these cells buried deep within vascular bundles (e.g., Amiard et al., 2007; Haritatos et al., 2000; Maeda et al., 2006). However, Edwards et al. (2010) developed a fluorescence based procedure exploiting the cellulose-rich composition of wall ingrowths to image PP TCs by using calcofluor white staining of leaves. Subsequent to this development, aniline blue was also used to stain callose associated with wall ingrowths in PP TCs. Thus, by combining the bioinformatics resources of *Arabidopsis* with relatively high-throughput analysis afforded by staining leaf tissue with either calcofluor white or aniline blue, preliminary identification of various MYB and NAC-domain transcription factors were identified as possible regulators of PP TC development. A review reporting on this development was published at the early stages of this PhD

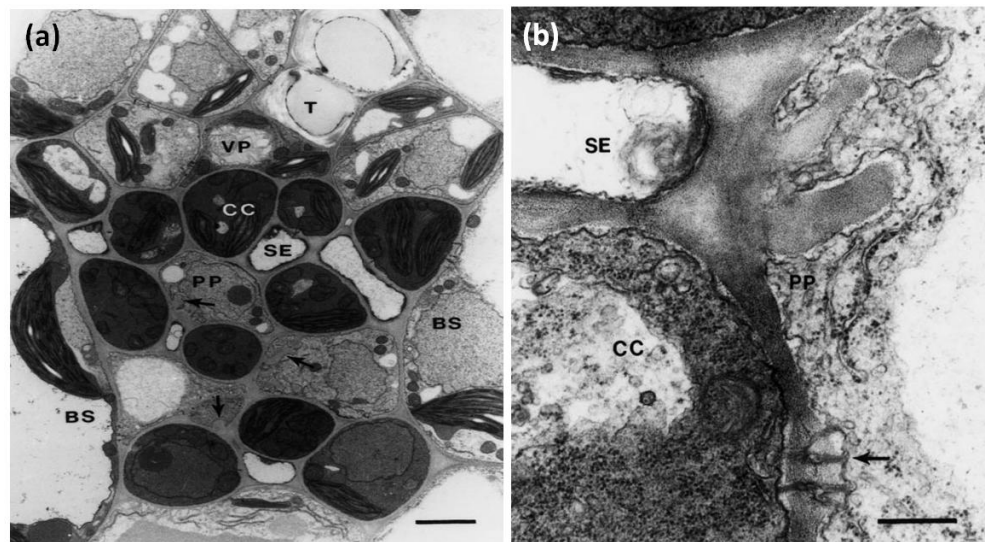


**Figure 1.5. TEM images of PP TCs in an *Arabidopsis* leaf minor vein.**

(a) Minor vein architecture showing the position of phloem parenchyma (PP) cells relative to cells of the SE/CC complex. Wall ingrowths in PP TCs are indicated by black arrows. (b) Higher magnification view of PP TC showing papillate wall ingrowths deposited adjacent to neighbouring cells of the SE/CC complex. Black arrow indicates plasmodesmata connecting the PP TC with neighbouring CC. BS, bundle sheath cell; CC, companion cell; PP, phloem parenchyma cell; SE, sieve element; T, tracheary element; VP, vascular parenchyma cell. Bar in (a) = 2  $\mu$ m; bar in (b) = 0.4  $\mu$ m. Images taken from Haritatos et al. (2000).

thesis and has been included as Appendix 1 (Arun Chinnappa et al., 2013). Subsequent to this review, more detailed observations using confocal microscopy of the cell types fluorescently stained by either calcofluor white or aniline blue came to the conclusion that neither stain, especially calcofluor white, could not be relied upon to exclusively stain

PP TCs in vascular bundles. With this realization, a new method involving propidium iodide staining of cell walls in combination with confocal microscopy was developed which allows unambiguous assessment of wall ingrowth deposition in PP TCs of Arabidopsis and TCs in other species (Nguyen and McCurdy, 2015; see Chapter 4). With this new capability in hand, the power of using Arabidopsis as a model system to investigate regulation of wall ingrowth deposition in PP TCs has been substantially increased. Chapter 4 of this thesis provides a description of using Arabidopsis for reverse genetics analysis of transcription factors identified from RNA-Seq analysis of epidermal TC development in *V. faba* cotyledons (Chapter 3) as putative regulators of wall ingrowth deposition in plant TCs.

## 1.7 AIMS AND HYPOTHESES

A major deficiency in understanding of TC biology is the identity and function of transcription factors which initiate the *trans*-differentiation of TCs and co-ordination of wall ingrowth deposition. The major focus of this thesis therefore is centred on undertaking molecular and genetic studies to identify such transcription factors. Two experimental systems to study TC development will be used for this task, namely development of epidermal TCs in cotyledons of *V. faba* and PP TCs in leaf minor veins in Arabidopsis. Both experimental systems provide unique attributes for both “targeted” and “non-targeted” strategies to identify hypothesized transcriptional regulators of TC development. The “Non-targeted” strategy will be undertaken employing RNA-Seq to profile transcriptional changes occurring during wall ingrowth deposition in epidermal TCs of *V. faba* cotyledons. Recent developments in *de novo* assembly of transcriptomes in non-model plants lacking genome information has paved the way for using RNA-Seq for transcript profiling (Garg et al., 2011a; Thiel et al., 2012a). NGS platforms like Illumina and 454 Sequencing have been successfully employed to perform *de novo* transcriptomics of non-model crop species such as chick pea (Garg et al., 2011a) and transcriptome sequencing of ETC in barley (Thiel et al., 2012a), respectively (although it is noted here that the barley genome was published later in the November 29, 2012 issue of *Nature* 491: 711-716, by The International Barley Genome Sequencing Consortium). Hence, *de novo* assembly can be used in combination with RNA-Seq to identify master transcriptional regulators of TC development, which ultimately may lead

to improved crop yields by targeting manipulation of TC development. The aims of this projects are as follows.

**Aim 1:** Generation of a genome-wide transcriptome map of *V. faba* using Illumina Next Generation Sequencing.

**Aim 2:** Identify potential transcription factors regulating wall ingrowth development by RNA-Seq analysis of adaxial epidermal TC development in *V. faba* cotyledons.

**Aim 3:** To investigate identified transcription factors as potential candidates regulating wall ingrowth deposition in PP TCs in Arabidopsis by phenotypic screening.

In Chapter 2 (Aim 1), a genome wide *de novo* transcriptome map of *V. faba* was generated from total RNA extracted from vegetative and reproductive tissue of plants at different stages of development along with cotyledons cultured to induce adaxial epidermal TC development. The transcriptome map was validated by comparison to *V. faba* cDNAs submitted to GenBank and unpublished cDNAs for three *VfCesA* genes. The goal of this exercise was to provide a transcriptome map for subsequent RNA-Seq analysis of epidermal TC development. A description of this work was published in *Frontiers in Plant Science* (Arun-Chinnappa & McCurdy, 2015), and Chapter 2 comprises the submitted manuscript plus additional unpublished material associated with this work.

Chapter 3 (Aim 3) describes an RNA-Seq analysis of transcriptional changes accompanying epidermal TC development in *V. faba* cotyledons. Total RNA was isolated from epidermal tissue and storage parenchyma harvested from cotyledons cultured for 0, 3, 9 and 24 h to induce epidermal TC development. Transcripts characterized as showing epidermal-specific or epidermal-enhanced transcriptional changes across epidermal TC development were identified, including a sub-set of transcription factors exceeding threshold values deemed as showing epidermal-specific expression and thus possibly functioning as transcriptional regulators of TC development. These expression characteristics were confirmed by qRT-PCR. A manuscript describing this RNA-Seq analysis and the possible involvement of the identified transcription factors in regulating TC development has been submitted to *Frontiers in Plant Science* (20.03.2016) and under review as on 30.03.2016, and Chapter 3 comprises the submitted manuscript plus additional unpublished material associated with this study.

Chapter 4 describes attempts to verify a role for the transcription factors identified from the RNA-Seq analysis by performing phenotyping of T-DNA insertional mutants in Arabidopsis of orthologous genes. Arabidopsis orthologues of the *V. faba* transcription factors were identified and relevant T-DNA insertional mutants for these genes were sourced from ABRC and NASC. In most instances double mutants of the orthologous gene and its paralog in the Arabidopsis genome were examined by confocal microscopy of propidium-iodide-stained leaves to determine effects on wall ingrowth deposition in PP TCs of minor veins. From this analysis of some 10 Arabidopsis transcription factors in total, no disrupted wall ingrowth phenotypes were identified, possibly due to additional gene redundancy effects, incomplete gene knockout in the mutants or lack of orthologous function between the *V. faba* gene and its Arabidopsis ortholog.

Chapter 5 provides a summary of the research undertaken in this thesis, the significance of the outcomes in providing new genes to investigate as possible transcriptional regulators of TC development, and future directions to build on this research in both *V. faba* and Arabidopsis to eventually build a more complete understanding of TC biology in plants and this understanding might be utilized to improve crop productivity in agriculture.

**CHAPTER 2**

***DE NOVO* ASSEMBLY OF A GENOME-WIDE  
TRANSCRIPTOME MAP OF *Vicia faba* (L.)  
FOR TRANSFER CELL RESEARCH**

## 2.1 OVERVIEW

The aim of this chapter was to generate a *de novo* transcriptome map of *Vicia faba* that can be used for transfer cell research. The genome of the grain legume *V. faba* is extremely large (~13000 Mb; Kaur et al., 2012) and consequently has not been sequenced to this point. Hence, a transcriptome map of *V. faba* sequences was generated using NGS (Next Generation Sequencing) techniques. This transcriptome map would then be used as a reference to discover TC-specific transcription factors revealed by RNA-Seq analysis as likely candidates functioning as transcriptional regulators of TC development.

This Chapter consists of a published paper (pdf) describing *de novo* construction of a transcriptome map from *V. faba*. In addition, Appendix 2 included in this chapter describes additional unpublished validation of the transcriptome map using sequenced *V. faba Cesa* genes.

Details of the published manuscript from this chapter are as follows:

Arun-Chinnappa, K.S., McCurdy, D.W. (2015). *De novo* assembly of a genome-wide transcriptome map of *Vicia faba* (L.) for transfer cell research. *Frontiers in Plant Science* **6**: 217. Doi: 10.3389/fpls.2015.00217

# ***De novo* assembly of a genome-wide transcriptome map of *Vicia faba* (L.) for transfer cell research**

Kiruba Shankari Arun-Chinnappa and David W. McCurdy\*

Centre for Plant Science, School of Environmental and Life Sciences, The University of Newcastle, Callaghan, NSW 2308, Australia.

\*Correspondence: David W. McCurdy, School of Environmental and Life Sciences, The University of Newcastle, Callaghan, NSW 2308, Australia

## **Abstract**

*Vicia faba* (L.) is an important cool-season grain legume species used widely in agriculture but also in plant physiology research, particularly as an experimental model to study transfer cell (TC) development. TCs are specialized nutrient transport cells in plants, characterized by invaginated wall ingrowths with amplified plasma membrane surface area enriched with transporter proteins that facilitate nutrient transfer. Many TCs are formed by *trans*-differentiation from differentiated cells at apoplasmic/symplasmic boundaries in nutrient transport. Adaxial epidermal cells of isolated cotyledons can be induced to form functional TCs, thus providing a valuable experimental system to investigate genetic regulation of TC *trans*-differentiation. The genome of *V. faba* is exceedingly large (ca. 13 Gb), however, and limited genomic information is available for this species. To provide a resource for future transcript profiling of epidermal TC differentiation, we have undertaken *de novo* assembly of a genome-wide transcriptome map for *V. faba*. Illumina paired-end sequencing of total RNA pooled from different tissues and different stages, including isolated cotyledons induced to form epidermal TCs, generated 69.5M reads, of which 65.8M were used for assembly following trimming and quality control. Assembly using a De-Bruijn graph-based approach generated 21,297 contigs, of which 80.6% were successfully annotated against GO terms. The assembly was validated against known *V. faba* cDNAs held in GenBank, including transcripts previously identified as being specifically expressed in epidermal cells across TC *trans*-differentiation. This genome-wide transcriptome map therefore provides a valuable tool for future transcript profiling of epidermal TC *trans*-differentiation, and also enriches the genetic resources available for this important legume crop species.

## INTRODUCTION

The introduction of RNA sequencing (RNA-Seq) has widened the use of plant species for molecular genetic analyses beyond those for which full genome sequences are available. *De novo* assembly of transcriptomes from such species has enabled gene discovery and marker identification in a wide variety of non-genome-sequenced agricultural species such as common wheat (Duan et al., 2012), peanut (Zhang et al., 2012) and rubber tree (Mantello et al., 2014), but especially in crop legumes such as pea (Franssen et al., 2011), yellow lupin (Parra-González et al., 2012), lentils (Verma et al., 2013) and chick pea (Garg et al., 2011a, 2011b), which are important to agriculture but genetic studies have been limited due to their often large genomes. In combination with *de novo* assembly of novel transcriptomes, RNA-Seq provides a platform for transcript profiling in these non-annotated species, thus enabling a deeper understanding at the transcriptional level of diverse but little studied biological processes in plants, such as fiber development in ramie (*Boehmeria nivea* L.; Chen et al., 2014), cell wall synthesising enzymes in paper mulberry (Xianjun et al., 2014), biomass production in *Panicum hallii* (Meyer et al., 2012) and plant sex determination in cucumber (Guo et al., 2010).

*Vicia faba* (L.) is an important cool-season grain legume species used widely for human nutrition, fodder for livestock and as a rotation crop for nitrogen replenishment of soils (Torres et al., 1993; El-Rodeny et al., 2014). In addition to its importance as a crop species worldwide, *V. faba* is also widely used in plant physiology research to study such processes as guard cell dynamics in leaves (Fukuda et al., 1998; Fellè et al., 2000), transport processes in phloem (Thorpe et al., 2010; Hafke et al., 2013), and importantly for this study, transfer cell (TC) development in cotyledons (Offler et al., 2003). In the latter case, when isolated cotyledons are placed in culture, adaxial epidermal cells *trans*-differentiate to become functional epidermal TCs (Farley et al., 2000; Dibley et al., 2009). This cotyledon culture system has been used extensively to investigate the development and composition of the reticulate wall ingrowth network that defines TC identity in these cells (Talbot et al., 2001, 2007a, 2007b; Vaughn et al., 2007), in addition to defining the role of inductive signals such as sugars (Wardini et al., 2007), auxin (Dibley et al., 2009), ethylene (Zhou et al., 2010; Andriunas et al., 2011), reactive oxygen species (Andriunas et al., 2012; Xia et al., 2012) and calcium (Zhang et al., 2014) in polarized wall ingrowth deposition in these cells. In an initial study to analyse transcriptional changes occurring across induction and development of adaxial epidermal TCs in cultured cotyledons,

Dibley et al. (2009) used cDNA-amplified fragment length polymorphism (AFLP) to detect 5795 transcript-derived fragments (TDFs), of which 264 showed epidermal-specific changes in expression. However, due to the limited capacity of cDNA-AFLP for high-throughput analysis, only 112 TDFs from this cohort of 264 were sequenced to provide a glimpse of the diversity of genes involved in signalling, metabolism, cell division, vesicle trafficking and cell wall biosynthesis putatively involved in TC *trans*-differentiation (Dibley et al., 2009). Importantly, however, this study estimated that TC formation in this system may involve differential expression of approximately 650 different genes (Dibley et al., 2009), a total approaching the minimum 815 genes determined by a 12K microarray analysis to be differentially expressed during nucellar projection and endosperm TC development in barley grains (Thiel et al., 2008).

To exploit the advantages offered by next-generation sequencing, RNA-Seq is being used to identify transcription factors putatively involved in regulating the substantial transcriptional changes occurring during adaxial epidermal TC *trans*-differentiation in *V. faba* cotyledons. The genome size of *V. faba* is estimated to be approximately 13 Gb (Kaur et al., 2012), one of the largest described to date for crop legumes, thus making this species an unattractive target for genome sequencing but nonetheless compatible for *de novo* transcriptome assembly (Kaur et al., 2012). In this communication, we report *de novo* assembly of a genome-wide transcriptome map of *V. faba* using Illumina-based 100 bp paired-end sequencing. Total RNA was isolated from diverse tissues and organs of *V. faba*, including isolated cotyledons induced to form epidermal TCs. Therefore, this genome-wide transcriptome database would be expected to contain genes involved in the *trans*-differentiation of epidermal TCs in *V. faba* cotyledons, and thus provide a reference transcriptome map suitable for transcript profiling of this process by RNA-Seq.

## **MATERIALS AND METHODS**

### **PLANT GROWTH AND HARVESTING**

*Vicia faba* L. (cv. Fiord) plants were grown in environmentally-controlled glasshouse conditions as previously described (Farley et al., 2000). To survey *V. faba* transcripts, selected tissues were harvested from flowering plants including expanding and fully expanded leaves, elongating and fully elongated stems and closed and open flowers. Whole roots including root hairs were isolated from 10-day old seedlings germinated on

filter paper. At least three independent biological samples of each tissue type were harvested and snap frozen in liquid nitrogen. To enrich the transcriptome with genes involved in induction and wall ingrowth deposition in epidermal TCs, isolated cotyledons cultured for 0, 3, 9 and 24 h were also sampled. For this process, *V. faba* cotyledons (100-120 mg FW) were removed from pods and either fixed immediately ( $t = 0$  h) in ice-cold ethanol:acetic acid (3:1 v/v) for 1 h, or placed adaxial surface down on filter paper soaked in Murashige and Skoog medium (MS; Sigma Australia) in Petri dishes (Dibley et al., 2009). The Petri dishes were sealed with tape and incubated in darkness at 22°C for 3, 9 or 24 h, then the cotyledons were fixed in ice-cold ethanol:acetic acid as described above. Fixation of cotyledons in this manner was used to rapidly inhibit RNA degradation (see Dibley et al., 2009). Fixed cotyledons were rinsed briefly in distilled water and snap frozen in liquid nitrogen and stored at -80°C before isolation of total RNA.

#### **TOTAL RNA ISOLATION AND cDNA LIBRARY PREPARATION**

Total RNA was extracted independently from each batch of isolated organs/tissues (harvested as described above) using an RNeasy Plant RNA isolation kit (Qiagen) incorporating on-column DNA digestion. For transcriptome assembly, up to 1 µg of total RNA from each organ/tissue sample type was pooled to achieve 20 µg in total, of which at least 4 µg was derived from cultured cotyledon tissue. The pooled total RNA was subjected to QA analysis using an Agilent 2100 Bioanalyzer. A single cDNA library for 100-bp paired-end sequencing was constructed from this pooled total RNA using the Illumina TrySeq Library kit and sequencing was performed using the Illumina HiSeq-2000 platform. QA analysis, library construction and sequencing were performed by the Beijing Genome Institute (Hong Kong).

#### **DE NOVO ASSEMBLY OF CONTIGS**

Illumina sequencing generated 69,543,694 100-bp paired-end reads from the pooled total RNA used for transcriptome assembly. Sequence filtering was performed by trimming adapter sequences, excluding low quality reads and ribosomal-derived reads and removing the last 10 bases from the 3' end of each read to increase sequence confidence. The resulting 65,795,198 90-bp reads were then assembled using a De-Bruijn graph-based *de novo* assembly program in CLC Genomics Workbench 6.1 run on an Intel®

Xeon<sup>®</sup> workstation with 64 Gb RAM. Word size (*k*-mer) and bubble size were varied to obtain optimum *de novo* assembled contigs (Henkel et al., 2012), based on assembly output parameters such as high N50, low total number of contigs, high average contig length and high percentage of mapped reads (Garg et al., 2011a; Annadurai et al., 2012).

## **VALIDATION OF *DE NOVO* ASSEMBLED CONTIGS**

The optimum assembly (*47x300* – see Results) derived from comparing *k*-mer and bubble size was used to create a BLAST database in CLC Genomics Workbench 6.1. Contig validation using 32 full-length *V. faba* cDNA sequences from GenBank was then performed by executing a BLASTN search for each cDNA against the *47x300* assembly and choosing the top two contigs with highest bit scores (Mizrachi et al., 2010). The outcome of BLASTN alignment parameters for each of the 32 cDNAs with their best hit contig was assessed for validating the contigs derived from the *47x300* assembly.

## **FUNCTIONAL ANNOTATION**

Contigs derived from the *47x300* assembly were functionally annotated by BLASTX analysis against both the Viridiplantae and *Arabidopsis* databases using default parameters in CLC Genomics Workbench 6.1. The BLASTX output files from both searches were then used to assign the three GO terms of Biological Process (BP), Molecular Function (MF) and Cellular Component (CC) separately using the Blast2GO plugin in CLC Genomics Workbench 6.1 (Conesa et al., 2005). The annotations from both datasets were merged to yield at least one annotation for most of the contigs. The “GO slim” routine in Blast2GO was performed on the merged annotation dataset in order to merge specific GO terms into higher-order generic terms for each contig. This merging eases the process of creating a “combined graph”, which is a directed acyclic graph (DAG) that summarizes the functional relationship within and between all three GO terms (BP, MF, CC) using Blast2GO (Conesa et al., 2005; Gotz et al., 2008).

## RESULTS

### GENERATION OF A *DE NOVO*-ASSEMBLED, GENOME-WIDE TRANSCRIPTOME MAP OF *V. FABA*

To construct a genome-wide transcriptome map of *V. faba*, total RNA was isolated from all major organs across different stages of development, including isolated cotyledons cultured for 0, 3, 9 and 24 h (see Material and Methods). Illumina sequencing of this pooled total RNA yielded approximately 69.5 M paired-end reads, and after sequence filtering and quality control, a total of nearly 65.8 M 90-bp paired-end reads were used for *de novo* assembly using CLC Genomics Workbench 6.1 (see Materials and Methods). *De novo* assembly was optimized by comparing word size (*k*-mer) and bubble size on assembly outcomes (Henkel et al., 2012). From 24 different assemblies (see **Supplementary Table 1**), assembly *47x300* (*k*-mer 47, bubble size 300) was chosen based on the maximum number of optimum parameters such as high N50 value (1,245), low total number of contigs (21,297), high values for both longest contig length (10,528) and percentage of mapped reads (82%) contributing to the assembly (see **Table 1**; Garg et al., 2011a; Annadurai et al., 2012; Henkel et al., 2012; Dorn et al., 2013). The parameter Reads Mapped Back to Transcripts (RMBT) is an indication of completeness of assembly for *de novo* assembled transcripts (Moreton et al., 2014), and assembly *47x300* returned a high score of 82% (see **Table 1**). This assembly was chosen in preference to assembly *20x300* due to the latter's low value for percentage mapped reads (see **Supplementary Table 1**). Furthermore, a *k*-mer value of 47 is consistent with previous studies using value as an optimum word size for *de novo* transcriptome assembly in other non-sequenced species such as chick pea (*Cicer arietinum*; Garg et al., 2011a) and insulin plant (*Costus pictus*; Annadurai et al., 2012). Contig length in assembly *47x300* varied from 432 bp to 10,528 bp, with an average of 1,114 bp. Contig number decreased with increasing contig length, with the majority of assembled contigs belonging to the size range 500-800 bp and >1500 bp (see **Figure 1**), while total reads mapped per contig ranged from 33 to 1,015,710 with an average of 2,528 (see **Table 2**). A majority of the reads were mapped to assembled contigs greater than 1,500 bp length, with the least amount of reads mapping to contigs of 400-600 bp (see **Table 2**). The contigs making up assembly *47x300* have been submitted to the Cool Season Food Legume Genome Database ([www.coolseasonfoodlegume.org](http://www.coolseasonfoodlegume.org)), while the 69.5 M paired-end raw reads have been submitted to SRA (NCBI) under the accession number SRP055969.

## VALIDATION OF THE GENOME-WIDE TRANSCRIPTOME MAP

To assess the validity of assembly *47x300*, 32 full-length *V. faba* cDNAs available in GenBank at the time of analysis were compared by BLASTN against the 21,297 contigs that make up assembly *47x300*. Of this cDNA collection, ranging in length from 259 to 3,426 bp, 29 cDNAs returned matches of 97-100% identity, while only three returned matches between 90-94% (see **Table 3**). This result indicates that the assembled contig closely matched the relevant cDNA across the length of the transcript-derived contig. Several of the cDNAs that best aligned to contigs in assembly *47x300* corresponded to *V. faba* cDNAs previously shown to have putative roles in signaling epidermal TC *trans*-differentiation (see **Table 3**; Zhou et al., 2010; Andriunas et al., 2012). For example, three ethylene response factor genes (*VfERF1-3*; Zhou et al., 2010), and two putative respiratory burst oxidase homologue genes (*VfrbohA*, *VfrbohC*; Andriunas et al., 2012), each of which shows epidermal-specific change in expression accompanying the *trans*-differentiation of epidermal TCs, all matched with 98-100% identity across corresponding contig sequence coverage present in assembly *47x300* (see **Table 3**).

## FUNCTIONAL ANNOTATION OF CONTIGS

Functional annotation was undertaken to assign GO terms to the 21,297 contigs comprising assembly *47x300*. BLASTX analysis in CLC Genomics Workbench yielded 20,325 and 20,052 annotation hits when compared against the Viridiplantae and *Arabidopsis* data sets, respectively. The Blast2GO plugin in CLC successfully annotated 12,192 and 15,794 contigs from the Viridiplantae and *Arabidopsis* datasets, respectively, and thus merging these two annotation datasets (Garg et al., 2011a) yielded at least one annotation term for 17,160 (80.6%) of the 21,297 contigs in *47x300*. This total of 80.6% is comparable to annotation statistics for *de novo* assemblies from other non-sequenced species, or yet to be sequenced at the time of experimentation, such as chick pea (85.5%; Garg et al., 2011a), eucalyptus (*Eucalyptus grandis* - 83.2%; Mizrachi et al., 2010), insulin plant (69.2%; Annadurai et al., 2012), sesame (*Sesamum indicum* - 54.0%; Wei et al., 2011) and sweet potato (*Ipomoea batatas* - 62.0%; Wang et al., 2010). As expected, *V. faba* transcripts compared against the Viridiplantae database by BLASTX showed highest similarity to closely related legume species for which full genome sequences are

now available, with *Cicer arietinum* (chick pea, 47%) and *Medicago truncatula* (38%) genes accounting for 47% and 38% of the annotated hits, respectively (see **Figure 2**).

The 17,160 annotated contigs (herein referred to as unigenes) were assigned GO terms in three categories, namely Biological Process, Molecular Function and Cellular Component (see **Figure 3**). Within Biological Process, the category “Response to different stress and stimulus”, which incorporates biotic, abiotic, endogenous and extracellular, was highly represented (25%) followed by “Metabolic process” (13%). Within Molecular Function, processes like “Nucleotide binding” (34%), “Transcriptional regulation and DNA binding” (14%), and “Kinase activity” (14%) were dominant in this category. Similarly, Cellular Component was highly represented by “Plasma membrane” (21%) followed by “Plastid” (20%) subgroups.

Analysis of the annotated data set showed that 726 unigenes (4.2% of 17,160 in total) were identified as coding for putative transcription factors based on the GO term 0003700 (Transcription factor activity) appearing in the output for Molecular Function category. Of this total, 376 could be assigned to 31 of the 58 families of known plant transcription factors identified in PlnTFDB (see **Figure 4**; Perez-Rodriguez et al., 2009). A similar representation of plant transcription factor families has been observed in *de novo* assembled transcriptomes from chick pea (Garg et al., 2011b), soybean (Schmutz et al., 2010) and other legumes (Libault et al., 2009). Of those unigenes assigned to the 31 families, 19% were classified as homeobox transcription factors, with WRKY and AP2-EREBP genes making up the next most prominent families at 8% each.

## DISCUSSION

We have generated a genome-wide transcriptome map of *V. faba* to provide a reference for subsequent RNA-Seq-based transcript profiling of transfer cell development. Despite the large genome size of this important crop legume (ca. 13 Gb; Kaur et al., 2012), the paired-end strategy using Illumina sequencing was successful in generating 21,297 contigs, of which 80.6% (17,160) could be annotated against GO terminology. The total number of gene loci in *V. faba* is not known, but the 17,160 unigenes identified in this study may represent at least half of the gene space in faba bean given the number of genes identified in flowering plants (~27,000-39,000; TAIR10 – [www.arabidopsis.org](http://www.arabidopsis.org); Rice Genome Annotation Project – [www.rice.plantbiology.msu.edu](http://www.rice.plantbiology.msu.edu)). This argument is based in part on a similar study by Lehnert and Walbot (2014) who reported that their *de novo*

assembly of 20,881 contigs from *Dahlia* may represent about half the gene loci in this species, which has a genome of approximately 9.4 Gb.

Validation of the *47x300* assembly against full-length *V. faba* cDNAs in GenBank established that the CLC assembly routine using a De-Bruijn graph-based approach gave 97-100% identity for 29 out of the 32 cDNAs tested across an average “Hit length” of 1,157 bp, thus providing high confidence that the *47x300* assembly accurately reflects the component of the *V. faba* transcriptome captured by the sequencing strategy. Furthermore, the value of the transcriptome map as a resource for future transcript profiling of TC *trans*-differentiation is indicated by the presence of several transcripts, such as three ethylene response factor genes (*VfERF1-3*), two respiratory burst oxidase homologues (*VfrbohA*, *VfrbohC*), two ethylene insensitive transcription factors (*VfEIN3-1*, *VfEIN3-2*), two putative ACC oxidase genes (*VfACO1*, *VfACO2*, and two putative ACC synthase genes (*VfACSI*, *VfACSI*). Each of these genes has been cloned from isolated epidermal tissue, with many displaying epidermal-specific differential expression during the *trans*-differentiation of epidermal TCs (Zhou et al., 2010; Andriunas et al., 2012).

A major aim of our future investigations is to identify transcription factors regulating the *trans*-differentiation of TCs. Annotation of the *47x300* assembly revealed that 4.2% (726) of the 17,160 unigenes encoded putative transcription factors, of which representatives from 31 of the 58 known families of transcription factors in plants were identified. Within this cohort, 19% were identified as homeobox genes, while WRKY and AP2-EREBP members were the next most prominently represented families at 8% each. Homeobox genes are commonly involved in regulating morphogenesis and cell identity, typically via switching on cascades of gene expression (Williams, 1998). WRKY transcription factors are involved in biotic and abiotic stress defense pathways in plants (Rushton et al., 2010), and members of the AP2-EREBP family have roles in stress signaling pathways induced by hormones like ethylene and methyl jasmonate (Dietz et al., 2010). Given that the *trans*-differentiation of TCs involves differential expression of many hundreds of genes (Thiel et al., 2008; Dibley et al., 2009) in response to biotic (Cabrera et al., 2014) and abiotic stresses that can involve ethylene (Zhou et al., 2010) and methyl jasmonate (Amiard et al., 2007), the diverse representation of transcription factors in this transcriptome map augers well as a reference tool to identify key transcriptional regulators of TC *trans*-differentiation.

Overall, these considerations support the conclusion that assembly *47x300* represents a high-quality, genome-wide transcriptome map of *V. faba* and thus provides a validated platform for subsequent transcript profiling of TC *trans*-differentiation by RNA-Seq.

## ACKNOWLEDGEMENTS

This project was supported by a University of Newcastle Faculty of Science and Information Technology Strategic Research Initiative Grant. KSAC was supported by UNIPRS and UNRS Scholarships. We thank Joe Enright for valuable assistance with plant growth.

## SUPPLEMENTARY MATERIAL

The Supplementary Material for this article can be found online at: <http://www.frontiersin.org/journal/> .....

## REFERENCES

- Amiard, V., Demmig-Adams, B., Mueh, K. E., Turgeon, R., Combs, A. F., and Adams, W. W. (2007). Role of light and jasmonic acid signaling in regulating foliar phloem cell wall ingrowth development. *New Phytol.* 173, 722-731. doi: 10.1111/j.1469-8137.2006.01954.x
- Andriunas, F. A., Zhang, H. M., Weber, H., McCurdy, D. W., Offler, C. E., and Patrick, J. W. (2011). Glucose and ethylene signalling pathways converge to regulate *trans*-differentiation of epidermal cells in *Vicia narbonensis* cotyledons. *Plant J.* 68, 987-998. doi: 10.1111/j.1365-313X.2011.04749.x
- Andriunas, F. A., Zhang, H. M., Xia, X., Offler, C. E., McCurdy, D. W., and Patrick, J. W. (2012). Reactive oxygen species form part of a regulatory pathway initiating *trans*-differentiation of epidermal transfer cells in *Vicia faba* cotyledons. *J. Exp. Bot.* 63, 3617-3629. doi: 10.1093/jxb/ers029
- Annadurai, R. S., Jayakumar, V., Mugasimangalam, R. C., Katta, M. A., Anand, S., Gopinathan, S., et al. (2012). Next generation sequencing and de novo transcriptome analysis of *Costus pictus* D. Don, a non-model plant with potent anti-diabetic properties. *BMC Genomics* 13:663. doi: 10.1186/1471-2164-13-663

- Cabrera, J., Barcala, M., Fenoll, C., and Escobar, C. (2014). Transcriptomic signatures of transfer cells in early developing nematode feeding cells of *Arabidopsis* focused on auxin and ethylene signaling. *Front. Plant Sci.* 5:107. doi: 10.3389/fpls.2014.00107
- Chen, J., Pei, Z., Dai, L., Wang, B., Liu, L., An, X., et al. (2014). Transcriptome profiling using pyrosequencing shows genes associated with bast fiber development in ramie (*Boehmeria nivea* L.). *BMC Genomics* 15:919. doi:10.1186/1471-2164-15-919
- Conesa, A., Gotz, S., Garcia-Gomez, J. M., Terol, J., Talon, M., and Robles, M. (2005). Blast2GO: a universal tool for annotation, visualization and analysis in functional genomics research. *Bioinformatics* 18, 3674-3676. doi: 10.1093/bioinformatics/bti610
- Dibley, S. J., Zhou, Y., Andriunas, F. A., Talbot, M. J., Offler, C. E., Patrick, J. W., et al. (2009). Early gene expression programs accompanying *trans*-differentiation of epidermal cells of *Vicia faba* cotyledons into transfer cells. *New Phytol.* 182, 863-877. doi: 10.1111/j.1469-8137.2009.02822.x.
- Dietz K. J., Vogel M. O., and Viehhauser A. (2010). AP2/EREBP transcription factors are part of gene regulatory networks and integrate metabolic, hormonal and environmental signals in stress acclimation and retrograde signalling. *Protoplasma* 245, 3-14. doi: 10.1007/s00709-010-0142-8
- Dorn, K. M., Fankhauser, J. D., and Marks, M. D. (2013). *De novo* assembly of the pennycress (*Thalasspi arvense*) transcriptome provides tools for the development of a winter cover crop and biodiesel feedstock. *Plant J.* 75, 1028-1038. doi: 10.1111/tpj.12267
- Duan, J., Xia, C., Zhao, G., Jia, J., and Kong, X. (2012). Optimizing *de novo* common wheat transcriptome assembly using short-read RNA-Seq data. *BMC Genomics* 13:392. doi: 10.1186/1471-2164-13-392
- El-Rodeny, W., Kimura, M., Hirakawa, H., Sabah, A., Shirasawa, K., Sato, S., et al. (2014). Development of EST-SSR markers and construction of a linkage map in faba bean (*Vicia faba*). *Breeding Sci.* 64, 252-263. doi: 10.1270/jsbbs.64.252

- Farley, S. J., Patrick, J. W., and Offler, C. E. (2000). Functional transfer cells differentiate in cultured cotyledons of *Vicia faba* L. seeds. *Protoplasma* 214, 102-117. doi: 10.1007/BF02524267.
- Fellè, H. H., Hanstein, S., Steinmeyer, R., and Hedrich, R. (2000). Dynamics of ionic activities in the apoplast of the sub-stomatal cavity of intact *Vicia faba* leaves during stomatal closure evoked by ABA and darkness. *Plant J.* 24, 297-304. doi: 10.1046/j.1365-313x.2000.00878.x
- Franssen, S. U., Shrestha, R. P., Brautigam, A., Bornberg-Bauer, E., and Weber A. P. M. (2011). Comprehensive transcriptome analysis of the highly complex *Pisum sativum* genome using next generation sequencing. *BMC Genomics* 12:227. doi: 10.1186/1471-2164-12-227
- Fukuda, M., Hasezawa, S., Asai, N., Nakajima, N., and Kondo, N. (1998). Dynamic organization of microtubules in guard cells of *Vicia faba* L. with diurnal cycle. *Plant Cell Physiol.* 39, 80–86.
- Garg, R., Patel, R. K., Tyagi, A. K., and Jain, M. (2011a). De novo assembly of chickpea transcriptome using short reads for gene discovery and marker identification. *DNA Research* 18, 53-63. doi: 10.1093/dnares/dsq028
- Garg, R., Patel, R. K., Jhanwar, S., Priya, P., Bhattacharjee, A., Yadav, G., Bhatia, S., Chattopadhyay, D., Tyagi, A. K., Jain, M. (2011b). Gene discovery and tissue-specific transcriptome analysis in chickpea with massively parallel pyrosequencing and web resource development. *Plant Physiol.* 156, 1661–1678. doi: 10.1104/pp.111.178616
- Gotz, S., Garcia-Gomez, J. M., Terol, J., Williams, T. D., Nagaraj, S. H., Nueda, M. J., et al. (2008). High-throughput functional annotation and data mining with the Blast2GO suite. *Nucl. Acids Res.* 36, 3420-3435. doi: 10.1093/nar/gkn176
- Guo, S. G., Zheng, Y., Joung, J. G., Liu, S. Q., Zhang, Z. H., Crasta, O. R., et al. (2010). Transcriptome sequencing and comparative analysis of cucumber flowers with different sex types. *BMC Genomics* 11:384. doi: 10.1186/1471-2164-11-384
- Hafke, J. B., Höll, S., Kühn, C., and van Bel, A. (2013). Electrophysiological approach to determine kinetic parameters of sucrose uptake by single sieve elements or phloem

- parenchyma cells in intact *Vicia faba* plants. *Front. Plant Sci.* 4:274. doi: 10.3389/fpls.2013.00274
- Henkel, C. V., Dirks, R. P., and De Wijze, D. L. (2012). First draft genome sequence of the Japanese eel, *Anguilla japonica*. *Gene* 511, 195-201. doi: 10.1016/j.gene.2012.09.064
- Kaur, S., Pembleton, L. W., Cogan, N. O., Savin, K. W., Leonforte, T., and Paull, J. (2012). Transcriptome sequencing of field pea and faba bean for discovery and validation of SSR genetic markers. *BMC Genomics* 13:104. doi: 10.1186/1471-2164-13-104
- Lehnert, E.M., and Walbot, V. (2014). Sequencing and *de novo* assembly of a *Dahlia* hybrid cultivar transcriptome. *Front. Plant Sci.* 5:340. doi:10.3389/fpls.2014.00340
- Libault, M., Joshi, T., Benedito, V. A., Xu, D., Udvardi, M. K., and Stacy, G. (2009). Legume transcription factor genes: what makes legumes so special. *Plant Physiol.* 151, 991-1001. doi: 10.1104/pp.109.144105
- Mantello, C. C., Cardoso-Silva, C. B., Da Silva, C. C., De Souza, L. M., Scaloppi Junior, E. J., Goncalves, P. S., et al. (2014). *De novo* assembly and transcriptome analysis of the rubber tree (*Hevea brasiliensis*) and SNP markers development for rubber biosynthesis pathways. *PLoS ONE* 9:e102665. doi: 10.1371/journal.pone.0102665.
- Meyer, E., Logan, T. L., and Juenger, T. E. (2012). Transcriptome analysis and gene expression atlas for *Panicum hallii* var. *filipes*, a diploid model for biofuel research. *Plant J.* 70, 879-890. doi: 10.1111/j.1365-313X.2012.04938.x
- Mizrachi, E., Hefer, C. A., Ranik, M., Joubert, F., and Myburg, A. A. (2010). *De novo* assembled expressed gene catalog of a fast-growing Eucalyptus tree produced by Illumina mRNA-Seq. *BMC Genomics* 11:681. doi: 10.1186/1471-2164-11-681
- Moreton, J., Dunham, S. P., and Emes, R. D. (2014). A consensus approach to vertebrate *de novo* transcriptome assembly from RNA-Seq data: assembly of the duck (*Anas platyrhynchos*) transcriptome. *Front. Genetics* 5:190. doi: 10.3389/fgene.2014.00190

- Offler, C. E., McCurdy, D. W., Patrick, J. W., and Talbot, M. J. (2003). Transfer cells: cells specialized for a special purpose. *Annu. Rev. Plant Biol.* 54, 431-454. doi: 10.1146/annurev.arplant.54.031902.134812
- Parra-González, L., Aravena-Abarzúa, G., Navarro-Navarro, C., Udall, J., Maughan, J., Peterson, L. M., et al. (2012). Yellow lupin (*Lupinus luteus* L.) transcriptome sequencing: molecular marker development and comparative studies. *BMC Genomics* 13:425. doi: 10.1186/1471-2164-13-425
- Perez-Rodriguez, P., Riano-Pachon, D. M., Correa L. G. G., Stefan A., Rensing S. A., Kersten, B., et al. (2009). PlnTFDB: updated content and new features of the plant transcription factor database. *Nucl. Acids Res.* 38:822. doi: 10.1093/nar/gkp805
- Schmutz, J., Cannon, S. B., and Schlueter, J. (2010). Genome sequence of the palaeopolyploid soybean. *Nature* 463, 178-183. doi: 10.1038/nature08670
- Rushton, P. J., Somssich, I. E., Ringler, P., and Shen, Q. J. (2010). WRKY transcription factors. *Trends Plant Sci.* 15, 247-258. doi: 10.1016/j.tplants.2010.02.006
- Talbot, M. J., Wasteneys, G., McCurdy, D. W., and Offler, C. E. (2007a). Deposition patterns of cellulose microfibrils in flange wall ingrowths of transfer cells indicate clear parallels with those of secondary wall thickenings. *Funct. Plant Biol.* 34, 307-313. doi : <http://dx.doi.org/10.1071/FP06273>
- Talbot, M. J., Wasteneys, G., Offler, C. E., and McCurdy, D. W. (2007b). Cellulose synthesis is required for deposition of reticulate wall ingrowths in transfer cells. *Plant Cell Physiol.* 48, 147-158. doi: 10.1093/pcp/pc1046
- Talbot, M. J., Franceschi, V. R., McCurdy, D. W., and Offler, C. E. (2001). Wall ingrowth architecture in epidermal transfer cells of *Vicia faba* cotyledons. *Protoplasma*, 215, 191-203. doi: 10.1007/BF01280314
- Thiel, J., Weier, D., Sreenivasulu, N., Strickert, M., Weichert, N., Melzer, M., et al. (2008). Different hormonal regulation of cellular differentiation and function in nucellar projection and endosperm transfer cells: A microdissection-based transcriptome study of young barley grains. *Plant Physiol.* 148, 1436-1452. doi: <http://dx.doi.org/10.1104/pp.108.127001>

- Thorpe, M. R., Furch, A. C. U., Minchin, P. E. H., Föllner, J., van Bel, A. J. E., and Hafke, J. B. (2010). Rapid cooling triggers forisome dispersion just before phloem transport stops. *Plant Cell Environ.* 33, 259-271. doi: 10.1111/j.1365-3040.2009.02079.x.
- Torres, A. M., Weeden, N. F., and Martin, A. (1993). Linkage among isozyme, RFLP and RAPD markers in *Vicia faba*. *Theor. Appl. Genet.* 85, 937-945. doi: 10.1007/BF00215032
- Vaughn, K. C., Talbot, M. J., Offler, C. E., and McCurdy, D. W. (2007). Wall ingrowths in epidermal transfer cells of *Vicia faba* cotyledons are modified primary walls marked by localized accumulations of arabinogalactan proteins. *Plant Cell Physiol.* 48, 159-168. doi: 10.1093/pcp/pc1047
- Verma, P., Shah, N., and Bhatia, S. (2013). Development of an expressed gene catalogue and molecular markers from the *de novo* assembly of short sequence reads of the lentil (*Lens culinaris* Medik.) transcriptome. *Plant Biotech. J.* 11, 894-905. doi: 10.1111/pbi.12082
- Wang, Z., Fang, B., Chen, J., Zhang, X., and Luo, Z. (2010). *De novo* assembly and characterization of root transcriptome using Illumina paired-end sequencing and development of cSSR markers in sweet potato (*Ipomoea batatas*). *BMC Genomics* 11:726. doi: 10.1186/1471-2164-11-726.
- Wardini, T., Talbot, M. J., Offler, C. E., and Patrick, J. W. (2007). Role of sugars in regulating transfer cell development in cotyledons of developing *Vicia faba* seeds. *Protoplasma* 230, 75-88. doi: 10.1007/s00709-006-0194-y
- Wei, W., Qi, X., Wang, L., Zhang, Y., Hua, W., Li, D., et al. (2011). Characterization of the sesame (*Sesamum indicum* L.) global transcriptome using Illumina paired-end sequencing and development of EST-SSR markers. *BMC Genomics* 12:451 doi: 10.1186/1471-2164-12-451
- Williams, R. (1998). Plant homeobox genes: many functions stem from a common motif. *BioEssays* 20, 280–282.

- Xia, X., Zhang, H-M., Andriunas, F. A., Offler, C. E., and Patrick, J. W. (2012). Extracellular hydrogen peroxide, produced through a respiratory burst oxidase/superoxidedismutase pathway, directs ingrowth wall formation in epidermal transfer cells of *Vicia faba* cotyledons. *Plant Signal. Behav.* 7, 1–4. doi: 10.4161/psb.21320.
- Xianjun, P., Linhong, T., Xiaoman, W., Yucheng, W., and Shihua, S. (2014). *De novo* assembly of expressed transcripts and global transcriptomic analysis from seedlings of the paper mulberry (*Broussonetia kazinoki* x *Broussonetia papyifera*). *PLoS ONE* 9:e97487. doi: 10.1371/journal.pone.0097487
- Zhang, H-M., Imtiaz, M. S., Laver, D. R., McCurdy, D. W., Offler, C. E., van Helden, D. F., and Patrick, J. W. (2014). Polarized and persistent Ca<sup>2+</sup> plumes define loci for formation of wall ingrowth papillae in transfer cells. *J. Exp. Bot.* – in press. doi:10.1093/jxb/eru460
- Zhang, J. A., Liang, S., Duan, J. L., Wang, J., Chen, S. L., Cheng, Z. S., et al. (2012). *De novo* assembly and characterisation of the transcriptome during seed development, and generation of genetic-SSR markers in peanut (*Arachis hypogaea* L.). *BMC Genomics* 13:90. doi: 10.1186/1471-2164-13-90
- Zhou, Y. C., Andriunas, F., Offler, C. E., McCurdy, D. W., and Patrick, J. W. (2010). An epidermal-specific ethylene signal cascade regulates *trans*-differentiation of transfer cells in *Vicia faba* cotyledons. *New Phytol.* 185, 931-943. doi: 10.1111/j.1469-8137.2009.03136.x

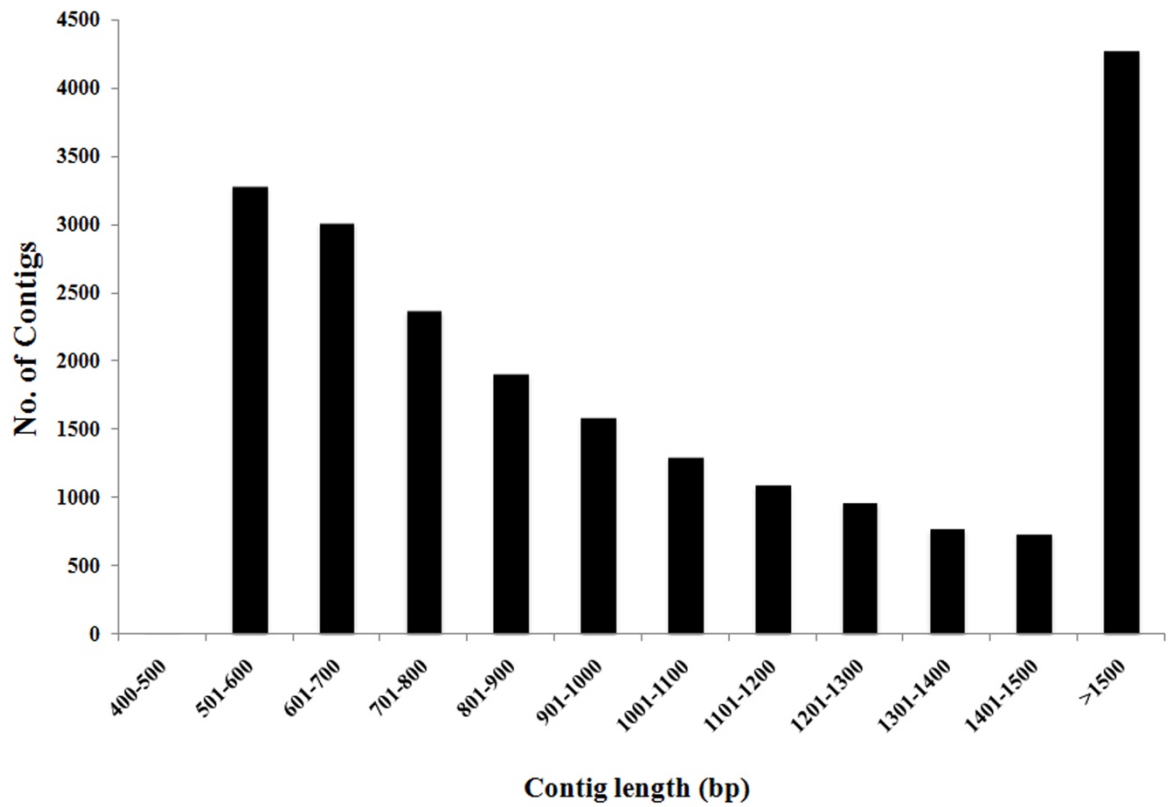


**Figure 1: Distribution of total number of *V. faba* contigs versus contig length.** Most contig lengths were in the range of 500-800 bp (50%) and above 1,500 bp (20%). Total number of contigs decreased as contig length increased.

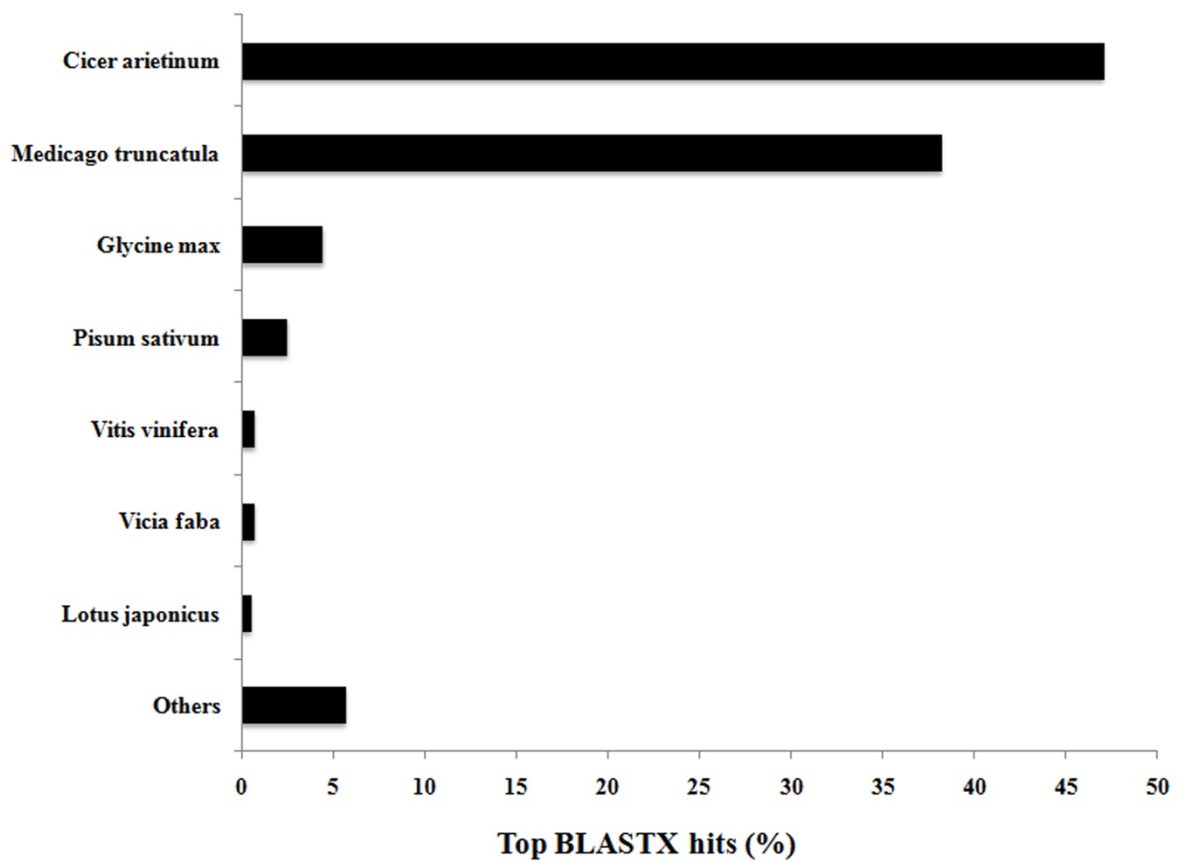


**Figure 2: Top BLASTX hits of *V. faba* contigs against the Viridiplantae database.** Contig sequences of *V. faba* are highly conserved with closely related and sequenced legume species, with 85% of the contigs showing similarity with *Cicer arietinum* (chick pea) and *Medicago truncatula*.

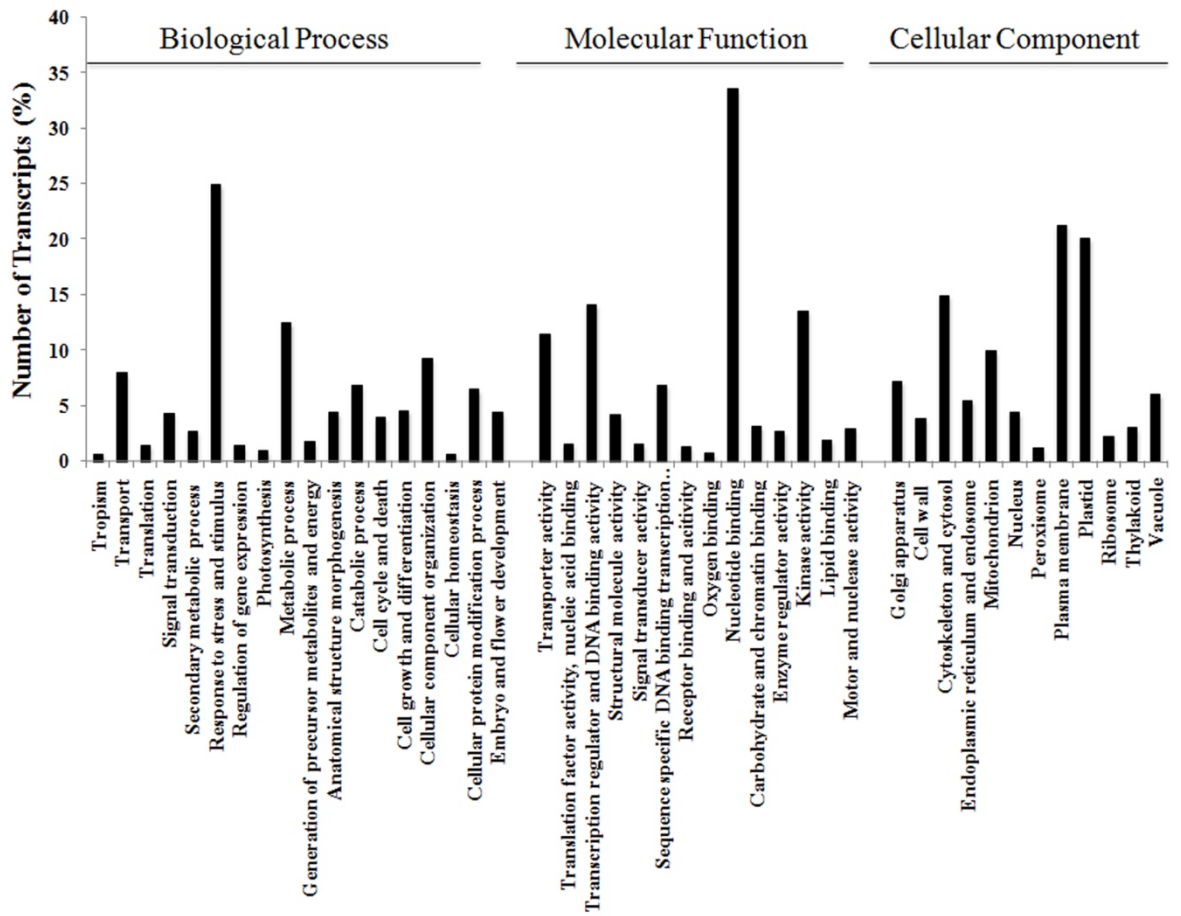


**Figure 3: Functional annotation of *V. faba* contigs.** Blast2GO characterization of GO terms in the three categories of Biological Process, Molecular Function and Cellular Component.

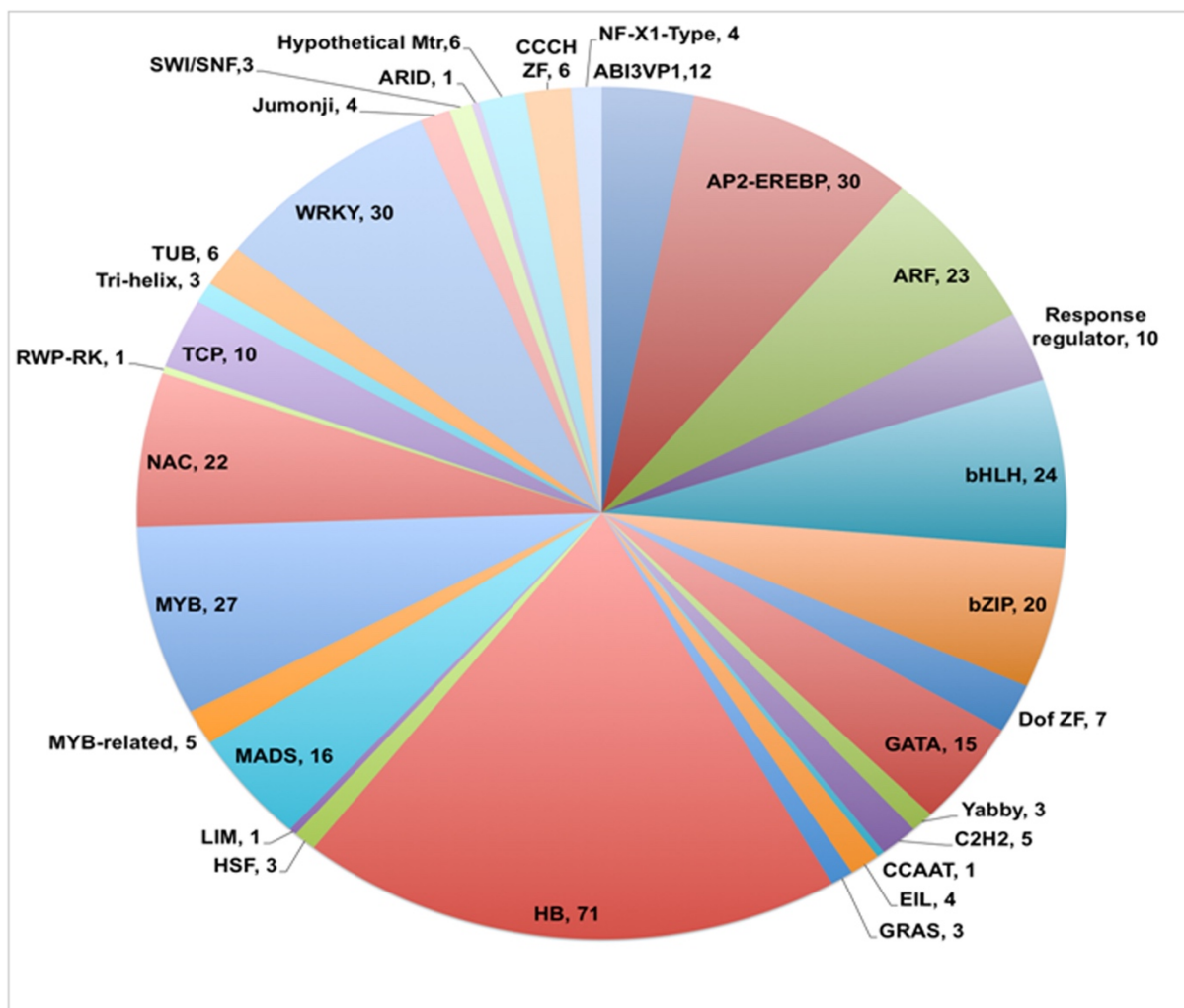


**Figure 4: Distribution of *V. faba* transcripts into different transcription factor families.** Pie chart showing families of transcription factors and total number of transcripts identified for each family. Homeobox family members (HB) contributed 19% of the total transcription factors identified and classified, followed by WRKY (8%) and AP2-EREBP (8%) sequences. The number listed after each family name represents the total number of transcription factors assigned to that family.

---

**Table 1| Statistics of RNA-Seq and *de novo* assembly (47x300) of *Vicia faba* transcriptome map.**

---

|                                    |            |
|------------------------------------|------------|
| Total number of filtered reads     | 65,795,198 |
| Reads used for assembling contigs  | 53,838,233 |
| Total number of contigs            | 21,297     |
| N50 (bp)                           | 1,245      |
| Average contig length (bp)         | 1,114      |
| Longest contig length (bp)         | 10,528     |
| Mapped reads (%)                   | 82         |
| Average number of reads per contig | 2,528      |

---

**Table 2 | Statistics of mapped reads assembled into contigs in assembly 47x300**

| Contig length<br>(bp) | Average total<br>read count | Total read count |         |
|-----------------------|-----------------------------|------------------|---------|
|                       |                             | Lowest           | Highest |
| 400-500               | 546                         | 55               | 1633    |
| 501-600               | 803                         | 33               | 401177  |
| 601-700               | 1471                        | 39               | 883766  |
| 701-800               | 1289                        | 53               | 135973  |
| 801-900               | 1774                        | 62               | 320721  |
| 901-1000              | 1759                        | 79               | 381139  |
| 1001-1100             | 2288                        | 101              | 425383  |
| 1101-1200             | 2229                        | 104              | 74043   |
| 1201-1300             | 2988                        | 162              | 552613  |
| 1301-1400             | 2642                        | 196              | 185390  |
| 1401-1500             | 3371                        | 207              | 502245  |
| >1500                 | 5793                        | 172              | 1015710 |

**Table 3 | BLASTN output for 32 full-length *Vicia faba* cDNAs assessed against assembly 47x300.**

| <b>GeneBank entry<br/>(Accession number)</b>                                 | <b>Hit<br/>length<br/>(bp)</b> | <b>Query<br/>length<br/>(bp)</b> | <b>Length<br/>coverage<br/>(%)</b> | <b>Identity<br/>%</b> |
|--|--------------------------------|----------------------------------|------------------------------------|-----------------------|
| UDP glucose D fructose 2 glycosyl transferase mRNA (M97551)                  | 1721                           | 2665                             | 64                                 | 99                    |
| VHA2 mRNA for P-type H <sup>+</sup> -ATPase (AB022442)                       | 3277                           | 3398                             | 96                                 | 99                    |
| Glutamate decarboxylase (JX444699)   | 1625                           | 1787                             | 91                                 | 99                    |
| Putative ABA induced guard cell protein ABG1 mRNA (AF218806)                 | 648                            | 753                              | 86                                 | 99                    |
| Pre-pro cysteine proteinase VFCYSPRO mRNA (U59465)                           | 1435                           | 1439                             | 100                                | 99                    |
| GPRP mRNA for glycine- and proline-rich protein (AB615379)                   | 850                            | 860                              | 99                                 | 99                    |
| NOI mRNA for putative nitrate induced NOI protein (AB615378)                 | 255                            | 259                              | 98                                 | 100                   |
| Calcium dependent protein kinase 1 CPK1 mRNA (AY753552)                      | 993                            | 1783                             | 56                                 | 100                   |
| Cyclophilin (L32095)   | 1101                           | 1160                             | 95                                 | 99                    |
| CBL1 mRNA calcineurin-B like calcium binding protein (AB370168)              | 722                            | 1007                             | 72                                 | 100                   |
| CIPK1 mRNA for CBL interacting protein (AB370167)                            | 1045                           | 1400                             | 75                                 | 99                    |
| Peptide transporter 1 PTR1 mRNA (AY289622)                                   | 1438                           | 2028                             | 71                                 | 99                    |
| Heat shock protein 17.9 gene (KC249973)                                      | 472                            | 483                              | 98                                 | 90                    |
| Putative glycerol-3-phosphate acyltransferase GPAT mRNA (AF090734)           | 1385                           | 1386                             | 100                                | 99                    |
| Ferredoxin NADP reductase precursor fnr mRNA (U14956)                        | 1455                           | 1474                             | 99                                 | 98                    |
| Putative ethylene responsive factor ERF3 mRNA* (EU543661)                    | 671                            | 672                              | 100                                | 100                   |
| Putative ethylene responsive factor ERF2 mRNA* (EU543660)                    | 670                            | 1232                             | 54                                 | 98                    |
| Putative ethylene responsive factor ERF1 mRNA* (EU543659)                    | 654                            | 688                              | 95                                 | 100                   |
| Putative ethylene insensitive transcription factor (EIN3-1) mRNA* (EU543660) | 2173                           | 2406                             | 90                                 | 99                    |
| Putative ethylene insensitive transcription factor EIN3-2 mRNA* (EU543658)   | 2296                           | 2353                             | 97                                 | 100                   |

|   |      |      |     |     |
|---|------|------|-----|-----|
| Putative respiratory burst oxidase-like protein A (rbohA) mRNA* (JF784279)  | 2824 | 3046 | 93  | 100 |
| Putative respiratory burst oxidase-like protein C (rbohC) mRNA * (JF784280) | 1121 | 3426 | 33  | 99  |
| Putative ACC synthase ACS2 mRNA * (EU543656)                                | 964  | 1519 | 63  | 97  |
| Putative aminocyclopropane carboxylic acid oxidase (ACO1)* (EU543653)       | 614  | 614  | 100 | 99  |
| Putative aminocyclopropane carboxylic acid synthase (ACO2)* (EU543654)      | 764  | 767  | 100 | 100 |
| Apyrase gene (AB088209)   | 294  | 2173 | 13  | 92  |
| Expansin EXP1 mRNA (EF190969)   | 1037 | 1127 | 92  | 99  |
| PP2Ac-3 mRNA for type 2A protein phosphatase-3 (AB039918)                   | 1342 | 1502 | 89  | 99  |
| PP2Ac-2 mRNA for type 2A protein phosphatase-2 (AB039917)                   | 1397 | 1475 | 95  | 99  |
| CyP mRNA (AB012947)   | 806  | 829  | 97  | 100 |
| MET mRNA for type 1 metallothionein (AB176562)                              | 345  | 501  | 69  | 94  |
| Guanine nucleotide regulatory protein mRNA (Z24678)                         | 632  | 946  | 67  | 100 |

Hit length refers to contig length homologous to *V. faba* cDNA sequence; Query length refers to total length of *V. faba* cDNA sequence. Asterisks (\*) indicate genes previously cloned from isolated epidermal TCs of *V. faba* cotyledons – many of these genes are reported as showing epidermal-specific differential expression across epidermal TC *trans*-differentiation in cultured cotyledons (see Zhou et al., 2010; Andriunas et al., 2012).

**Supplementary Table 1. *De novo* assembly outputs resulting from varying bubble size and word size.**

| WORD SIZE<br>( <i>k</i> -mer) | BUBBLE SIZE | N50<br>(bp) | TOTAL No.<br>OF<br>CONTIGS | LARGEST<br>CONTIG<br>LENGTH<br>(bp) | AVERAGE<br>CONTIG<br>LENGTH<br>(bp) | MAPPED<br>READS<br>% |
|-------------------------------|-------------|-------------|----------------------------|-------------------------------------|-------------------------------------|----------------------|
| 20                            | 200         | 1527**      | 22066                      | 11541*                              | 1299                                | 75                   |
| 20                            | 300         | 1577*       | 19153*                     | 10589                               | 1320*                               | 65                   |
| 23                            | 200         | 1518        | 21706                      | 9455                                | 1291                                | 79                   |
| 23                            | 300         | 1521        | 21680                      | 9456                                | 1293**                              | 80                   |
| 25                            | 200         | 1512        | 22052                      | 9700                                | 1289                                | 78                   |
| 25                            | 300         | 1512        | 22020                      | 9702                                | 1290                                | 76                   |
| 27                            | 200         | 1499        | 22397                      | 9646                                | 1276                                | 77                   |
| 27                            | 300         | 1501        | 22402                      | 9646                                | 1275                                | 77                   |
| 30                            | 200         | 1467        | 22563                      | 9478                                | 1256                                | 84*                  |
| 30                            | 300         | 1466        | 22541                      | 9481                                | 1255                                | 81                   |
| 33                            | 200         | 1447        | 22429                      | 9304                                | 1243                                | 78                   |
| 33                            | 300         | 1452        | 22429                      | 9305                                | 1247                                | 79                   |
| 35                            | 200         | 1423        | 22444                      | 9916                                | 1228                                | 79                   |
| 35                            | 300         | 1426        | 22447                      | 9916                                | 1229                                | 80                   |
| 37                            | 200         | 1394        | 22314                      | 9304                                | 1208                                | 79                   |
| 37                            | 300         | 1396        | 22298                      | 9304                                | 1209                                | 80                   |
| 40                            | 200         | 1364        | 22120                      | 11455**                             | 1190                                | 81                   |
| 40                            | 300         | 1352        | 22079                      | 11455                               | 1184                                | 81                   |
| 43                            | 200         | 1324        | 21884                      | 10668                               | 1160                                | 80                   |
| 43                            | 300         | 1326        | 21868                      | 10668                               | 1162                                | 80                   |
| 45                            | 200         | 1282        | 21697                      | 10621                               | 1132                                | 81                   |
| 45                            | 300         | 1283        | 21709                      | 10621                               | 1133                                | 81                   |
| 47                            | 200         | 1245        | 21295**                    | 10528                               | 1114                                | 82**                 |
| 47                            | 300         | 1245        | 21297**                    | 10528                               | 1114                                | 82**                 |

Single asterisk (\*) indicates best score and double asterisk (\*\*) indicates second best score, for each criteria as follows: highest N50 score, lowest number of contigs, largest contig length of all assemblies, average length of contigs (includes all contigs in the assembly), highest mapped reads %.

**CHAPTER 3**

**IDENTIFICATION OF CANDIDATE  
TRANSCRIPTIONAL REGULATORS OF  
EPIDERMAL TRANSFER CELL  
DEVELOPMENT IN *Vicia faba* COTYLEDONS**

### 3.1 OVERVIEW

The aim of this chapter was to identify transcription factors putatively involved in regulating epidermal TC development in *V. faba* cotyledons by using RNA-Seq analysis. As described in Chapter 1, adaxial epidermal cells of *V. faba* cotyledons, which do not form TCs *in planta*, can be induced to *trans*-differentiate into epidermal TCs when cotyledons are cultured adaxial side down on nutrient media, whereas cells of the adjacent storage parenchyma tissue in the cotyledons do not form such cells (Offler et al., 2003). The temporal and spatial development of these functional adaxial epidermal TCs has been studied in some detail (Farley et al., 2000; Wardini et al., 2007b), and this system has been used extensively to discover signaling pathways regulating epidermal TC development in *V. faba* cotyledons (Dibley et al., 2009; Zhou et al., 2010; Andriunas et al., 2012; Zhang et al., 2015a,c). Subsequently, this experimental system is well suited to use RNA-Seq as a means to discover transcription factors putatively involved in regulating epidermal TC development in this system, and thus possibly in all TCs developing reticulate wall ingrowths.

This chapter comprises a manuscript that has been submitted to *Frontiers in Plant Science* (20/12/2015) and is currently under *Interactive Review* with a revised version of the manuscript having been submitted (03/04/2016) in response to Reviewer comments. The manuscript focuses on identifying transcription factors from the RNA-Seq data as showing transcriptional responses consistent with a role in regulating the *trans*-differentiation of epidermal TCs. Additional analysis of the data set derived from the RNA-Seq analysis but not included in the manuscript is described in Appendix 3.

Note: Supplementary material associated with the submitted manuscript (Supplementary Tables 1-4) and the Appendix for this Chapter (Supplementary Tables 3A.1-3A.4.) are supplied on the USB drive submitted with this thesis.

**Manuscript title: Identification of Candidate Transcriptional Regulators of Epidermal Transfer Cell Development in *Vicia faba* Cotyledons**

**Kiruba Shankari Arun-Chinnappa and David W. McCurdy**

Submitted to *Frontiers in Plant Science* (20/12/2015) and in revised form (03/04/2016).

# **Identification of Candidate Transcriptional Regulators of Epidermal Transfer Cell Development in *Vicia faba* Cotyledons**

***Kiruba S Arun-Chinnappa<sup>1</sup>, David W McCurdy\****

*Centre for Plant Science, School of Environmental and Life Sciences, The University of Newcastle, Callaghan, NSW 2308, Australia.*

*<sup>1</sup>Current address: Centre for Crop Health, University of Southern Queensland, Toowoomba, QLD 4350, Australia*

*\*E-mail: David.McCurdy@newcastle.edu.au*

## Abstract

Transfer cells (TCs) are anatomically-specialized cells formed at apoplastic-symplasmic bottlenecks in nutrient transport pathways in plants. TCs form invaginated wall ingrowths which provide a scaffold to amplify plasma membrane surface area and thus increase the density of nutrient transporters required to achieve enhanced nutrient flow across these bottlenecks. Despite their importance to nutrient transport in plants, little is known of the transcriptional regulation of wall ingrowth formation. Here, we used RNA-Seq to identify transcription factors putatively involved in regulating epidermal TC development in cotyledons of *Vicia faba*. Comparing cotyledons cultured for 0, 3, 9 and 24 h to induce *trans*-differentiation of epidermal TCs identified 42 transcription factors that showed either epidermal-specific or epidermal-enhanced expression, and 10 that showed epidermal-specific down regulation. Members of the WRKY and ethylene-responsive families were prominent in the cohort of transcription factors showing epidermal-specific or epidermal-enhanced expression, consistent with the initiation of TC development often representing a response to stress. Members of the MYB family were also prominent in these categories, including orthologs of MYB genes involved in localized secondary wall deposition in *Arabidopsis thaliana*. Among the group of transcription factors showing down regulation were various homeobox genes and members of the MADs-box and zinc-finger families of poorly defined functions. Collectively, this study identified several transcription factors showing expression characteristics and orthologous functions that indicate likely participation in transcriptional regulation of epidermal TC development in *V. faba* cotyledons.

**Keywords:** *Vicia faba*, transfer cell, wall ingrowth, *trans*-differentiation, transcription factors, RNA-Seq

## Introduction

Transfer cells (TCs) commonly *trans*-differentiate from various differentiated cell types at anatomical locations where enhanced rates of nutrient transport are required for programmed development or in response to stress (Offler et al., 2003). The characteristic feature of TCs is their development of extensive and morphologically varied wall ingrowth networks which provide a scaffold to increase plasma membrane surface area to enable high densities of membrane transporters and thus accommodate increased demand for nutrient transport (Offler et al., 2003; McCurdy et al., 2008).

Wall ingrowth formation in TCs represents a novel example of wall deposition in plant cells (McCurdy et al., 2008; McCurdy, 2015), presumably involving unique sets of genes to both initiate and then orchestrate the cellular events required for this highly localized wall deposition event. Indeed, transcript profiling in endosperm TCs of barley (Thiel et al., 2008, 2012) and epidermal TCs of *Vicia faba* cotyledons (Dibley et al., 2009; Zhang et al., 2015b) established that wall ingrowth deposition involves differential expression of many hundreds of genes, presumably organized within transcriptional cascades to coordinate expression of the biosynthetic machinery required for wall ingrowth deposition and TC function (Arun-Chinnappa et al., 2013). These studies identified a role for auxin and ethylene signaling in inducing TC development, and details of the involvement of epidermal-specific ethylene and reactive oxygen species signaling pathways in epidermal TC induction have been elucidated (Zhou et al., 2010; Andriunas et al., 2011; Andriunas et al., 2012).

A major unresolved question in TC biology is the identity of transcription factors which respond to these inductive signals to coordinate the downstream expression of biosynthetic machinery required for wall ingrowth building. In maize, *ZmMRP-1*, a member of the MYB-Related family of transcription factors, has been identified as a key regulator of basal endosperm TC development (Gómez et al., 2009). *ZmMRP-1* is expressed specifically in endosperm TCs (Gómez et al., 2002) and regulates the expression of several maize TC-specific genes such as *MEG-1* (*Maternally Expressed Gene 1*; Gutiérrez-Marcos et al., 2004), *BETL-1* and *BETL-2* (Gómez et al., 2002), and *TCRR-1* (*Transfer Cell Response Regulator 1*; Múniz et al., 2006). When transformed into *Arabidopsis thaliana* (*Arabidopsis*) or *Nicotiana tabacum*, the *ZmMRP-1* promoter drives expression at tissue locations involved in active transport (Barrero et al., 2009). Thus, while *ZmMRP-1* clearly plays a key role in regulating basal endosperm TC

development, the genetic origin of these cells which develop in the triploid endosperm as part of a cell fate specification pathway (Thiel, 2014) is clearly different from most TCs which develop via *trans*-differentiation. Thus, transcriptional regulation of the *trans*-differentiation of TCs forming reticulate wall ingrowths may likely be different from that occurring in basal endosperm TCs.

Dibley et al. (2009) used cDNA-AFLP to survey differential expression across the *trans*-differentiation of epidermal TCs in cultured cotyledons of *V. faba*. The cotyledon culture system provides a valuable experimental approach for transcriptional profiling of TC development, since the adaxial epidermal cells form an experimentally accessible and homogenous population of cells which *trans*-differentiate into functional TCs when isolated cotyledons are placed adaxial surface down on nutrient agar (Farley et al., 2000; Offler et al., 2003; Dibley et al., 2009; Zhou et al., 2010; Andriunas et al., 2012). Dibley et al. (2009) used this experimental system in combination with cDNA-Amplified Fragment Length Polymorphism (AFLP) analysis to identify extensive transcriptional changes occurring across the *trans*-differentiation of epidermal cells to become functional epidermal TCs. However, due to the technical limitations of cDNA-AFLP as a platform for high-throughput gene discovery, this study identified only a small cohort of the larger population of genes predicted to display changes in epidermal-specific temporal expression. Amongst this analysis, only a few transcription factors were identified as differentially expressed, and thus the depth of discovery of such genes putatively involved in regulating the *trans*-differentiation of TCs was limited.

The development of RNA-Seq for transcriptional profiling in species without a sequenced genome, with its deep sequencing capabilities to detect changes in transcript abundance with high sensitivity (Simon et al., 2009; Martin et al., 2013; Weber, 2015), provides an opportunity to re-visit transcript profiling using the *V. faba* cotyledon culture system. Zhang et al. (2015b) used this approach to identify genes putatively involved in the process of building the ingrowth wall. In this current study we used RNA-Seq to identify at least 42 transcription factors which show differential up-regulated expression in adaxial epidermal cells of *V. faba* cotyledons undergoing *trans*-differentiation to form epidermal TCs, and 10 which are similarly down-regulated. Many of the transcription factors showing up-regulation belong to the WRKY and Ethylene Response Factor families, consistent with *trans*-differentiation of epidermal TCs representing a stress response involving ethylene (Zhou et al., 2010; Andriunas et al., 2012). Furthermore,

several members of the MYB family of transcription factors were also identified as differentially up-regulated, in particular *VfMYB20*, the ortholog of which in Arabidopsis, *AtMYB20*, is a key target of the NAC-domain secondary wall master regulators *VNT6* and *VNT7* (Kubo et al., 2005; Zhong and Ye, 2010). This result implies possible similarity in the transcriptional pathways regulating secondary wall deposition and wall ingrowth formation in plants.

## **Materials and Methods**

### **Plant Growth and Cotyledon Culture**

*Vicia faba* L. (cv. Fiord) plants were grown in environmentally-controlled glasshouse and growth cabinet conditions as previously described (Offler et al., 1997; Farley et al., 2000). To sample transcripts from cotyledons undergoing epidermal TC development, cotyledons (100-120 mg FW) were removed from pods and either fixed immediately (t = 0-h) in ice-cold ethanol:acetic acid (3:1 v/v) for 1 h, or placed adaxial surface down on filter paper soaked in Murashige and Skoog medium (MS; Sigma Australia) in petri dishes. The Petri dishes were sealed with tape and incubated in darkness at 22°C for 3, 9 or 24 h, then the cotyledons were fixed in ice-cold ethanol:acetic acid as described above. The ethanol-acetic acid fixation was used for all cotyledons to minimize wounding responses associated with handling. Fixed cotyledons were rinsed briefly in distilled water and sheets of adaxial epidermal cells and discs of storage parenchyma were then isolated from each cotyledon as described (Dibley et al., 2009). For each time-point (0, 3, 9, 24 h) epidermal peels and storage parenchyma disks were collected from a minimum of 10 cotyledons derived from pods harvested from at least three different plants, and were snap frozen in liquid nitrogen and stored at -80°C prior to RNA isolation.

### **Total RNA Isolation and cDNA Library Preparation**

Total RNA was extracted from the samples described above using an RNeasy Plant RNA isolation kit (Qiagen) incorporating on-column DNase digestion. For RNA-Seq, between 1-2 µg of total RNA was isolated as described above from each sample and subjected to QA analysis using an Agilent 2100 Bioanalyzer. One hundred-bp single-end read libraries were prepared for each sample using the Illumina TrySeq Library kit and sequencing was

performed using the Illumina HiSeq-2000 platform. The QA analysis, library construction and 100-bp single-end sequencing were performed by the Australian Genome Research Facility (Melbourne).

## **RNA-Seq Analysis**

Sequencing of the poly(A)<sup>+</sup> transcriptome of epidermal cells and storage parenchyma of cultured cotyledons yielded 368 M reads in total (42-48 M reads for each of the eight samples). Raw reads from each sample were trimmed to remove low quality bases and then mapped against a *de novo* assembled, genome-wide transcriptome map generated using CLC Genome Workbench (Arun-Chinnappa and McCurdy, 2015). To determine transcript abundance, Reads Per Kilobase per Million (RPKM) mapped read values were calculated to determine normalized gene expression of each transcript at each time point using default settings in CLC Genome Workbench. The RPKM values were exported into Microsoft<sup>®</sup> Excel<sup>®</sup> 2010 for all subsequent data calculations. To rationalise fold-change calculations, contigs with RPKM values less than 0.1 were assigned a value of 0.1, and a value of 0.5 or above for a given contig was deemed to be expressed (Sweetman et al., 2012).

Calculated RPKM values for both epidermal cells and storage parenchyma, at all four time points, were used for differential expression analysis. Transcripts with RPKM values less than 0.5 in all time points, and thus deemed not to be expressed, were removed from all data sets, and fold-change based on RPKM values at 3, 9 and 24 h relative to the 0-h control was calculated for all transcripts expressed in each tissue type. To identify transcripts showing epidermal-specific up-regulation, a two-step filtering process was undertaken. First, all transcripts expressed in epidermal cells showing a two-fold ( $\text{Log}_2 2=1$ ) or greater increase across at least one culture time point relative to 0-h were selected. Next, transcripts from this list that showed a fold-change of 1.2 ( $\text{Log}_2 1.2=0.26$ ) or greater change in expression in storage parenchyma tissue across any of the culture time points relative to 0-h were eliminated from this cohort. However, these threshold levels yielded an excessively high number of transcripts. Hence, to refine this list, the same two-step filtering process was undertaken but this time using fold-change of five ( $\text{Log}_2 5=2.3$ ) or above to identify changes in epidermal gene expression, and then eliminate from this cohort transcripts that showed a fold-change of two ( $\text{Log}_2 2=1$ ) or greater in storage parenchyma. This analysis identified a cohort of 444 transcripts that

showed a five-fold or greater increase in expression in adaxial epidermal cells but two-fold or less change in storage parenchyma tissue across the three culture time points relative to 0-h control. A similar strategy was undertaken to identify transcripts which were down-regulated specifically in epidermal tissue in any of the three culture time points relative to 0-h, with this analysis identifying 172 transcripts categorized as epidermal-specific, down-regulated. For all transcripts excluded from this epidermal-specific, differential expression category (i.e., either up- or down-regulated specifically in epidermal tissue), fold-change in expression between 0- and 3-h culture was calculated for both epidermal and storage parenchyma data sets. The difference of fold-change for each transcript between epidermal and storage parenchyma was then calculated, and transcripts with a difference of 25 or greater were deemed to show “epidermal-enhanced, up-regulated” expression. The rationale for this analysis is described in Results. This analysis identified 198 transcripts displaying epidermal-enhanced, up-regulated expression.

### **Reverse Transcription-Quantitative PCR (RT-qPCR)**

Total RNA was extracted from both isolated epidermal peels and storage parenchyma disks of cotyledons cultured for 0- and 3-h as described above. For this analysis, epidermal peels and storage parenchyma were obtained from a minimum of 5-8 cotyledons from three replicate plants. cDNA was synthesized from 1 µg of total RNA from each sample using Superscript® III first strand synthesis system (Invitrogen) as per the manufacturer’s instructions. PCR reactions were carried out using RotorGene SYBR Green PCR kit (Qiagen) as per manufacturer’s instructions and using a RotorGene-Q (Qiagen) thermocycler. Cycling conditions were as follows: 95<sup>0</sup>C for 2 min followed by 40 cycles of 95<sup>0</sup>C for 10 s, 60<sup>0</sup>C for 30 s and 72<sup>0</sup>C for 30 s. Expression analysis was performed using the delta-delta method using Q-gene software (Simon, 2003) with *VjEFα* (*V. faba Elongation Factor alpha*, AJ222579) as the reference gene (Andriunas et al., 2012). Primer and gene details used for the RT-qPCR analysis are listed in Supplementary Table 4.

## Results

### RNA-Seq Analysis of Adaxial Epidermal TC Development

Adaxial epidermal cells of cultured *V. faba* cotyledons *trans*-differentiate to become epidermal TCs but cells of the adjacent storage parenchyma tissue do not (Farley et al., 2000; Talbot et al., 2007; Dibley et al., 2009). Consequently, genes showing epidermal-specific change in expression upon cotyledon culture represent a pool of candidates likely to be involved in the *trans*-differentiation of epidermal TCs (Dibley et al., 2009; Zhang et al., 2015b). To identify transcription factors showing epidermal-specific up-regulation, we performed RNA-Seq of epidermal cells and storage parenchyma isolated from cultured cotyledons. An initial analysis of transcriptional changes using a two-fold or greater change in expression in epidermal cells across cotyledon culture compared to a 1.2-fold change in storage parenchyma yielded more than 2,000 transcripts (data not shown). To provide a more stringent analysis of epidermal-specific expression we identified transcripts showing a five-fold ( $\text{Log}_2=2.3$ ) or greater change in epidermal cells across all three culture time points (3-, 9-, 24-h) relative to 0-h cotyledon culture compared to a two-fold ( $\text{Log}_2=1$ ) or less change in storage parenchyma. This analysis identified 444 transcripts (see Supplementary Table 1) that matched this definition for “epidermal-specific, up-regulation”. Of this collection, 22 were identified as transcription factors (Table 1) based on annotation against both Viridiplantae and Arabidopsis gene sets as determined previously (Arun-Chinnappa and McCurdy, 2015). From this list of transcription factors, 13 were up-regulated within the first 3-h of culture, while the remaining nine were up-regulated in epidermal cells by either 9- or 24-h of cotyledon culture (Table 1). The list of 22 transcription factors was headed by a GT-3B-like member of the trihelix gene family (Unigene 13378), which showed early and sustained epidermal-specific up-regulation across the 24-h culture period (Table 1). The remaining list of transcription factors shown in Table 1 is dominated by members of the MYB and MYB-like families (9/22) followed by ethylene responsive (3/22) and bHLH (3/22) transcription factors (Table 1).

A similar strategy was undertaken to identify 172 transcripts that showed epidermal-specific down-regulation, defined as a five-fold or greater decrease in epidermal tissue with a two-fold or less change in storage parenchyma, across any culture time point

relative to the 0-h control (see Supplementary Table 2). This list included 10 transcription factors, including two homeobox leucine zipper proteins, and transcription factors belonging to the MADS-box and zinc finger CCCH-domain families (Table 2).

The criteria of using a five-fold or greater change to define a biologically relevant change in expression, and conversely a two-fold or less value to denote no change in expression, provides a stringent basis for claiming “epidermal-specific” change in expression, given the sensitivity of RNA-Seq to detect transcript abundance (e.g., Sweetman et al., 2012; Zhao et al., 2014). From this collective analysis, therefore, a total of 32 transcription factors were identified as showing epidermal-specific differential expression across adaxial epidermal TC development in *V. faba* cotyledons.

In addition to the genes listed in Table 1, we noted numerous examples in the RNA-Seq dataset where expression of a given transcript increased substantially in epidermal tissue within the first 3-h of cotyledon culture but its change in storage parenchyma was comparably less substantial but nonetheless greater than two-fold. To account for this cohort of genes excluded from the category of “epidermal-specific”, we calculated differences in fold-change between epidermal and storage parenchyma for each transcript at 3-h culture compared to 0-h control. Transcripts showing a numerical fold-change difference of 25 or greater were deemed as displaying “epidermal-enhanced, up-regulated” expression, whereby differential expression of these transcripts was 25 times greater in epidermal tissue compared to storage parenchyma. In total, 198 transcripts were identified in this category (see Supplementary Table 3), of which 20 were identified as putative transcription factors (Table 3). This cohort of transcription factors is characterized by high representation (nearly 50%) of members of the plant-specific WRKY family (Table 3), a result consistent with the *trans*-differentiation of epidermal TCs being a stress-related phenomenon regulated by ethylene (Andriunas et al., 2011, 2012).

## **Verification of expression by RT-quantitative PCR**

To verify temporal expression of transcripts revealed by RNA-Seq, we performed RT-qPCR on a cohort of transcription factors showing substantial epidermal-specific (Table 1) or epidermal-enhanced (Table 3) up-regulated change in expression within 3-h of cotyledon culture. All six of the selected transcription factors (*VfTrihelix GT-3B*,

*VfMYB20*, *VfRAP2.4*, *VfMYB30*, *VfMYB31*, *VfERF1*) showing epidermal-specific up-regulation as determined by RPKM showed expression essentially identical to or closely matching that obtained by RT-qPCR (Figure 1). This result therefore confirmed both the temporal (0-h vs 3-h) and spatial (epidermal vs storage parenchyma) changes in expression for these genes across epidermal TC development. Of the four genes chosen as representative of epidermal-enhanced, up-regulated expression, RT-qPCR confirmed the expression profile of two, namely *VfWRKY28* and *VfERF*, whereas RT-qPCR recorded disparately high expression of *VfPERF2* and *VfWRKY23* in storage parenchyma tissue compared to RPKM values (Figure 2). The reason for this discrepancy for these two genes, and only in storage parenchyma tissue, is not known but may be due to non-specific amplification of a closely related sequence expressed predominantly in storage parenchyma. Irrespective of this possibility, in both cases RPKM values reported high differential expression of the relevant gene in epidermal tissue from 0- to 3-h compared to storage parenchyma (Figure 2). Collectively, the RT-qPCR analysis (Figures 1 and 2) provide support for concluding that the RPKM values derived from the RNA-Seq analysis of cultured cotyledons accurately revealed temporal and spatial changes in expression across cotyledon culture, a conclusion supported by numerous studies using RNA-Seq for transcript profiling in non-sequenced plant species (e.g., Liu et al., 2014; O'Rourke et al., 2013).

## Discussion

In this study we used RNA-Seq to identify transcription factors putatively regulating the *trans*-differentiation of epidermal TCs in cultured *V. faba* cotyledons. Culturing *V. faba* cotyledons induces adaxial epidermal cells to form TCs, but cells of the neighbouring storage parenchyma tissue do not, thus offering an experimental system to identify signaling pathways inducing epidermal TC *trans*-differentiation (Zhou et al., 2010; Andriunas et al., 2011, 2012) as well as global gene expression events associated with this process (Dibley et al. 2009; Zhang et al., 2015b). Using cotyledon culture in combination with RNA-Seq, 444 transcripts were identified as showing epidermal-specific differential expression, defined in this study as showing five-fold or greater temporal change in epidermal tissue across cotyledon culture, but only a two-fold or less change for the same transcript in storage parenchyma. These parameters were chosen to

provide stringent criteria for classification as epidermal-specific differential expression, thus maximizing the potential to identify regulatory transcription factors based on substantive epidermal-specific change in expression, given that change in mRNA levels is the primary indicator for change in protein abundance (Weber, 2015). The total of 444 transcripts showing epidermal-specific differential regulation approaches the number of genes identified by cDNA-AFLP analysis of *V. faba* TCs (650 genes; Dibley et al., 2009) and microarray analysis of barley endosperm TCs (815 genes; Thiel et al., 2008). This correlation, however, is dependent on the criteria used to define epidermal-specific expression, and increased dramatically when a two-fold change was used in this instance (see Zhang et al., 2015b). Furthermore, excluded from our definition of epidermal-specific were a large number of transcripts showing substantial fold change in epidermal tissue and significantly less so in storage parenchyma, but nonetheless being two-fold or greater across cotyledon culture. This cohort was defined as showing epidermal-enhanced expression (Table 3), and as such contributed to the total number of genes displaying expression characteristics at least consistent with a role in regulating epidermal TC development.

A feature of the list of transcription factors showing epidermal-specific up-regulation is the prominence of members of the MYB gene family (Table 1). MYBs represent likely candidates to function as transcriptional regulators of wall ingrowth development in epidermal TCs since members of this family function as “second tier” transcriptional regulators of localized secondary wall deposition in plants (Zhong et al., 2010). In addition, the only transcription factor known to this point to regulate TC development, *ZmMRB1* from maize, is a member of the MYB-related family (Gomez et al., 2009). No *V. faba* ortholog of *ZmMRP1* was identified in the current study, but prominent among the list of MYBs was the *V. faba* ortholog of *AtMYB20* (Unigene 9668, Table 1), which showed a  $\log_2$  fold change of 7.1 within 3 h of cotyledon culture. In Arabidopsis, *AtMYB20* sits downstream of *SND1* and *VND6/7*, both being NAC domain transcription factors identified as master switches for secondary wall deposition (Zhong et al., 2010). *AtMYB20* and its paralog *AtMYB43* are amongst a cohort of MYB factors activated by *SND1/VND6/7* and proposed to regulate transcriptional pathways responsible for deposition of cellulosic and hemicellulosic components of secondary walls (Nakano et al., 2010; Zhong et al., 2010). At later stages of cotyledon culture, a *V. faba* ortholog of *AtMYB63* (Unigene 19002, Table 1) was also up-regulated specifically in epidermal cells.

*AtMYB63* is a transcriptional activator of lignin biosynthesis required for secondary wall formation in Arabidopsis (Zhou et al., 2009; Zhong et al., 2010). The construction of secondary wall thickenings in xylem elements and wall ingrowths in TCs both represent examples of localized wall deposition in plants, thus the finding that *V. faba* orthologs of Arabidopsis genes known to be involved in secondary wall deposition are up-regulated specifically in epidermal cells upon wall ingrowth building, suggests overlapping roles in these processes. Contrary to this suggestion, however, is the observation that wall ingrowths do not contain lignin (Gunning and Pate, 1974; Vaughn et al., 2007), a circumstance consistent with the predicted diffusional properties of wall ingrowths (Gunning and Pate, 1974). However, Rocha et al. (2014) recently used TEM-energy dispersive X-ray spectrometry and acriflavine staining with confocal microscopy to demonstrate the presence of lignin in flange and so-called reticulate wall ingrowths in maize basal endosperm TCs. In this context, therefore, both the transcriptional data reported here and the findings of Rocha et al. (2014) suggest that the assumed absence of lignin in wall ingrowths may need to be revisited.

The transcription factor showing the highest fold-increase in epidermal cells upon cotyledon culture was an ortholog of the trihelix transcription factor GT-3B from chickpea (Unigene 13378, Table 1). The trihelix family of transcription factors contains 30 genes in Arabidopsis, but the majority have not been functionally defined (Ayadi et al., 2004; Kaplan-Levy et al., 2012). *AtGT-3B* is rapidly expressed in response to pathogen or salt stress (Park et al., 2004). In soybean, a similar response to these stresses is mediated by a calmodulin signaling gene, *SCaM-4*, which contains a GT-like element in its promoter recognised by *AtGT-3B* (Park et al., 2004). The function of the *V. faba* ortholog significantly up-regulated specifically in epidermal TCs is unclear, but wall ingrowth deposition in these cells involves calcium signaling (Zhang et al., 2015a), thus a *GT-3B-like* gene may be involved in this process.

Ethylene has been demonstrated to play a clear role in signaling the induction of epidermal TCs in *V. faba* cotyledons (Zhou et al., 2010; Andriunas et al., 2011). These TCs form by a *trans*-differentiation process which is preceded by dedifferentiation of the epidermal cells (Dibley et al., 2009). In this context it is noteworthy that a *V. faba* ortholog of the ERF/AP2 transcription factor *RAP2.4* (Unigene 7266, Table 1), now referred to as *WOUND INDUCED DEDIFFERENTIATION 1 (WIND1)*, was strongly induced in

epidermal cells by 3-h of cotyledon culture. *WINDI* in *Arabidopsis* acts as a regulator of wound-induced dedifferentiation in young tissues, including cotyledon epidermal cells (Iwase et al., 2011). The culture-induced *trans*-differentiation of epidermal TCs represents a wound response in this tissue, this being an example of indirect *trans*-differentiation involving dedifferentiation without cell division (Nguyen and McCurdy, 2016). Consequently, rapid epidermal-specific expression of a *V. faba* ortholog of *WINDI* to drive dedifferentiation as a first step of *trans*-differentiation is consistent with this proposition. Another ERF/AP2 ortholog (Unigene 10245, Table 1) was induced specifically in epidermal cells at 9 h culture. The ortholog of this gene, *ERF BUD ENHANCER (EBE)*, functions in regulating cell proliferation and is highly expressed during S-phase of the cell cycle (Mehrnia et al. 2013), an observation consistent with the endopolyploid status of adaxial epidermal cells of *V. faba* cotyledons (Dibley et al., 2009) and up-regulation of a TCP ortholog involved in endoreduplication in *Arabidopsis* (Unigene 18946, Table 1). The delayed expression of *EBE* upon cotyledon culture, however, does not correlate with the temporal increase in mitotic index in these cells (Dibley et al., 2009; Zhang et al., 2015b), thus a definitive role for the *V. faba* ortholog of *EBE* is unclear. Finally, expression of the *V. faba* ortholog of *AtERF98* (Unigene 7356, Table 3) suggests a role for ascorbic acid in wall ingrowth deposition. Ascorbic acid, via its capacity for generating reactive oxygen species in the cell wall (Fry, 1992), can increase wall extensibility during growth (Schopfer, 2002). *AtERF98* plays an important role in ascorbic acid production (Zhang et al., 2012) and the substantial up-regulation of the *V. faba* ortholog in an epidermal-enhanced manner (Table 3) suggests it may have a role in increasing ascorbic acid production in adaxial epidermal cells to promote cell wall loosening required for wall ingrowth deposition.

A prominent feature of the list of genes showing epidermal-enhanced up-regulation is the abundance of WRKY transcription factors (Table 3). This gene family is commonly involved in regulating stress tolerance in plants (Rushton et al., 2010), and thus it is not surprising that many are up-regulated throughout the whole cotyledon upon transfer to culture conditions. However, since these *WRKY* genes show substantial fold-increase in epidermal expression compared to storage parenchyma, a role in stress-induced induction of epidermal TCs is reasonable to conclude. This conclusion is strengthened by considering the *V. faba* ortholog of *AtWRKY28* which shows a fold increase of 378 in epidermal cells by 3 h of culture (Unigene 11848, Table 3). In *Arabidopsis*, the paralog

of *AtWRKY28*, *AtWRKY8*, is up-regulated in the tocopherol-deficient mutant *vte2* (*vitamin E 2*) when grown at low temperature (Maeda et al., 2014). The low temperature phenotype of *vte2* includes enhanced levels of delocalized wall ingrowth deposition in phloem parenchyma TCs (Maeda et al., 2006, 2008), an observation consistent with participation of both *AtWRKY8* and the *V. faba* ortholog in genetic pathways regulating wall ingrowth deposition. A role for WRKYs in signaling epidermal TC development is also suggested by the epidermal-enhanced up-regulation of an ortholog of *AtWRKY23* (Unigene 2088, Table 3). This gene in Arabidopsis is expressed during syncytia and giant cell formation in roots of nematode-infected cells (Grunewald et al. 2008; Cabrera et al., 2014), structures with distinct wall ingrowth-like characteristics. Furthermore, the Arabidopsis ortholog of Unigene 12104 (Table 3), *AtWRKY33*, regulates genes involved in the ethylene biosynthesis pathway (Birkenbihl et al., 2012), while the expression of both *AtWRKY23* and *AtWRKY33* is regulated by auxin (Berendzez et al., 2012; Grunewald et al., 2012). Hence, these two *WRKY* orthologs in *V. faba*, both of which show strong epidermal-enhanced expression (Table 3), are possibly induced by auxin and in turn act to promote ethylene biosynthesis as part of the auxin/ethylene signaling pathway which drives epidermal TC development in *V. faba* cotyledons (Zhou et al., 2010; Andriunas et al., 2011). Interestingly, of the *WRKY* genes appearing in Tables 1 and 3, four of them (*AtWRKY23*, 28, 71 and 48) cluster within the Ib subgroup of this family (Wu et al., 2005), suggesting structurally-conserved roles in signaling wall ingrowth deposition in TCs.

Homeobox transcription factors are prominent among the list of *V. faba* genes showing epidermal-specific down-regulated expression across cotyledon culture (Table 2). One of these, the Arabidopsis ortholog of Unigene 2074 (Table 2), *ATHB-1*, which belongs to the HD-Zip I class of transcription factors (Ariel et al., 2007), regulates genes involved in cell wall composition and cell elongation (Capella et al., 2015), and thus the downregulation of the *V. faba* ortholog may contribute to the altered compositional profile of wall ingrowths in epidermal TCs compared to the primary wall (Vaughn et al., 2007). A second *V. faba* homeobox transcription factor (Unigene 1229, Table 2), the Arabidopsis ortholog of which is *HAT3*, is a member of the HD-Zip II sub-family and participates in regulating apical embryo development and meristem function (Turchi et al., 2013). The functional significance in switching off expression of such a gene to involvement in the *trans*-differentiation of epidermal TCs is not immediately obvious, but this observation extends to many of the genes listed in Table 2. The *trans*-

differentiation of epidermal TCs involves dedifferentiation followed by redifferentiation, processes that require substantial genomic reorganization and modifications (Dibley et al., 2009), thus switching off many of the genes listed in Table 2 may be a requirement to achieve these outcomes.

Collectively, this study has identified several transcription factors which due to their expression characteristics and orthologous functions in other systems represent likely candidates to participate in the transcriptional pathways leading to wall ingrowth deposition in epidermal TCs. The challenge now is to establish causal relationships between these genes and roles in regulating aspects of epidermal TC development in *V. faba* cotyledons. A robust transformation system for *V. faba* is not available, thus making a genetic approach to this challenge difficult. However, the induction of wall ingrowth deposition in epidermal TC of cultured cotyledons can be substantially delayed in the presence of inhibitors affecting auxin and ethylene signaling (Zhang et al., 2015a), thus making delivery of RNAi or other constructs by biolistic bombardment a possibility to demonstrate a role for these candidates in regulating epidermal TC development.

## Acknowledgements

We thank Dr Damien Drew for advice on RNA-Seq data analysis and Joe Enright for valuable help with plant growth. This project was supported by funds from an ARC Discovery Grant (DP110100770) and a University of Newcastle Faculty of Science and Information Technology Strategic Research Initiative Grant to DWMcC. KSAC was supported by UNIPRS and UNRSC Scholarships.

## Supplementary Material

The Supplementary Material for this article can be found online at:

## References

- Andriunas, F.A., Zhang, H.M., Weber, H., McCurdy, D.W., Offler, C.E., and Patrick, J.W. (2011). Glucose and ethylene signaling pathways converge to regulate *trans*-differentiation of epidermal transfer cells in *Vicia narbonensis* cotyledons. *Plant J.* 68, 987–998.
- Andriunas, FA, Zhang, H.M., Xia, X., Offler, C.E., McCurdy, D.W., and Patrick, J.W.

- (2012). Reactive oxygen species form part of a regulatory pathway initiating *trans*-differentiation of epidermal transfer cells in *Vicia faba* cotyledons. *J. Exp. Bot.* 63, 3617-3629.
- Ariel, F.D., Manavella, P.A., Dezar, C.A., and Chan, R.L. (2007). The true story of the HD-Zip family. *Trends Plant Sci.* 12, 419-426.
- Arun-Chinnappa, K.S., and McCurdy, D.W. (2015). De novo assembly of a genome-wide transcriptome map of *Vicia faba* (L.) for transfer cell research. *Front. Plant Sci.* 6:217. doi: 10.3389/fpls.2015.00217
- Arun-Chinnappa, K.S., Nguyen, T.T., Hou, J., Wu, Y., and McCurdy, D.W. (2013). Phloem parenchyma transfer cells in *Arabidopsis* – an experimental system to identify transcriptional regulators of wall ingrowth formation. *Front. Plant Sci.* 4:102. doi: 10.3389/fpls.2013.00102
- Ayadi, M., Delaporte, V., Li, Y.F., and Zhou, D.X. (2004). Analysis of GT-3a identifies a distinct subgroup of trihelix DNA-binding transcription factors in *Arabidopsis*. *FEBS Lett.* 562, 147–154.
- Barrero, C., Royo, J., Grijota-Martinez, C., Faye, C., Paul, W., Sanz, S., et al. (2009). The promoter of *ZmMRP-1*, a maize transfer cell-specific transcriptional activator, is induced at solute exchange surfaces and responds to transport demands. *Planta* 229, 235–247.
- Berendzen, K.W., Weiste, C., Wanke, D., Kilian, J., Harter, K., and Dröge-Laser, W. (2012). Bioinformatic *cis*-element analyses performed in *Arabidopsis* and rice disclose bZIP- and MYB-related binding sites as potential AuxRE-coupling elements in auxin-mediated transcription. *BMC Plant Biol.* 12:125. doi: 10.1186/1471-2229-12-125
- Birkenbihl, R.P., Diezel, C., and Somssich, I.E. (2012). *Arabidopsis* WRKY33 is a key transcriptional regulator of hormonal and metabolic responses towards *Botrytis cinerea* infection. *Plant Physiol.* 159, 266–285.
- Cabrera, J., Barcala, M., Fenoll, C., and Escobar, C. (2014). Transcriptomic signatures of transfer cells in early developing nematode feeding cells of *Arabidopsis* focused on auxin and ethylene signaling. *Front. Plant Sci.* 5:107. doi: 10.3389/fpls.2014.00107
- Capella, M., Ribone, P.A., Arce, A.L., and Chan, R.L. (2015). *Arabidopsis thaliana* HomeoBox 1 (AtHB1), a Homeodomain-Leucine Zipper I (HD-Zip I) transcription factor, is regulated by PHYTOCHROME-INTERACTING FACTOR 1 to promote hypocotyl elongation. *New Phytol.* 207, 669–682.

- Dibley, S.J., Zhou, Y., Andriunas, F.A., Talbot, M.J., Offler, C.E., Patrick, J.W., et al. (2009). Early gene expression programs accompanying *trans*-differentiation of epidermal cells of *Vicia faba* cotyledons into transfer cells. *New Phytol.* 182, 863–877.
- Farley, S.J., Patrick, J.W., and Offler, C.E. (2000). Functional transfer cells differentiate in cultured cotyledons of *Vicia faba* L. seeds. *Protoplasma* 214, 102-117.
- Fry, S.C. (1992). Oxidative scission of plant cell wall polysaccharides by ascorbate-induced hydroxyl radicals. *Biochem. J.* 332, 507–515.
- Gómez, E., Royo, J., Guo, Y., Thompson, R., and Hueros, G. (2002). Establishment of cereal endosperm expression domains: identification and properties of a maize transfer cell-specific transcription factor, ZmMRP-1. *Plant Cell* 14, 599-610.
- Gómez, E., Royo, L.M., Sellam, O., Paul, W., Gerentes, D., Barrero, C., et al. (2009). The maize transcription factor Myb-related protein-1 is a key regulator of the differentiation of transfer cells. *Plant Cell* 21, 2022-2035.
- Grunewald, W., De Smet, I., Lewis, D.R., Lofke, C., Jansen, L., Goeminne, G. et al. (2012). Transcription factor WRKY23 assists auxin distribution patterns during *Arabidopsis* root development through local control on flavonol biosynthesis. *Proc. Natl. Acad. Sci. USA* 109, 1554–1559.
- Grunewald, W., Karimi, M., Wieczorek, K., Van de Cappelle, E., Wischnitzki, E., Grundler, F., et al. (2008). A role for AtWRKY23 in feeding site establishment of plant-parasitic nematodes. *Plant Physiol.* 148: 358–368.
- Gunning, B.E.S., and Pate, J.S. (1974). “Transfer cells” in *Dynamic Aspects of Plant Ultrastructure*, ed. A.W. Robards (London: McGraw-Hill), 441–479.
- Gutierrez-Marcos, J.F., Costa, L.M., Biderre-Petit, C., Khbaya, B., O'Sullivan, D.M., Wormald, M., et al. (2004). Maternally expressed gene1 is a novel maize endosperm transfer cell-specific gene with a maternal parent-of-origin pattern of expression. *Plant Cell* 16, 1288-1301.
- Iwase, A., Mitsuda, N., Koyama, T., Hiratsu, K., Kojima, M., Arai, T., et al. (2011). The AP2/ERF transcription factor WIND1 controls cell dedifferentiation in *Arabidopsis*. *Curr. Biol.* 21, 508–514.
- Kaplan-Levy, R.N., Brewer, P.B., Quon, T., and Smyth, D.R. (2012). The trihelix family of transcription factors – light, stress and development. *Trends Plant Sci.* 17, 163-171.

- Kubo, M., Udagawa, M., Nishikubo, N., Horiguchi, G., Yamaguchi, M., Ito, J., et al. (2005). Transcription switches for protoxylem and metaxylem vessel formation. *Genes Dev.* 19, 1855–1860.
- Liu Q., Wen C., Zhao H., Zhang L., Wang J., Wang Y. (2014). RNA-Seq reveals leaf cuticular wax-related genes in welsh onion. *PLoS ONE* 9: doi: e113290. doi:10.1371/journal.pone.0113290
- Maeda, H., Sage, T.L., Isaac, G., Welti, R., and DellaPenna D. (2008). Tocopherols modulate extraplastidic polyunsaturated fatty acid metabolism in *Arabidopsis* at low temperature. *Plant Cell* 20, 452–470.
- Maeda, H., Song, W., Sage, T.L., and DellaPenna D. (2006). Tocopherols play a crucial role in low-temperature adaptation and phloem loading in *Arabidopsis*. *Plant Cell* 18, 2710–2732.
- Maeda, H., Song, W., Sage, T.L., and DellaPenna, D. (2014). Role of callose synthases in transfer cell wall development in tocopherol deficient mutants. *Front. Plant Sci.* 5:46. doi: 10.3389/fpls.2014.00046
- Martin, L.B.B., Fei, Z., Giovannoni, J.J. and Rose, J.K.C. (2013). Catalyzing plant science research with RNA-seq. *Front. Plant Sci.* 4:66. doi: 10.3389/fpls.2013.00066
- McCurdy, D.W. (2015). “Transfer cells: novel cell types with unique wall ingrowth architecture designed for optimal nutrient transport” in *Plant Cell Wall Patterning and Cell Shape*, ed. H. Fukuda (Hoboken, New Jersey: Wiley-Blackwell), 287-317.
- McCurdy, D.W., Patrick, J.W., and Offler, C.E. (2008). Wall ingrowth formation in transfer cells: novel examples of localized wall deposition in plant cells. *Curr. Opin. Plant Biol.* 11, 653-661.
- Mehrnia, M., Balazadeh, S., Zanol, M.-I., and Mueller-Roeber, B. (2013). EBE, an AP2/ERF transcription factor highly expressed in proliferating cells, affects shoot architecture in *Arabidopsis*. *Plant Physiol.* 162, 842-857.
- Müniz, L.M., Royo, J., Gómez, E., Barrero, C., Bergareche, D., and Hueros, G. (2006). The maize transfer cell-specific type-A response regulator ZmTCRR-1 appears to be involved in intercellular signaling. *Plant J.* 48, 17-27.
- Nakano, Y., Nishikubo, N., Goué, N., Ohtani, M., Yamaguchi, M., Katayama, Y., et al. (2010). MYB transcription factors orchestrating the developmental program of xylem vessels in *Arabidopsis* roots. *Plant Biotechnol.* 27, 267–272.
- Nguyen, T.T.S., and McCurdy, D.W. (2016). “Transdifferentiation – a plant perspective”

- in *Molecular Cell Biology of the Growth and Differentiation of Plant Cells*, ed. R.J. Rose (Boca Raton: CRC Press), in press.
- Offler, C.E., Liet, E., and Sutton, E.G. (1997). Transfer cell induction in cotyledons of *Vicia faba* L. *Protoplasma* 200, 51–64.
- Offler, C.E., McCurdy, D.W., Patrick, J.W., and Talbot, M.J. (2003). Transfer cells: cells specialized for a special purpose. *Annu. Rev. Plant Biol.* 54, 431–454.
- O'Rourke, J.A., Yang, S.S., Miller, S.S., Bucciarelli, B., Liu, J., Rydeen, A., et al. (2013). An RNA-Seq transcriptome analysis of orthophosphate-deficient white lupin reveals novel insights into phosphorus acclimation in plants. *Plant Physiol.* 161, 705-724.
- Park, H.C., Kim, M.L., Kang, Y.H., Jeon, J.M., Yoo, J.H., Kim, M.C., et al. (2004). Pathogen- and NaCl-induced expression of the SCaM-4 promoter is mediated in part by a GT-1 box that interacts with a GT-1-like transcription factor. *Plant Physiol.* 135, 2150–2161.
- Rocha, S., Monjardino, P., Mendonça, D., Machado, AC., Fernandes, R., Sampaio, P., et al. (2014). Lignification of developing maize (*Zea mays* L.) endosperm transfer cells and starchy endosperm cells. *Front. Plant Sci.* 5:102. doi: 10.3389/fpls.2014.00102
- Rushton, P.J., Somssich, I.E., Ringler, P., and Shen, Q.J. (2010). WRKY transcription factors. *Trends Plant Sci.* 15, 247–258.
- Schopfer, P. (2002). Hydroxyl radical-induced cell-wall loosening in vitro and in vivo: implications for the control of elongation growth. *Plant J.* 28, 679–688.
- Simon, P. (2003). Q-Gene: processing quantitative real-time RT-PCR data. *Bioinformatics* 19, 1439–1440.
- Simon, S.A., Zhai, J., Nandety, R.S., McCormick, K.P., Zeng, J., Mejia, D., et al. (2009). Short-read sequencing technologies for transcriptional analyses. *Annu. Rev. Plant Biol.* 60, 305–333.
- Sweetman, C., Wong, D., Ford, C., and Drew, D. (2012). Transcriptome analysis at four developmental stages of grape berry (*Vitis vinifera* cv. Shiraz) provides insights into regulated and coordinated gene expression. *BMC Genomics* 13:691. doi: 10.1186/1471-2164-13-691
- Talbot, M.J., Wasteneys, G., McCurdy, D.W., Offler, C.E. (2007). Deposition patterns of cellulose microfibrils in flange wall ingrowths of transfer cells indicate clear parallels with those of secondary wall thickenings. *Func. Plant Biol.* 34: 307-313.
- Thiel, J. (2014). Development of endosperm transfer cells in barley. *Front. Plant Sci.*

5:108. doi: 10.3389/fpls.2014.00108

- Thiel, J., Hollmann, J., Rutten, T., Weber, H., Scholz, U., and Weschke, W. (2012). 454 transcriptome sequencing suggests a role for two-component signaling in cellularization and differentiation of barley endosperm transfer cells. *PLoS ONE* 7: e41867-e41867.
- Thiel, J., Weier, D., Sreenivasulu, N., Strickert, M., Weichert, N., Melzer, M., Czauderna, T., Wobus, U., Weber, H., and Weschke, W. (2008). Different hormonal regulation of cellular differentiation and function in nucellar projection and endosperm transfer cells: a microdissection-based transcriptome study of young barley grains. *Plant Physiol.* 148, 1436-1452.
- Turchi, L., Carabelli, M., Ruzza, V., Possenti, M., Sassi, M., and Peñalosa, A. et al. (2013). *Arabidopsis* HD-Zip II transcription factors control apical embryo development and meristem function. *Development* 140, 2118-2129.
- Vaughn, K.C., Talbot, M.J., Offler, C.E., and McCurdy, D.W. (2007). Wall ingrowths in epidermal transfer cells of *Vicia faba* cotyledons are modified primary walls marked by localized accumulations of arabinogalactan proteins. *Plant Cell Physiol.* 48, 159–168.
- Weber, A.P.M. (2015). Discovering new biology through sequencing of RNA. *Plant Physiol.* 169, 1524-1531.
- Wu, K.L., Guo, Z.J., Wang, H.H., and Li, J. (2005). The WRKY family of transcription factors in rice and *Arabidopsis* and their origins. *DNA Res.* 12, 9–26.
- Zhang, H.-M., van Helden, D.F., McCurdy, D.W., Offler, C.E., and Patrick, J.W. (2015a). Plasma membrane Ca<sup>2+</sup>-permeable channels are differentially regulated by ethylene and hydrogen peroxide to generate persistent plumes of elevated cytosolic Ca<sup>2+</sup> during transfer cell *trans*-differentiation. *Plant Cell Physiol.* 56, 1711-1720.
- Zhang, Z., Wang, J., Zhang, R., and Huang, R. (2012). ERF protein AtERF98 enhances tolerance to salt through the transcriptional activation of ascorbic acid synthesis in *Arabidopsis*. *Plant J.* 71, 273–287.
- Zhang, H.-M., Wheeler, S., Xia, X., Radchuk, R., Weber, H., Offler, C.E., et al. (2015b). Differential transcriptional networks associated with key phases of ingrowth wall construction in *trans*-differentiating epidermal transfer cells of *Vicia faba* cotyledons. *BMC Plant Biol.* 15:103 doi: 10.1186/s12870-015-0486-5
- Zhao, S., Fung-Leung, W.P., Bittner, A., Ngo, K., and Liu, X. (2014). Comparison of

- RNA-Seq and microarray in transcriptome profiling of activated T cells. *PLoS ONE* 9:e78644.10.1371/journal.pone.0078644
- Zhong, R., Lee, C., and Ye, Z.H. (2010). Evolutionary conservation of the transcriptional network regulating secondary cell wall biosynthesis. *Trends Plant Sci.* 15, 625-632.
- Zhou, Y.C., Andriunas, F., Offler, C.E., McCurdy, D.W., and Patrick, J.W. (2010). An epidermal-specific ethylene signal cascade regulates *trans*-differentiation of transfer cells in *Vicia faba* cotyledons. *New Phytol.* 185, 931-943.
- Zhou, J., Lee, C., Zhong, R., and Ye, Z.H. (2009). MYB58 and MYB63 are transcriptional activators of the lignin biosynthetic pathway during secondary cell wall formation in *Arabidopsis*. *Plant Cell* 21, 248–266.

**Table 1 Transcription factors displaying epidermal-specific, up-regulated expression in epidermal transfer cells of cultured *Vicia faba* cotyledons.**

| Unigene ID | Gene Product (Viridiplantae)                            | Species (Accession number)            | E value (BLASTX) | Arabidopsis gene product (AT number)                       | Log <sub>2</sub> Fold Change Epidermal and storage parenchyma (brackets) tissue compared to 0-h |            |            |
|------------|---|---------------------------------------|------------------|--|---|------------|------------|
|            |   |                                       |                  |  | 3-h   | 9-h        | 24-h       |
| 13378      | Trihelix transcription factor GT-3B-like                | <i>C. arietinum</i> (XP_004514215)    | 8e-49            | Homeodomain-like superfamily                               | 8.9 (-)   | 7.1 (-)    | 6.5 (-)    |
| 9668       | P-type R <sub>2</sub> R <sub>3</sub> MYB protein        | <i>M. truncatula</i> (XP_003600714.1) | 4e-115           | ATMYB20 (AT1G66230)  | 7.1 (-)   | 5.6 (0)    | 4.9 (0.5)  |
| 7266       | Ethylene-responsive transcription factor                | <i>M. truncatula</i> (XP_003638785.1) | 2e-97            | ERF/AP2 transcription factor RAP2.4 (AT1G78080)            | 4.3 (0)   | 3.2 (0)    | 3.3 (0.4)  |
| 20101      | Transcription factor bHLH122-like                       | <i>C. arietinum</i> (XP_004486946.1)  | 1e-97            | Basic Helix-Loop-Helix (bHLH) (AT2G42280)                  | 4.0 (-)   | 1.0 (-)    | - (-)      |
| 19492      | MYB family transcription factor-like protein            | <i>M. truncatula</i> (XP_003618488.1) | 4e-124           | ATMYB30 (AT3G28910)  | 3.8 (0)   | 1.0 (-0.9) | 0 (-1)     |
| 3890       | R <sub>2</sub> R <sub>3</sub> -MYB transcription factor | <i>M. truncatula</i> (XP_003599668.1) | 5e-152           | ATMYB31 (AT1G74650)  | 3.7 (1)   | 2.3 (-0.2) | 2.0 (0.4)  |
| 13430      | DOF zinc finger protein                                 | <i>M. truncatula</i> (XP_003638640.1) | 1e-42            | DOF zinc finger protein 1 (AT1G51700)                      | 3.6 (0)   | 1.0 (0.4)  | 2.0 (0.8)  |
| 14644      | Zinc finger (GATA type) family protein                  | <i>T. repens</i> (ADD09603.1)         | 6e-136           | GATA transcription factor 5 (AT5G66320)                    | 3.5 (0)   | 1.0 (0)    | 2.3 (-0.4) |
| 12504      | MYB transcription factor                                | <i>M. truncatula</i> (XP_003616176.1) | 6e-144           | MYB-like transcription factor (AT5G17300)                  | 3.3 (-1)  | 2.0 (-0.6) | 2.3 (-0.1) |
| 20627      | bHLH transcription factor                               | <i>M. truncatula</i> (XP_003626938.1) | 6e-97            | Basic Helix-Loop-Helix (bHLH) (AT3G07340)                  | 3 (-)   | 1 (1.0)    | 1 (-)      |
| 9906       | Homeobox protein SBH1-like                              | <i>C. arietinum</i> (XP_004491125.1)  | 4e-147           | KNOX/ELK homeobox transcription factor (AT1G62360)         | 2.8 (-)   | 1.0 (-)    | 1.0 (-)    |
| 7007       | Ethylene-responsive transcription factor                | <i>M. truncatula</i> (XP_003616666.1) | 2e-56            | ERF/AP2 transcription factor ABA INSENSITIVE 4 (AT2G40220) | 2.6 (1)   | 1.0 (0.3)  | 1.0 (-0.1) |
| 18946      | TCP family transcription factor-like protein            | <i>M. truncatula</i> (XP_003613691.1) | 7e-103           | TCP family transcription factor (AT1G69690)                | 2.3 (-)   | 1.0 (-)    | 1.0 (-)    |

|       |   |  |        |   |           |               |              |
|-------|---|--|--------|---|-----------|---------------|--------------|
| 771   | Transcription factor bHLH78-like                | <i>C. arietinum</i><br>(XP_004492265.1)  | 1e-173 | Basic Helix-Loop-Helix (bHLH)<br>(AT3G07340)                | -<br>(0)  | 2.8<br>(-0.5) | 2.0<br>(0.2) |
| 7111  | MYB transcription factor                        | <i>M. truncatula</i><br>(XP_003624757.1) | 9e-100 | ATMYB60<br>(AT1G08810)                                      | -<br>(-)  | 4.4<br>(-)    | 3.8<br>(-)   |
| 17302 | MYB transcription factor MYB56                  | <i>G. max</i><br>(NP_001235662.1)        | 2e-68  | ATMYB4<br>(AT4G38620)                                       | -<br>(-1) | 3.3<br>(-0.9) | 3.3<br>(-)   |
| 19002 | MYB-related protein MYB4-like                   | <i>C. arietinum</i><br>(XP_004488797.1)  | 4e-75  | ATMYB63<br>(AT1G79180)                                      | -<br>(-)  | 3.6<br>(-)    | 5.0<br>(-)   |
| 12445 | Transcription factor MYB113-like                | <i>G. max</i><br>(XP_003529126.1)        | 3e-139 | ATMYB114<br>(AT1G66380)                                     | -<br>(-)  | 0<br>(-)      | 2.8<br>(-)   |
| 13120 | Transcription factor ASG4-like isoform X1       | <i>C. arietinum</i><br>(XP_004497454.1)  | 2e-158 | MYB-like transcription factor LHY-CCA1-LIKE5<br>(AT3G09600) | -<br>(-)  | 0<br>(-)      | 2.3<br>(-)   |
| 10245 | Ethylene-responsive transcription factor RAP2-6 | <i>M. truncatula</i><br>(XP_003602747.1) | 4e-99  | ERF/AP2 transcription factor<br>(AT5G61890)                 | -<br>(-)  | 5.8<br>(-)    | 6.5<br>(-)   |
| 14898 | WRKY transcription factor 28-like isoform X1    | <i>C. arietinum</i><br>(XP_004491329.1)  | 3e-77  | ATWRKY71<br>(AT1G29860)                                     | 0<br>(-)  | 1.0<br>(-)    | 4.7<br>(-)   |
| 21012 | Ovate family protein 1                          | <i>M. truncatula</i><br>(AFK43560.1)     | 1e-25  | Ovate family protein 1<br>(AT5G01840)                       | 0<br>(0)  | 1.0<br>(0.9)  | 3.3<br>(0)   |

Gene name and species correspond to annotation based on Viridiplantae data set. *E* value refers to BLASTX comparison of the unigene sequence with the Viridiplantae gene. The orthologous gene from Arabidopsis and its AT number is listed. Log<sub>2</sub> Fold Change was determined by calculating ratio of RPKM values at 3-, 9- and 24-h culture compared to 0-h, for both epidermal (open numbers) and storage parenchyma (bracketed numbers). The term “-“ indicates no expression, while the value “0” indicates fold change of 1, i.e., no difference in gene expression between the two time points.

**Table 2 Transcription factors displaying epidermal-specific, down-regulated expression in epidermal transfer cells of cultured *Vicia faba* cotyledons**

| Unigene ID | Gene Product (Viridiplantae)                          | Species (Accession number)            | E value (BLAST X) | Arabidopsis gene name (AT number)   | Log <sub>2</sub> Fold Change Epidermal and storage parenchyma (brackets) tissue compared to 0-h |           |            |
|------------|---|---------------------------------------|-------------------|---|---|-----------|------------|
|            |   |                                       |                   |   | 3-h   | 9-h       | 24-h       |
| 2074       | Homeobox-leucine zipper protein ATHB-16               | <i>M. truncatula</i> (XP_003613578.1) | 1e-167            | ATHB-1 (AT3G01470)  | 3.6 (-0.6)  | 0 (0.9)   | 0 (1.0)    |
| 1229       | Homeobox-leucine zipper protein                       | <i>C. arietinum</i> (XP_004515372.1)  | 7e-113            | Homeobox-leucine zipper protein 3 (AT3G60390)                             | 3.5 (-0.2)  | 1.6 (0.2) | 1.0 (0.3)  |
| 20713      | MADS-box protein SOC1-like                            | <i>C. arietinum</i> (XP_004510894.1)  | 2e-84             | AGAMOUS-like 20 (AT2G45660)   | 3.2 (-)   | 3.2 (-)   | 1.6 (-)    |
| 21180      | Squamosa promoter-binding protein 1-like isoform X1   | <i>G. max</i> (XP_003541730.1)        | 1e-48             | Squamosa promoter binding protein-like 3 (AT2G33810)                      | 2.8 (-)   | 3.3 (-)   | 3.3 (-)    |
| 7803       | Zinc finger CCCH domain-containing protein 53-like    | <i>C. arietinum</i> (XP_004513268.1)  | 0                 | Zinc finger (CCCH-type) family protein (AT3G51950)                        | 2.6 (-0.2)  | 1.6 (0.6) | 1.6 (-0.1) |
| 16720      | MADS-box transcription factor 12                      | <i>P. sativum</i> (AGV40795.1)        | 3e-139            | MADS-box transcription factor family protein (AT4G18960)                  | 2.3 (-)   | 2.8 (-)   | 1 (-)      |
| 14359      | TMV resistance protein N                              | <i>M. truncatula</i> (XP_003612869.1) | 5e-133            | Disease resistance protein (TIR-NBS-LRR class) family (AT5G36930)         | 2.3 (-)   | 1.6 (-)   | 3.2 (-)    |
| 19507      | mTERF domain-containing protein                       | <i>M. truncatula</i> (XP_003617710.1) | 5e-157            | Mitochondrial transcription termination factor family protein (AT5G55580) | 1.6 (0.2)   | 2.6 (0.3) | 1.0 (0)    |
| 464        | AP2-like ethylene-responsive transcription factor ANT | <i>M. truncatula</i> (XP_003608564.1) | 1e-75             | AINTEGUMENTA (AT4G37750)  | 1 (0.8)   | 1.6 (1.8) | 3.8 (0)    |
| 16491      | High mobility group B protein 6-like                  | <i>C. arietinum</i> (XP_004503638.1)  | 6e-80             | HMG (high mobility group) box protein (AT4G11080)                         | 0 (-0.1)  | 1.0 (0)   | 2.8 (-0.4) |

Gene name and species correspond to annotation based on Viridiplantae data set. E value refers to BLASTX comparison of the unigene sequence with the Viridiplantae gene. The orthologous gene from Arabidopsis and its AT number is listed. Log<sub>2</sub> Fold Change was determined by calculating ratio of RPKM values at 0-h compared to 3-, 9- and 24-h culture, for both epidermal (open numbers) and storage parenchyma (bracketed numbers). The term “-” indicates no expression, while the value “0” indicates fold change of 1, i.e., no difference in gene expression between the two time points.

**Table 3 Transcription factors displaying epidermal-enhanced, up-regulated expression in epidermal transfer cells of cultured *Vicia faba* cotyledons**

| Unigene ID | Gene Product (Viridiplantae)                    | Species (Accession number)            | E value (BLAST X) | Arabidopsis gene name (AT number)                        | Fold change |           | Fold difference                     |
|------------|---|---------------------------------------|-------------------|--|-------------|-----------|-------------------------------------|
|            |   |                                       |                   |  | EP          | SP        |                                     |
|            |   |                                       |                   |  | 3-h v 0-h   | 3-h v 0-h | EP fold change minus SP fold change |
| 11848      | WRKY transcription factor 28-like               | <i>C. arietinum</i> (XP_004504707)    | 2e-71             | ATWRKY28 (AT4G18170)                                     | 378         | 1         | 377                                 |
| 19283      | Ethylene-responsive transcription factor        | <i>M. truncatula</i> (XP_003630161.1) | 1e-74             | ABA REPRESSOR1 (AT5G64750)                               | 332         | 7         | 325                                 |
| 10055      | Transcription factor WRKY                       | <i>M. truncatula</i> (XP_003610463.1) | 4e-142            | ATWRKY6 (AT1G62300)                                      | 278         | 1         | 277                                 |
| 12104      | WRKY transcription factor 33-like               | <i>C. arietinum</i> (XP_004506827.1)  | 0                 | ATWRKY33 (AT2G38470)                                     | 191         | 1         | 190                                 |
| 7382       | Hypothetical protein PHAVU_007G102900g          | <i>P. vulgaris</i> (ESW15796.1)       | 5e-42             | MYB-like transcription factor family protein (AT1G68670) | 131         | 4         | 127                                 |
| 7356       | Putative ethylene responsive factor             | <i>V. faba</i> (ACD87816.1)           | 1e-50             | ATERF98 (AT3G23230)                                      | 121         | 3         | 118                                 |
| 2088       | WRKY transcription factor                       | <i>M. truncatula</i> (XP_003625994.)  | 5e-135            | ATWRKY23 (AT2G47260)                                     | 81          | 2         | 79                                  |
| 10876      | Ethylene-responsive transcription factor ERF110 | <i>M. truncatula</i> (XP_003592075.1) | 1e-61             | ABA REPRESSOR1 (AT5G64750)                               | 78          | 2         | 76                                  |
| 11312      | WRKY transcription factor                       | <i>M. truncatula</i> (XP_003629812.1) | 2e-137            | ATWRKY65 (AT1G29280)                                     | 73          | 12        | 61                                  |
| 15437      | Zinc finger and SCAN domain-containing protein  | <i>M. truncatula</i> (XP_003604663.1) | 1e-111            | Homeodomain-like superfamily protein (AT2G38250)         | 69          | 1         | 68                                  |
| 3427       | WRKY transcription factor 48-like               | <i>C. arietinum</i> (XP_004486582.1)  | 3e-64             | ATWRKY48 (AT5G49520)                                     | 64          | 1         | 63                                  |
| 20862      | MYB family transcription factor APL             | <i>M. truncatula</i> (XP_003613820.1) | 1e-82             | Homeodomain-like superfamily protein (AT1G69580)         | 48          | 2         | 46                                  |

|       |   |  |        |   |    |   |    |
|-------|---|--|--------|---|----|---|----|
| 5690  | Transcriptional repressor NF-X1                                 | <i>M. truncatula</i><br>(XP_003605239.1) | 0      | ATNFXL1<br>(AT1G10170)                                    | 46 | 2 | 44 |
| 2809  | WRKY transcription factor WRKY100630                            | <i>M. truncatula</i><br>(ACD40316.1)     | 0      | ATWRKY6<br>(AT1G62300)                                    | 46 | 2 | 44 |
| 10215 | WRKY family transcription factor                                | <i>C. arietinum</i><br>(ABX10954.1)      | 5e-140 | AtWRKY41<br>(AT4G11070)                                   | 42 | 2 | 40 |
| 18475 | Transcription factor DIVARICATA-like isoform X1                 | <i>C. arietinum</i><br>(XP_004500230.1)  | 4e-69  | Homeodomain-like transcriptional regulator<br>(AT5G58900) | 31 | 2 | 29 |
| 10039 | Putative C <sub>2</sub> H <sub>2</sub> type zinc finger protein | <i>M. truncatula</i><br>(XP_013457625.1) | 2e-93  | Unknown Protein<br>(AT4G12450)                            | 30 | 1 | 29 |
| 1309  | NAC-domain protein  | <i>M. truncatula</i><br>(XP_003602684.1) | 2e-165 | ANAC002<br>(AT1G01720)                                    | 29 | 2 | 27 |
| 19791 | WRKY transcription factor 56                                    | <i>M. sativa</i><br>(AEI83414.1)         | 2e-110 | ATWRKY40<br>(AT1G80840)                                   | 27 | 2 | 25 |
| 18219 | NAC domain-protein  | <i>M. truncatula</i><br>(XP_003607287.1) | 3e-142 | ANAC036<br>(AT2G17040)                                    | 27 | 2 | 25 |

Gene name and species correspond to annotation based on Viridiplantae data set. *E* value refers to BLASTX comparison of the unigene sequence with the Viridiplantae gene. The orthologous gene from Arabidopsis and its AT number is listed. “Fold Change” represents ratio derived for RPKM value from epidermal (EP) and storage parenchyma (SP) tissues at 3-h compared to 0-h culture. Fold difference is the difference between the fold change in epidermal tissue and storage parenchyma tissue. Only those transcripts showing a numerical fold-difference of  $\geq 25$  were selected, whereby differential expression of these transcripts in epidermal tissue is 25 times greater than in storage parenchyma.

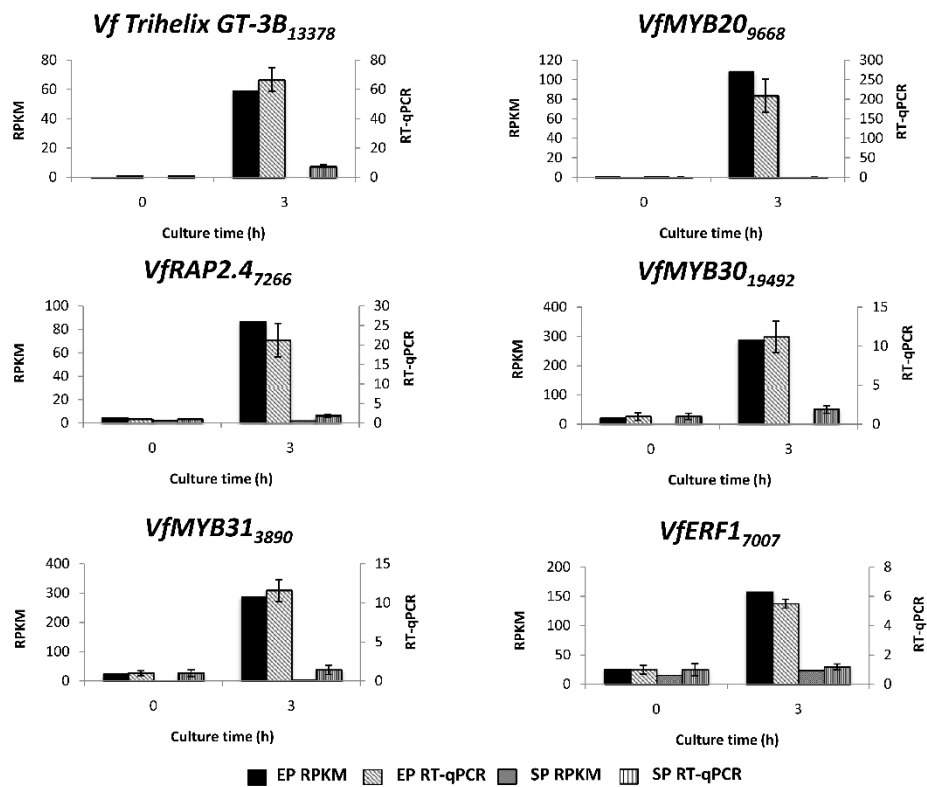


**FIGURE 1 | Validation by RT-qPCR of selected transcription factor genes displaying epidermal-specific up-regulation as determined by RNA-Seq analysis.** Comparison of transcript expression determined by RNA-Seq (RPKM) and RT-qPCR across cotyledon culture (0- and 3-h) in both epidermal (EP) and storage parenchyma (SP) tissue. The RT-qPCR data is presented as expression normalized against *Vf Elongation Factor alpha* (Andriunas et al., 2012) at 0-h culture and is derived from the average of three biological replicates, with each replicate consisting of epidermal peels and storage parenchyma tissue obtained from 5-8 cotyledons (data shows mean  $\pm$  SEM). Expression derived by RNA-Seq is indicated as RPKM. The subscript number associated with each *V. faba* transcript name indicates the relevant Unigene number.

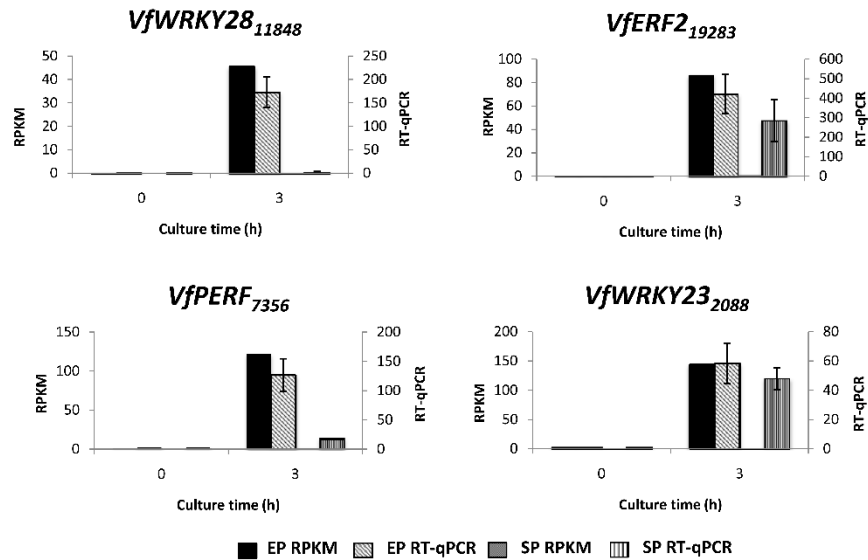


**FIGURE 2 | Validation by RT-qPCR of selected transcription factor genes displaying epidermal-enhanced up-regulation as determined by RNA-Seq analysis.** Comparison of transcript expression determined by RNA-Seq (RPKM) and qRT-PCR across cotyledon culture (0- and 3-h) in both epidermal (EP) and storage parenchyma (SP) tissue. The RT-qPCR data is presented as expression normalized against *Vf Elongation Factor alpha* (Andriunas et al., 2012) at 0-h culture and is derived from the average of three biological replicates, with each replicate consisting of epidermal peels and storage parenchyma tissue obtained from 5-8 cotyledons (data shows mean  $\pm$  SEM). Expression derived by RNA-Seq is indicated as RPKM. The subscript number associated with each *V. faba* transcript name indicates the relevant Unigene number.

**CHAPTER 4**  
**PHENOTYPIC ANALYSIS OF**  
**TRANSCRIPTION FACTORS AS CANDIDATE**  
**REGULATORS OF TC DEVELOPMENT**  
**USING *Arabidopsis thaliana***

## 4.1 INTRODUCTION

The RNA-Seq analysis of adaxial epidermal TC development in *Vicia faba* cotyledons reported in Chapter 3 identified several transcription factors with expression characteristics and orthologous functions that identified them as potentially involved in regulating wall ingrowth deposition during TC development. Many of these transcription factors are members of the MYB, WRKY and homeodomain families in plants, families which collectively have numerous roles in plant development (Mukherjee and Brocchieri, 2010; Rushton et al., 2010; Ambawat et al., 2013). Many of these transcription factors showed substantial fold-increase in epidermal-specific and epidermal-enhanced expression by 3 h of cotyledon culture, leading to the hypothesis that they may have roles in the *trans*-differentiation of epidermal TCs. Testing a role for these transcription factors through genetic modification of *V. faba* is not feasible due to the lack of an efficient and widely adopted transformation protocol (see Bahgat et al., 2009). Hence an alternative genetic system to test the putative role of these transcription factors is needed. *Arabidopsis thaliana* (Arabidopsis), a flowering plant from family brassicaceae, is the most widely used genetic model in plant biology. The fully sequenced genome, availability of a huge collection of T-DNA insertion mutants, and extensive transcriptional databases derived from microarray and now NGS databases, provides a unique set of experimental tools for molecular and genetic analysis of biological processes occurring in plants (Meinke et al., 1998; Arabidopsis Genome, 2000; Koornneef and Meinke, 2010). PP cells in vascular bundles of Arabidopsis leaves *trans*-differentiate to form PP TCs with reticulate-type wall ingrowths (Haritatos et al., 2000; Amiard et al., 2007), and the extent of wall ingrowth deposition is responsive to abiotic stresses such as high light and low temperature (Maeda et al., 2006; Amiard et al., 2007; Maeda et al., 2008). Consequently, PP TCs provide a good system to study the transcriptional regulation of reticulate-type wall ingrowth deposition.

The original descriptions of PP TCs in Arabidopsis used transmission electron microscopy (TEM), as these cells are located deep within the vascular tissue and are not easily accessible for manipulation and experimentation. To address this situation, McCurdy and colleagues developed calcofluor white as a stain to detect wall ingrowth deposition in PP TCs by fluorescence microscopy (Edwards et al., 2010), and later used aniline blue to detect callose putatively associated with wall ingrowths in these cells (see

Arun-Chinnappa et al., 2013; Appendix 1). Both stains were used for fluorescence microscopy to survey PP TC abundance across leaf development and in response to different experimental conditions, but subsequent imaging by confocal microscopy revealed that both stains could not be relied upon to exclusively report the presence of PP TCs (Nguyen – unpublished data). However, to overcome this problem, Nguyen and McCurdy (2015) recently adapted a modified pseudo-Schiff-propidium iodide (mPS-PI) method for staining cell walls (see Truernit et al., 2008; Wuyts et al., 2010) to develop a convenient procedure for confocal imaging of wall ingrowth deposition in PP TCs. While the mPS-PI procedure labels cell walls generally, the high local abundance of polysaccharide-rich wall ingrowths in PP TCs made these structures easily identifiable (Nguyen & McCurdy, 2015). Therefore, development of this staining protocol coupled with high-resolution three-dimensional analysis by confocal imaging has proven to be an efficient tool for studying wall ingrowth deposition in PP TCs (Nguyen and McCurdy, 2015). This efficiency therefore opened the possibility to rapidly screen T-DNA insertional mutants of orthologous genes identified from the RNA-Seq analysis for altered wall ingrowth phenotypes in PP TCs.

In this chapter, a genetics approach has been used to test the role of genes identified by RNA-Seq analysis as putatively involved in regulating epidermal TC development in *V. faba* cotyledons. This approach was undertaken by identifying the closest orthologous gene in Arabidopsis and analysing PP TC development in mutant lines carrying a T-DNA insertion in that gene. To address functional redundancy issues when using single mutants, this approach was extended for most genes by testing PP TC development in double mutants of the orthologous gene and its Arabidopsis paralog. Numerous studies have successfully used panels of T-DNA insertion mutants to identify genes responsible for a particular phenotype (Motose et al., 2001; Tzafrir et al., 2004; Prigge et al., 2005). However, as reported here, this approach was ultimately unsuccessful in identifying a defective wall ingrowth phenotype in any of the single or double mutants of orthologous Arabidopsis genes identified from the *V. faba* RNA-Seq study reported in Chapter 3. This result included a double knockout mutant for *AtMYB20* and *AtMYB43*, two genes that function in co-ordinating gene expression pathways required for cellulose/hemicellulose biosynthesis as part of the biosynthesis of secondary walls (Zhong et al., 2008; Zhong and Ye, 2014). A discussion of the applicability of this approach to test orthologous genes

for involvement in regulating wall ingrowth deposition is provided.

## **4.2 MATERIALS AND METHODS**

### **4.2.1 Plant growth conditions**

*Arabidopsis* plants (*Arabidopsis thaliana* Col-0 ecotype, unless otherwise stated) were grown in Adaptis CMP6010 growth cabinets (Conviron). Seeds were obtained from the *Arabidopsis* Biological Resource Centre (ABRC) and from the Nottingham *Arabidopsis* Stock Centre (NASC). Seeds were germinated under sterile conditions on agar plates (see section 4.2.2 below) or alternatively directly on a potting mix soil, and were stratified at 4°C in darkness for three days before transfer to the growth cabinets with a 16 h photoperiod, day/night temperature regime of 22/18°C, and light intensity of 90-120  $\mu\text{mol}\cdot\text{m}^{-2}\cdot\text{s}^{-1}$ . For some experiments, testing effects of low temperature, plants were grown in normal conditions for 19 days and then transferred to cold (8.5°C; 16 h light/8h dark; 75  $\mu\text{mol}\cdot\text{m}^{-2}\cdot\text{s}^{-1}$ ) for 5 days.

### **4.2.2 Preparation of agar plates**

Media for growing *Arabidopsis* was prepared from half-strength MS powder (Sigma M5524), 1% (w/v) sucrose and pH adjusted to 5.8 with 1M KOH and solidified with 0.8% (w/v) Bacto Agar. The media was then autoclaved and poured into sterile 9 cm petri dishes (approximately 25 mL) and allowed to solidify. The plates were then stored at 4°C for later use.

### **4.2.3 Seed sterilisation and plating**

Seeds of T-DNA insertion mutants of *Arabidopsis* orthologs selected from the RNA-Seq study (Chapter 3) were obtained from ABRC and NASC (Table 4.1) and sterilised using vapour phase sterilisation technique as follows. Seeds (10-15) were transferred to a microfuge tube (1.5 mL) and placed in a rack inside a desiccator leaving the cap of the microfuge tube open. The desiccator was kept in a fume hood. A beaker filled with about 100 mL of bleach (White King™) was placed inside the desiccator and 1.5 mL of concentrated hydrochloric acid was added slowly to the bleach. The desiccator was immediately closed and seeds were surface sterilised by chlorine fumes for a period of 45 min to 1 h. After sterilisation, the desiccator was opened and the microfuge tubes were closed. These sterilised seeds were then taken to a biosafety cabinet for plating. The

MS/agar plates were UV sterilised in the biosafety cabinet by exposure to UV light for 30 min and labelled individually for plating of sterilised seed lines. Seeds were distributed over the corresponding labelled sterile plates, which were then sealed with parafilm. After one week post-stratification growth, seedlings were then transferred to soil pots (5 plants each pot) and grown as described in section 4.2.1.

#### **4.2.4 Extraction of genomic DNA for genotyping**

A small piece of leaf tissue (~0.25 cm<sup>2</sup>) was excised from each seedling using sterile scissors, placed in a labelled tube and snap-frozen in liquid nitrogen. The tissue was quickly ground using a sterile pestle and 700 µl of extraction buffer (200 mM Tris-HCl, pH 8; 250 mM NaCl; 25 mM EDTA; 0.5% SDS) was added to the powder and vortexed thoroughly for 10-30 s. Samples were then centrifuged at 12000g for 2 min at room temperature. The supernatant (~600 µL) was transferred to a fresh tube and an equal volume of ice cold iso-propanol was added to the tube and mixed by inverting the tube and then held on ice. The tubes were spun at 16000g at 4°C for 10 min. The supernatant was carefully removed and the pellet was washed with 70% ethanol and centrifuged again at 12000g for 2 min. The supernatant was removed and the pellet was air-dried to remove ethanol and then resuspended in 20 µL of sterile Milli-Q water and stored in -20°C until further use.

#### **4.2.5 Genotyping of Arabidopsis mutants**

Arabidopsis mutants were genotyped for identifying homozygous individuals. In order to identify plants homozygous for each T-DNA insertion, PCR with two primer sets was performed; a control primer set with left primer (LP) and right primer (RP) that amplifies the WT CDS, and a primer set for the insertion line using the RP and a left border primer (LBP) that amplifies a product with a part of the gene and T-DNA insertion. Each primer was used at a final concentration 0.5 µM. Total volume of 15 µL reaction was carried out using ThermoScientific Fermentas PCR Master Mix (2X), primers and 1 µl of genomic DNA. Primer sequences for each individual line is shown in Appendix 4A. For each individual plant, two reactions: control and T-DNA insertion reaction was carried out using the following PCR conditions:

Step 1: Initiation denaturation - 94°C (3 min); Step 2: Denaturation - 94°C (15 s); Step 3: Annealing (T<sub>m</sub> - 5°C) - 55°C (30 s); Step 4: Extension - 72°C (60 s); Step 5: Repeat steps

2-4 another 39 times to give a total of 40 cycles; Step 6: Hold at 22°C.

After PCR, 3 µL of 6x Loading Dye was added to each sample followed by agarose gel electrophoresis at 110V on a 1% (w/v) agarose gel containing 0.1% (v/v) ethidium bromide. Gels were visualised using the GelDoc XR Imaging System (BIORAD) and Quantity One Ver. 4.6.3 software.

#### **4.2.6 Semi-quantitative RT-PCR**

Mature rosette leaves of same leaf number and size were harvested from 3 week-old T-DNA insertional mutants and WT Col-0 plants grown alongside them. Harvested leaves (less than 100 mg) were snap frozen in liquid nitrogen. The leaf tissue was ground thoroughly using a sterile micropestle. Total RNA was isolated from these samples using QIAGEN RNeasy Plant mini-kit as per manufacturer's instructions along with on-column DNase treatment for eliminating DNA. Total RNA extracted was quantified using a Nanodrop spectrophotometer (Mettler, Toledo). Up to 1 µg of total RNA was used for first strand cDNA synthesis using Superscript III™ First-Strand Synthesis System for RT-PCR (Invitrogen) as per the manufacturer's instructions. Relative expression levels of genes of interest in their corresponding T-DNA insertional lines were determined by semi-quantitative RT-PCR along with WT. Master mixes were prepared separately for both gene of interest and *AtACTIN2* (AT3G18780) with gene specific forward and reverse primer (see Appendix 4B), and *AtACTIN2* primer pairs (Sigma), respectively. Each reaction volume comprised of 10 µl autoclaved Milli-Q water, 12.5 µl of 2X ThermoScientific Fermentas PCR Master Mix and 0.75 µl (2 µM) each of forward and reverse primers and 1 µl of cDNA. All the reagents were thoroughly mixed by vortexing and pulse-spin centrifugation. PCR reactions were performed and the gel electrophoresis undertaken as described in section 4.2.5. Primers were designed downstream of insertion sites for all the T-DNA insertion mutants with approximate product size of 300 bp (Appendix 4C). Quantification of gene expression was carried out by Image J analysis, such that pixel intensity of each band was measured and percentage of knockdown for each mutant was calculated after normalising expression levels to the *AtACT2* gene.

#### **4.2.7 Generation of double mutants**

##### *Growth of plants and genetic crossing*

Double mutants were generated by crossing homozygous T-DNA insertion lines of both the selected gene and its closest paralog. Healthy plants were grown in standard conditions and once the primary inflorescence bolted, it was removed at the base with scissors to promote the growth of secondary inflorescence. Inflorescence branches with at least two buds were selected for crossing. For the female parent, all siliques, opened flowers and very small flowers were removed from the selected branch. Sepals, petals and stamens were removed from the selected buds with fine tweezers and care was taken to ensure that the stem was not damaged by crushing or squeezing. Once all these structures were removed, the carpel was visible. Care was taken that the carpel was undamaged for pollination. Pollen from 4-5 opened flowers from the male parent of the reciprocal mutant line was dusted onto the stigma of emasculated carpel of female parent. Once both the carpels were dusted with pollen, an identifying thread was gently tied just below the carpels without damaging the stem. This thread was an indication that the carpels that were pollinated and was used as point of reference to monitor silique formation. At least 16-20 carpels were pollinated in order to obtain eight successful siliques for each set of plants crossed. Once the carpels were crossed they were covered with small white paper bags in such a way that they did not touch the carpel. The bags remained covering the carpel for two days after pollination. After two days, bags were removed and the carpel was examined to see if it had started elongating. Once the carpel had started elongating, the plants were kept well-watered and cool for enhancing carpel elongation. The siliques then started forming, matured and started drying. The siliques developed through hand pollination and crossing were usually shorter than normal siliques. Dried siliques were collected into a clean and dry autoclaved 1.5mL eppendorf tube. All the siliques from the same cross were collected in the same tube.

##### *Genotypic screening of double mutants*

Approximately six seeds of T1 generation for each pair of crosses were grown as described in section 4.2.1. Genotyping was performed using primers specific for each gene as described in section 4.2.5 to confirm the plants were heterozygous for both T-DNA insertions. Once confirmed, the plants were allowed to set seed and this seed was collected separately from each confirmed heterozygous T1 plant and labelled as T2 seeds.

T2 seeds were therefore segregating populations, containing different genetic combinations for T-DNA insertions.

At least 40 seeds from two T2 plants (confirmed heterozygous for each T-DNA insertion) were sown for identifying homozygous double mutants for T-DNA insertions of selected gene pairs. Since the genetic ratio of segregation will be 9:3:3:1 (WT:homozygous gene 1/heterozygous gene 2:heterozygous gene 1/homozygous gene 2:homozygous gene 1/gene 2), theoretically, in 40 plants, at least two double homozygous mutants could be expected to be identified. Genotyping was carried out in two-week old plants as described in section 4.2.1.

#### **4.2.8 Phenotyping of T-DNA insertional mutants**

##### *Propidium iodide staining of leaf tissue*

Juvenile leaves 1 and 2 were harvested from 3-week old plants at the end of their night period to minimize starch levels and processed for propidium iodide staining according to Nguyen and McCurdy (2015). Similarly, for cold-treated plants, immature adult leaves 7 and 8 were harvested from plants after 19 days growth in standard conditions and then cold-stressed for 5 days. These leaves were also harvested at the end of their night period. For staining, leaves were fixed in ethanol:acetic anhydride (1:3) overnight at 4°C then transferred to 70% (v/v) ethanol and stored at 4°C until further processing. Fixed leaf tissue was then extracted by bleaching leaves in diluted White King™ bleach (1:3 in MQ water) for 1-3 hrs followed by repeated washes in MQ water. Leaves were then treated with 1% (w/v) periodic acid for 10 mins prior to staining using a pseudo-Schiff solution containing 100 mM Na<sub>2</sub>S<sub>2</sub>O<sub>5</sub> and 0.15 N HCl. Propidium iodide staining solution was prepared by mixing 9 ml of pseudo-Schiff solution with 1 mL of propidium iodide (1 mg/mL), and used to stain the leaves for at least 1 h in darkness. The leaves were then mounted on glass slides in a chloral hydrate (4 g of chloral hydrate + 2 ml of MQ water + 1 ml of glycerol) clearing solution with abaxial surface facing up and left overnight in darkness at RT. Staining of adult leaves was performed similarly except immediately before fixation, the abaxial epidermis and associated mesophyll tissue were removed by peeling using sticky tape (Nguyen and McCurdy, 2015).

### *Confocal microscopy*

Stained leaf tissue was observed using an Olympus FluoView™ FV1000 confocal microscope. Minor veins of the leaves were examined for abundance of wall ingrowths in PP TCs in each T-DNA insertional mutant compared with WT plants grown alongside in standard growth condition or cold treatment. Z-stack images of PP TCs stained with PI were captured using 488 nm Argon-ion laser excitation and a 60X 1.35 NA Olympus oil-immersion objective, with a resolution of 1600 X 800 and thickness of each section set between 2–3 µm. Images were imported into Olympus Fluoro viewer FV10-ASW version 4.0, and the extent of wall ingrowth deposition was scored visually based on the intensity and pattern of staining in PP TCs as described by Nguyen and McCurdy (2015). For statistical analysis, scoring was undertaken by examining two regions of minor veins from fully-expanded leaf 1 (a juvenile leaf) from three replicate plants of each mutant and WT, and calculating mean scores and standard error for each line analysed. A Student t-test was undertaken to assess statistical significance of any changes.

## **4.3 RESULTS**

### **4.3.1 Genotyping of T-DNA insertional mutants**

To assess the putative involvement of Arabidopsis orthologs of *V. faba* transcription factors identified by RNA-Seq as candidate transcriptional regulators of wall ingrowth deposition in TCs, T-DNA insertional mutants of each Arabidopsis ortholog (*AtGT-3B*, *AtMYB20*, *AtWRKY33*, *AtWRKY48*, *AtWRKY41*, – see Table 4.1) were identified and seeds obtained from ABRC and NASC. In addition, to address the issue of potential redundancy of function, insertional mutants for each Arabidopsis paralog of the genes listed above were also obtained. The paralogous genes selected for this investigation are also shown in Table 4.1. The genomic structure for each gene, along with relevant T-DNA insertion details, and phylogenetic relationship of each paralog, is shown in Appendix 4C. An example genotyping result for seed carrying a T-DNA insertion in *AtWRKY44* is shown in Figure 4.1. Amplification products of the expected size of 1167bp were seen in WT and plants 1, 2 and 3 using the LP/RP primer set (lanes 1C, 2C, 3C), but not in the PCRs using the LBP/RP primer set (lanes 1M, 2M, 3M). In contrast, plants 4 and 6 did not yield the WT band (lanes 4C and 6C), but rather, amplification of an ~600 bp band using the LBP/RP primer set occurred (lanes 4M and 6M, indicated by asterisk),

indicating these plants to be homozygous for the T-DNA insertion (Figure 4.1). Line 5 was heterozygous as it showed bands from both primer sets (lanes 5C, 5M). Similar genotyping was undertaken for all lines listed in Table 4.1, including seed supplied as homozygous stock from ABRC (seed stock identified with a terminal “C”). A summary of these outcomes is listed in Table 4.1. The corresponding gel results for these genotyping experiments are shown in Appendix 4D. From each seed stock listed in Table 4.1, at least one individual carrying a homozygous insertion for the T-DNA was successfully identified.

**Table 4.1: Details of orthologous and paralogous Arabidopsis transcription factors selected from the *Vicia faba* RNA-Seq analysis and their genotyping results.**

| <i>Vicia faba</i> Unigene No. | Arabidopsis Gene (Ortholog/paralog) | Gene number | Identity with <i>V. faba</i> sequence (%) (Bit score) | Mutant allele | Insertion Location | Results of genotyping |
|-------------------------------|-------------------------------------|-------------|---|---------------|--------------------|-----------------------|
| 9668                          | <b><i>AtMYB20</i></b>               | AT1G66230   | 93 (268)  | GK-109C11     | Exon 2             | Homozygous            |
|                               | <i>AtMYB43</i>                      | AT5G16600   | 58 (263)  | SALK_023509C  | Intron 1           | Homozygous            |
| 12104                         | <b><i>AtWRKY33</i></b>              | AT2G38470   | 46 (312)  | SALK_064436   | 3' UTR             | Homozygous            |
|                               | <i>AtWRKY44</i>                     | AT2G37260   | 43 (200)  | SALK_058009   | Promoter           | Homozygous            |
| 3427                          | <b><i>AtWRKY48</i></b>              | AT5G49520   | 69 (77)   | SALK_066438C  | Exon 1             | Homozygous            |
|                               | <i>AtWRKY57</i>                     | AT1G69310   | 87 (65)   | GK_078H12     | Exon 1             | Homozygous            |
| 10215                         | <b><i>AtWRKY41</i></b>              | AT4G11070   | 40 (168)  | SALK_068648C  | Exon 3             | Homozygous            |
|                               | <i>AtWRKY53</i>                     | AT4G23810   | 44 (152)  | SALK_034157C  | Exon 2             | Homozygous            |
| 13378                         | <b><i>AtGT-3B</i></b>               | AT2G38250   | 75 (212)  | SALK-133090C  | Promoter           | Homozygous            |
|                               | <i>AtGT-3A</i>                      | AT5G01380   | 72 (126)  | GK-591B09     | Exon 2             | Homozygous            |

The Arabidopsis ortholog of the *V. faba* gene identified by RNA-Seq (Chapter 3) is shown in bold and its paralog is listed immediately below.

### 4.3.2 Analysis of T-DNA insertions on candidate gene expression

To test the effect on gene expression of T-DNA insertion events in each Arabidopsis gene, total RNA was isolated from mature rosette leaves of 3-week-old plants and RT-PCR was performed (see section 4.2.6). The T-DNA insertion events in both *AtMYB20* (GK-109C11) and its closest paralog *AtMYB43* (SALK\_023509C) resulted in gene knockout as shown in Figure 4.2A. This result is expected given the insertion in *AtMYB20* is located in the second of the two exons in this gene, and close to the beginning of intron 1 for *AtMYB43* (Appendix 4C). In contrast, the T-DNA insertion in the 3'-UTR of *AtWRKY33* (SALK\_064436) resulted in only an approximately 47% reduction in transcript abundance (Appendix 4C), albeit with *AtWRKY33* being expressed at low levels in mature rosette leaves (Figure 4.2B).

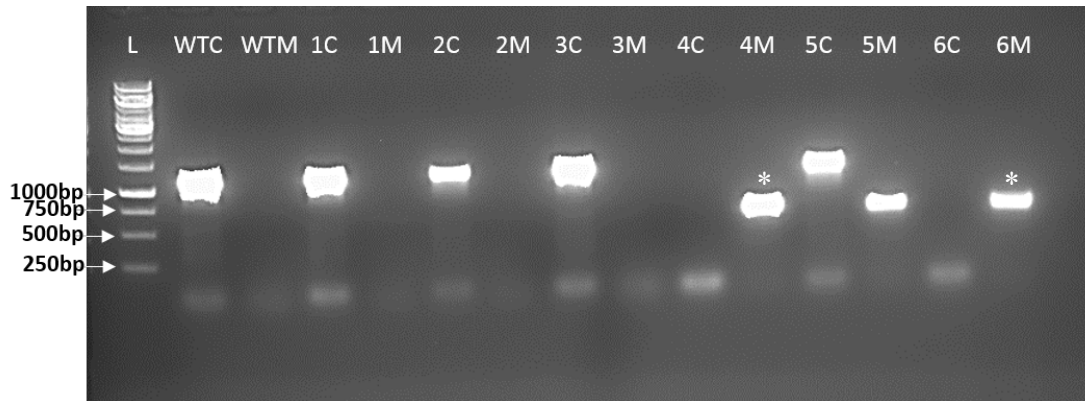


**Figure 4.1 An example genotyping result – SALK\_058009 (*AtWRKY44*).**

**L:** GeneRuler™ 1 Kb ladder. **WT:** WT Col-0 sample. **C:** Control primer pair (LP/RP). **M:** Mutant primer pair (LBP/RP). Plant lines 1, 2 and 3 are WT as indicated by presence of a WT band (1167 bp) in lanes 1C, 2C and 3C lanes, and absence of a band in lanes 1M, 2M and 3M. Lines 4 and 6 are homozygous based on the absence of the WT band in lanes 4C and 6C, and bands (~600 bp) in lanes 4M and 6M (indicated by asterisk). Line 5 shows a heterozygous individual as indicated by presence of both the WT (1167 bp) and mutant (~600 bp) bands.

The T-DNA insertion in the promoter region of *AtWRKY44* (SALK\_058009; Appendix 4C) caused severe knockdown (approx. 82%) of expression (Figure 4.2B). Surprisingly, the T-DNA insertion in the first exon of *AtWRKY48* (SALK\_066438C; Appendix 4C) only caused a modest (42%) knockdown of expression (Figure 4.2C), whereas a first exon insertion in *AtWRKY57* (GK\_078H12; Appendix 4C) caused complete knockout as expected (Figure 4.2C). *AtWRKY41* was expressed to very low levels in mature rosette leaves, and the T-DNA insertion towards the 5' end of the third and last exon in *AtWRKY41* (SALK\_068648C; Appendix 4C) appeared to cause knockout of expression (Figure 4.2D). Similarly, expression of *AtWRKY53* (SALK\_034157C; Appendix 4C) was knocked-out by T-DNA insertion in the 5' end of the second exon in this gene (Figure 4.2D). Interestingly, expression of *AtWRKY41* in *atwrky53* was substantially increased compared to WT (Figure 4.2D). This result was confirmed in three independent experiments using the *atwrky53* line. *AtWRKY41* is not represented on the Affymetrix ATH1 gene chip and thus its expression details are not available on the eFP Browser database (Schmid et al., 2005). This database, however, broadly confirmed the expression of these genes in WT tissue (see Appendix 4E). Unfortunately, a T-DNA insertion in the promoter region of *AtGT-3B* (approximately 88 bp from the ATG start codon) did not cause any visible reduction in expression of *AtGT-3B* in the *atgt-3b* (SALK-133090C) mutant (Figure 4E, Appendix 4C). A second mutant line (SALK\_038142C) carrying a T-DNA insertion in the 3'-UTR region of *AtGT-3B* also showed no effect on expression of

*AtGT-3B* (data not shown). A T-DNA insertion (GK-591B09) in *AtGT-3A* in the second exon (Appendix 4C) caused knockout of this gene in *atgt-3a* (Figure 4.2E, Appendix 4C).

### 4.3.3 Generation of homozygous double mutants

To pursue a strategy to minimize effects of gene redundancy, each homozygous mutant of the four Arabidopsis MYB and WRKY orthologs listed in Table 4.1 was crossed with a homozygous individual carrying a T-DNA insertion in its closest paralog. T1 plants obtained from such crosses were all confirmed to be heterozygous, as shown in Appendix 4F. T2 seed from heterozygous T1 were collected and sown, and genotyping of the double mutants was undertaken. Results of this double mutant screening are shown in Table 4.2. Homozygous double mutants were identified for all crosses performed except for the gene pair *AtWRKY33xAtWRKY44*, in which case plants were identified as homozygous for *AtWRKY33* and heterozygous for *AtWRKY44* or *vice versa*, depending on which plant was used as pollen donor (Table 4.2).

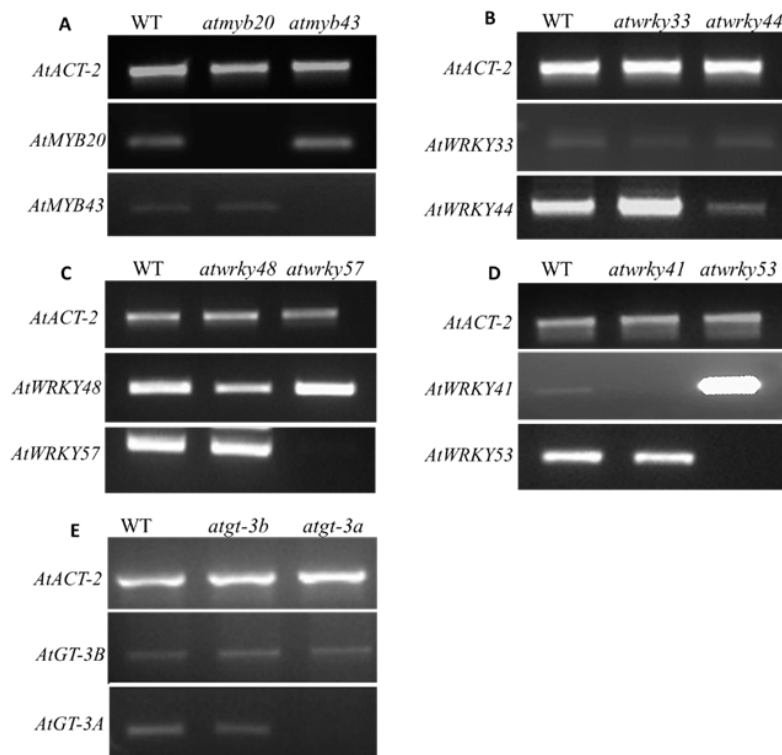


**Figure 4.2 Semi-quantitative RT-PCR analysis of gene expression in T-DNA insertional mutants.**

(A) *AtMYB20* and *AtMYB43* in GK-109C11 (*atmyb20*) and SALK\_023509C (*atmyb43*), respectively in relation to expression of *AtACT2*. (B) *AtWRKY33* and *AtWRKY44* in SALK\_064436 (*atwrky33*) and SALK\_058009 (*atwrky44*), respectively in relation to *AtACT2*. (C) *AtWRKY48* and *AtWRKY57* in SALK\_066438C (*atwrky48*) and GK\_078H12 (*atwrky57*), respectively in relation to *AtACT2*. (D) *AtWRKY41* in SALK\_068648C (*atwrky41*) in relation

to *AtACT*, and expression of *AtWRKY41* in the *atwrky53* mutant. **(E)** *AtGT-3B* and *AtGT-3A* in SALK\_133090C and GK-591B09 respectively in relation to *AtACT2*.

**Table 4.2 Summary of genotyping results for double mutant screening**

| Mutant pairs crossed       | Results of genotyping |                           |
|----------------------------|-----------------------|---------------------------|
|                            | T1 Plants             | T2 Plants                 |
| <i>atmyb20 x atmyb43</i>   | Heterozygous          | Homozygous Double mutants |
| <i>atwrky33 x atwrky44</i> | Heterozygous          | **                        |
| <i>atwrky48 x atwrky57</i> | Heterozygous          | Homozygous Double mutants |
| <i>atwrky41 x atwrky53</i> | Heterozygous          | Homozygous Double mutants |

\*\*Homozygous double mutants were not identified, only mutants homozygous for *AtWRKY33*, heterozygous for *AtWRKY44*, and *vice versa*.

#### 4.3.4 Phenotypic analysis of T-DNA insertional double mutants

Single and double mutants of homozygous T-DNA insertion mutants were analysed for a wall-ingrowth phenotype by comparing mPS-PI staining of PP TCs compared to WT Col-0 plants. For this analysis, the classification system of Nguyen and McCurdy (2015) was employed to semi-quantify the extent of wall ingrowth deposition in PP TCs and their abundance, as determined by confocal microscopy (see Figure 4.3). In this system, Class I corresponds to PP cells with no evidence of wall ingrowth deposition (Figure 4.3A); Class II is defined as showing the first evidence of discrete, punctate-like deposition of wall ingrowths (Figure 4.3B); Class III corresponds to substantial levels of reticulate wall ingrowth deposition seen as continuous stretches of fluorescence in most PP TCs in a given field of view (Figure 4.3C); and Class IV is defined as extensive wall ingrowth deposition seen as thick bands of fluorescence staining in essentially all PP cells in a field of view (Figure 4.3D; Nguyen and McCurdy, 2015). This fluorescence labelling of wall ingrowths occurs along the face of PP TCs adjacent to cells of the SE/CC complex. To provide a semi-quantitative analysis of wall ingrowth deposition in a given leaf, Class I, II, III and IV were assigned 0, 2, 4 and 6 points, respectively, according to Nguyen and McCurdy (2015).

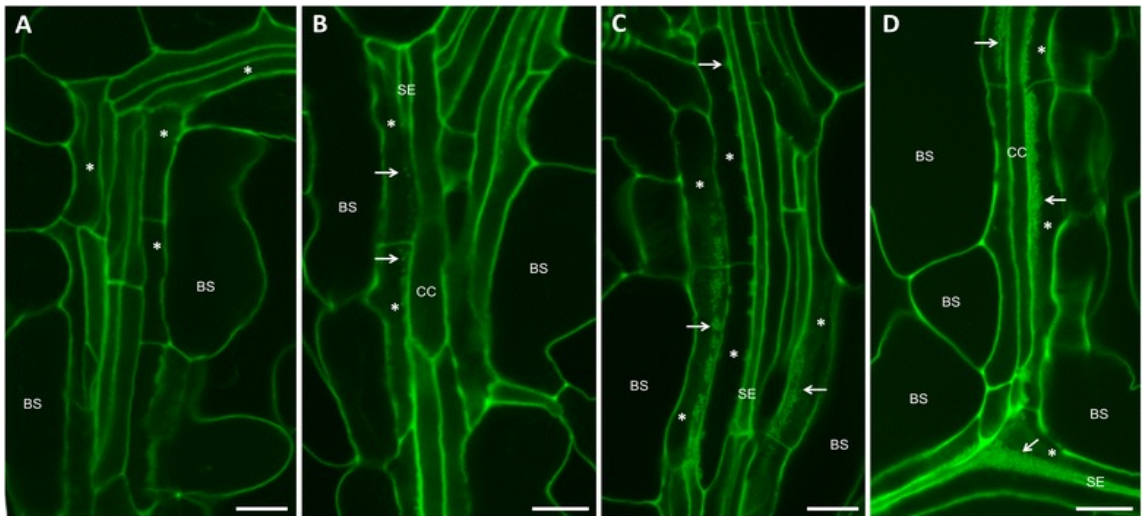


**Figure 4.3: Categorization of wall ingrowths based on extent of PI staining.**

**(A)** Class I type with no wall ingrowths in PP cells (asterisks). **(B)** Class II type shows evidence of early wall ingrowth deposition seen as discrete and punctate-like dots (asterisks). **(C)** Class III type shows substantial amount of wall ingrowths seen either as clusters or continuous bands (arrows) in PP TCs adjacent to SE/CC complex (asterisks). **(D)** Class IV type shows extensive wall ingrowths appearing as thick bands (arrows) in PP TCs (asterisks) adjacent to SE/CC complex. BS, bundle sheath cell; CC, companion cell; SE, sieve element; Scale bars = 10µm. The figure is reproduced from Nguyen and McCurdy (2015).

#### *Phenotyping results for plants grown in standard conditions*

Juvenile leaves were harvested from each single or double mutant (Table 4.3) along with WT plants grown alongside under standard growth conditions. At least two juvenile leaves (leaf 1 and leaf 2) from three different plants of each genotype were stained and examined. Juvenile leaves of three week-old plants were chosen because they show abundant wall ingrowth deposition (Class III-IV; Suong Nguyen – personal communication), and thus a mutation causing reduced levels of wall ingrowth deposition may be expected to be readily identified compared to WT. Each juvenile leaf harvested from WT or a mutant was carefully examined for wall ingrowth deposition by selecting two minor veins per leaf, one from the apical half and one from the basal half of the leaf. Each leaf 1 was scored according to the system described above and mean scores were derived from all leaves for each single or double mutant (Table 4.3). A mean score of 5 and above indicates Class IV type wall ingrowths. Wall ingrowth deposition in PP TCs was observed as an unevenly thickened and mottled layer of staining localized towards

cells of the SE/CC complex (Figure 4.4A, B). The examples of wall ingrowth deposition shown in WT (Figure 4.4A, B) clearly indicates Class IV PP TCs ( $5.7\pm 0.2$  - Table 4.3, Figure 4.4A, B), as indicated by the abundance of ingrowth deposition in essentially all PP TCs in the field of view. From this basis, wall ingrowth deposition in the *atmyb20/atmyb43* double mutant was also assigned as Class IV ( $5.6\pm 0.1$  - Table 4.3; Figure 4.4C). Since both *AtMYB20* and *AtMYB43* are involved in the transcriptional cascades required for cellulose/hemicellulose deposition in localised secondary wall biosynthesis (Zhong et al., 2008), xylem elements in minor veins adjacent to PP TCs were also carefully analysed for any sign of abnormal secondary wall thickenings. The results from this analysis, which showed no detectable effects on secondary wall thickenings in xylem elements, plus further investigations of potential phenotypes in this double mutant, are described in Appendix 4G.

Similar analyses were performed for the *WRKY* double mutants shown in Figure 4.4. Similar to the result with *atmyb20/atmyb43*, however, the double homozygous mutant for *AtWRKY48* and *AtWRKY57*, namely *atwrky48/atwrky57*, also showed Class IV ( $5.8\pm 0.1$ ) wall ingrowth deposition in PP TCs as defined by propidium iodide staining (Table 4.3; Figure 4.4F). Similarly, the double homozygous mutant for *AtWRKY41* and *AtWRKY53* also displayed Class IV ingrowth deposition ( $5.7\pm 0.1$ ; Table 4.3, Figure 4.4 G). For analysis of crosses between homozygous mutants *atwrky33* and *atwrky44*, however, double homozygous mutants could not be recovered from the T<sub>2</sub> population. Substantial lethality (failure to germinate) of seed was observed in this population and thus it was suspected that double homozygous mutants of this gene combination were seedling lethal. Hence, double mutants of *AtWRKY33/atwrky44* (heterozygous for *AtWRKY33*, homozygous for *atwrky44* for the T-DNA insertions) and *atwrky33/AtWRKY44* (homozygous for *atwrky33*, heterozygous for *AtWRKY44*) were analysed. However, similar to *atwrky48/atwrky57*, both combinations of double mutants displayed PP TCs defined as Class IV (*AtWRKY33/atwrky44* -  $5.7\pm 0.2$ ; *atwrky33/AtWRKY44* -  $5.9\pm 0.1$ ; Table 4.3; Figure 4.4D, E).

This observation continued for the single mutants for *AtGT-3B* ( $5.8\pm 0.1$  - Table 4.3) and *AtGT-3A* ( $5.4\pm 0.2$  - Table 4.3), which also showed Class IV wall ingrowths in the knockout mutant for *AtGT-3A* (Figure 4.4I), and not unexpectedly for the *atgt-3b* mutant

(Figure 4.4H), since the T-DNA insertion in this line was located in the promoter and did not disrupt expression of *AtGT3B* (Figure 4.2). Thus, despite careful confocal analyses of all these mutants, as either single or double mutants, none showed detectable reductions in wall ingrowth deposition compared to WT as determined by mPS-PI staining (Table 4.3; Figure 4.4).

**Table 4.3 Summary of phenotyping screening of T-DNA insertional mutants in comparison with WT.**

| Mutant name               | Gene(s)                   | Single gene/double gene mutants    | Class and Phenotypic Score (Mean±SE) |
|---------------------------|---------------------------|------------------------------------|--------------------------------------|
| WT Col-0                  | N/A                       | N/A                                | Class IV<br>5.7±0.2                  |
| <i>atmyb20/atmyb43</i>    | <i>AtMYB20, AtMYB43</i>   | Double mutant                      | Class IV<br>5.6±0.1                  |
| <i>atwrky48 /atwrky57</i> | <i>AtWRKY48, AtWRKY57</i> | Double mutant                      | Class IV<br>5.8±0.1                  |
| <i>atwrky41/atwrky53</i>  | <i>AtWRKY41, AtWRKY53</i> | Double mutant                      | Class IV<br>5.7±0.1                  |
| <i>AtWRKY33/atwrky 44</i> | <i>AtWRKY33, AtWRKY44</i> | Double mutant ( <i>atwrky44</i> )* | Class IV<br>5.7±0.2                  |
| <i>atwrky33/AtWRKY 44</i> | <i>AtWRKY33, AtWRKY44</i> | Double mutant ( <i>atwrky33</i> )* | Class IV<br>5.9±0.1                  |
| <i>atgt-3b</i>            | <i>AtGT-3B</i>            | Single mutant                      | Class IV<br>5.8±0.1                  |
| <i>atgt-3a</i>            | <i>AtGT-3A</i>            | Single mutant                      | Class IV<br>5.4±0.2                  |

\*These mutants were obtained by crossing T-DNA insertional mutants of genes *AtWRKY33* and *AtWRKY44*. Double mutants for these genes could not be identified, however T-DNA insertional mutants that were homozygous for one gene and heterozygous for the other gene were identified. Homozygous mutants for the relevant gene are indicated by gene name in brackets. Values greater than 5 are categorised as Class IV wall ingrowths. Phenotypic score was determined as described in section 4.3.4. N/A, Not applicable; SE, Standard Error.

*Phenotypic analysis of WRKY double mutants subjected to cold-treatment.*

*WRKY* genes are typically involved in numerous stress responses including cold stress (Bakshi and Oelmuller, 2014), and cold treatment has been reported to enhance wall ingrowth deposition in PP TCs in both WT and the *vte2* mutant (Maeda et al., 2006). Furthermore, Maeda et al. (2014) reported that several *WRKY* genes are up-regulated by cold-treatment in the *vte2* mutant (Maeda et al., 2014). Based on these observations, the deposition of wall ingrowths in *WRKY* double mutants in response to cold treatment was

also investigated. Plants grown under standard conditions (section 4.2.1) for 19 days were then transferred to cold treatment (8.5°C; 16h light/8h dark; 75  $\mu\text{mol m}^{-2} \text{s}^{-1}$ ) for five days. Immature adult leaves (leaf 7 and 8) were then harvested from all double mutants along with the WT from both control and cold-stressed plants. In total, three biological replicates for each mutant, for each growth condition, were analysed. These leaves were fixed and stained using mPS-PI staining as described in section 4.2.8.

Maeda et al. (2006) reported that cold treatment, similar to the conditions used here, resulted in enhanced deposition of wall ingrowths in PP TCs. Consequently, to test if any of the WRKY genes were involved in signalling this process, immature adult leaves of WT, which have mostly Class I PP TCs (Figure 4.5A; Nguyen and McCurdy - unpublished), were used for this analysis, with the prediction that cold treatment would cause increased deposition of wall ingrowths in WT, and this response would be absent or attenuated if one of the selected WRKY genes was involved in signalling this response.

Surprisingly, however, based on propidium iodide staining, no increase in wall ingrowth deposition in WT (Col-0) plants exposed to cold treatment was detected (Figure 4.5B). PP cells are easily identified in stained leaves due to their thin elongated morphology, with a common wall shared along its length with larger bundle sheath cells (Figure 4.5). However, none of these PP cells from plants exposed to 5 days of cold treatment displayed evidence of wall ingrowth deposition adjacent to cells of the SE/CC complex or indeed elsewhere in PP cells (Figure 4.5A, B). The low temperature response of plants exposed to cold was evident by the abundant accumulation of starch grains, seen as irregularly shaped fluorescent structures in bundle sheath and mesophyll cells (Figure 4.5B). Analysis of each of the WRKY double mutants revealed similar results to WT; no evidence of increased wall ingrowth deposition in PP cells in response to cold (Figure 4.5C-J). In each case, however, the low temperature-induced accumulation of starch grains was evident.

#### **4.4 DISCUSSION**

RNA-Seq analysis of *Vicia faba* adaxial epidermal TC reported in Chapter 3 identified several transcription factors that showed strong epidermal-specific differential expression in response to induction of wall ingrowth deposition, thus marking these genes as putative regulators of TC development. Verification of the putative role of these transcription

factors via a genetics approach in *V. faba* is not feasible given the absence of a robust transformation protocol for this species. For example, Böttinger et al. (2001) reported that regeneration of transformed *V. faba* explants takes 16-24 months and yields very low regeneration frequencies of 2-6%, possibly due to mortification of explant tissues caused by excess production of phenolic compounds (Böttinger et al., 2001). Therefore, in the absence of a viable transformation protocol for *V. faba*, the approach taken in this research was to assess the function of orthologous genes in regulating wall ingrowth deposition in TCs of Arabidopsis. As the leading model system in plant research, a huge array of bioinformatics and mutant resources are available in Arabidopsis to study individual gene functions (Koornneef and Meinke, 2010). In Arabidopsis, PP cells in leaf minor veins *trans*-differentiate to become PP TCs involved in phloem loading (Haritatos et al., 2000; Maeda et al., 2006). The genetic resources available in Arabidopsis, including numerous microarray data and access to thousands of mutants, have been used to identify several genes putatively involved in either directly or indirectly regulating PP TC development (Edwards et al., 2010; Arun-Chinnappa et al., 2013). In this study it was hypothesised that Arabidopsis orthologs of the transcription factors identified from the *V. faba* RNA-Seq study (Chapter 3) may function as regulators of PP TC development in Arabidopsis. Both epidermal TCs in *V. faba* cotyledons and PP TCs in Arabidopsis leaves form reticulate-type wall ingrowths (Talbot et al., 2001; Maeda et al., 2008; Edwards et al., 2010), thus mechanisms involved in regulating deposition of these types of wall ingrowths might be conserved.

To test this hypothesis, Arabidopsis orthologs of the *V. faba* sequences displaying epidermal-specific up-regulation upon cotyledon culture (Trihelix GT-3B-like and P-type R<sub>2</sub>R<sub>3</sub> MYB proteins – see Table 1 from Chapter 3) and those displaying epidermal-enhanced up-regulation (WRKY33, WRKY48, WRKY41 – see Table 3 from Chapter 3) were selected for phenotypic analysis. The cohort of Arabidopsis genes listed in Table 3 was finalized by the availability of homozygous T-DNA insertional mutants for each gene, and to a lesser extent on a plausible role for the Arabidopsis protein in regulating TC development based on known functions of the orthologous genes. A full discussion of the possible functional involvement in regulating TC development of the *V. faba* genes identified from the RNA-Seq study is presented in Chapter 3.

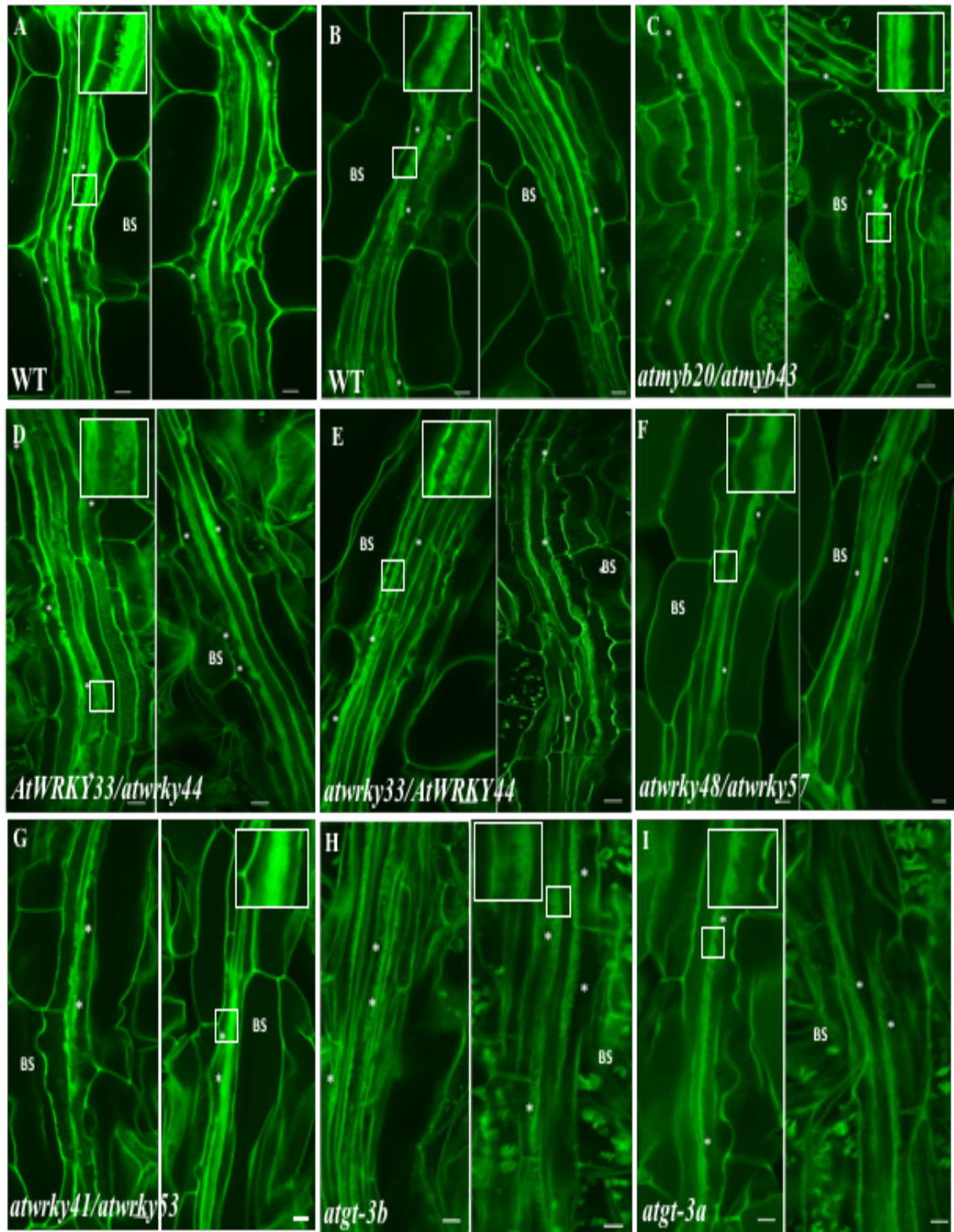


**Figure 4.4: Confocal imaging of PP TCs in juvenile leaves of WT and selected double mutants.**

Examples of wall ingrowth deposition in PP TCs of minor veins from the apical (left image) or basal (right image) half of mature juvenile leaves. PP TCs are characterised as elongated cells bordered by larger bundle sheath cells on one side and thin cells of the SE/CC complex on the opposite side. Wall ingrowth deposition is seen as mottled fluorescence staining along the wall of PP TCs adjacent to cells of the SE/CC complex. **(A, B)** WT (Col-0). **(C)** *atmyb20/atmyb43* double mutant. **(D)** *AtWRKY33/atwrky44* double mutant. **(E)** *atwrky33/AtWRKY44* double mutant. **(F)** *atwrky48/atwrky57* double mutant. **(G)** *atwrky41/atwrky53* double mutant. **(H)** *atgt-3b* single

mutant. **(I)** *atgt-3a* single mutant. In each panel, two images for each genotype are shown. Each small boxed area in white is enlarged to show details wall ingrowth deposition in the PP TCs. In all genotypes, wall ingrowth deposition was determined to be Class IV. Asterisks indicate PP TCs in which thick bands of wall ingrowth deposition are clearly seen. BS, Bundle sheath cells. Scale bars = 5µm.

To address as best as possible the high occurrence of functional redundancy amongst Arabidopsis genes (Krysan et al., 1999), and in particular transcription factors (e.g., Taylor-Teeples et al., 2015), a double mutant strategy was employed whereby T-DNA insertional mutants for each orthologous Arabidopsis gene and those for its closest paralog were crossed to obtain double mutants.

This strategy was achieved for all of the Arabidopsis orthologs listed in Table 4.1 (except *AtGT-3B*), and phenotypic analysis of these mutants using propidium iodide staining of leaf tissue was used to assess whether disruption of these genes caused altered levels of wall ingrowth deposition in PP TCs, either reduced or elevated levels, depending on whether the gene(s) was acting as an activator or repressor, respectively, of wall ingrowth deposition.

However, while a total of five double mutants (three double homozygous mutants and two heterozygous/homozygous combinations) and two single mutants were tested, making a total of 10 genes, no significant phenotype consisting of altered levels of wall ingrowth deposition in PP TCs was observed in any of these mutant lines (Table 4.3). All single and double mutants showed Class IV-type wall ingrowths equivalent to that seen in WT. This collective result may be due to several factors negatively impacting either individually or collectively on the assumptions of this approach. Such factors could include functional redundancy, lack of complete knockout of gene function in certain T-DNA mutants, or lack of functional conservation between orthologous genes in the legume *V. faba* and in the non-legume Arabidopsis. These issues are discussed below.

T-DNA insertional mutagenesis is the primary tool in Arabidopsis used to assess gene function, since the T-DNA insertion event typically causes loss of mRNA production and consequently loss of functional protein (Krysan et al., 1999). However, depending on

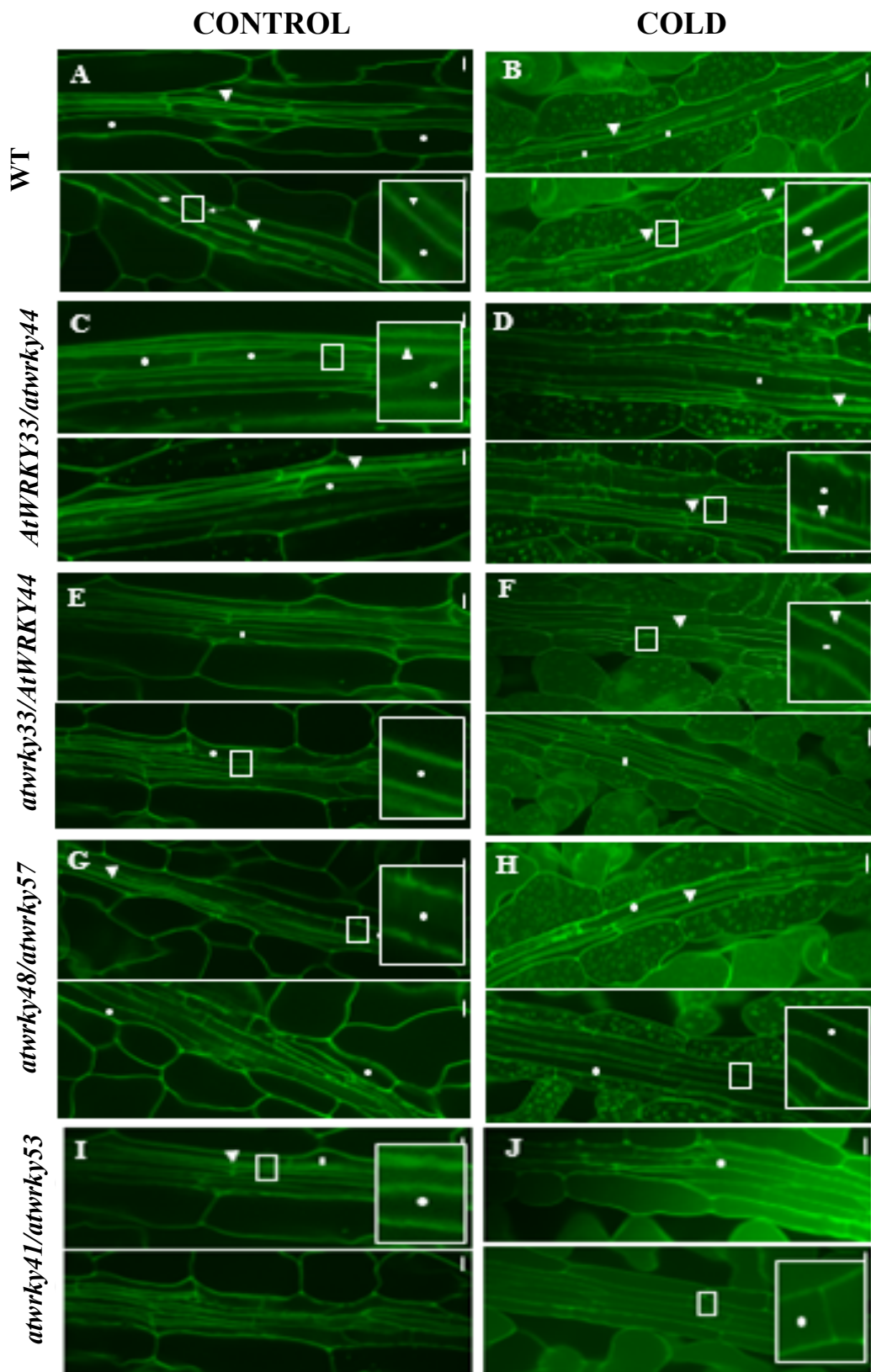


**Figure 4.5: Confocal imaging of PP cells from immature adult leaves of cold-stressed WT and double mutants of *WRKY* transcription factors.**

Plants were grown in two different condition, standard growth condition and cold-treatment to study the role of *WRKY* genes in TC development with respect to WT. Left panel (A, C, E, G,

**I**) indicates confocal imaging of vascular bundles in minor veins of plants grown under standard conditions (Control). Right panel (**B, D, F, H, J**) indicates confocal imaging of vascular bundles in minor veins of cold-treated plants (Cold). (**A, B**) WT plants showing Class I PP cells (no wall ingrowths) in either control or cold-treated plants. (**C, D**) *AtWRKY33/atwrky44*. (**E, F**) *atwrky33/AtWRKY44*. (**G, H**) *atwrky48/atwrky57*. (**I, J**) *atwrky41/atwrky53* Class I PP cells were observed in all *atwrky* double mutants, irrespective of the growth conditions. Note that all plants subjected to cold show accumulation of starch granules in bundle sheath/mesophyll cells, which is typical of cold-treated leaves (Maeda et al., 2006). In each panel, two separate images from the same genotype are shown. Boxed area in each image is shown at larger magnification to demonstrate lack of wall ingrowths as viewed by mPS-PI staining. White dots indicate PP cells; arrowheads indicate cells of the SE/CC complex. BS, Bundle sheath cells. Scale bars = 5µm.

where the T-DNA insertion event occurs in the structure of the gene, or sometimes independently of this location, some level of primary transcript may remain and this can be translated into functional or semi-functional protein (Wang, 2008). In the case of the 10 genes analysed here, only six (*AtMYB20*, *AtMYB43*, *AtWRKY57*, *AtWRKY41*, *AtWRKY53*, *AtGT-3A*) were knockout mutants (absence of detectable mRNA), while of the remaining four, knockdown of expression was detected for two (*AtWRKY44*, *AtWRKY48*) and expression of *AtWRKY33* and *AtGT-3B* was not apparently affected (Figure 4.2). While these variable effects on gene expression can in most instances be explained by the location of the T-DNA insert in the relevant gene (e.g., exon, intron, 5'/3'-UTR, promoter, etc), only two double mutants tested in this study (*atmyb20/atmyb43*, *atwrky41/atwrky53*) were double homozygous knockouts, where expression of both genes was ablated. In the case of the *atwrky53* mutant, however, expression of *AtWRKY41* was substantially up-regulated, thus complicating phenotypic analysis in this double mutant (Figure 4.2). Further, only one of the GT trihelix genes, *AtGT-3A*, was knocked out in the relevant single mutant. Thus, in each of the remaining double mutants tested, at least one of the two gene paralogs may have retained full or partial functionality, thus masking a potential PP TC phenotype if the paralogous genes were involved in regulating PP TC development but functioned redundantly with each other. Thus, while phenotypes have been identified in literally thousands of single homozygous T-DNA insertional mutants in Arabidopsis, the combined effects of incomplete gene knockout and redundancy common within families of transcription factors (see later) may have conspired to mask any wall ingrowth phenotype, even if the genes involved play some role in regulating this process. Functional redundancy is particularly acute in the WRKY gene family (Shen et al., 2007; Hu et al., 2013), with one

example being the three Group IIa transcription factors, *AtWRKY18*, *AtWRKY40* and *AtWRKY60*. These three genes act together as negative regulators of basal defence (Xu et al., 2006) and abscisic acid signalling during seed germination and early post-germination growth (Chen et al., 2010). Whilst *AtWRKY18*, *AtWRKY40* and *AtWRKY60* act synergistically in plant basal defence, redundancy is nonetheless observed within this group since a functional copy of *AtWRKY18* can still perform in the absence of functional *AtWRKY40* and *AtWRKY60* (Xu et al., 2006). In another example, two WRKY genes *AtWRKY70* and *AtWRKY54* regulate leaf senescence in a redundant manner (Li, 2014).

A further example of redundancy highly relevant to cell wall biology is the study by Taylor-Teeples et al. (2015) characterizing the signalling network involved in transcriptional regulation of secondary cell wall biosynthesis. This study showed that every transcription factor identified to have a role in regulating secondary cell wall deposition in xylem was shown to act redundantly with at least one other transcription factor, but often more than one, resulting in extremely complex regulatory networks to achieve secondary wall deposition (Taylor-Teeples et al., 2015). In other examples of extreme redundancy in Arabidopsis, quadruple or quintuple mutants have been necessary to distinguish individual roles of phosphate transporters (Ayadi et al., 2015) and members of the myosins XI gene family (Peremyslov et al., 2015). These high levels of redundancy seen in Arabidopsis are thought to be due mainly to extensive duplication events in the Arabidopsis genome (Vision et al., 2000).

A further consideration in assessing the validity of the orthologous phenotyping approach used in this chapter is whether the similarity in sequence identity between a specific *V. faba* gene and its Arabidopsis ortholog extended to functional similarity. Table 4.1 shows that percent identity at the amino acid level between the translated *V. faba* contig and the Arabidopsis ortholog ranged from as high as 93% for the AtMYB20 pair, to as low as 40% for the AtWRKY41 pair. These identity values were derived by BLASTX comparing contigs encoding, in most instances, truncated versions of the *V. faba* sequence, hence the percent identity score may be an underestimate. In most cases, however, orthologous proteins that are at least 40% identical at sequence level are likely to have functional similarity (Pearson, 2013). Not surprisingly, functional similarity of orthologous genes in Arabidopsis and *V. faba* have been reported; for example, the *V.*

*V. faba* ABA-activated serine-threonine protein kinase, AAPK, shares 79% identity at the amino acid level with *Arabidopsis OST1* protein kinase and is considered to be a functional ortholog (Mustilli et al., 2002). Against this example, however, is the study by Zhu et al. (2003) showing a relatively high degree of microsynteny degeneration between *Arabidopsis* and *Medicago truncatula* (*Medicago*), a legume species closely related to *V. faba*. Their study concluded that most genes in *Arabidopsis* cannot be selected as orthologs for legume genes as the genomic structures in the two species lack appropriate syntenic relationships (Zhu et al., 2003.). However, after taking these observations into account, in the absence of a transformation protocol for *V. faba*, the orthologous phenotyping approach used in this study represented the best available genetic approach to test the functions of transcription factors identified from the RNA-Seq study as being putatively involved in regulating TC development.

Finally, an additional consideration in assessing the orthologous phenotyping approach is whether the propidium iodide staining used for confocal imaging of wall ingrowths was sufficiently sensitive to detect possibly subtle wall ingrowth phenotypes in the mutant lines. Phenotypes seen in complete knockout or null lines for a given gene may only be partial or incomplete compared to the WT. This scenario is frequently seen in cell wall mutants, such as *lac4-1/lac17* and *lac4-2/lac17* double mutants, where knockout of expression of two laccases *LAC4* and *LAC17* caused only partial loss of lignification in *Arabidopsis* stems (Berthet et al., 2011). Similarly, *fra8*, which encodes a glucuronyltransferase, showed only partial reduction in fibre wall thickness and stem strength due to defective xylan synthesis (Zhong et al., 2005). Thus, a question remains as to whether confocal imaging of propidium iodide stained wall ingrowths in PP TCs would be sufficiently sensitive to detect partial reduction or other subtle changes in wall ingrowth deposition. TEM could be used to answer this question, although considerable time would be required to use this approach to screen every mutant analysed in this study. In this context, however, the confocal imaging of the various double mutants shown in Figure 4.4 clearly detected abundant wall ingrowth deposition in PP TCs comparable to that seen in WT, and the semi-quantitative scoring (Table 4.3) provided a statistical basis for claiming that no significant differences were observed between WT and the mutants. This point is critical in light of recent published (Nguyen and McCurdy, 2015) and unpublished observations from the McCurdy lab showing that wall ingrowth deposition

in PP TCs is highly variable, being abundant in mature juvenile leaves but less abundant and variable along the apical-basal axis in developing adult leaves. Thus, the scoring approach used in this study of examining comparable minor veins in mature leaf 1 ensured that this variability did not influence conclusions regarding wall ingrowth phenotypes. Collectively, therefore, it is reasonable to assume that propidium iodide staining and confocal microscopy provides an appropriate method to screen T-DNA insertional mutants for disrupted levels of wall ingrowth deposition in PP TCs.

After taking into consideration all of the above points put forward as reasons why the orthologous gene phenotyping approach may not have been successful, several results emerging from this analysis remain surprising, in particular the *atmyb20/atmyb43* double mutant. As discussed in Chapter 3 and Appendix 4G, *AtMYB20* and *AtMYB43* function as second-tier transcriptional regulators of the gene cascade required for cellulose/hemicellulose biosynthesis during localized secondary wall formation (Zhong et al., 2008, 2010). The *V. faba* ortholog of *AtMYB20* (Unigene 9668 - Table 1; Chapter 3) showed a log<sub>2</sub> fold-change of 7.1 within 3 h of induction of epidermal TCs (Table 1, Chapter 3), suggesting that the machinery for cell wall synthesis was activated to support wall ingrowth deposition in these cells. Given that localized secondary wall formation and wall ingrowth deposition both represent different examples of highly polarized cell wall biosynthesis in plants, it was hypothesized that the gene pathways regulating cellulose/hemicellulose biosynthesis may be conserved between these two types of wall deposition. However, the *atmyb20/atmyb43* double mutant, even as a double homozygous knockout, displayed normal levels of wall ingrowth formation (Figure 4.4, Table 4.3). This result was surprising, especially given the 93% identity at the amino acid level of *AtMYB20* and the *Vicia* protein, providing a strong case for assuming conserved functions between the two proteins. However, the absence of a wall ingrowth phenotype in the double mutant needs to be considered in light of the apparent absence of any effect on localized secondary wall deposition in minor veins in this double mutant (Appendix 4G). FTIR spectroscopy revealed a clear reduction in total polysaccharides (predominantly cellulose/hemicelluloses) in leaf tissue of the double mutant compared to WT (Figure 4G.2A), however xylem formation in vascular bundles of minor veins was not significantly reduced (Figure 4G.1). One possibility explaining these results is that *AtMYB20* and *AtMYB43* can act redundantly with other MYB transcription factors in

directing cellulose/hemicellulose synthesis during secondary wall deposition in xylem elements and wall ingrowth deposition in PP TCs. This possibility is likely given the extensive levels of functional redundancy built into the transcriptional regulation of secondary wall biosynthesis (Taylor-Teeple et al., 2015). Nonetheless, the *atmyb20/atmyb43* double mutant represents a valuable genetic resource to investigate the role of these two genes in regulating secondary wall biosynthesis, and possibly wall ingrowth deposition, because as far as the author is aware, no studies have investigated the role of these two genes using T-DNA insertional mutants.

A striking feature of the RNA-Seq study reported in Chapter 3 was the abundance of WRKY transcription factors appearing in the list of genes showing epidermal-enhanced up-regulation within the first 3 h of cotyledon culture. A discussion of this observation is presented in Chapter 3. The analysis of WRKY genes reported here was compromised by a number of issues, the first being accessibility of suitable homozygous knockout lines. For example, no T-DNA insertion line was available for *AtWRKY28*, the transcription factor showing the highest fold-difference between “epidermal fold-change” minus “storage parenchyma fold-change” (Table 3, Chapter 3). The paralog of *AtWRKY28*, *AtWRKY8*, is up-regulated in the *vte2* mutant upon exposure to cold (Maeda et al., 2014), a condition reported by Maeda et al. (2006, 2008) to increase wall ingrowth deposition in PP TCs. Attempts are on-going in the McCurdy lab to eliminate expression of both *AtWRKY28* and *AtWRKY8* by artificial microRNA technology (see Eamens et al., 2014), but this analysis is yet to be completed.

Of the six *AtWRKY* genes analysed in this chapter by the orthologous phenotyping approach, only one pair, *AtWRKY41* and *AtWRKY53*, were analysed as a homozygous double knockout mutant (Figure 4.2). Potentially complicating this analysis, however, was the observation that the *atwrky53* mutant showed very strong up-regulation of *AtWRKY41* expression (Figure 4.2), potentially compromising detection of a wall ingrowth phenotype in the double mutant by over-expression of *AtWRKY41*. A similar example of over-expression of a paralog in a knockout mutant of the paralogous partner has been seen in the NH<sup>4+</sup> transporter family (AMT) genes in Arabidopsis. Knockout of *AtAMT1;1* in the *amt1;1* mutant enhanced the expression of other *AtAMT* genes such as

*AtAMT1;3* and *AtAMT3;1*, which compensated the loss of functional *AtAMT1;1* (Kaiser et al., 2002).

For the *atwrky48/atwrkyb57* double mutant, knockout of gene expression was seen for *AtWRKY57*, but *AtWRKY48* was knocked down by some 42%. Thus, similar to the *atwrky41/atwrky53* mutant, the presence of non-basal levels of *AtWRKY48* may too have compromised development of a wall ingrowth phenotype in *atwrky48/atwrky57*. A similar complication exists in interpreting lack of a wall ingrowth phenotype in the *AtWRKY33/AtWRKY44* mutant combinations. Since it was not possible to identify a plant line homozygous for T-DNA insertions in both genes, either of the double mutants (i.e., *atwrky33/AtWRKY44* or *AtWRKY33/atwrky44*) contained a functional copy of at least one of the two genes. In all of these cases regarding analysis of WRKY genes, since it was formally possible that single WRKY transcription factors could be operating independently in a non-redundant manner to regulate wall ingrowth deposition, it was nonetheless valid to undertake phenotypic analysis in each case.

Maeda et al. (2014) demonstrated that *AtWRKY8* (the paralog of *AtWRKY28*) and two other WRKY transcription factors were up-regulated in the vitamin-E deficient *vte2* mutant when exposed to cold stress. Maeda's group reported that cold stress caused increased wall ingrowth deposition in PP TCs in both WT plants and the *vte2* mutant (Maeda et al., 2006, 2008), thus indicating a possible link between WRKY-regulated wall ingrowth deposition in response to cold. Therefore, to test this possible link, the WRKY double mutants described in Table 4.2 were tested in response to cold. After five days exposure to cold, however, again no differences in wall ingrowth deposition in any of the double mutants compared to WT was detected (Figure 4.5). Surprisingly in this experiment, however, no evidence of increased wall ingrowth deposition in response to cold was seen in WT (Figure 4.5A, B), which contradicts the result reported by Maeda et al. (2006). An explanation for this difference may lie with differences in developmental status of the leaf tissue used in both studies. Maeda et al. (2006) used "mature leaves" for their analysis, while this study used immature adult leaves which show little if any wall ingrowth deposition in PP TCs (Class I according to Figure 4.3). Immature adult leaves were chosen because any cold-induced increase in wall ingrowth deposition would

presumably be more easily detected against a baseline of little or no deposition. Mature adult leaves (assumed to be the leaf type chosen by Maeda et al. in their 2006 publication) in contrast contain relatively abundant but highly variable levels of wall ingrowth deposition in PP TCs depending on where the vein is sampled along the axis of the leaf blade (Nguyen and McCurdy, 2015). Thus, depending on where the TEM analysis by Maeda et al. (2006) imaged wall ingrowth deposition along the length of a “mature leaf”, these authors may have mis-interpreted the effect of cold on wall ingrowth deposition in PP TCs.

The *V. faba* trihelix transcription factor GT-3B-like (Unigene 13378; Table 1, Chapter 3) showed the highest epidermal-specific log<sub>2</sub> fold-increase of 8.9 in the list of transcription factors shown in Table 1 of Chapter 3. This very substantial fold-increase in epidermal cells occurred in the absence of expression in nearby storage parenchyma, and thus presumably reflects a role in the *trans*-differentiation of epidermal TCs by this gene. Unfortunately in this case, however, the two available T-DNA insertion lines for *AtGT-3B* showed no effect on expression levels for this gene, thus orthologous phenotyping to demonstrate a role for this gene in regulating TC development was not possible. Complete knockout of the paralog of this gene, *AtGT-3A*, however, also failed to cause any effect on wall ingrowth deposition in PP TCs (Figure 4.4; Table 4.3). As discussed in Chapter 3, *AtGT-3B* is rapidly expressed in response to pathogen and salt stress (Park et al., 2004), and thus the response of the *V. faba* gene may reflect involvement in a TC-specific stress induction pathway. *AtGT-3B* can bind to a GT element in the stress-responsive calcium-signalling gene *SCaM-4* in soybean, and since wall ingrowth deposition in *V. faba* involves calcium signalling (Zhang et al., 2015a,c), the *V. faba* gene and its Arabidopsis ortholog *AtGT-3B* may be involved in these processes. Interestingly, while no functional studies of *AtGT-3B* have been reported, microarray analysis has shown that *AtGT-3B* is up-regulated five-fold in response to H<sub>2</sub>O<sub>2</sub> (Inzé et al., 2012). This ROS induces wall ingrowth deposition in epidermal TCs of *V. faba* cotyledons (Andriunas et al., 2012), hence *AtGT-3B* may be similarly involved in induction of PP TCs in Arabidopsis. Given the potential significance of *AtGT-3B* to regulating wall ingrowth deposition, gene disruption of both *AtGT-3B* and *AtGT-3A* by amiRNA technology represents a high priority experiment for future investigations.

An alternative explanation as to why PP TC phenotypes may not have been detected in any of the single or double mutants of genes associated with stress responses, namely the WRKY genes and possibly *AtGT-3B*, is that the two examples of TC development analysed in this study may be responding to different inductive cues. In the *V. faba* system, stress seems to be a major inductive mechanism due to isolation and *in vitro* culture of the cotyledons. In contrast, developmental cues associated with source/sink physiology may be the primary inductive signalling required for PP TC development in Arabidopsis. Consequently, genes associated with stress responses seen in the *V. faba* study may not be prominent players in the Arabidopsis pathway. If this scenario is valid, then the orthologous phenotyping strategy used in this research may not be the best avenue to demonstrate a functional role for this collection of transcription factors in regulating TC development in plants.

**CHAPTER 5**  
**GENERAL DISCUSSION**

## 5.1 INTRODUCTION

This research project focused on identifying key participants in the transcriptional regulation of TCs in plants. This goal is significant because TCs play key roles in plant productivity and thus understanding how the induction of these unique plant cell types occurs at the genetic level may provide new avenues for optimizing plant productivity by targeting manipulation of TC development. TCs occur in all plant taxonomic groups and develop at “bottlenecks” along nutrient transport routes within plants (Gunning and Pate, 1969; Offler et al., 2003), thus increasing plasma membrane surface area and thus membrane transporter density to achieve this enhanced transport outcome. By achieving this increase in membrane transport capacity, TCs play critical roles in transport processes and consequently contribute to important processes such as nutrient distribution to growth and storage organs (Borisjuck et al., 2002; Charlton et al., 1995; Haritatos et al., 2000), adaptive responses of plants to abiotic stresses (e.g., Schikora and Schmidt, 2002) and symbiotic and pathogenic relationships (e.g., Gheysen and Fenoll, 2002). Therefore, identifying transcriptional regulators of TC development may provide means to manipulate such processes to achieve optimized plant productivity.

Little is known about transcriptional regulators of TCs that build reticulate wall ingrowths. This contrasts with TCs containing flange wall ingrowths where the maize MYB-related gene, *ZmMRP-1*, regulates basal endosperm TC development exclusively in maize kernels (Gómez et al., 2002). Somewhat surprisingly, over-expression of this gene product in heterologous systems is not well tolerated (Gómez et al., 2009), and thus information about *ZmMRP-1* as a regulator of TC development is restricted to these pioneering studies by Gómez et al. (2002, 2009) and limited to basal endosperm TCs occurring in maize kernels. The review by Arun Chinnappa et al. (2013; see Appendix 1) lists previously uncharacterized NAC-domain and MYB-related transcription factors as putative regulators of PP TC development in Arabidopsis, but this conclusion was based on using aniline blue to specifically stain PP TCs in vascular bundles of leaves. Subsequently, however, this result has been questioned based on using the more definitive technique of propidium-iodide staining followed by confocal microscopy to visualize wall ingrowth deposition in PP TCs (Nguyen and McCurdy, 2015; see Chapter 4). Using this procedure, mutants of the NAC-domain and MYB-related sequences reported in Arun

Chinnappa et al. (2013; Appendix 1) show some level of decreased wall ingrowth deposition in PP TCs of Arabidopsis, but not statistically significant across all stages of leaf development compared to WT (S. Nguyen – personal communication). Therefore, from this perspective, a large gap in understanding of transcriptional regulation of reticulate wall ingrowth deposition in plant TCs exists, and consequently this project addressed this issue by using a combination of RNA-Seq in *V. faba* cotyledons and ‘orthologous phenotyping’ in Arabidopsis.

## **5.2 TRANSCRIPTIONAL REGULATION OF *V. faba* TRANSFER CELLS**

### **5.2.1 *De novo* assembly of genome-wide transcriptome map of *V. faba* for TC research (Chapter 2)**

During cotyledon development in *V. faba*, expanding cotyledons crush against the seed coat creating a mechanical stress on the abaxial surface of the cotyledons, which in turn triggers an ethylene signalling pathway which induces abaxial epidermal and sub-epidermal cells of the cotyledons to *trans*-differentiate to form TCs. In contrast, adaxial epidermal cells of the cotyledons do not form TCs *in planta*, but remarkably these epidermal cells can be induced to form TCs when isolated cotyledons are placed in culture. This experimental system provides access to a specific cell type to study TC biology (Farley et al., 2000; Offler et al., 2003). The temporal development of TC induction in this system is well understood (Wardini et al., 2007b), and hence has been utilized to identify roles for auxin, ethylene and ROS signalling pathways and Ca<sup>2+</sup> signalling in forming reticulate wall ingrowth deposition in epidermal TC development (Dibley et al., 2009; Zhou et al., 2010; Andriunas et al., 2012; Xia et al., 2012; Zhang et al., 2015a,c). However, despite the transcript profiling studies of Dibley et al. (2009) and Zhang et al. (2015b) using this system, the identity of transcription factors responding to these signals remains unknown. In this project, therefore, RNA-Seq was employed using the *V. faba* cotyledon culture system to identify transcriptional regulators of TC development. However, since the genome sequence of *V. faba* is not available, a *de novo* transcriptome map of *V. faba* was developed (Chapter 2) for use as a reference map for RNA-Seq. Next Generation Sequencing (NGS) has been widely used as a tool for transcriptome analysis in non-sequenced species (Egan et al., 2012; Unamba et al., 2015),

as *de novo* generation of a transcriptome maps provides a valuable cost-effective alternative to whole genome sequencing (Xia et al., 2011). This approach provides direct access to functional information of transcripts and is not burdened by sequencing of repetitive sequences (Gayral et al., 2011), which in the case of *V. faba* with a huge genome of approximately 13 Gb (Kaur et al., 2012), represents a considerable advantage.

A genome-wide transcriptome map of *V. faba* was generated by capturing transcripts from different vegetative and reproductive tissues at different developmental stages of the plant, and in particular from cultured cotyledons induced to form adaxial epidermal TCs. Consequently, the genome-wide transcriptome map contained transcripts expressed across the 24 h culture period in which adaxial epidermal cells were *trans*-differentiating to become epidermal TCs. Optimization routines varying *K*-mer and bubble size parameters in CLC Genomics Workbench software based on De-bruijn graph principles for *de novo* assembly (Egan et al., 2012) generated 24 initial assemblies, of which assembly *47x300* (*K*-mer value of 47 and bubble size of 300) was chosen due to optimal assembly statistics like high number of mapped reads, high N50 value and low total number of contigs. The CLC Genomics Workbench software has been used successfully to generate *de novo* assemblies of transcriptomes in other non-model plants such as *Thalasspi arvense* (Pennycress, Dorn et al., 2013) and *Cleome spinosa* (*C*<sub>3</sub> species), *Cleome gynandra* (*C*<sub>4</sub> species) (Bräutigam et al., 2011), and performed well compared to other *de novo* assembly software in a study investigating chick pea (Garg et al., 2011b). The quality of the *47x300* assembly was indicated by the validation procedure comparing contigs against 32 full-length *V. faba* cDNAs in GenBank and three sequenced *V. faba* *CesA* genes (Chapter 2; Appendix 2). A total of 21297 contigs were generated in this assembly with average contig length of 1114bp, this being higher than *de novo* assemblies of chick pea (Garg et al., 2011a) and insulin plant (Annadurai et al., 2012). These statistics indicate that the De-bruijn graph-based assembly generated contigs that showed a high representation of unique genes in *V. faba*. This conclusion was particularly relevant to TC biology, since many of the contigs comprising assembly *47x300* were identical in nucleotide sequence to, or very closely matched, *V. faba* genes previously identified as having roles in inductive signalling of epidermal TCs, such as ethylene response factors (*VjERF1-3*), ethylene insensitive transcription factors (*VjEIN3-1*, *VjEIN3-2*), ethylene synthesis (*VjACO1*, *VjACO2*, *VjACS2*) and respiratory burst oxidases (*VjrbhA*, *VjrbhC*), all of which are differentially expressed specifically in epidermal TCs of *V.*

*faba* (Zhou et al., 2010; Andriunas et al., 2012). Annotation of the 21,297 contigs from 47x300 using Blast2GO resulted in assigning GO terms for 17,180 contigs (80.6%), this being higher than those achieved in *de novo* assembly of other non-model plants (Mizrachi et al., 2010; Wang et al., 2010; Garg et al., 2011a; Wei et al., 2011). As expected, contigs from the *V. faba* assembly were highly conserved with other legume sequences such as chick pea (47%) and *Medicago truncatula* (38%). Analysis of the 47x300 transcriptome map revealed that 756 contigs were predicted to encode for transcription factors, of which 326 could be classified into different families of plant transcription factor based on GO terminology. This corresponded to about 31 of the 58 known families of transcription factors in plants (Plant Transcription Factor Database (PlnTFDB), <http://plntfdb.bio.uni-potsdam.de/v3.0>), a total being similar to *de novo* assemblies in other legumes (Libault et al., 2009; Schmutz et al., 2010; Garg et al., 2011a). Prominent among these families were members of the homeobox gene family (19%) and WRKY and AP2/EREBP families (at 8% each) in the *V. faba* transcription factor family. These families are commonly associated with stress signalling pathways in plants (Williams, 1998; Dietz et al., 2010; Rushton et al., 2010), thus indicating the suitability of the *V. faba* transcriptome map as a reference to identify transcription factors putatively involved in regulating epidermal TC development in *V. faba* cotyledons. Overall, the characteristics of the *V. faba* transcriptome map generated in this project provides valuable new genomics resources for genetic studies in *Vicia* generally and specifically for transcript profiling of epidermal TC development in *V. faba* cotyledons.

### **5.2.2 Putative roles of identified transcription factors in *V. faba* TCs (Chapter 3)**

The RNA-Seq experiments reported in Chapter 3 were designed to identify both temporal and spatial changes in gene expression accompanying epidermal TC development. Temporal changes were identified by harvesting cotyledon tissues at 0, 3, 9 and 24 h culture, time points which correlate with known landmark stages in epidermal TC development (Wardini et al., 2007b). Spatial specificity was determined by comparing gene expression in *trans*-differentiating epidermal cells at these time points with storage parenchyma that does not form TCs (Farley et al., 2000). Hence transcript profiling of epidermal tissue along with storage parenchyma tissue at these time points was designed to identify transcription factors showing epidermal-specific expression and thus likely to be involved in epidermal-specific TC development. To identify such genes, a stringent

criteria was set whereby epidermal-specific expression was defined as a fold change of five or greater ( $\text{Log}_2 5 = 2.3$ ) across at least one culture time point relative to 0h, with storage parenchyma expression for that genes changing by only two-fold or less ( $\text{Log}_2 2 = 1$ ) across cotyledon culture. Most microarray studies use two-fold change as a minimum cutoff to identify differentially expressed genes (McCarthy and Smyth, 2009), however applying this criteria to the RNA-Seq dataset identified several thousand genes in this category. In contrast, applying the five-fold criteria resulted in 444 transcripts being defined as epidermal-specific, up-regulated, and a total of 172 transcripts identified as epidermal-specific, down-regulated. This stringent fold-change criteria applied to the RNA-Seq dataset revealed the substantial numbers of genes displaying significant levels of epidermal-specific change in gene expression accompanying the *trans*-differentiation of epidermal TCs. This result is consistent with specialized cell wall building events in plant cells requiring substantial regulatory gene networks (e.g., secondary wall biosynthesis; Taylor-Teeple et al., 2015).

The cohort of epidermal-specific up-regulated genes contained 22 transcription factors of which 13 were up-regulated within the first 3 h of cotyledon culture, a characteristic expected of a transcription factor operating in a signal transduction cascade responsible for induction of epidermal TCs. The most prominently up-regulated gene was GT-3B like, a member of the trihelix family of transcription factors. A functional role for *VfGT-3B-like* in TC development is not clear, however, the Arabidopsis ortholog *AtGT-3B* is involved in regulating expression of a soybean calmodulin gene, *SCaM-4* (Park et al., 2004). Since wall ingrowth deposition involves  $\text{Ca}^{2+}$  signalling (Zhang et al., 2015a,c), this gene could be operating via calmodulin signalling to regulate this process. MYB family transcription factors were commonly present in the epidermal-specific, up-regulated category (10 out of 22 transcription factors). As discussed previously, *ZmMRP1*, a member of the MYB-related family in plants, is the only transcription factor experimentally confirmed as a regulator of wall ingrowth deposition in TCs (Gómez et al., 2009). Several Arabidopsis orthologs of *Vicia* MYB transcription factors identified in this study are known to play roles in cell wall polymer synthesis, namely *AtMYB20* (*V. faba* Unigene 9668) as a regulator of cellulose/hemicellulose deposition in secondary walls (Zhong et al., 2008), and *AtMYB63* (*V. faba* Unigene 19002) which regulates lignin biosynthesis (Zhou et al., 2009; Zhong et al., 2010).

Also prominent amongst the category of epidermal-specific up-regulated genes were members of the ERF family. This is not surprising as ethylene is a component of the signalling pathway acting downstream of auxin signalling to promote epidermal TC development in *V. faba* cotyledons (Zhou et al., 2010; Andriunas et al., 2011). The Arabidopsis ortholog of *V. faba* Unigene 7266, known as RAP2.4, is proposed to be involved in dedifferentiation (Iwase et al., 2011), which is a precursor event of the subsequent *trans*-differentiation of epidermal TCs. Auxin is proposed to stimulate dedifferentiation via inducing ethylene production during root formation (Sun and Bassuk, 1993), hence these ERFs may act downstream of ethylene promoting dedifferentiation to prepare cells for *trans*-differentiation to become epidermal TCs. Furthermore, the Arabidopsis ortholog of *V. faba* Unigene 7356, namely *AtERF98*, regulates ascorbic acid production (Zhang et al., 2012), which in turn may promote cell wall loosening required for wall ingrowth deposition.

The category of epidermal-specific, down-regulated genes contained 172 transcripts, of which 10 were transcription factors, including two homeobox leucine zipper proteins, and transcription factors belonging to the MADS-box and zinc finger CCCH-domain families. One of the *V. faba* homeobox ortholog genes, *ATHB-1*, which was down regulated by 3 h cotyledon culture, belongs to the HD-Zip I class of transcription factors (Ariel et al., 2007). This gene regulates other genes involved in cell wall composition and cell elongation in hypocotyls of Arabidopsis (Capella et al., 2015), and thus down regulation of the *V. faba* ortholog may reflect altered compositional profile of wall ingrowths in epidermal TCs compared to the primary wall (Vaughn et al., 2007).

In addition to identifying epidermal-specific differential expression during cotyledon culture, analysis of expression data revealed numerous genes showing epidermal-enhanced differential expression. This category consisted of genes showing up-regulation in both epidermal and storage parenchyma, but the magnitude of this differential expression was significantly greater in epidermal cells across cotyledon culture compared to storage parenchyma. Many of the transcription factors identified as epidermal-enhanced, up-regulated, belong to the WRKY gene family, known generally to be stress responsive and play regulatory roles in both biotic and abiotic plant stress response (Rushton et al., 2010). The high proportion of WRKY genes in this category is consistent with cotyledon culture causing stress throughout the organ, but the significant increase in

epidermal cells points to the involvement of at least some of these WRKY genes in signalling the *trans*-differentiation of epidermal TCs. This conclusion is supported by the observation that various Arabidopsis orthologs of these *V. faba* WRKYs are indirectly associated with TC responses in other systems. For example, the Arabidopsis ortholog of Unigene 11848 (fold-increase difference of 377 in epidermal tissue) is *AtWRKY28*, the closest paralog of which, *AtWRKY8*, is up-regulated in the *vte2* mutant which displays cold-dependent increased wall ingrowth deposition in PP TCs (Maeda et al., 2006, 2014). Furthermore, the *V. faba* ortholog of Unigene 2088, *AtWRKY23*, is expressed during syncytia and giant cell formation, cells with TC-like wall ingrowths, in roots of nematode-infected cells (Grunewald et al. 2008; Cabrera et al., 2014). Similar connections to TC biology can be made for other WRKY genes, whereby *AtWRKY33* (*V. faba* Unigene 12104) is known to regulate genes in the ethylene biosynthesis pathway (Birkenbihl et al., 2012), while *AtWRKY23* (*V. faba* Unigene 2088) and *AtWRKY33* (*V. faba* Unigene 12104) are regulated by auxin (Berendzen et al., 2012; Grunewald et al., 2012). Collectively, these observations point to a role(s) of these WRKY genes in the process of regulating epidermal TC development, but the precise contributions of these WRKYs to this process requires further investigation.

### **5.3 IS ARABIDOPSIS A GOOD MODEL TO TEST ORTHOLOGS OF *V. faba*? (Chapter 4)**

#### **5.3.1 Functional characterization of *V. faba* transcription factors using Arabidopsis orthologs**

Chapter 4 of this research project presented an attempt to experimentally demonstrate a role for the transcription factors identified from RNA-Seq of *V. faba* cotyledons in regulating TC development. Using *V. faba* for genetic modification in order to study these putative transcriptional regulators is challenging due to the recalcitrance of *V. faba* to stable genetic transformation (Böttinger et al., 2001). Hence an alternative model system to investigate genetic regulation of TCs with reticulate wall ingrowth deposition was needed. In this case, analysis of PP TC in Arabidopsis was chosen because these TCs deposit reticulate wall ingrowths (Haritatos et al., 2000), there is a vast array of T-DNA insertional mutants available in this model species, and a procedure to image wall ingrowth deposition in these cells by confocal imaging of propidium iodide-stained tissue

(Nguyen and McCurdy, 2015) provided a convenient methodology to examine these cells in numerous mutants (Nguyen and McCurdy, 2015). Furthermore, abiotic stresses such as high light, cold temperature and exposure to jasmonic acid were known to induce elevated levels of wall ingrowth deposition in these cells (Amiard et al., 2007; Maeda et al., 2006), thus providing a platform to experimentally manipulate wall ingrowth deposition in PP TCs. However, extensive confocal analysis of single and double T-DNA insertional mutants in various Arabidopsis orthologs of the candidate *V. faba* genes failed to identify any evidence of altered wall ingrowth deposition in these mutants, either tested under standard growth conditions or in the case of the WRKY orthologs, in response to cold-treatment. This outcome may be attributed to several possible reasons, either operating independently or in combination. First, the T-DNA insertional strategy was compromised by situations where expression of individual genes in a single or double mutant was not completely knocked out, thus compromising testing the function of that gene by mutant analysis. In-complete knockout occurred for 6 of the 10 genes tested, thus 60% of the genes tested were done so under some degree of compromise based on this observation. This circumstance arose from the unavoidable characteristics of each T-DNA insertional line, and could possibly be addressed in future studies by using additional T-DNA insertion lines for each gene as they become available, although it is stressed here that each mutant line used was the best available based on predictions of the insertion event showing the highest probability for complete knockout. Thus, for many genes, no other preferable insertion line was available. In such cases, targeting gene suppression by amiRNA approaches may be more effective (see Future Directions).

In addition to gene knockout effects, or lack thereof, gene redundancy may also be impacting significantly on the approach used to test the function of each Arabidopsis ortholog. It is well established that functional redundancy amongst transcription factors in Arabidopsis is very common (Mitsuda and Ohme-Takagi, 1999; Alves et al., 2014). For example, in the case of secondary wall deposition, complex transcriptional regulation of different cell wall polymer genes occurs and this regulation involves extensive redundancy for most if not all transcription factors involved in this process (Taylor-Teeple et al., 2015). Since wall ingrowth deposition and secondary wall deposition both represent examples of highly polarized wall deposition in plants, it may be expected that wall ingrowth deposition also involves extensive transcriptional redundancy (see Arun Chinnappa et al., 2013; Appendix 1). Such redundancy may be expected amongst the

MYB, WRKY and ERF genes identified as showing epidermal-specific/enhanced expression during epidermal TC development (Dubos et al., 2010; Chen et al., 2010; Taylor-Teeple et al., 2015). Similarly, functional redundancy amongst the GT trihelix factors caused difficulties in identifying physiological functions by using a mutant screening approach (Ayadi et al., 2004).

### **5.3.2 Arabidopsis as a model to test *V. faba* orthologs**

Arabidopsis has been widely used as model system in plants to study various biological process especially plant cell wall biology (Koornneeff and Meinke, 2010; Liepman et al., 2010). However, in the current study, *V. faba* orthologs in Arabidopsis showed similarities ranging from 40-93% identity at the amino acid level, but based on orthologous phenotyping, no functions associated with wall ingrowth deposition could be identified for these genes using T-DNA insertional mutagenesis. This observation could be interpreted as showing minimal functional relatedness between Arabidopsis and *V. faba* genes. This possibility is supported by a study comparing genome structure of *Medicago truncatula* with Arabidopsis, which revealed a low degree of microsyteny between the two genomes (Zhu et al., 2003) and thus minimal functional conservation between “orthologous” genes (Zhu et al., 2003). This observation is particularly acute given that *V. faba* is a very close relative with *Medicago truncatula* (Doyle et al., 1996; Ellwood et al., 2008). However, in the absence of a transformation system in *V. faba*, and the time-frame for thesis research, the reverse genetics approach using T-DNA insertional mutants in Arabidopsis was the best available phenotyping approach to test the functional roles of *V. faba* genes selected as putative transcriptional regulators of TC development based on RNA-Seq. In conclusion, due to the limitations of the T-DNA insertional approach, the role of these transcription factors as putative regulators of TC development remains to be demonstrated.

## **5.4 FUTURE DIRECTIONS**

A cohort of transcription factors identified from their spatial and temporal expression characteristics as possibly involved in regulating the *trans*-differentiation of adaxial epidermal TCs in *V. faba* cotyledons were identified. However, the approach of using reverse genetics, or “orthologous phenotyping” to test the role of orthologous genes in Arabidopsis was unsuccessful. Consequently, new experimental approaches to test the

role of these transcription factors are required. One possibility is to invest in the effort to develop a robust transformation protocol for *V. faba*. While the current transformation efficiency of *V. faba* is unacceptably low using stem sections as explant (Böttinger et al., 2001), a better choice of explant tissue might increase the frequency of successful regeneration. *De novo* regeneration of transformed explants in legumes is highly challenging, so explants derived from meristematic tissues like shoot apices could be used. Using shoot apices as explant material for transformation allows axillary shoot formation from the embryonic axis with less tissue culture steps, and also the genotype of the plant will have no influence on regeneration (Pigeaire et al., 1997). Another possibility to study the role of the *V. faba* transcription factors identified in this study is through biolistic bombardment of adaxial epidermal cells with amiRNA vectors for gene silencing (Eamens and Waterhouse, 2011). These amiRNA vectors can be designed to target individual genes or closely related sequences, thus silencing two or more genes simultaneously. The induction of epidermal TCs in *V. faba* cotyledons can be reversibly delayed by culture in the presence of inhibitors of ROS (diphenyleneiodonium) and ethylene (aminoethoxyvinylglycine) production (Andriunas et al., 2012), thus enabling constructs bombarded into epidermal cells to be expressed prior to experimental induction of epidermal TCs. Co-expression with a GFP marker could allow identification of transformed epidermal cells prior to analysing the effect of gene suppression on wall ingrowth deposition. Protocols for biolistic bombardment into epidermal cells of leaves (Ueki et al., 2013) could be followed in the first instance.

Other alternatives could be to investigate the role of orthologous transcription factors in other legume species. *Medicago sativa* (alfalfa) and *Pisum sativum* (pea – the closest relative to *V. faba*) both develop CC TCs (Joshi et al 1993; Gunning et al., 1974), and both species are transformable (alfalfa – Weeks et al., 2008; pea – Zhang et al., 2015). Thus, it would be feasible to either over-express the *V. faba* transcription factors to assess effects on development of CC TCs in these species, or suppress expression of orthologous genes by amiRNA.

Instead of using a reverse genetics approach (loss-of-function) to test Arabidopsis orthologs, selected *V. faba* transcription factors could be cloned and over-expressed in Arabidopsis (gain-of-function) under control of a constitutive promoter like CaMV35S, or more precisely by control of a phloem-specific promoter such as *rolC* (Booker et al.,

2003; Srivastava et al., 2009), to study their effect on TC development. Gain-of-function approaches have been used as an alternative to where loss-of-function was not successful (e.g., Mitsuda and Ohme-Takagi, 2009; Kondou et al., 2010). Gain-of-function strategies have identified the function of transcription factors such as *PAP1*, *AtMYB23* and *NST1* (Kirik et al., 2001; Esch et al., 2004; Mitsuda et al., 2005; Mitsuda and Ohme-Takagi, 2009), and this approach was successful in demonstrating the role of *VfPIP1*, a putative aquaporin gene isolated from *V. faba* leaf epidermis (Cui et al., 2008). Cloning of the *V. faba* sequences would be straightforward given the *de novo* transcriptome map detailed in Chapter 2.

Since many of the double mutants analysed in Chapter 4 were compromised by lack to various degrees of gene knockout, undertaking gene suppression by amiRNA strategies could be useful. Indeed, as mentioned earlier, this approach is currently being used to investigate the possible role of *AtWRKY8* and *AtWRKY28* as regulators of TC development, and this approach would be timely to investigate *AtGT-3B* and *AtGT-3A*, given the inability to assess the functions of these potentially important genes due to the absence of gene knockdown in the *atgt-3b* mutant. Sequence analysis of each gene pair listed in Table 4.1 has revealed that a single amiRNA construct could simultaneously target expression of both genes in each pair, a minimal requirement to address functional redundancy.

One distinct possibility emerging from this study and previously discussed is that the Arabidopsis orthologs of the *V. faba* genes do not actually function in regulating TC development, despite their strong epidermal-specific or epidermal-enhanced expression profiles. Given this possibility, non-targeted forward genetics may eventually be the best approach to identify transcriptional regulators of TC development. A forward genetics screen looking for an altered wall ingrowth phenotype in PP TCs of Arabidopsis might be feasible by developing high-throughput capability of the propidium iodide staining procedure to identify aberrant levels of wall ingrowth deposition. Genotyping an ethyl methanesulfonate mutant by Next Generation Mapping (NGM) is now straightforward (Austin et al., 2011), thus making this approach more realistic and timely. This approach offers the long-realized benefit of forward genetics in discovering essential genes required for a particular biological process, in this case wall ingrowth building in TCs.

In addition, RNA-Seq of PP TC development in Arabidopsis could be undertaken similar to the *V. faba* study to directly identify endogenous regulators in Arabidopsis, thus allowing loss-of-function and gain-of-function approaches to be used to assess the role of identified transcription factors. This approach would be more powerful than the current study using *V. faba* cotyledons as identified genes could be directly tested rather than testing orthologous genes in a different species. Furthermore, performing RNA-Seq in Arabidopsis provides the availability of computational approaches to investigate relationships between putative transcriptional regulators using transcriptomic data (Koryachko et al., 2015; Smita et al., 2015).

## 5.5 CONCLUSIONS

This project initiated a study to identify transcriptional regulators of TC development in plants, using the *V. faba* cotyledon culture system to undertake transcript profiling using RNA-Seq, followed by phenotypic analysis of orthologous genes in Arabidopsis. Transcript profiling by RNA-Seq necessitated *de novo* assembly of a transcriptome map in *V. faba*, which was successfully undertaken and now provides a genetic resource for this cool-season grain legume species. A panel of transcription factors displaying epidermal-specific or epidermal-enhanced transcriptional regulation in *V. faba* cotyledons were identified from the RNA-Seq analysis, with many showing predicted functions at least consistent with a role in regulating epidermal TC development. However, functional characterization of orthologous transcription factors in Arabidopsis using a reverse genetics approach was not successful in establishing a role for these genes in regulating TC development. This outcome may have been caused by technical or biological explanations, or a combination of both. Nonetheless, the substantial epidermal-centred transcriptional regulation of these transcription factors accompanying the *trans*-differentiation of epidermal TCs in *V. faba* cotyledons strongly implies a functional role for these genes, and thus alternative experimental possibilities to analyse these genes in *V. faba* have been discussed. Ultimately, however, unequivocal identification of transcriptional regulators of TC development in plants may require gain-of-function or loss-of-function studies in Arabidopsis focusing on PP TCs in minor veins. A forward genetics screen may ultimately prove to be the most compelling experimental approach

to achieve this goal, all with the long-term goal of manipulating TC development to improve crop yield.

# APPENDICES

## APPENDIX 1: Chapter 1 Supplementary Data

### Mini-Review

# **Phloem parenchyma transfer cells in *Arabidopsis* – an experimental system to identify transcriptional regulators of wall ingrowth formation**

**Kiruba Shankari Arun Chinnappa, Thi Thu Suong Nguyen, Jiexi Hou, Yuzhou Wu and David W. McCurdy\***

School of Environmental and Life Sciences, The University of Newcastle, NSW, Australia

**\*Correspondence:**

David McCurdy  
School of Environmental and Life Sciences  
The University of Newcastle  
University Drive, Callaghan  
NSW 2308, Australia  
e-mail: David.McCurdy@newcastle.edu.au

**Keywords:** *Arabidopsis*; phloem parenchyma; transfer cells; wall ingrowths; transcription factors

**Running title:** *Arabidopsis* phloem parenchyma transfer cells

**Word count:** 2,725

**Number of Figures:** 1

**Number of Tables:** 1

## ABSTRACT

In species performing apoplastic loading, phloem cells adjacent to sieve elements often develop into transfer cells (TCs) with wall ingrowths. The highly invaginated wall ingrowths serve to amplify plasma membrane surface area to achieve increased rates of apoplastic transport, and may also serve as physical barriers to deter pathogen invasion. Wall ingrowth formation in TCs therefore plays an important role in phloem biology, however the transcriptional switches regulating the deposition of this unique example of highly localized wall building remain unknown. Phloem parenchyma (PP) TCs in *Arabidopsis* veins provide an experimental system to identify such switches. The extent of ingrowth deposition responds to abiotic stress, enabling bioinformatics to identify candidate regulatory genes, and simple fluorescence staining of PP TCs in leaves enables phenotypic analysis of relevant mutants. Combining these approaches resulted in the identification of *GIGANTEA* as a regulatory component in the pathway controlling wall ingrowth development in PP TCs. Further utilization of this approach has identified two NAC-domain and two MYB-related genes as putative transcriptional switches regulating wall ingrowth deposition in these cells.

## Introduction

The plant cell wall profoundly defines cell shape and functioning. This observation is particularly acute for transfer cells (TCs) which develop extensive wall ingrowths to aid nutrient transport. These cells *trans*-differentiate from various differentiated cell types at sites where nutrient distribution pathways encounter apoplasmic/symplasmic discontinuities (Pate and Gunning, 1969; Offler et al., 2003). The increase in plasma membrane surface area resulting from wall ingrowth deposition enables increased densities of nutrient transporters to facilitate localized flux of nutrients across these apoplasmic/symplasmic junctions.

TCs are prominent at anatomical sites required for phloem loading and post-phloem unloading processes. In species that perform apoplasmic phloem loading, vascular cells adjacent to sieve elements (SEs) often develop extensive wall ingrowths. Well known examples include companion cells (CCs) in pea (Gunning and Pate, 1969; Henry and Steer, 1980; Wimmers and Turgeon, 1991), phloem parenchyma (PP) in *Arabidopsis* (Haritatos et al., 2000; Amiard et al., 2007), and both CCs and PP in *Senecio vulgaris* (Pate and Gunning, 1969; Amiard et al., 2007). In pea, the onset of assimilate export from young leaves coincides with the differentiation of leaf minor vein TCs (Gunning & Pate, 1974), and in *Arabidopsis*, sucrose export from leaves is affected if wall ingrowth abnormalities occur in the PP TCs (Maeda et al., 2006). TCs are also commonly observed in cells involved in post-phloem unloading pathways (Patrick, 1997), particularly in seed of cereal crops such as wheat and barley (Thompson et al 2001). Wall ingrowth formation therefore plays an important role in efficient phloem loading and post-phloem unloading strategies in many species, however the genetic pathways which regulate wall ingrowth deposition in TCs remain largely unknown.

TC development occurs across normal developmental windows but also in response to biotic and abiotic stress (Offler et al., 2003). Recent studies using epidermal TCs of *Vicia faba* cotyledons have established that auxin (Dibley et al., 2009), ethylene (Zhou et al., 2010; Andriunas et al., 2011) and reactive oxygen species (ROS) (Andriunas et al., 2012) function as inductive signals for TC development. Furthermore, expression profiling in epidermal TCs of *V. faba* cotyledons (Dibley et al., 2009) and in endosperm TCs in barley (Thiel et al., 2008, 2012) indicates that wall ingrowth deposition involves differential expression of hundreds of genes. The missing link in this developing molecular understanding of TC biology, however, is the identity of key transcriptional regulators which respond to inductive signals and switch on the downstream cascades of gene expression required to build wall ingrowths. A genetic approach is well suited to identify such transcription factors. In this mini-review we discuss the features of PP TCs in *Arabidopsis* that enabled a combined bioinformatics and reverse genetics approach to be undertaken to discover that *GIGANTEA* is a component of a pathway regulating wall ingrowth deposition in PP TCs. Further, we describe preliminary results using this approach to identify previously uncharacterized members of the NAC-domain and MYB-

related gene families as putative transcriptional regulators of wall ingrowth deposition in PP TCs.

### **Phloem parenchyma transfer cells in *Arabidopsis***

TCs in *Arabidopsis* are known to occur in PP of the minor vein network in both leaves (Haritatos et al., 2000) and sepals (Chen et al., 2012). These PP TCs are defined as Type B TCs (Gunning and Pate, 1969), characterized by having bulky wall ingrowths predominantly abutting SEs and to a lesser extent CCs (Haritatos et al., 2000; Amiard et al., 2007). These three cell types together constitute phloem tissue of the minor vein in *Arabidopsis*, with proportionate numbers of cells of each type relatively consistent throughout the vein system regardless of vein order (Haritatos et al., 2000). SEs are smaller than CCs, as is typical of collection phloem described by van Bel (1996), and PP cells are larger than CCs (Haritatos et al., 2000). Vein order in *Arabidopsis* leaves typically extends to three or four (Haritatos et al., 2000) or sometimes to five orders (Kang et al., 2007). This number is lower than the typically six or seven vein orders seen in most dicot species, and may in part account for the suggestion that both major and minor veins, being in close proximity to mesophyll tissue, are likely to be involved in phloem loading and thus functionally defined as “minor veins” (Haritatos et al., 2000).

A role for PP TCs in phloem loading is based on structural and molecular observations. Prominent symplasmic connections occur between PP and neighboring bundle sheath cells (Haritatos et al., 2000), providing a symplasmic delivery pathway for sucrose from photosynthetic mesophyll cells. Prominent wall ingrowths deposited adjacent to abutting cells of the SE/CC complex infers that the symplasmically delivered sucrose is effluxed across the plasma membrane of PP TCs into the apoplasm (Amiard et al., 2007). Subsequent movement of sucrose into the SE/CC complex occurs via carrier-mediated uptake by SUC2, a sucrose/H<sup>+</sup> co-transporter localized to the plasma membrane of CCs in *Arabidopsis* (Truernit and Sauer, 1995; Gottwald et al., 2000). The machinery responsible for sucrose efflux from PP TCs into the apoplasm was recently identified as members of the AtSWEET family of sugar transporters (Chen et al., 2012). AtSWEET11 and 12 function as sucrose uniporters that facilitate sucrose efflux, and both localize to the plasma membrane of PP TCs (Chen et al., 2012). An *atsweet11 atsweet12* double mutant shows various physiological traits consistent with impaired sucrose export from leaves (Chen et al., 2012). These authors concluded that PP TCs participate in a two-step phloem loading strategy in *Arabidopsis* – unloading of sucrose from PP TCs into the apoplasm, followed by active uptake of this apoplasmic sugar into the SE/CC complex by SUC2. Interestingly, Chen et al. (2012) propose that the highly localized deposition of wall ingrowths in PP TCs adjacent to cells of the SE/CC complex enables restricted diffusion of sucrose into the apoplasm, thus potentially reducing access to this apoplasmic sugar by pathogens. Others have suggested that the extensive deposition of bulky and highly localized wall ingrowths in PP TCs adjacent to SEs provides a physical barrier to protect against pathogen infection of sieve tissues which commonly target PP cells of the vascular network (Amiard et al., 2007).

Haritatos et al. (2000) observed that PP TCs also form asymmetric plasmodesmatal connections with adjacent CCs in *Arabidopsis* veins, implying that phloem loading in this system may also occur passively via plasmodesmatal pathways under certain physiological conditions. This observation implies that phloem loading strategies in different scenarios may be developmentally plastic, switching alternately from active, apoplasmic loading, to passive, symplasmic loading, even along a single vascular bundle (Slewinski and Braun, 2010). The molecular signals that may control such plasticity are unknown, however the identification by Chen et al. (2012) that the promoter for *AtSWEET11* drives expression in leaf tissue specifically in PP cells provides a valuable addition to the molecular tool box to investigate such processes.

### ***Arabidopsis* phloem parenchyma transfer cells as an experimental system to investigate genetic control of wall ingrowth deposition**

Importantly for genetic analysis of TCs in a model species, wall ingrowth deposition in *Arabidopsis* PP TCs is responsive to various stresses. The extent of wall ingrowth invaginations in PP TCs of leaf minor veins was significantly increased in response to stress caused by high light or exposure to methyl jasmonate (Amiard et al., 2007). Furthermore, the high-light response was reduced in the jasmonate-deficient double mutant *fad7-1 fad8-1* (Amiard et al., 2007), implying the unexpected conclusion that chloroplast-derived jasmonates signal wall ingrowth deposition in PP TCs in response to oxidative stress. In support of this conclusion, a *npq1-2 lut2-1* double mutant showed increased levels of wall ingrowth deposition compared to wild-type when subjected to high-light stress (Demmig-Adams et al., 2013). The double mutant lacks zeaxanthin and its isomer lutein, photoprotective agents which suppress lipid peroxidation and most likely oxylipin (methyl jasmonate and its precursors jasmonic acid and 12-oxo-phytodienoic acid) formation. The absence of this suppression in the *npq1-2 lut2-1* double mutant presumably leads to higher levels of jasmonic acid when plants are switched from low to high light, thus the observed increase in deposition of wall ingrowths in PP TCs (Demmig-Adams et al., 2013).

Wall ingrowth deposition in PP TCs is also responsive to cold stress. As part of their study investigating the role of tocopherols in photoprotection, Maeda et al. (2006) reported that growth of wild-type plants at low temperature caused increased deposition of polarized wall ingrowths in PP TCs. In contrast, at low temperature the vitamin E-deficient mutant, *vte2*, displayed greatly increased levels of abnormal wall ingrowth deposition, including loss of polarized deposition and substantial accumulation of callose in and around the wall ingrowths (Maeda et al., 2006). Not surprisingly, the *vte2* plants showed reduced sugar export and consequently increased levels of soluble sugar in leaves of cold-treated plants (Maeda et al., 2006). This result indicates not only that low temperature in itself causes increased wall ingrowth deposition, but at low temperature

the signal(s) causing localized wall ingrowth deposition are lost or over-ridden in the *vte2* mutant. Irrespective of this issue, however, the study by Maeda et al. (2006) adds low temperature to high light and exposure to methyl jasmonate (Amiard et al., 2007) as stress signals causing wall ingrowth deposition in *Arabidopsis* PP TCs. From the perspective of identifying transcriptional regulators of wall ingrowth deposition, the importance of these observations is that they enable bioinformatics approaches to be used to identify candidate genes.

### **Fluorescence staining of phloem parenchyma transfer cells in *Arabidopsis* leaves**

TCs typically occur deep within tissue systems and consequently have mostly been studied by electron microscopy, a process which is not compatible for high throughput genetic screening using *Arabidopsis*. Wall ingrowths lack lignin but are abundant in cellulose and hemicelluloses (DeWitt et al., 1999; Dahiya and Brewin, 2000; Vaughn et al., 2007), therefore Edwards et al. (2010) used Calcofluor White staining of cleared leaf tissue as a means to rapidly assess the abundance of PP TC development across whole leaves. Staining showed strong patches of fluorescence in terminating minor veins but also more continuous, linear regions of fluorescence often seen as one or two rows of staining within each vein (**Figure 1A, B**). Higher magnification views revealed that the Calcofluor White staining showed a distinctive mottled appearance, a characteristic consistent with staining the patchy and tangled wall ingrowths seen in leaf PP TCs by scanning electron microscopy (**Figure 1C, D**; Edwards et al., 2010). The non-continuous staining pattern for PP TCs along a given vein is consistent with observations by transmission electron microscopy that not all PP cells contain wall ingrowths (Amiard et al., 2007), a situation possibly reflecting potential plasticity in phloem loading mechanisms as discussed by Slewinski and Braun (2010). Furthermore, the ability to survey whole leaves for the presence of PP TCs clearly established that these cells are prominent in both minor and major veins of the vascular network, an observation consistent with the conclusion that both vein types in *Arabidopsis* are likely to be involved in phloem loading (Haritatos et al., 2000).

A recent improvement for fluorescence staining to detect PP TCs in *Arabidopsis* leaves has been the use of Aniline Blue rather than Calcofluor White. Callose is an abundant component of the electron translucent outer layer of wall ingrowths in both epidermal TCs of *V. faba* cotyledons (Vaughn et al., 2007) and *Arabidopsis* PP TCs (Maeda et al., 2006, 2008). Other than being deposited in sieve plates, callose is mostly absent from other tissues in unwounded leaves, thus giving superior signal-to-noise staining of PP TCs compared to Calcofluor White (**Figure 1E, F**). Double labeling experiments have shown that Aniline Blue gives the same mottled patterns of staining for PP TCs as does Calcofluor White (J. Hou – unpublished observation and see Edwards et al., 2010), thus confirming that Aniline Blue can be used as a convenient and high throughput fluorescence stain for wall ingrowth deposition in PP TCs.

### **Identification of GIGANTEA as a component in the regulatory pathway controlling wall ingrowth deposition in PP TCs**

Combining the experimental features of PP TCs as described above, Edwards et al. (2010) performed a hierarchical bioinformatics analysis of publically available microarray datasets and identified *GIGANTEA* (*GI*) as one of about 46 genes commonly up-regulated in leaves subjected to either high-light or cold stress. Phenotypic analysis using Calcofluor White staining of leaves revealed that in both *gi-2* and *gi-3* plants, the abundance of PP TCs in veins was reduced up to 15-fold compared to wild-type. Over-expression of *GI* in the *gi-2* mutant background restored PP TC abundance back to wild-type levels, whereas rescue of wall ingrowth deposition in *gi-2* did not occur after exposure to high light, methyl jasmonate or cold. Based on these outcomes, Edwards et al. (2010) proposed that *GI* may be regulating wall ingrowth deposition downstream of inputs from stress signals, possibly through detoxification of ROS (see Cao et al., 2006). In epidermal TCs of *V. faba* cotyledons, extracellular H<sub>2</sub>O<sub>2</sub> is known to act as a polarizing signal to direct aspects of wall ingrowth deposition (Andriunas et al., 2012; Xia et al., 2012). In *Arabidopsis*, however, H<sub>2</sub>O<sub>2</sub> is abundant in leaf vasculature, even in the absence of stress (Mullineaux et al., 2006), hence its ability to act as a local signal directing polarized wall ingrowth formation in PP TCs needs further investigation.

### **Identification of NAC-domain and MYB-related transcription factors as putative regulators of wall ingrowth deposition**

Based on the successful approach used by Edwards et al. (2010), we recently performed an extended bioinformatics analysis to identify transcription factors commonly up-regulated in leaf tissue in response to high light, methyl jasmonate and cold. Phenotypic analysis using Aniline Blue staining of leaves from homozygous T-DNA insertional mutants from this list identified several previously uncharacterized NAC-domain (At3g04420 and At1g33060) and MYB-related genes (At1g25550 and At1g49560) which showed significantly reduced abundance of PP TCs in veins of mature leaves compared to wild-type (**Table 1**). The levels of reduced abundance in each line, while significant, were not comparable to that seen for the *gi-2* mutant (**Table 1**), indicating the possibility that these transcription factors may be acting redundantly with unidentified orthologs in controlling wall ingrowth deposition. *In silico* expression data (eFP and Genevestigator) shows that all four genes are expressed at very low levels in leaves, and qPCR confirmed this observation directly for both expanding and fully expanded leaves (J. Hou, Y. Wu – unpublished observations). Low expression might be expected for genes operating as putative regulators of wall ingrowth deposition specifically in PP TCs, since the number of these cells relative to most other cell types in the leaf is exceedingly low (Haritatos et al., 2000, Edwards et al., 2010), and many plant transcription factors are expressed at low levels (Czechowski et al., 2004). Given these factors, we are using both constitutive

(CaMV-35S promoter) and PP-specific (*AtSWEET11* promoter) over-expression to test the role of these transcription factors as regulators of wall ingrowth deposition in *Arabidopsis*.

**TABLE 1.** Phenotypic analysis showing reduced abundance of PP TC staining for two NAC-domain and two MYB-related genes identified by bioinformatics as candidate transcriptional regulators of wall ingrowth deposition in PP TCs of *Arabidopsis* leaf veins.

| Gene number        | Mutant allele | % vein length showing staining for PP TCs <sup>§</sup> |
|--------------------|---------------|--|
| WT (Col-0)         |               | 45.3 ± 3.6   |
| <u>NAC-domain</u>  |               |  |
| At3g04420          | FLAG_009F02   | 18.2 ± 3.8**   |
| At1g33060          | SALK_085596   | 27.5 ± 2.9*  |
|                    | SALK_024241   | 31.5 ± 4.7*  |
| <u>MYB-related</u> |               |  |
| At1g25550          | SALK_144656   | 16.3 ± 2.4**   |
| At1g49560          | SALK_085182   | 20.5 ± 2.9*  |
|                    | SALK_095775   | 15.6 ± 2.7**   |
| <u>GIGANTEA</u>    |               |  |
| At1g22770          | <i>gi-2</i>   | 3.3 ± 1.0** <sup>†</sup>                               |

<sup>§</sup> This value was measured from mature, Aniline Blue-stained leaves according to our previously published method (Edwards et al., 2010). Data is presented as mean ± SE from two leaves from each of three plants per line. \**P*<0.01, \*\**P*<0.001.

<sup>†</sup> Data for *gi-2* taken from Edwards et al. (2010).

Interestingly, ectopic over-expression of VND6 or VND7, both NAC-domain transcription factors, causes *trans*-differentiation of non-vascular cells into metaxylem- and protoxylem-like vessels elements, respectively (Kubo et al., 2005), a process involving localized secondary wall deposition. Over-expression of various MYB transcription factors such as AtMYB46 (Zhong et al., 2007) and AtMYB83 (McCarthy et al., 2009) also causes ectopic secondary wall formation, leading to the conclusion that hierarchical transcriptional pathways, with NAC-domain and MYB transcription factors acting as either first- or second-level “master switches”, co-ordinate the gene expression programs required for localized secondary wall deposition (Zhong et al., 2010). Building wall ingrowths in TCs is also an example of highly localized wall deposition (McCurdy et al., 2008), thus our finding that two NAC-domain and two MYB-related genes are putative regulators of this process in PP TCs may indicate evolutionarily-conserved roles for members of these two large gene families in regulating transcriptional cascades involved in localized wall deposition. Further support for this proposition is that ZmMRP-1, a transcription factor which regulates basal endosperm TC development in maize, is a member of the MYB-related family of transcription factors in plants (Gómez et al., 2002, 2009).

### **Conclusions and future directions**

The formation of wall ingrowths in TCs impacts on phloem loading and post-phloem unloading processes in many species, with corresponding impacts on plant development and reproduction. Development of an experimental system to investigate PP TCs in *Arabidopsis* has proven useful to identify candidate genes operating as putative transcriptional regulators of wall ingrowth deposition in TCs. The discovery of *GI* as a component in the pathway regulating wall ingrowth deposition, and identification of NAC-domain and MYB-related genes as putative “master switches” involved in controlling this process, provides new lines of investigation to understand the genetic control of TC development and the cell biology of localized wall ingrowth deposition. Ultimately, identifying master switches which respond to various inductive signals to coordinate wall ingrowth deposition in TCs may provide new opportunities for improving crop yield by manipulating this process.

### **ACKNOWLEDGEMENTS**

This work was supported by an Australian Research Council Discovery Project Grant (DP110100770) and by a University of Newcastle FSCIT Strategic Research Initiative Grant.

## REFERENCES

- Amiard, V., Demmig-Adams, B., Mueh, K. E., Turgeon, R., Combs, A. F., and Adams, W. W. (2007). Role of light and jasmonic acid signaling in regulating foliar phloem cell wall ingrowth development. *New Phytol.* 173, 722-731.
- Andriunas, F., A., Zhang, H. M., Weber, H., McCurdy, D. W., Offler, C. E., and Patrick, J. W. (2011). Glucose and ethylene signalling pathways converge to regulate *trans*-differentiation of epidermal cells in *Vicia narbonensis* cotyledons. *Plant J.* 68, 987–998.
- Andriunas, F. A., Zhang, H. M., Xia, X., Offler, C. E., McCurdy, D. W., and Patrick, J. W. (2012). Reactive oxygen species form part of a regulatory pathway initiating *trans*-differentiation of epidermal transfer cells in *Vicia faba* cotyledons. *J. Exp. Bot.* 63, 3617-3629.
- Cao, S., Jiang, S., and Zhang, R. (2006). The role of GIGANTEA gene in mediating the oxidative stress response and in *Arabidopsis*. *Plant Growth Regul.* 48, 261–270.
- Chen, L. Q., Qu, X. Q., Hou, B. H., Sosso, D., Osorio, S., Fernie, A. R., and Frommer, W. B. (2012). Sucrose efflux mediated by SWEET proteins as a key step for phloem transport. *Science* 335, 207-210.
- Czechowski, T., Bari, R.P., Stitt, M., Scheible, W.-R., and Udvardi, M.K. (2004). Real-time RT-PCR profiling of over 1400 *Arabidopsis* transcription factors: unprecedented sensitivity reveals novel root- and shoot-specific genes. *Plant J.* 38, 366-379.
- Dahiya, P., and Brewin, N. J., (2000). Immunogold localization of callose and other cell wall components in pea nodule transfer cells. *Protoplasma* 214, 210-218.
- Demmig-Adams, B., Cohu, C. M., Amiard, V., Zadelhoff, G., Veldink, G. A., Muller, O., and Adams, W. W. (2013). Emerging trade-offs - impact of photoprotectants (PsbS, xanthophylls, and vitamin E) on oxylipins as regulators of development and defense. *New Phytol.* 197, 720-729.
- DeWitt, G., Richards, J., Mohnen, D., and Jones, A.M. (1999). Comparative compositional analysis of walls with two different morphologies: archetypical versus transfer cell like. *Protoplasma* 209, 238-245.
- Dibley, S. J., Zhou, Y., Andriunas, F. A., Talbot, M. J., Offler, C. E., Patrick, J. W., and McCurdy, D. W. (2009). Early gene expression programs accompanying *trans*-differentiation of epidermal cells of *Vicia faba* cotyledons into transfer cells. *New Phytol.* 182, 863–877.
- Edwards, J., Martin, A. P., Andriunas, F., Offler, C.E., Patrick, J.W., and McCurdy, D.W. (2010). GIGANTEA is a component of a regulatory pathway determining wall

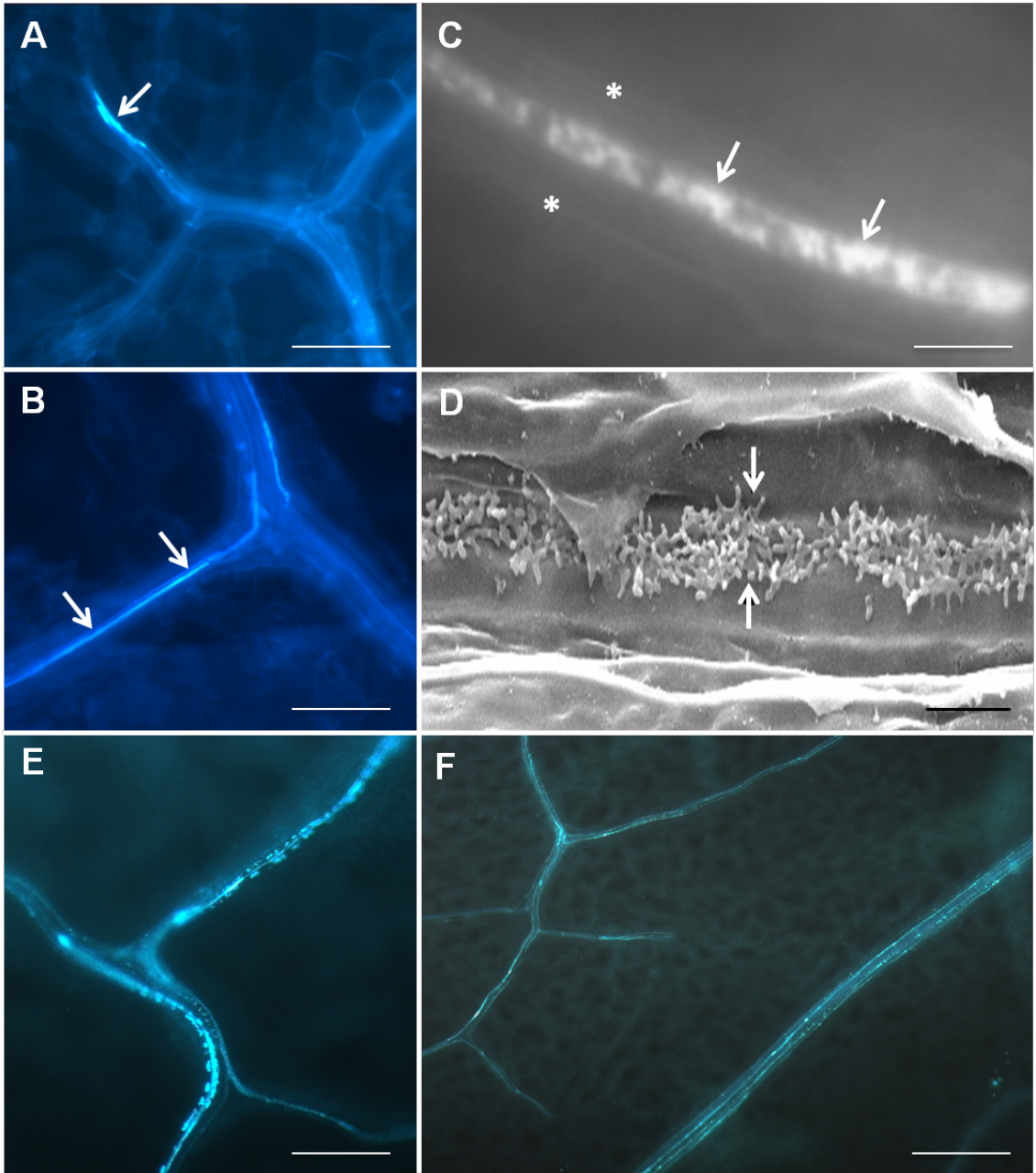
- ingrowth deposition in phloem parenchyma transfer cells of *Arabidopsis thaliana*. *Plant J.* 63, 651–661.
- Gómez, E., Royo, J., Muñiz, L.M., Sellam, O., Paul, W., Gerentes, D., Barrero, C., López, M., Perez, P., and Hueros, G. (2009). The maize transcription factor Myb-Related Protein-1 is a key regulator of the differentiation of transfer cells. *Plant Cell* 21, 2022-2035.
- Gómez, E., Royo, J., Guo, Y., Thompson, R., and Hueros, G. (2002). Establishment of cereal endosperm expression domains: Identification and properties of a maize transfer cell-specific transcription factor, ZmMRP-1. *Plant Cell* 14, 599-610.
- Gottwald, J. R., Krysan, P. J., Young, J. C., Evert, R. F., and Sussman, M. R. (2000). Genetic evidence for the *in planta* role of phloem-specific plasma membrane sucrose transporters. *Proc. Natl. Acad. Sci. U.S.A.* 97, 13979-13984.
- Gunning, B. E. S., and Pate, J. S. (1969). Transfer cells plant cells with wall ingrowths, specialized in relation to short distance transport of solutes - their occurrence, structure, and development. *Protoplasma* 68, 107-133.
- Gunning, B. E. S., and Pate, J. S. (1974). “Transfer cells”, in *Dynamic Aspects of Plant Ultrastructure*, ed. A.W. Robards (London: McGraw-Hill), 441–479.
- Haritatos, E., Medville, R., and Turgeon, R. (2000). Minor vein structure and sugar transport in *Arabidopsis thaliana*. *Planta*, 211, 105-111.
- Henry, Y., and Steer, M. W. (1980). A re-examination of the induction of phloem transfer cell development in pea leaves (*Pisum sativum*). *Plant, Cell & Environ.* 3, 377–380.
- Kang, J., Mizukami, Y., Wang, H., Fowke, L., and Dengler, N.G. (2007). Modification of cell proliferation patterns alters leaf vein architecture in *Arabidopsis thaliana*. *Planta* 226, 1207-1218.
- Kubo, M., Udagawa, M., Nishikubo, N., Horiguchi, G., Yamaguchi, M., Ito, J., Mimura, T., Fukuda, H., and Demura, T. (2005). Transcription switches for protoxylem and metaxylem vessel formation. *Genes Dev.* 19, 1855–1860.
- Maeda, H., Song, W., Sage, T. L., and DellaPenna, D. (2006). Tocopherols play a crucial role in low-temperature adaptation and phloem loading in *Arabidopsis*. *Plant Cell* 18, 2710-2732.
- Maeda, H., Sage, T. L., Isaac, G., Welti, R., and DellaPenna, D. (2008). Tocopherols modulate extraplastidic polyunsaturated fatty acid metabolism in *Arabidopsis* at low temperature. *Plant Cell* 20, 452-470.
- McCarthy, R. L., Zhong, R., and Ye, Z. H. (2009). MYB83 is a direct target of SND1 and acts redundantly with MYB46 in the regulation of secondary cell wall biosynthesis in *Arabidopsis*. *Plant Cell Physiol.* 50, 1950–1964.

- McCurdy, D.W., Patrick, J. W., and Offler, C. E. (2008). Wall ingrowth formation in transfer cells: novel examples of localized wall deposition in plant cells. *Curr. Opin. Plant Biol.* 11, 653-661.
- Mullineaux, P.M., Karpinski, S., and Baker, N.R. (2006). Spatial dependence for hydrogen peroxide-directed signaling in light-stressed plants. *Plant Physiol.* 141, 346-350.
- Offler, C. E., McCurdy, D. W., Patrick, J. W., and Talbot, M. J. (2003). Transfer cells: cells specialized for a special purpose. *Annu. Rev. Plant Biol.* 54, 431-454.
- Pate, J. S., and Gunning, B. E. S. (1969). Vascular transfer cells in angiosperm leaves. A taxonomic and morphological survey. *Protoplasma* 68, 135–156.
- Patrick, J. W. (1997). Phloem unloading: sieve element unloading and post-sieve element transport. *Annu. Rev. Plant Physiol. Plant Mol. Biol.* 48, 191-222.
- Slewinski, T.L., and Braun, D.M. (2010). Current perspectives on the regulation of whole-plant carbohydrate partitioning. *Plant Sci.* 178, 341–349.
- Thiel, J., Weier, D., Sreenivasulu, N., Strickert, M., Weichert, N., Melzer, M., Czauderna, T., Wobus, U., Weber, H., and Weschke, W. (2008). Different hormonal regulation of cellular differentiation and function in nucellar projection and endosperm transfer cells: A microdissection-based transcriptome study of young barley grains. *Plant Physiol.* 148, 1436-1452.
- Thiel, J., Riewe, D., Rutten, T., Melzer, M., Friedel, S., Bollenbeck, F., Weschke, W., and Weber, H. (2012). Differentiation of endosperm transfer cells of barley: a comprehensive analysis at the micro-scale. *Plant J.* 71, 639-655.
- Thompson, R. D., Hueros, G., Becker, H., and Maitz, M. (2001). Development and functions of seed transfer cells. *Plant Sci.* 160, 775-783.
- Truernit, E., and Sauer, N. (1995). The promoter of the *Arabidopsis thaliana* SUC2 sucrose-H<sup>+</sup> symporter gene directs expression of beta-glucuronidase to the phloem: evidence for phloem loading and unloading by SUC2. *Planta* 196, 564-570.
- van Bel, A. J. E. (1996) Interaction between sieve element and companion cell and the consequences for photoassimilate distribution: two structural hardware frames with associated physiological software packages in dicotyledons. *J. Exp. Bot.* 47, 1129–1140.
- Vaughn, K. C., Talbot, M. J., Offler, C. E., and McCurdy, D. W. (2007). Wall ingrowths in epidermal transfer cells of *Vicia faba* cotyledons are modified primary walls marked by localized accumulations of arabinogalactan proteins. *Plant Cell Physiol.* 48, 159-168.

- Wimmers, L. W., and Turgeon, R. (1991). Transfer cells and solute uptake in minor veins of *Pisum sativum* leaves. *Planta* 186, 2–12.
- Xia, X., Zhang, H.-M., Andriunas, F.A., Offler, C.E., and Patrick, J.W. (2012). Extracellular hydrogen peroxide, produced through a respiratory burst oxidase/superoxide dismutase pathway, directs ingrowth wall formation in epidermal transfer cells of *Vicia faba* cotyledons. *Plant Signal. & Behav.* 7, 1-4.
- Zhong, R., Richardson, E.A., and Ye, Z-H. (2007). The MYB46 transcription factor is a direct target of SND1 and regulates secondary wall biosynthesis in *Arabidopsis*. *Plant Cell* 19, 2776-2792.
- Zhong, R., Lee, C., and Ye, Z.H. (2010). Evolutionary conservation of the transcriptional network regulating secondary cell wall biosynthesis. *Trends Plant Sci.* 15, 625-632.
- Zhou, Y. C., Andriunas, F., Offler, C. E., McCurdy, D. W., and Patrick, J. W. (2010). An epidermal-specific ethylene signal cascade regulates trans-differentiation of transfer cells in *Vicia faba* cotyledons. *New Phytol.* 185, 931-943.

## Figure Legends

**FIGURE 1.** Imaging of PP TCs in *Arabidopsis* veins using fluorescence staining and scanning electron microscopy. Calcofluor White staining of cleared leaf tissue (**A-C**) showing presence of PP TCs in a terminating minor vein (arrow in **A**) and as more continuous linear strands of staining running along major veins (arrows in **B**). Higher magnification reveals a central band of mottled fluorescence (arrows in **C**, asterisks mark cell edges) in a PP TC which corresponds to the deposition pattern of reticulate wall ingrowths seen by scanning electron microscopy in these cells (arrows in **D**). Staining of PP TCs by Aniline Blue (**E, F**) shows the same patterns of staining as revealed by Calcofluor White, albeit with superior signal-to-noise properties (see **F**). Punctate staining indicating the non-continuous development of PP cells into PP TCs along a given length of vein is particularly evident in **E**. The images in **A-D** are reproduced from Edwards et al. (2010) and **E** and **F** are unpublished data. Staining with Aniline Blue was performed identically to that of Calcofluor White, except that 0.01 (w/v) Aniline Blue in 70 mM phosphate buffer, pH 8.5, was used to replace 0.05% (w/v) Calcofluor White. Scale bars: **A, B, E** = 100  $\mu\text{m}$ ; **F** = 200  $\mu\text{m}$ ; **C** = 5  $\mu\text{m}$ ; **D** = 2  $\mu\text{m}$ .



## APPENDIX 2: Chapter 2 Supplementary Data

### Validation of the *V. faba* transcriptome map using *CesA* genes

#### 2A.1 Introduction

A total of 24 assemblies were generated in CLC by varying the *K*-mer and bubble size. The three best assemblies arising from this analysis were chosen based on optimum parameters. These assemblies were initially validated by comparing the contig sequences against three cellulose synthase (*CesA*) genes (*VfCesA1*, *VfCesA2*, *VfCesA3a*) previously sequenced in the Plant Science Group at the University of Newcastle by S. Dibley using degenerate PCR and 5' and 3' RACE (unpublished data). *CesA* genes were chosen for validation purposes since they are relatively long sequences and typically contain a central hypervariable region which differs between *CesA* family members (Liang and Joshi, 2004), hence providing a good test for validating a given *de novo* assembly. This validation exercise provided initial insights which contributed to the validation routine published in Arun-Chinnappa and McCurdy (2015).

#### 2A.2 Primary validation of assembly using *CesA* sequences

The three best assemblies (*20 x 300*, *23 x 300* and *47 x 300*) were selected based on the optimum assembly parameters (see Supplementary Table 1 in Arun-Chinnappa & McCurdy, 2015) and BLAST databases were created in CLC Workbench, named after *K*-mer size (20, 23 and 47 respectively). The three *V. faba CesA* sequences, *VfCesA1*, *VfCesA2*, *VfCesA3a* (see Appendix 2A.3), were uploaded into CLC Workbench as individual *fasta* files. These genes were then analyzed by BLASTN against the created databases (*K*-mer assemblies) and the top contig hits with highest identity were selected for further analysis. All three assemblies successfully differentiated between the hypervariable regions of the *CesA* genes by identifying different contigs for each *CesA* gene (Table 2A.1). Pairwise alignment of the top hit contigs for each gene was performed with their corresponding gene to analyse global alignment using EMBOSS NEEDLE program from EMBL ([http://www.ebi.ac.uk/Tools/psa/emboss\\_needle/](http://www.ebi.ac.uk/Tools/psa/emboss_needle/)), and assemblies were assessed for good alignment parameters, such as identity percentage, similarity percentage and gaps. Pairwise alignment of these genes against the three assemblies showed that *47x300* assembly returned the best alignments for high identity and similarity percentage with less gaps, for two of the three genes tested (Table 2A.2). Two of the

contigs showed full length matching (i.e., including START and STOP codons) of the relevant *CesA* gene. The best performed assembly (47 x 300) was selected and a large scale contig validation using 32 complete *V. faba* cDNA sequences from GenBank was then performed, as described in Arun-Chinnappa and McCurdy (2015 – this Chapter).

**Table 2A.1: BLASTN output of the *V. faba CesA* genes against three assemblies.**

| Assembly | <i>VfCesA1</i> |           |            | <i>VfCesA2</i> |           |            | <i>VfCesA3a</i> |           |            |
|----------|----------------|-----------|------------|----------------|-----------|------------|-----------------|-----------|------------|
|          | Contig #       | Identity% | Hit length | Contig #       | Identity% | Hit length | Contig #        | Identity% | Hit length |
| 20x300   | 154            | 100       | 2567       | 104            | 99        | 4093       | 114             | 99        | 2628       |
| 23x300   | 158            | 100       | 3047       | 1135           | 99        | 4129       | 1342            | 99        | 3474*      |
| 47x300   | 143            | 98        | 3757*      | 1134           | 99        | 4148*      | 1086*           | 99        | 3474*      |

Asterisk (\*) indicates the best result for each gene in terms of maximum hit length.

**Table 2A.2: Comparison of pairwise alignment parameters of three *V. faba CesA* genes against the three best performing assemblies.**

| Assembly | <i>VfCesA1</i> |             |            | <i>VfCesA2</i> |             |             | <i>VfCesA3a</i> |             |          |
|----------|----------------|-------------|------------|----------------|-------------|-------------|-----------------|-------------|----------|
|          | Identity%      | Similarity% | Gaps       | Identity%      | Similarity% | Gaps        | Identity%       | Similarity% | Gaps     |
| 20x300   | 65.3           | 65.3        | 34.5       | <b>59.2</b>    | <b>59.2</b> | <b>39.8</b> | 39.8            | 39.8        | 49.1     |
| 23x300   | 77.8           | 77.8        | 21.8       | 40.8           | 40.8        | 48.3        | 90              | 90          | 9.4      |
| 47x300   | <b>93.8</b>    | <b>94.6</b> | <b>4.6</b> | 41             | 41          | 48          | <b>91.4</b>     | <b>91.4</b> | <b>8</b> |

Values highlighted in bold indicates the best result for each gene. Assembly 47x300 showed best outcome as it contained full length contigs (bold) for at least two of the three genes compared.

## Appendix 2A.3 Nucleotide Sequences of *VfCesA* genes

### *VfCesA1*

#### Nucleotide Sequence (3918 bp)

TATTTAGGTGACACTATAGAATACTCAAGCTATGCATCCAACGCGTTGGGAGCTCTCCCATATGGTCGAC  
CTGCAGGCGGCCGGAATTCAGTAGTGATTAAGCAGTGGTATCAACGCAGAGTACGCGGGGGCAGTGTG  
TTTTAATAAGCAAAGTACAAAGTGGAAAAATGGCGTGTAAAGTGGGCGAAGATTTTCATGCTTTGCCGC  
AAAATCTAAACGCAGATCGTGAACCTCACTTCATTGATCTGCATCAATCAATCTCCGTCGCTATAACAAC  
**ATG**GAAAGCTTCTTCCGGAATGGTTGCTGGGTCCACAAACGTAACGAGCTTGTTCGGATTTCGTCACGATT  
CTTCCGACAGCGGGCCGAAACCATTGAAGAATTTGAACGGACAAAATCTGTCAAATATGCGGTGAAAATGT  
TGGATTGACAGCTACTAGTGATGTGTTTGTGCTTGTAAATGAGTGTGGTTTCCCGTTTTGTCGACCTTGT  
TATGAATATGAGCGAAAAGATGGGAATCAGTCTTGTCCCTCAGTGCAAACTAGATACAAAAGGCACAAAG  
GGAGTCTTAGAGTGGATGGAGATGATGATGAGGATGATGGTGTATATAGAAAATGAGTTTAGTTATGG  
ACAAGGAAATACAAAGTCAAGGAGGCAATGGGAAGATGATGCTGAGCTTTCTTCGCTCTCTAGACGTGAT  
TATCAGCAACCGATTCTCTTCTTACTAATGGTCAAACGATGTCCGGTGAGATCCCGTGTGCTACGCCAG  
ATACTCAATCGATCCGAACTACTTCAGGTCTTTGGGCCATCTGAGAAAAGGTCACGCACTTCCCTATAT  
CGATCCAAGGCAACCGATTCTCTGTGAGAATTTGTGGATCCATCAAAGGACTTAAATTTCTTATGGTTTGGGA  
AACGTTGACTGGAAGGAAAGGGTTGAAGGTTGGAAGTTGAAGCACGAGAAAAATATGGTACAAATGACTG  
GTAGATATGCTGAGGGGAAAGGAGGAGGGGATATTGAAGGGACTGGTTCTAATGGAGAAGAATTCAC  
AATGGTTGATGATGCTCGACAACCTATGAGTCGGATTGTACCTATTTCTTCATCTCAATTGACCCCTTAT  
CGCGTTGTCATCGTACTCCGGCTGATAATTTCTCGGTTCTTCTTGCAATATCGTGTAACTCACCCAGTAA  
ATGATGCATATCCACTGTGGTTGACATCAGTTATCTGTGAGATTTGGTTTGCCTTATCCTGGATTTTGGGA  
TCAGTTTCCAAAGTGGTCACCCATTAATCGCGAGACTTATCTTGACAGGCTTGCTATAAGATACGATCGT  
GACGGAGAACCATCACAGTTGGCTCCTGTTGACGTTTTTGTGACGACAGTGGACCCCTCTCAAAGAGCCGC  
CTCTTGTCACTGCAAATACTGTTTTGTCTATACTCTCTGTTGATTACCCTGTCGACAAGGAATTTCTGTTA  
TGTGTCTGATGATGGTTTCACTATGTTGACTTTTTGAAGCCTTATCAGAAACAGCTGAGTTTGCAAAGAAG  
TGGGTGCCCTTTTTGCAAAAAACACAATATTGAGCCTAGAGCCCTGAGTTTTATTTTGCCCAGAAGATTG  
ATTACTTAAAGGACAAGATTCAACCTTCTTTTGTAAAGGAGCGACGGCAATGAAGAGAGAATATGAAGA  
ATTCAAAGTAGGGATCAATGCCTATGTTGCCAAAGCTCAGAAGACGCCAGAGGAAGTTGGACAATGCAG  
GATGGAACCTCCTTGGCCTGGAAATAATTCTAGGGATCATCCTGGAATGATTGAGGTGTTTTTAGGTCATA  
GCGGAGGGCTTGACACAGATGGTAATGAGCTGCCTAGGCTTGCTATGTTTTCTCGTGAAAAGCGGCCTGG  
CTTCCAACATCACAAGAAGGCTGGAGCTATGAATGCTTTGATTTCGAGTTTCTGCTGTTTTGACCAACGGT  
GCATATCTTTTGAATGTTGATTGTGATCACTACTTCAATAATAGCAAAGCTCTTAAAGAAGCAATGTGTT  
TCATGATGGATCCCACTTATGCAAAGAAGACATGCTATGTGCAATTTCTCAGAGATTTGATGGCATTGA  
CTTGCACGATCGATATGCCAATCGCAATATTGTCTTCTCGATATCAACATGAAAGGTCATGATGGTATT  
CAGGGCCCAGTCTATGTGGAACTGGTTGCTGTTTCAATAGGCAAGCTTTGTATGGTTATGATCCTGTTT  
TGACCAGGAGAAGATCTCGAACCTAACATTATTGTGAAGAGCTGTTGTGGTTCTAGAAAAGAAGGGAAAGGG  
TGGCAATAAAGAAGTACGGGTGACAAGAAGAGGGGTGTCAAAAGAACCAGTCCACCATTTCCATATTTAAT  
ATGGAGGATATAGAGGAGGGTGTGAAGGTTATGATGATGAAAGGTCACCTTAAATGCTCAGAAGAGTT  
TGGAGAAGCGTTTTTGGACAGTACCAGTTTTTATTTCTGCTACCTTCATGGAGCAGGGTGGCATTCCACC  
TACAACCAATCCTGCAACTCTTCTTAAAGGAAGCAATACACGTTATCAGCTGCGGTTACGAAGACAAGACA  
GAATGGGGCAAAGAGATTGGATGGATCTATGGTTCTGTGACTGAAAGATATCTTGACTGGGTTTAAAGATGC  
ATGCGCGAGGTTGGATTTCCGTCTATTGCATGCCACCTCGTCCAGCATTTAAGGGTCTGCACCCATCAA  
TCTTTCTGATCGTCTCAATCAAGTGCTTCGGTGGGCCCTGGGTTCAATCGAGATTTTCTTAGCAGGCAT  
TGTCCCTTATGGTATGGCTACAACGGAAGGATGAGGCCTCTCATGAGGCTTGCTTATATCAACACAATTG  
TCTACCCCTTTACCTCACTCCCGCTATTGCGTATTGACTCTTCTCCTGCATTTTGTCTTCTCACAAATAA  
ATTTATTATTTCCCGAGATAAGTAACTTTGCAAGTATGTGGTTTATCCTTCTCTTTATATCCATTTTTACC  
ACTTCAATTTCTCGAGCTAAGGTGGAGTGGTGTGCGGTATAGAAGACTGGTGGAGAAACGAACAGTTTTGGG  
TTATCGGTGGAACATCCGCACATCTTTTCGCCGTGTTCCAAGGGCTTCTCAAAGTGCTTGCAGGGATTGA  
CACAAATTTTACTGTACATCAAAGGCATCCGACGAAGACGGGGACTTCGCCGAGCTATACGTGTTCAA  
TGGACATCACTTCTCATCCCTCCCAACAGTGCTTATTGTGAACTTGGTAGGTATTGTGGCTGGTGTAT  
CTTTTGCATAAACAGTGGTTACCAATCTTGGGGTCCACTATTTGGAAAGCTTTTCTTTGCCATATGGGT  
CATTGCCCATTTATACCTTTCTTGAAGGGTCTATTGGGGAGACAAAATCGTACTCCAACGATCGTTATC  
GCTGTTCTATTCTCCTCGCTTCTATATTCTCCTTATTGTGGGTCAGGATTGACCCCTTCATCACTGATC  
CCAACAAAGCATCAGCCAATGGTCAATGTGGTATCAACTGT**TAG**TTTATCCTTGAAGATTCCTTTTGKAT  
TTTTACCACACCCCTTTTGATTTGGGAGAAGACWTTCCARATTTGCCAAGGGTTATTACCAAAAATTCMGCT



CCCATTGATAGTCTATTGTACTTTACCAGCCATATGTCTTCTCACTGGAAAATTTATTGTGCCTGAGATA  
AGCAACTATGCAAGTATTGTGTTTCATGGCCCTCTTCATATCCATTGCAGCAACGGGCATCCCTCGAGATGC  
AATGGGGTGGTGTGGGAATAGATGATTGGTGGAGAAAATGAACAGTTTTGGGTGATTGGAGGTGCTTCATC  
ACATCTTTTTCGCACTTTTCCAAGGTTTACTCAAGGTTTTAGCTGGTGTGCACACAACTTCACCGTTACA  
TCAAAAGCAGCCGACGACGGAGAATTCTCAGAGCTCTACATCTTCAAATGGACCTCGCTCTTAATCCCTC  
CGATGACATTACTGATAATGAATATTGTTGGTGTGATTGTTCGGTGTCTCAGATGCCATCAATAATGGTTA  
TGAGTCATGGGGTCTCTTTTTGGGAGACTTTTCTTCGCTCTTTGGGTCAATTGTTCAATTTATACCCATTC  
CTCAAGGGAATGCTTGGGAAGCAAGACAGAATGCCAACCATTTGTGTTGGTTGGTCCATCTTGTAGCTT  
CCATCTTGACCCTCTTGTGGGTTAGAGTTAACCTTTTTGTTTCAAGAGACGGTCTGTGTTAGAAAATTTG  
TGGATTGAATTGTGATGATACA**TGA**AATAAATGAAGGTGTTTATGAAGAAGCATTTGAATACGACACGCTT  
CACATCACAAAAACGCGTTGCACAAATTTTTGGATGGAAGTTGTATTTTTTCGGTGGTGTGTGTAGATA  
AAGAGGAAGAGGAAAGATAATGGAAGGGAAGGAAAAGGGGAGTTTGACACATTGTTGCCTGCAATAGAG  
GTTTTCTTTTCATTTATTCTTTGATTATATTTTTCTGTGGTTTTTAAGTGTGTTGTTATTCTTTTTTAT  
CTTTCTAGTTGTTTCACTTTCATGTATTCTTATATAAGAAAAGGGCATTGAATATATATGATAAGTTAT  
TCCCTCTTCAAACAGAGGGATAAGCAGTCTCAAGAATTAGAGTTATGTCATATTTTTAAGGTATGGTTTT  
TTGTTGAAACCTTTGTGACATGAGAGATTTCTTCTCATTTGTAATACCATCAGCTAT

### **VfCesA3a**

#### **Nucleotide Sequence (3590 bp)**

TCTGAGAGCTGAGTAGGAGACT**ATG**ATGGACTCAGAAGGGGAATCTGGGGATAAGCCGATGAAGACGATG  
GGTAGCCAAGTCTGCCAGATATGTGGTGAATAATTTGGTAGCACTGTTGATGGGAATCCGTTTCATTGCTT  
GCGGTGTTTTGTGCCTTCCCTGTCTGTAGGCCGTGTTATGAGTATGAAAGGAAAAGATGGGAATCAGTCTTG  
CCCCAGTGCAAACTCGGTACAATAAGCACAAAGGTAGTCTGCAATCTTTGGAGACCGGGAAGAGGAT  
GGTGGTGTGATAATGATGCCAATGACTTCAAGTACAACCTCAGAACTCAGAGTCAAAAGCAAAAGATTG  
CAGAACGCATGTTGAGCTGGCAAATGGCTTATGGCCGAGGTGAGGAGTTCGATGCTCCAAATTTATGATAA  
GGAAGTTTCTCACAATCACGTTTCTCGGCTAACCGGCGGACAAGAGACATCTGGAGAATTTGTCTGCAGCC  
TCACCTGAGGGGATGTCAATGGCATCTCTCGGAAATCTTCGTGGGAAACGAGTTTCATAATCATCTATCAT  
ATTCGTCCGATCTTAATCAATCACCGAATATCAGGGTTGTTGAACCAGGATTTGGGAAATGTAGCATGGAA  
AGAAAGAGTTGATGGGTGGAAAATGAAGCACGATAATAAGAACGCTATTTCCAATGAGCACTGGTCAAGCT  
ACATCTGAAAGAGGAATCGGAGATATTGATGCCAGTACTGATGTGTTTTTCGATGATTCCTTGTGTAATG  
ATGAAGCTCGGCAACCTCTGTGCGAGGAAGGTTTCTATTCATCTTCCAGAATAAATCCATACCGTATGGT  
CATTGTTCTGCGGCTTATTATCCTCTGCATTTTCTTGCACTACCGAATTACAAATCCTGTACCCAATGGC  
TATGCATTGTGGTTAATATCAGTTATATGTGAAATTTGGTTGCTTTTCTTGGATATTTGGATCAGTTCC  
CCAAATGGCTTCTGTGAACCGTGAACATATCTTGACAGGCTTTCATTAAGATATGATCAGGAAGGGGA  
ACTGTACAGCTAGCAGCAGTTGACATTTTCTGTCAGTACTGTTGATCCCTTAAAGGAGCCCCAATTGTG  
ACAGCCAATACTGTACTCTCAATTTCTGCTGTTGACTACCCAGTAGACAAGGTCTCCTGTTATGTGTCTG  
ATGATGGTGTGCTATGTTGACATTTGAGGCTCTTGCCGAGACATCAGAGTTTCGCTAGGAAATGGGTCCC  
TTTCAGTAAGAAATATGCAATTTGAACCGCAGCTCCTGAGTGGTACTTTTCAAAGAAAATGACTATTTG  
AAAGATAAGGTCCAACCTTCGTTTCGTCAAAGATCGTAGAGCAATGAAGAGAGAATATGAAGAATTTAAAA  
TTCGTATCAATGGACTTGTGCAAAAGCAACGAAAGTTCTTGAAGAAGGATGGGTGATGCAAGATGGTAC  
ACCTTGGCCTGGAAACAACACCAGAGACCATCCAGGAATGATCCAGGTTTTCTTGGGCCAAAGTGGAGGA  
CTTGATACTGAGGGTAATGAACCTCCGCGTTTTAGTCTATGTTTCTCGTGAAAAGCGTCCAGGGTTCCAAC  
ATCACAAGAAGGCTGGTGCCATGAATGCACCTGTTTCGAGTATCAGCTGTCTTACCAATGGACCTTTCTT  
ATTGAATCTTGATTGTGATCATTACATAAAACAACAGCAAGGCCCTTGAGGGGAAGCTATGTGTTTTATGATG  
GATCCCAACCTTGGAAAAAATGTTTGTATGTCCAATTTCCACAGAGGTTTGTATGGTATTGATAGAAATG  
ATCGATATGCCAATCGTAATACCGTTTTCTTTGACATTAACCTTGCAGGATTTGGATGGCATTCAAGGCC  
AGTTTATGTGGGTACTGGATGTGTCTTCAATAGAACTGCTTTATATGGTTATGATCCTCCTATTTAAACCC  
AAGCATAAAAAGCCTGGATTTGTTTCTTCACTTTGTGGTGGAGATCGAAAGGGCTCAAAATCTGGCAAGA  
AAGGCTCAAAAAGAAATCTAGCAAGCATGTTGATCCAACCTGTGCCATCTTTAGTCTAGAGGATATAGA  
AGAAGTGTGGAAGGTGCTGGATTTGATGATGAGAAATCCCTTCTCATGTCTCAAATGAGCCTCGAGAAA  
AGGTTTTGGTCAATCTGCTGTTTTTGTGTCATCTACACTATGGAATAATGGCGGCTTCCCTCAGTCTGCAA  
CTCCAGAACTCTCCTTAAGGAGGCAATTCATGTTATCAGTTGTGGTTACGAAAGATAAATCGAATGGGG  
AACTGAGATTGGATGGATCTATGGTTCTGTACAGAAAGATATTCTTACTGGATTTAAGATGCATGCCCGC  
GGTTGGAGGTCTATATACTGCATGCCCAAGCTTGCAGCATTTAAAGGTTCTGCTCCCATCAATCTTTCTG  
ATCGTTTTGAACCAAGTGTCTTCGGTGGGCTTTAGGCTCAGTGGAAAATCTACTAAGTCGACATTTGCCAT  
CTGGTACGGTTATAGTGAAGGCTTAAGGTTCTTGTAGAGGTTTGCCTATATAAACACCACAATCTATCCA

ATCACTTCCATTCCCCTCCTCATGTATTGTACCTTACCTGCTGTTTGTCTCTTGACTAACAAAGTTCATTA  
TTCCACAGATTAGTAACATTGCAAGTATTTGGTTTATATCTCTCTTTCTTTCCATCTTTGCAACCGGTAT  
CCTAGAGATGAGGTGGAGTGGTGTCCGAATCGATGAATGGTGGAGAAACGAACAATTTTGGGTATCGGT  
GGTGTTCAGCTCATCTTTTCGCCGTGTTCCAAGGTTTACTCAAAGTACTTGTGGAATTGACACAAACT  
TCACTGTCACCTCAAAGCATCCGACGAAGACGGAGACTCTGCAGAACTATACATGTTTAAATGGACAAC  
ACTTCTCATTCCACCAACGACCCCTTCTTATTATAAACCTCGTCGGAGTCGTTGCAGGAATCTCCTACGCT  
GTTAACAGTGGCTACCAATCATGGGGACCACTCTTTGGTAAACTTTTGCTTTGCATTTTGGGTGATCAGT  
CCATTTATAACCTTTCTTAAAGGTCTTATGGGACGCCAGAACCGAAGCGCCAACCATCGTGGTTGTTTG  
GTCYATTCTTCTTGCATCCATCTTTTCGCTTTTATGGGTTCGAATCGACCCCTTTACAACCCGAGTCACC  
GGTCCTGATTCTCAGATGTGTGGAATCAACTGCT**TAG**AGAAAATAAAAAGTTGGCAGATTGAATAACCATGT  
CACGTTGTCACCTCCACCTGTTGTGATTGTATTGCAATCTTTTGTACCACGGTTACCACGTTATTTT  
TTTATATTTATTTGTTACACTGCACTGTTGTCTAAATTATGTGCCACGTTGTTGGACTATACCACGAAGG  
ATAACCAAATTAGGAATCCAAGTTATTTTGGAGAGGGTGTATTATTTTAAATTTTTTTTTTTGGGTTT  
TGTAAGGGTGTATTATTTGTATAATTGTTTTGAACACAGCTCCTTTTTTTTTGGGAGAAGTAAAAAAAA  
AAAAAGGGGGTAAAGGGG

## APPENDIX 3: Chapter 3 Supplementary Data

### Cluster analysis and functional categorization of transcripts showing epidermal differential regulation

#### 3A.1 INTRODUCTION

RNA-Seq of adaxial epidermal TCs of *V. faba* identified differentially expressed transcripts that were categorized into four major categories: epidermal-specific up- or down-regulated, and epidermal-enhanced, up- or down-regulated. The primary goal of this study was to identify transcription factors putatively involved in regulating TC development, and thus transcripts identified as coding transcription factors based on Gene Ontology analysis were extracted from these categories and analysed as part of the manuscript submitted to *Frontiers in Plant Science*. In addition to this analysis, the entire transcript data set was analysed by cluster analysis to determine temporal expression of functionally-related genes across the *trans*-differentiation of epidermal TCs.

This appendix provides preliminary analysis undertaken by cluster analysis to assess functional classes of genes across the period of *trans*-differentiation of epidermal TCs. Transcripts showing either epidermal-specific up- or down-regulation were assigned to groups using cluster analysis, and functional categories in each cluster were analysed. The potential role of each functional class in each cluster, in each category in TC development is discussed here. In addition, transcripts identified as showing epidermal-enhanced up- or down-regulation were categorised into different functional classes and their potential roles in TC development discussed.

#### 3A.2 METHODS

##### 3A.2.1 *K-means* Cluster analysis

To identify patterns of gene expression across cotyledon culture time points of 0-, 3-, 9- and 24-h, *K-means* clustering was performed using Cluster 3.0 software. *K-means* clustering uses Euclidean similarity to identify similar patterns of expression of individual genes across a time series (de Hoon et al., 2004). It identifies co-expressed genes that are functionally related based on their expressed patterns and groups them into clusters (Chandrasekar et al., 2011). To perform this analysis, RPKM values of each transcript at

different time points were normalized between -1.0 and 1.0 in Cluster 3 by multiplying values with a scale factor such that the sum of the squares of all four values are equal to 1. Later, the values were centred to 0 by subtracting mean of the four values from each data point so that the mean of each row was zero (Sweetman et al., 2012). Cluster analysis was performed with six clusters and 100 iterations for epidermal-specific, up-regulated transcripts and with four clusters and 100 iterations for epidermal-specific, down-regulated transcripts. The percentage of transcripts from each cluster identified as belonging to different functional classes were categorised based on the biological component in the GO terms relating to functional classes (see Dibley et al., 2009; Thiel et al., 2012b). For example, transcripts classified into “signal transduction” were identified by GO: 0007165, “transcription factors” by GO: 0003700, “transport” by GO: 0006810. Transcripts belonging to “cell wall biogenesis” were identified by multiple GO terms such as GO: 0009505 for “plant-type cell wall”, GO: 0071668 for “plant-type cell wall assembly”, GO: 0009828 for “plant-type cell wall loosening”, GO: 0009832 for “plant-type cell wall biogenesis”, GO: 0009664 for “plant-type cell wall organization” and GO: 0009827 for “plant-type cell wall modification.” Similarly multiple GO terms have been used for identifying transcripts belonging to metabolism and energy transfer, such as GO: 0008152 for “metabolic process” and many GO terms for “energy transfer” such as GO: 0009453 for “energy taxis”, GO: 0006091 for “generation of precursor metabolites and energy”, etc., as defined by the European Bioinformatics Institute ([www.ebi.ac.uk](http://www.ebi.ac.uk)). Similarly, transcripts in epidermal-enhanced category, were classified into different functional classes and their potential roles discussed.

### **3A.3 RESULTS AND DISCUSSION**

#### ***3A.3.1 Cluster analysis for epidermal-specific, up-regulated transcripts***

Cluster analysis was carried out to identify groups of genes displaying common expression patterns within the category of genes identified as showing epidermal-specific, up-regulated expression. The 444 transcripts showing a five-fold or greater epidermal-specific increase in expression (Supplementary Table 3A.1) were grouped into six clusters with distinct temporal patterns of expression (Figure 3A.1). These clusters were grouped under the names of “Early up-regulation” (Cluster 1 and 2), “Intermediate up-regulation” (Cluster 3 and 4) and “Late up-regulation” (Cluster 5 and 6) (Figure 3A.1).

Nearly 50% of the transcripts (201 out of 444) belonged to Cluster 1, showing specific up-regulation in epidermal cells within 3 hrs of cotyledon culture and then declining to basal levels by 24 h. In addition to this number, the 22 and 59 transcripts in Clusters 2 and 3, respectively, also peaked mostly by 3 h, but then declined slowly across the next 21 h (Cluster 3) or temporally by 9 h before rising again by 24 h (Cluster 2; Figure 3A.1). These clusters emphasize the major transcriptional changes occurring within the first 3 h of cotyledon culture, as noted in the studies by Dibley et al. (2009) and Zhang et al. (2015b). The 68 transcripts in Cluster 4 peaked at 9 h cotyledon culture and declined by 24 h, while the 31 transcripts in Cluster 5 gradually increased over the duration of cotyledon culture. The 64 transcripts making up Cluster 6 were characterized by increased expression from 9 to 24 h (Figure 3A.1).

The distribution of functional classes within each cluster for transcripts showing epidermal-specific, up-regulation is listed in Table 3A.1. This analysis shows that transcripts associated with signal transduction functions are prominent in Clusters 1-3, which is consistent with components of the auxin, ethylene and ROS signaling pathways being expressed within the first 3 h of cotyledon culture to induce *trans*-differentiation of epidermal TCs (Dibley et al., 2009; Zhou et al., 2010; Andriunas et al., 2011, 2012). Further, this result is consistent with Wardini et al. (2007b) who showed that all genetic machinery required to build a papillate wall ingrowth is switched on within the first 1 h of cotyledon culture. Wall ingrowth deposition in epidermal TCs is an on-going process required to construct the multi-layered fenestrated network of wall ingrowth material (Talbot et al., 2001, 2007b), hence signaling processes presumably continue across this period.

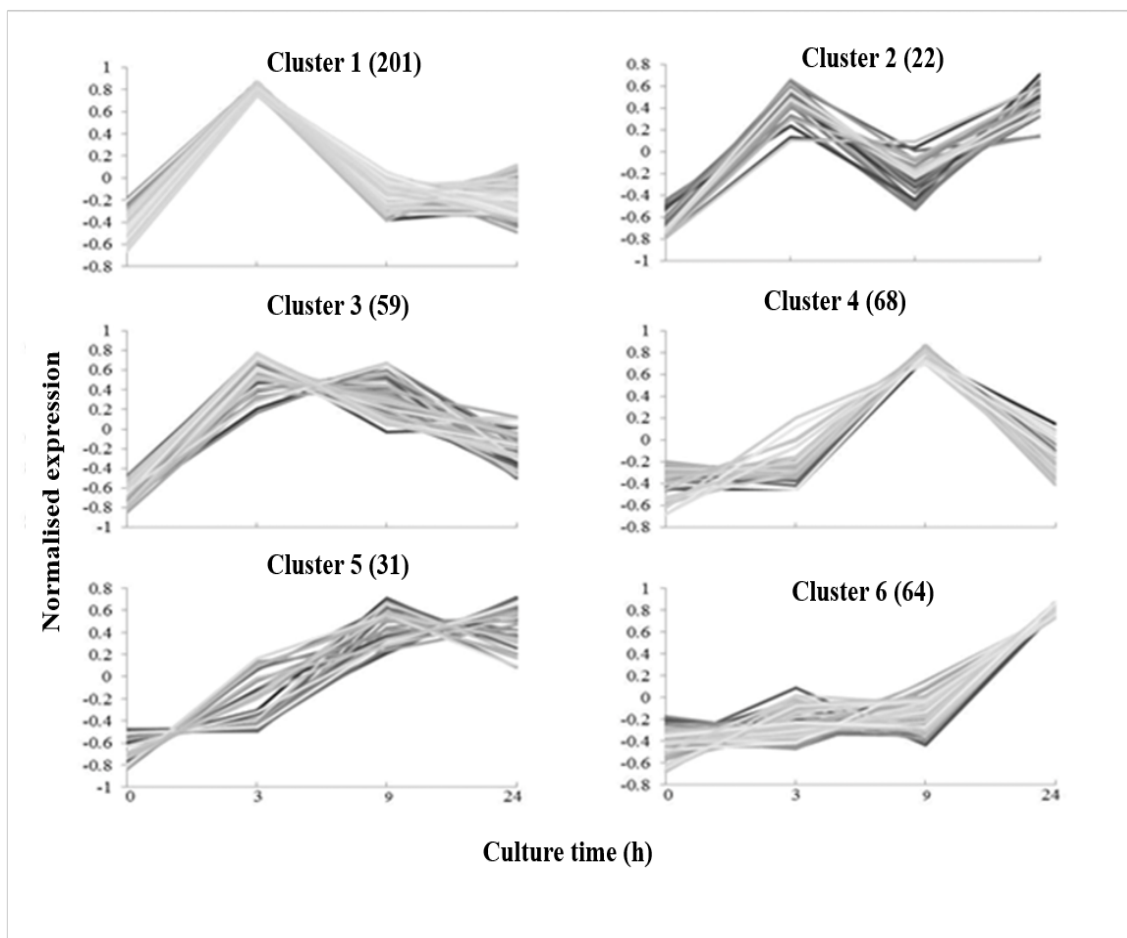


**Figure 3A.1: Cluster analysis of transcripts showing epidermal specific, up-regulated expression.**

*K-means* cluster analysis showing six clusters of gene expression profiles of the 444 transcripts showing epidermal-specific up-regulation. Clusters 1 & 2, Early up-regulation; Clusters 3 & 4, Intermediate up-regulation; Clusters 5 & 6, Late up-regulation. Transcripts in Clusters 3 and 4 show transient up-regulation. Number of transcripts in each cluster is indicated within brackets

**Table 3A.1: Functional categories of epidermal-specific, up-regulated transcripts assigned to each Cluster.**

| Functional Classes                 | Cluster 1 | Cluster 2 | Cluster 3 | Cluster 4 | Cluster 5 | Cluster 6 |
|------------------------------------|-----------|-----------|-----------|-----------|-----------|-----------|
| Signal Transduction (%)            | 36        | 24        | 22        | 8         | 10        | 22        |
| Transcription factors (%)          | 7         | 5         | 3         | 4         | 0         | 4         |
| Cell wall biosynthesis (%)         | 12        | 5         | 24        | 4         | 19        | 25        |
| Metabolism and energy transfer (%) | 13        | 9.5       | 10        | 34        | 13        | 22        |
| Transport (%)                      | 9         | 19        | 10        | 19        | 19        | 27        |
| Others (%)                         | 23        | 38        | 31        | 31        | 39        | 0         |

The percentage of each functional class assigned to each of the six Clusters is indicated.

The predicted functions of the transcripts assigned to functional classes within Clusters 1-6 covering epidermal-specific, up-regulated genes is shown in Supplementary Table 3A.1. The sequences classified as Signal Transduction were dominated by receptor kinases/kinases in all the clusters making up the epidermal-specific, up-regulated category (10% of 444 transcripts, Supplementary Table 3A.1). This observation is consistent with the study of Zhang et al. (2015b), indicating the importance of signal transduction pathways in initiating TC development. Similarly, transcripts involved in auxin biology, namely auxin signaling pathways, auxin induced proteins and auxin efflux components (Supplementary Table 3A.1) were found to be prominent in the Signal Transduction category across all clusters. This observation is consistent with inhibitor experiments showing that auxin signaling is involved in inducing the *trans*-differentiation of epidermal TC development in *V. faba* cotyledons (Dibley et al., 2009), and is required for development of TC-like nematode feeding cells in Arabidopsis roots (Cabrera et al., 2014). For example, *auxin induced protein AtIG04240* (Cluster 1, Supplementary Table 3A.1), promotes response in endoreduplication in root apical meristem of Arabidopsis (Ishida et al., 2010). This is consistent with endopolyploid status of *V. faba* TCs (Dibley et al., 2009). Further, several calcium- dependent protein kinases were also up-regulated by 3 h of cotyledon culture (Cluster 1, Supplementary Table 3A.1), which may indicate a role in calcium signaling of wall ingrowth deposition (Zhang et al., 2015a, c, d).

Transcription factors were generally more abundant in Clusters 1-3 compared to Clusters 4-6 (Figure 3A.1). This observation is again consistent with a requirement to initiate the extensive transcriptional cascades that accompany wall ingrowth deposition in epidermal TCs (Dibley et al., 2009; Arun-Chinnappa et al., 2013; Zhang et al., 2015b). MYB family members accounted for 37% of the “Transcription factors” category in Clusters 1-3 (Supplementary Table 3A.1). Members of this family are prominent regulators of secondary wall synthesis (Zhong et al., 2008, Nakano et al., 2015), and thus may be equally involved in regulating localized wall ingrowth deposition. A detailed analysis of the putative functions of these transcription factors in regulating TC development is presented in Arun-Chinnappa and McCurdy, 2016 – see submitted manuscript for this chapter).

An intriguing observation from Table 3A.1 is the high proportion of transcripts associated with “Cell wall biosynthesis” in Cluster 3 and 6, and to a slightly lesser degree in Cluster

5. Wall ingrowth deposition in adaxial epidermal TCs of *V. faba* cotyledons is a progressive event whereby at 3 h culture only 10% of epidermal cells contain early stage papillate wall ingrowths, but by 24 h this number increases to about 90% as the formation of a multilayered fenestrated network of wall deposition is being initiated (Wardini et al., 2007b). Thus, total levels of wall ingrowth deposition may be expected to be greater from 9-24 h than in the first 9 h of culture, hence explaining the high relative abundances of cell wall biosynthesis genes in Clusters 5 and 6 in particular. In general, transcripts involved in cell wall biosynthesis were dominated by extensins, expansins, endo-beta glucanases and phenyl alanine ammonia lyase (Supplementary Table 3A.1). Extensins have been detected in TCs depositing flange wall ingrowths in barley (Thiel et al., 2012b) and maize (Xiong et al., 2011) as well as reticulate wall ingrowths in root giant cells in rice (Ji et al., 2013) and epidermal TCs in *V. faba* (Zhang et al., 2015b). Extensins are a family of hydroxyproline-rich glycoproteins which presumably assemble into flexible cross-linked networks to support wall ingrowth formation. Expansins are another class of cell wall proteins that in turn play a role in hormone-induced cell wall loosening required for tip-growth processes (Cho and Cosgrove 2002), but whether expansins perform a similar role in wall ingrowth formation is yet to be determined. Beta-glucanases were generally highly represented in the cell wall biosynthesis functional class in most clusters. Beta-glucanases represent a large family of cell wall modelling enzymes hypothesised to function in remodelling to facilitate the highly sculptured reticulate wall ingrowth architecture (Dibley et al., 2009; Zhang et al., 2015b). Finally, enzymes involved in the phenyl propanoid pathway such as phenyl alanine ammonia lyase, cinnamoyl reductase and coumaroyl-CoA were also found to be highly represented in this functional class assigned as “Cell wall biosynthesis” (Supplementary Table 3A.1). These enzymes are mostly associated with lignin biosynthesis, and while lignin has long been assumed to be absent in reticulate wall ingrowths (Gunning and Pate, 1969; Vaughn et al., 2007), genes encoding these enzymes have been detected in nematode-forming giant cells in tomato roots (Portillo et al., 2013). Recently, lignin has been reported to be a component of both flange and so-called “reticulate” wall ingrowths in maize BETCs (Rocha et al., 2014), thus the assumption that wall ingrowths are devoid of lignin to assure optimal diffusion of nutrients through the wall ingrowth apoplasm may need to be re-visited. Cellulose microfibril deposition in TCs is proposed to involve a novel mechanism whereby the microfibrils may be deposited at right angles to the underlying primary wall (Talbot et

al., 2007b). Consistent with this, *β-glucosidases* were also up-regulated by 24 h which may be playing role in re-directing dislodgement of cellulose microfibrils (Cluster 6, Supplementary Table 3A.1; Zhang et al., 2015b). A somewhat surprising result was the high representation of endo- $\beta$ -xylanases represented in Cluster 3 (Supplementary Table 3A.1). Endo- $\beta$ -xylanases breakdown arabinoxylans (Juge et al., 2004) which are major cell wall components of TCs in wheat (Robert et al., 2011). Up-regulation of these genes in adaxial epidermal TCs might be explained by a necessity for extensive remodelling or reutilization of arabinoxylans during wall ingrowth formation.

Transcripts encoding genes involved in metabolism and energy transfer were especially abundant across the later stages of cotyledon culture, particularly in Clusters 4 and 6 (Table 3A.1). Transcripts in these clusters correlate with maximum occurrence of wall ingrowth deposition between 9 and 24 h, thus reflecting the requirement of energy and sugar demand across this period (Wardini et al., 2007a; Dibley et al., 2009). Increased sugar demand is presumably met by re-mobilizing stored reserves in starch and fatty acids, as evidenced by the presence of proteins involved in fatty acid metabolism and glucose metabolism (glycerol-3-phosphate hydrogenase - Cluster 4; 6-phosphofructo kinase 5 - Cluster 3) (Supplementary Table 3A.1). Energy is derived from mitochondria as evidenced by the presence of transcripts encoding cytochromes across all clusters and NADH dehydrogenase (Cluster 4; Supplementary Table 3A.1) which are components of the electron transport chain (Nelson and Cox, 2005). Similar observations were noted by Dibley et al. (2009) using cDNA-AFLP analysis of *V. faba* epidermal TC development. Many UDP glycosyl transferases were abundant in Cluster 6 (Supplementary Table 3A.1). One of these UDP-glycosyl transferase, UGT85A5, enhances salt stress tolerance in plants. Sun et al. (2013) suggested that UGT85A5 may have a role in regulating ion transporters and also in accumulation and transport of ions through glycosylation of certain molecules. Hence, increased expression of this gene at later stages suggests that it might play a similar role in TCs.

Roughly similar to metabolism and energy transfer, transcripts encoding transporter proteins were especially abundant in the later stages of epidermal TC development represented by Clusters 4-6 (Table 3A.1). This result is expected on the basis that the transport function of epidermal TCs is achieved by targeting incorporation of membrane transporters into the increased plasma membrane surface area resulting from wall

ingrowth deposition. Farley et al. (2000) demonstrated that adaxial epidermal TCs displayed enhanced transport capacity by 3 days of cotyledon culture, the earliest time point assayed in this study. Nonetheless, they made the important observation that transport capacity corresponds with the induction of adaxial epidermal TCs (Farley et al., 2000), and the high percentage of transcripts associated with transport function, particularly in Clusters 4-6, is consistent with this conclusion. ABC (ATP-binding cassette) transporters and nitrate transporter proteins were abundant in these clusters, which was also observed by Zhang et al. (2015b). ABC transporters promote the transport of IAA across the plasma membrane (Remy and Duque, 2014), which is consistent with auxin involvement in the induction of epidermal TCs in *V. faba* cotyledons (Dibley et al., 2009). Nitrate transporters presumably are involved in meeting the demand for protein synthesis by recruiting nitrogen compounds for various events underpinning wall ingrowth deposition (Zhang et al., 2015b). Change in membrane transporter profiles across different stages of TC development indicate the substantial enhancement of transport function of TCs.

Collectively, cluster analysis of transcripts identified as showing epidermal-specific up-regulation reflected in a general sense a predominance of signaling functions early in induction of epidermal TCs followed by cellular processes associated with cell wall biogenesis and metabolism to provide energy requirements for this process. Expression of transporter genes were more evident once plasma membrane enhancement as a consequence of wall ingrowth deposition had been achieved.

### **3A.3.2 Cluster analysis for epidermal-specific, down-regulated transcripts**

Cluster analysis similar to epidermal-specific up-regulated transcripts was carried out for the 172 epidermal-specific, down-regulated transcripts. This analysis identified 4 clusters showing distinct expression patterns characterized as “Early down-regulation” (Clusters 7 and 8; Figure 3A.2), “Continuous down-regulation” (Cluster 9; Figure 3A.2) and “Transient down-regulation” (Cluster 10; Figure 3A.2). Clusters 7 and 8 are characterized by transcripts showing dramatic down-regulation within the first 3 h of cotyledon culture, albeit with Cluster 8 transcripts returning to initial levels by 24 h culture. Cluster 10 transcripts mostly show a modest decline from 0-9 h culture, followed by strong up-regulation by 24 h (Figure 3A.2). All four clusters, however, show a decrease in

expression at either 3, 9 or 24 h compared to 0 h at the start of cotyledon culture, hence categorizing these genes as being down-regulated. Cluster 7 accounted for 33% (57 transcripts) of these transcripts, followed by 27% (47 transcripts) in Cluster 9, 22% (38 transcripts) in Cluster 8, with Cluster 10 making up 17% (30 transcripts) of the transcripts (Figure 3A.2).

A general observation is the consistent representation of Signal transduction functions across all Clusters (Figure 3A.2). In this context, it is relevant to point out that epidermal TC development is a *trans*-differentiation process presumably involving substantial genomic reorganization required to undertake de-differentiation prior to re-differentiation to become epidermal TCs. In three of the four clusters, substantial levels of increased gene expression occurs following an initial or mid-culture drop, indicating probably extensive signaling mechanisms to achieve *trans*-differentiation. In terms of specific signaling genes, Serine/threonine protein kinases, especially those with leucine rich repeats (LRR), were heavily represented, followed by several auxin regulatory proteins, indicating these families play a key role in initial signaling pathways in *trans*-differentiation (Supplementary Table 3A.2). Genes regulated by auxin contributed to the cohorts that were down-regulated specifically in epidermal TCs of *V. faba* (Dibley et al., 2009). While the specific serine/threonine kinases identified in this study have not been characterized, a serine/threonine protein kinase with LRR domain in bamboo functions in production of cellulose (Ghosh et al., 2013). Down-regulation of similar serine/threonine LRR protein kinases in *V. faba* epidermal TCs might contribute to the remodelling of the cell wall associated with wall ingrowth deposition, or reduced levels of cellulose biosynthesis associated with switching from primary wall to wall ingrowth deposition (Vaughn et al., 2007). Single mutants of *FEI1* and *FEI2*, receptor kinases with LRR domains, showed cellulose deficiency and were predicted to play role in synthesis of cell wall components under stress conditions (Xu et al., 2008). Serine/threonine protein kinases have been reported to play a role in cell wall signaling as a result of developmental and environmental cues (Steinwand and Kieber, 2010).

Two proteins involved in two-component signaling system (TCS) were down-regulated (Cluster 9; Supplementary Table 3A.2). This observation is in contrast to the prominent up-regulation of two-component signaling genes associated with development of barley endosperm TCs (ETCs) (Thiel et al., 2012a), which appears to be a clear difference

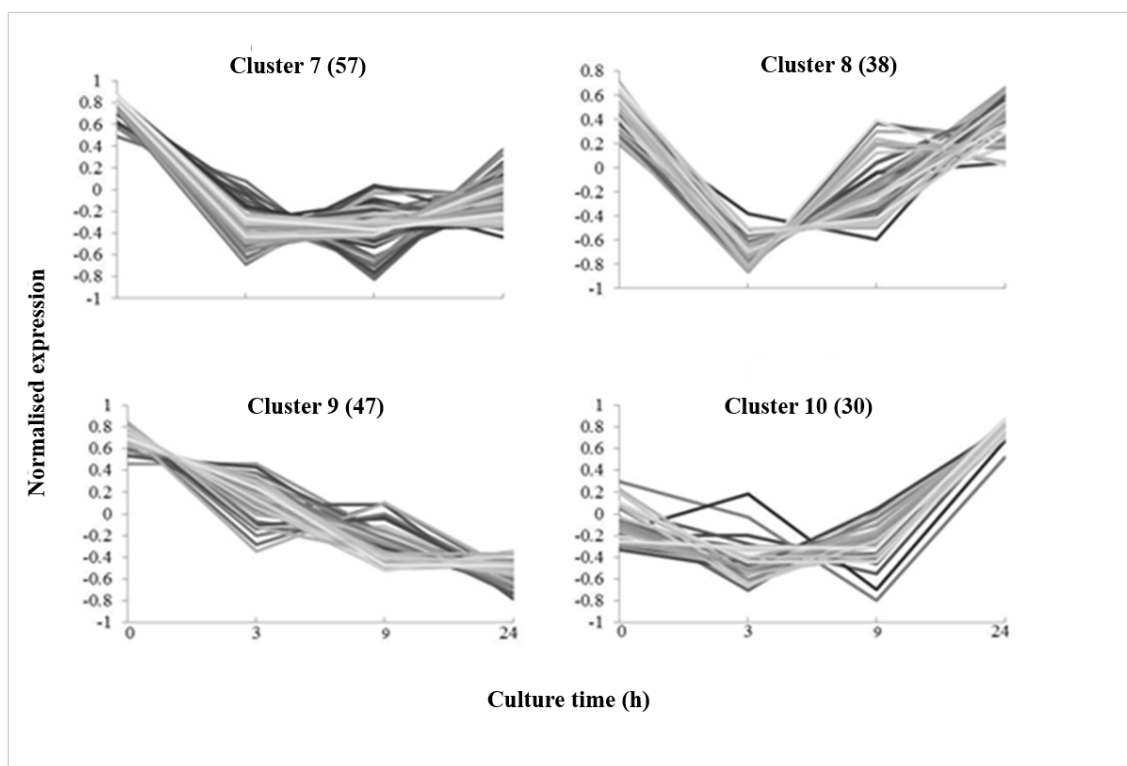


**Figure 3A.2: Cluster analysis of transcripts showing epidermal-specific, down-regulated expression.**

*K-means* cluster analysis showing four clusters of gene expression profiles of the 172 transcripts showing epidermal-specific, down-regulation. Clusters 7 & 8, Early down-regulation; Clusters 9, Continuous down-regulation; Cluster 10, Transient down-regulation. Number of transcripts in each cluster is indicated within brackets.

**Table 3A.2: Functional categories of epidermal-specific, down-regulated transcripts assigned to each Cluster.**

| Functional Classes                 | Cluster 7 | Cluster 8 | Cluster 9 | Cluster 10 |
|------------------------------------|-----------|-----------|-----------|------------|
| Signal Transduction (%)            | 30        | 24        | 28        | 20         |
| Transcription factors (%)          | 12        | 3         | 4         | 0          |
| Cell wall biosynthesis (%)         | 19        | 21        | 23        | 3          |
| Metabolism and energy transfer (%) | 0         | 0         | 15        | 17         |
| Transport (%)                      | 16        | 13        | 15        | 50         |
| Others (%)                         | 23        | 39        | 15        | 10         |

The percentage of each functional class assigned to each of the four Clusters is indicated

between genetic regulation of flange-type compared to reticulate-type wall ingrowths (Dibley et al., 2009; Zhang et al., 2015b; McCurdy, 2015). A discussion of the

transcription factors predominant in the early down-regulation category and their putative functions in regulating TC development is presented in the Arun-Chinnappa and McCurdy manuscript presented as part of Chapter 3.

Somewhat surprisingly, transcripts representing cell wall biosynthesis were substantially down-regulated and represented the second most-abundant functional class across the cohort of genes in Clusters 7-10. Several transcripts encoding cellulose synthase-like proteins were present in the “Cell wall biosynthesis” class, particularly in Cluster 7 and Cluster 9 (Supplementary Table 3A.2). As stated previously, this collective result most likely represents temporal switching off of genes to accommodate re-modelling of cell wall biosynthesis as it switches from deposition of primary wall to predominantly wall ingrowth cell wall. While wall ingrowths in epidermal TCs have been described as “primary wall-like” based on immunogold analysis (Vaughn et al., 2007), at the micro-scale level considerable changes in cell wall biosynthesis presumably occur across the transition from primary wall to wall ingrowth, hence it is not surprising that numerous cell wall biosynthesis genes may be switched off during this transition.

This conclusion is supported by the observation that various *CesA* genes, namely *AtCesA3* and *AtCesA6*, are down-regulated during giant cell formation resulting from nematode infection in tomato roots (Portillo et al., 2013). Double mutants of *AtCesA2/AtCesA6* in *Arabidopsis* produced random and aggregated cellulose microfibrils (Persson et al., 2007), which was interpreted as indicating that the combination of *CesA* genes forming rosette complexes reflects the type of cellulose fibres produced (McCurdy et al., 2008). Collectively, these results suggest the possibility that the structure of cellulose microfibrils in wall ingrowths may be distinct from that occurring within the underlying primary wall, a conclusion that is consistent with differences in cellulose microfibril organisation between the two type of cell wall (Talbot et al., 2001, 2007b).

Surprisingly, transcripts representing metabolism and energy transfer were absent in Clusters 7 and 8 (Table 3A.2) indicating that no genes recognizably associated with energy metabolism were switched off during early stages of cotyledon culture. In contrast, a cohort of genes contributing to metabolism and energy transfer were down-regulated throughout cotyledon culture (Cluster 9), whereas those associated with Cluster 10 showed increased expression following the first 9 h of cotyledon culture (Figure 3A.2; Table 3A.2). GDSL (Gly-Asp-Ser-Leu) esterase/lipases were strongly represented in Cluster 9, this being transcripts showing continuous decline in expression across cotyledon culture and thus epidermal TC development. Why this class of lipases, which contain a characteristic GDSL sequence motif and are associated with a broad spectrum

of functions such as defence and morphogenesis (Chepysenko et al., 2012), are strongly down-regulated during epidermal TC development is unclear.

Transcripts associated with transport functions represent 50% of the transcript functions in Cluster 10 (Table 3A.2). While listed in the category of epidermal-specific, down-regulated genes, transcripts in Cluster 10 are actually strongly up-regulated from about 9 h, hence explaining a predominance of transcripts encoding transporter functions coinciding with later stages of wall ingrowth production. Consequently, in agreement with transporter transcripts showing up-regulation, this grouping was dominated by ABC transporters in addition to peptide transporters. This indicates that the ABC family of transporter proteins possibly play an important role in TC development.

### **3A.3.3 Epidermal-enhanced, up-regulation**

A feature of the RNA-Seq analysis reported in this chapter (Arun-Chinnappa and McCurdy, 2016 – manuscript submitted) was the identification of transcripts, expressed in both epidermal and storage parenchyma, which underwent substantial epidermal-enhanced expression across the development of epidermal TCs. In total, 198 transcripts (Supplementary Table 3A.3) displayed this feature, in which up-regulation in epidermal tissue was at least 25-fold higher compared to that occurring in storage parenchyma at 3 h (Arun-Chinnappa and McCurdy, 2016 – manuscript submitted). Transcripts in this category were classified into functional classes as described above. Transcripts encoding signal transduction function were the most abundant (26%) (Table 3A.3), consistent with transcripts showing early epidermal-specific up-regulation (Clusters 1 and 2, Table 3A.1). Prominent among the epidermal-enhanced category were serine/threonine protein kinases (Supplementary Table 3A.3), commonly recognized as a major class of signaling genes initiating responses from endogenous or exogenous signals to initiate transcriptional changes in the plant (Hardie, 1999). This class of protein kinases are known to function in signaling pathways responsive to stress including pathogen attack (Becraft, 2002; Afzal et al., 2008; Lin et al., 2015). Surgical excision of cotyledons from the seed coat and subsequent culture imposes stress to cotyledons, hence such pathways might be triggered accordingly. Excision of cotyledons from seed also induces ethylene signaling which is evident from the enhanced up-regulation of the ethylene precursor 1-aminocyclopropane-

1-carboxylate synthase, up-regulated some 70-fold in epidermal TCs within 3 h of cotyledon culture (Supplementary Table 3A.3, and see Zhou et al., 2010).

Consistent with cotyledon culture inducing stress responses, transcription factors in this cohort were dominated by members of the WRKY family (Supplementary Table 3A.3; Rushton et al., 2010). A discussion of these transcription factors and others in this cohort in the context of regulating epidermal TC development is presented in this chapter (Arun-Chinnappa and McCurdy, 2016 - manuscript submitted). Ethylene-responsive transcription factors were also prominent in this cohort of epidermal-enhanced transcripts (Supplementary Table 3A.3), consistent with earlier studies showing the involvement of ethylene signaling in inducing epidermal TCs in *V. faba* cotyledons (Andriunas et al., 2011, 2012).

Cell wall biosynthesis functions contributed to 18% of the transcripts showing epidermal-enhanced up-regulation (Table 3A.3). Most of these transcripts are predicted to be involved in synthesis of cell wall components such as xyloglucan (Thiel et al., 2012b; Cabrera et al., 2014; Supplementary Table 3A.3), a common component of wall ingrowths in TCs (Vaughn et al., 2007). Somewhat surprisingly, the transcript showing the highest fold-difference is phenylalanine ammonia-lyase 1 involved in lignin biosynthesis. As stated previously, lignin has historically been regarded as absent from wall ingrowths (Gunning and Pate, 1969), but the recent publication by Rocha et al. (2014) detecting lignin in endosperm TCs of maize suggests further analysis is needed. The substantial fold-difference increase for this gene in epidermal TCs implies a significant change in lignin biosynthesis status during early stages of epidermal TC development, but the functional implications of this result remains unknown.

Transcripts representing metabolism and energy transfer accounted for 12% of the epidermal-enhanced genes and were dominated by cytochrome family members (Supplementary Table 3A.3). Cytochrome family proteins are major components of mitochondria that function in electron transport (Nelson and Cox, 2005). Energy requirements presumably increase as whole cotyledons are excised from seed coat creating sugar demand as the cells are expanding in the cotyledons. However, the increased demand for energy in epidermal cells undergoing *trans*-differentiation to TCs compared to energy requirements of expanding storage parenchyma cells presumably accounts for this difference (Harrington et al., 2005; Wardini et al., 2007a).

Transcripts encoding transporter functions constituted the second largest functional class (20%) in the epidermal-enhanced category (Table 3A.3). Early nodulin-like protein (ENOD) showed very high fold-difference within the first 3 h of cotyledon culture (Supplementary Table 3A.3). ENOD proteins are known to play major regulatory roles in cell wall re-organization in legumes (Scheres et al., 1990; Brewin, 2004), thus similar *V. faba* transcripts may be co-ordinating similar cell wall re-organization processes during epidermal TC development. Similar to epidermal-specific up-regulated transporter genes, ABC transporters, which play a major role in auxin transport (Remy and Duque, 2014) were also prominent in epidermal-enhanced, suggesting a major role for this process in the *trans*-differentiation of epidermal TCs (see also Zhang et al., 2015b).

**Table 3A.3:** Functional categories of epidermal- enhanced, up-regulated transcripts.

| Functional Class                   | Epidermal-enhanced up-regulation |
|------------------------------------|----------------------------------|
| Signal Transduction (%)            | 26                               |
| Transcription factors (%)          | 10                               |
| Cell wall biosynthesis (%)         | 18                               |
| Metabolism and energy transfer (%) | 12                               |
| Transport (%)                      | 20                               |
| Others (%)                         | 14                               |

### 3A.3.4 Epidermal-enhanced down-regulation:

Epidermal-enhanced, down-regulated transcripts showed down-regulation in both epidermal and storage parenchyma tissue by 3 h cotyledon culture, but the extent of down-regulation in epidermal tissue was at least 25 fold higher than compared to storage parenchyma. In total, 13 transcripts displayed this expression pattern. These transcripts did not contain genes in the functional classes mentioned above. However, a transcript encoding cellulose synthase was present in this category (Supplementary Table 3A.4), similar to epidermal-specific, down-regulated. This result suggests that cellulose synthesis in wall ingrowth deposition may not be dependent on CesAs in *V. faba* TCs, as suggested by Zhang et al. (2015b). However, this result could simply reflect that one *CesA* gene from the *V. faba* family may be switched off or down-regulated, while other genes in this family undertake the role of cellulose biosynthesis required for cell wall deposition.

**Conclusion:**

The RNA-Seq analysis reported in part here indicates that major transcriptional changes occur rapidly within 3 h of cotyledon culture which is evident from the proportion of genes differentially expressed specifically in adaxial epidermal TCs of *V. faba* cotyledons. Transcript profiling has confirmed that signaling pathways like ethylene and auxin play major roles during early stages of wall ingrowth deposition. Differential expression of cell wall and transporter genes indicate onset of *trans*-differentiation process which includes changes in the cell wall and transport properties of adaxial epidermal TCs. Identification of substantial levels of transcription factors differentially expressed in epidermal-specific and epidermal-enhanced categories indicate the *trans*-differentiation process is genetically regulated. Each stage of TC development was highly regulated by unique genes representing corresponding transcriptional change at that stage. The precise role of a major proportion of transcripts identified through this RNA-Seq study as showing differential expression accompanying epidermal TC development remains unclear. However, this study has identified numerous genes that require further investigation to understand their role(s) in regulating epidermal TC development in *V. faba* cotyledons and thus TCs more broadly.

## APPENDIX 4: Chapter 4 Supplementary Data

### Appendix 4A: List of primers used for genotyping

| Orthologous Arabidopsis Gene | Gene number | Mutant allele | Primer Sequences  |
|------------------------------|-------------|---------------|---|
| <i>AtMYB20</i>               | AT1G66230   | GK_109C11     | LP:GAGAGAAATGGGGAGACAACC<br>RP:ACACGAGGAAGTATGGAACCC    |
| <i>AtMYB43</i>               | AT5G16600   | SALK_023509C  | LP:ATGGGTCAAAGGGTCAATACC<br>RP:ACAAGACACCGTTTGTGATGG    |
| <i>AtWRKY33</i>              | AT2G38470   | SALK_064436   | LP:TTGCACATTTCTCAAAAAGGG<br>RP:TACGAAGGGAAACACAACCAC    |
| <i>AtWRKY44</i>              | AT2G37260   | SALK_058009   | LP:CTTGACTGTCCTAGCATTGGC<br>RP:AGCCGACACTGTGATGGATAC    |
| <i>AtWRKY48</i>              | AT5G49520   | SALK_066438C  | LP:AAATCCGTTCCGCCATATAAC<br>RP:ACCGCTGAATAACCAACAATG    |
| <i>AtWRKY57</i>              | AT1G69310   | GK_078H12     | LP:TTGCACAGTCAAAACAACCAC<br>RP:ACGATCCTGATAATCCCGATC    |
| <i>AtWRKY41</i>              | AT4G11070   | SALK_068648C  | LP:GAAAGGTTCCAGGATCTCCAG<br>RP:GGGGAAGCCTGTGTTAATCTC    |
| <i>AtWRKY53</i>              | AT4G23810   | SALK_034157C  | LP:TCAGGCACGACTTAGAGAAGC<br>RP:GGGAAAGTTGTGTCAATCTCG    |
| <i>AtGT-3B</i>               | AT2G38250   | SALK_133090   | LP:TGAATGAAAAAGCAGATTAACAG<br>RP:GTGACGAGGTTCTTCCACTTG  |
| <i>AtGT-3A</i>               | AT5G01380   | GK_591B09     | LP:AATCTCTCTTCTGAGCCCTAGCTT<br>RP:GAAGTCGTGGCTGCTAAGATG |

LP: Left primer; RP: Right Primer.

#### Primers used as left borders:

SALK\_LBP: ATTTTGCCGATTTTCGGAAC

GABI\_KAT LBP: ATATTGACCATCATACTCATTGC

#### Appendix 4B: List of primers used for semi-quantitative RT-PCR

| Orthologous Arabidopsis Gene | Gene number | Mutant allele | Primer Sequences   |
|------------------------------|-------------|---------------|--|
| <i>AtMYB20</i>               | AT1G66230   | GK-109C11     | <b>FP:</b> CAAGAAACAATGGAGCGTCCT<br><b>RP:</b> GCGAAGATGTGGACGTGGAT    |
| <i>AtMYB43</i>               | AT5G16600   | SALK_023509C  | <b>FP:</b> TTGGAGAGCTCTTCCCAAGC<br><b>RP:</b> TCTTCCTGGTAGATGAGAGGCA   |
| <i>AtWRKY33</i>              | AT2G38470   | SALK_064436   | <b>FP:</b> AAGCACACACACACACACACA<br><b>RP:</b> TCTCTTTGCAATAATGTGCTTCA |
| <i>AtWRKY44</i>              | AT2G37260   | SALK_058009   | <b>FP:</b> ATCTCCGCAAACGACTTGCC<br><b>RP:</b> GACATTTCCGGGTGTGTGCAT    |
| <i>AtWRKY48</i>              | AT5G49520   | SALK_066438C  | <b>FP:</b> GCGTTTCTGACGAAGAGCGA<br><b>RP:</b> CCAAAGCCGGGGAATGATGA     |
| <i>AtWRKY57</i>              | AT1G69310   | GK_078H12     | <b>FP:</b> ACCACTCCTCCGATCATCCT<br><b>RP:</b> CCACGAGGGAATCCAATGGT     |
| <i>AtWRKY41</i>              | AT4G11070   | SALK_068648C  | <b>FP:</b> AGCCAGAGAGAGGCTTAGA<br><b>RP:</b> AAACGTTCCACCACCGTTGA      |
| <i>AtWRKY53</i>              | AT4G23810   | SALK_034157C  | <b>FP:</b> AGGAGGTTCTAGCGAGAGTCA<br><b>RP:</b> ACTATCAACGGCGAGTTCGG    |
| <i>AtGT-3B</i>               | AT2G38250   | SALK_133090   | <b>FP:</b> AAGAACCTCGTCACTCGTTT<br><b>RP:</b> ATTACTACCGCCTTTTCGCT     |
| <i>AtGT-3A</i>               | AT5G01380   | GK_591B09     | <b>FP:</b> GAAGTCGTGGCTGCTAAGATG<br><b>RP:</b> TTCACCGTTTGCCTCATAAAC   |

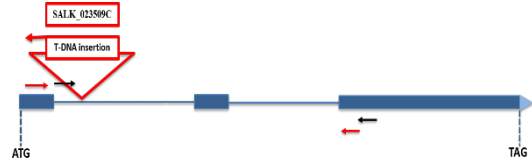
**FP:** Forward Primer; **RP:** Reverse Primer

## Appendix 4C: Structure of candidate genes, T-DNA insertions and phylogenetic relationships

*AtMYB20* (AT1G66230)



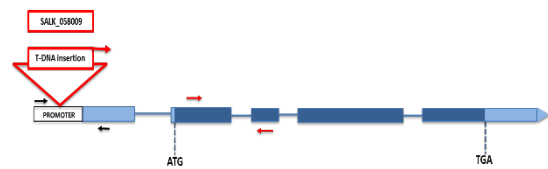
*AtMYB43* (AT5G16600)



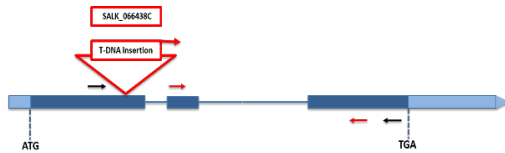
*AtWRKY33* (AT2G38470)



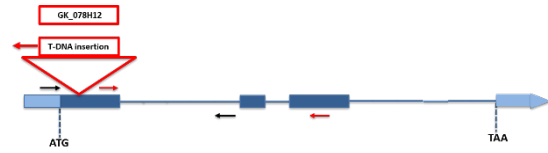
*AtWRKY44* (AT2G37260)



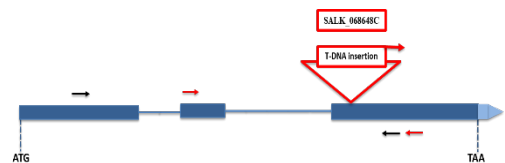
*AtWRKY48* (AT5G49520)



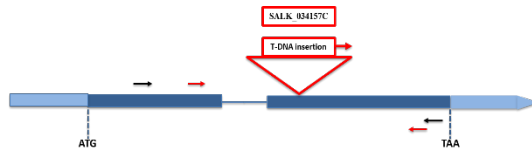
*AtWRKY57* (AT1G69310)



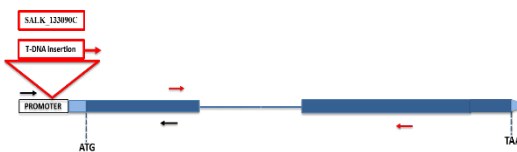
*AtWRKY41* (AT4G11070)



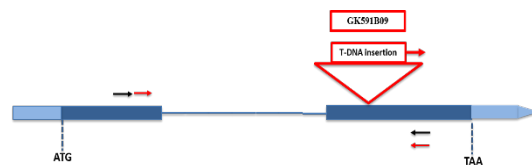
*AtWRKY53* (AT4G23810)



*AtGT-3B* (AT2G38250)

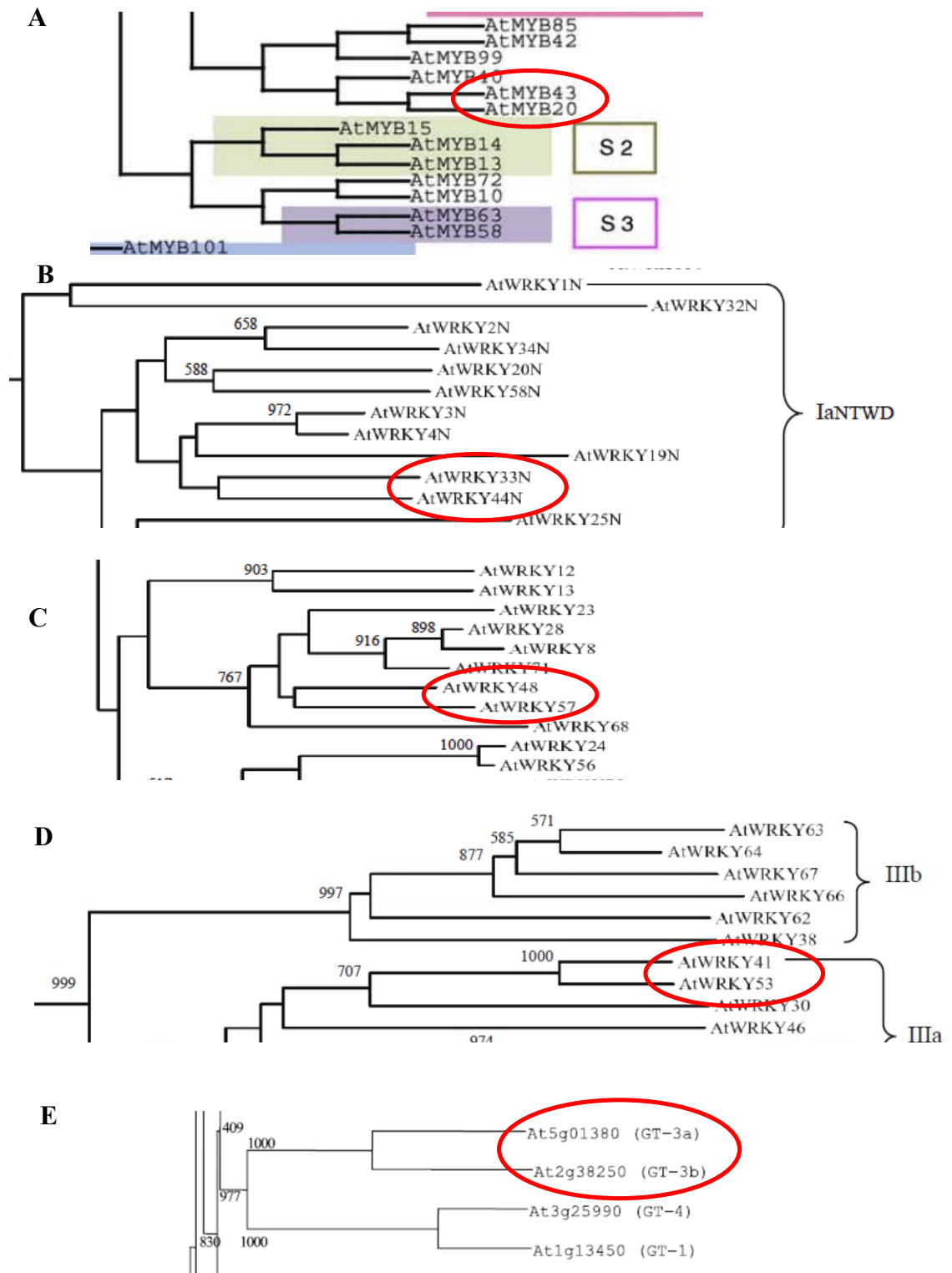


*AtGT-3A* (AT5G01380)



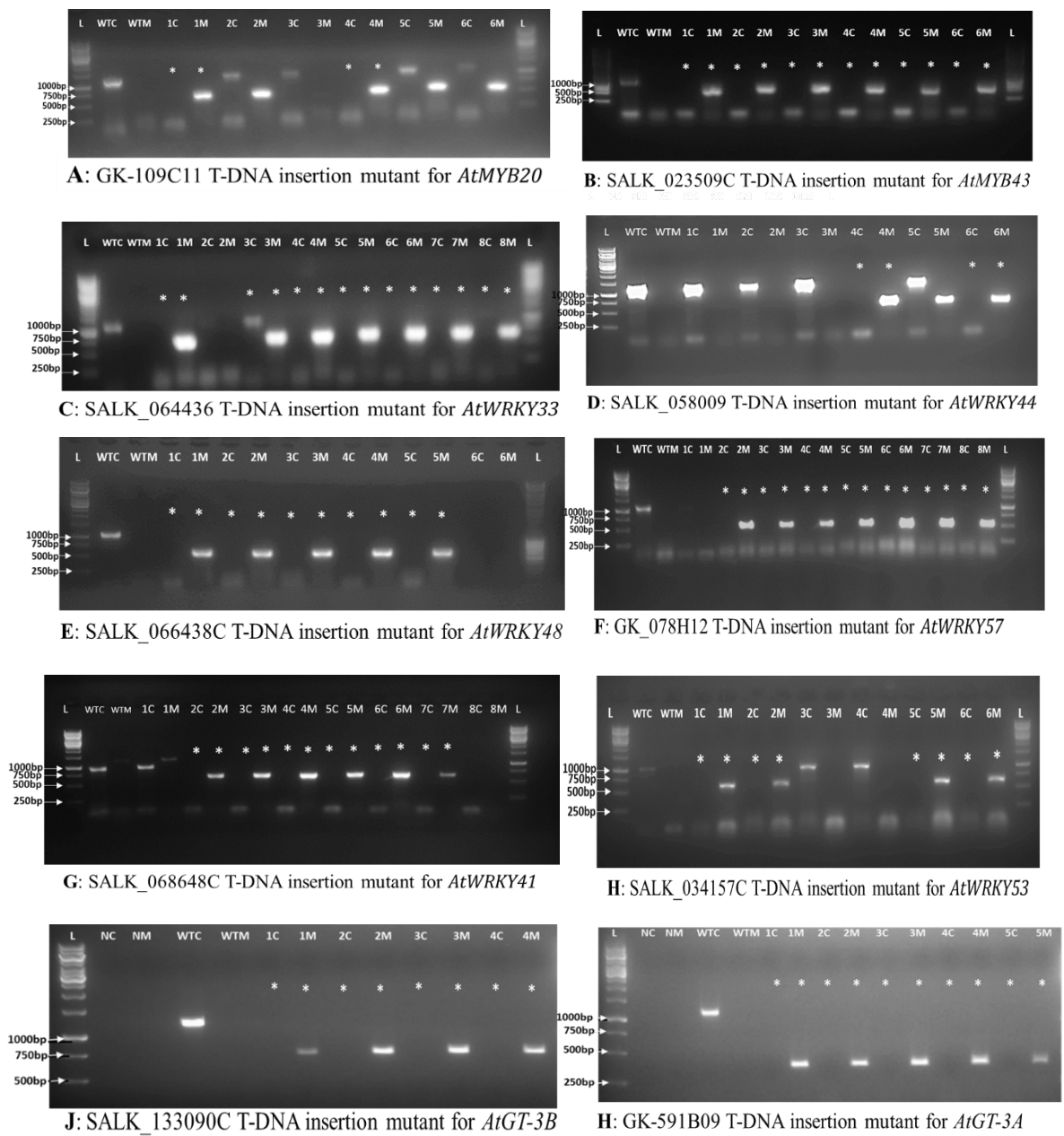
Black arrows indicate the location of primers designed for genotyping experiments. Red arrows indicate primers for semi-quantitative PCR. Primers for semi-quantitative PCR were designed either downstream or flanking the T-DNA insertion.

**Phylogenetic relationship of Arabidopsis MYB, WRKY and GT transcription factors**



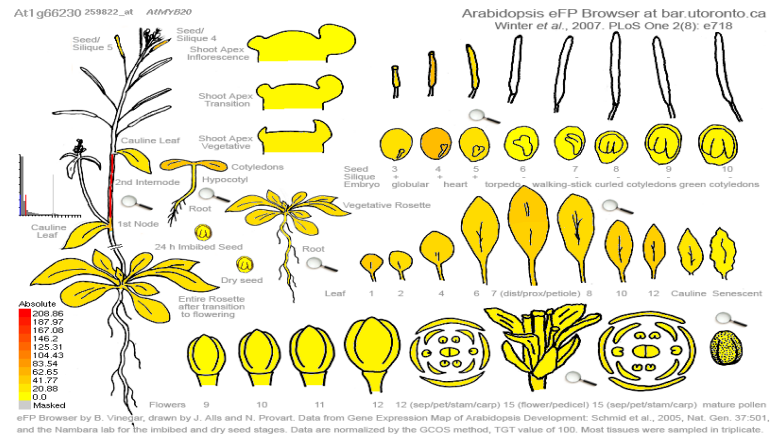
**A:** Phylogenetic tree of MYB transcription factors. Picture adapted and modified from Dubos et al. (2010). **B, C, D:** Phylogenetic tree of WRKY transcription factors. Picture adapted and modified from Wu et al. (2005). **E:** Phylogenetic tree of GT transcription factors. Picture adapted and modified from Ayadi et al. (2004). Red oval boxes indicate the paralogous gene pairs chosen for this study.

## Appendix 4D: Results of genotyping individual T-DNA insertion lines

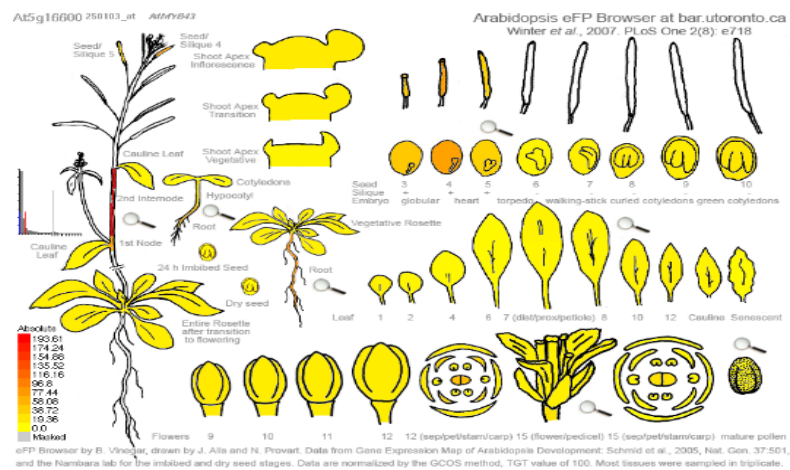


Individual gels for genotyping lines as indicated are shown. Homozygous individual for each seed line are indicated by asterisks (\*). NC corresponds to negative control where water was used as a replacement for template DNA.

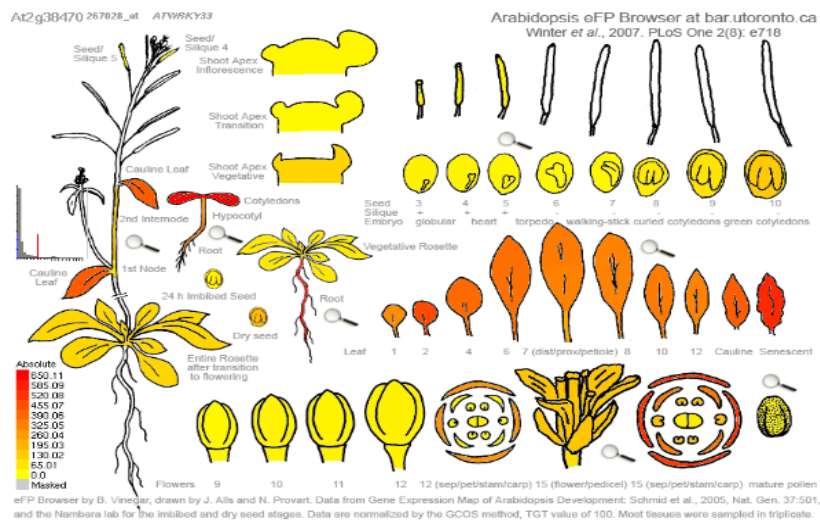
## Appendix 4E: Arabidopsis expression analysis of genes in eFP browser across whole plants



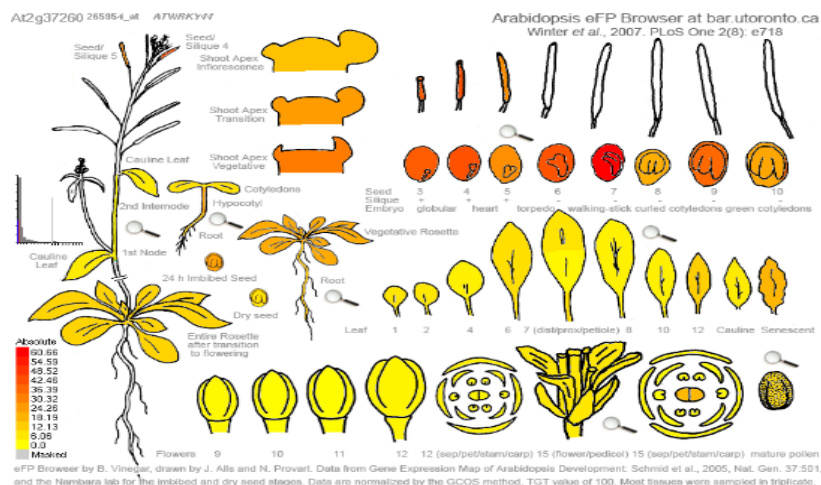
**A: Expression analysis for *AtMYB20***



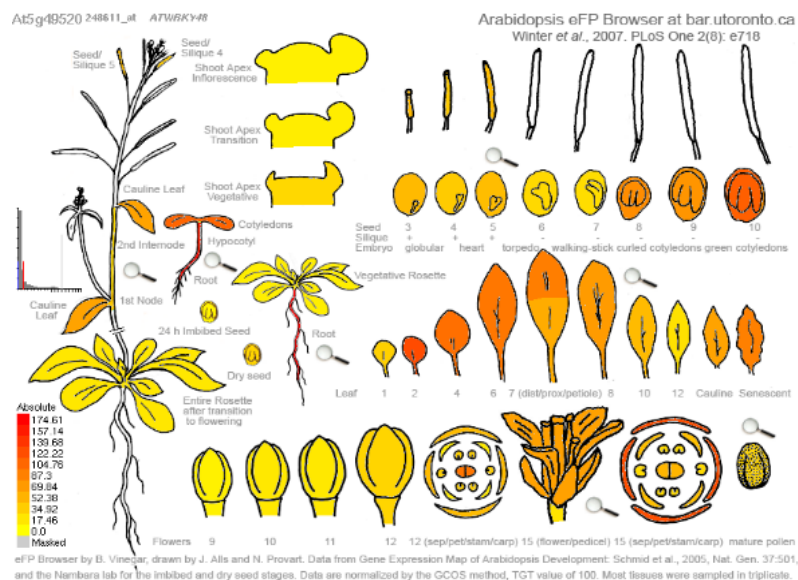
**B: Expression analysis for *AtMYB43***



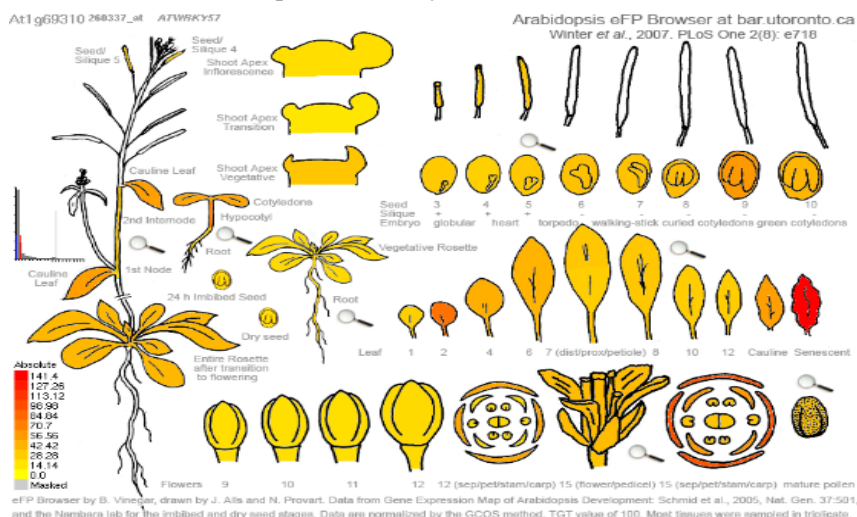
**C: Expression analysis for *AtWRKY33***



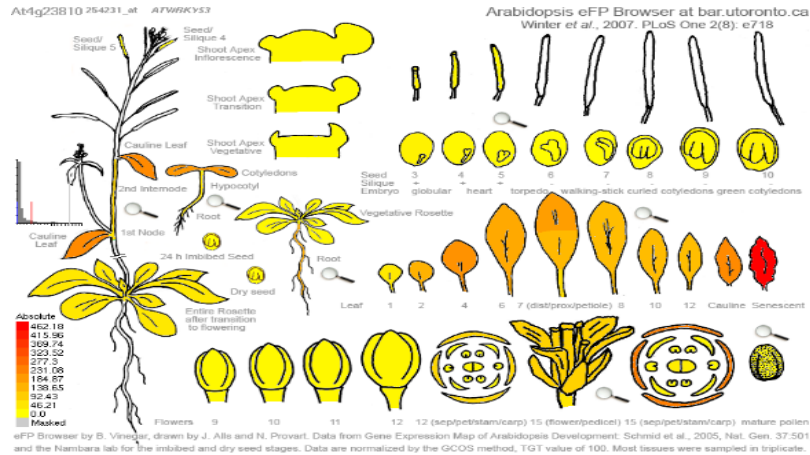
D: Expression analysis for *AtWRKY44*



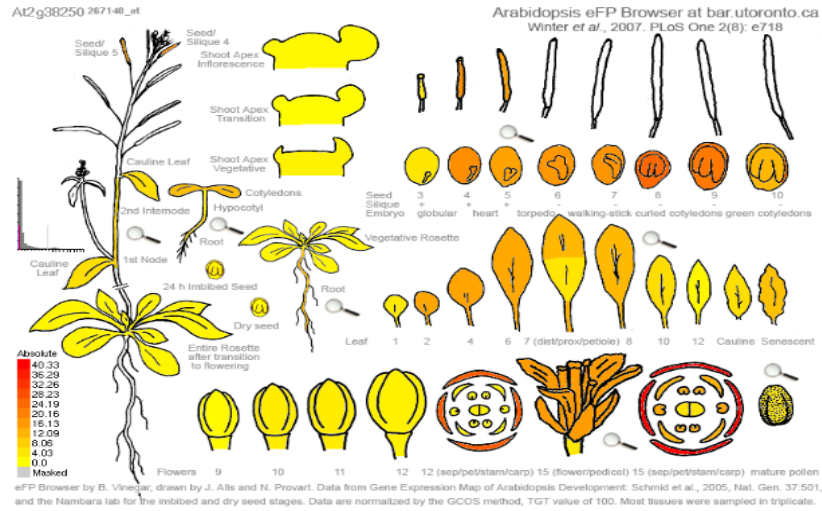
E: Expression analysis for *AtWRKY48*



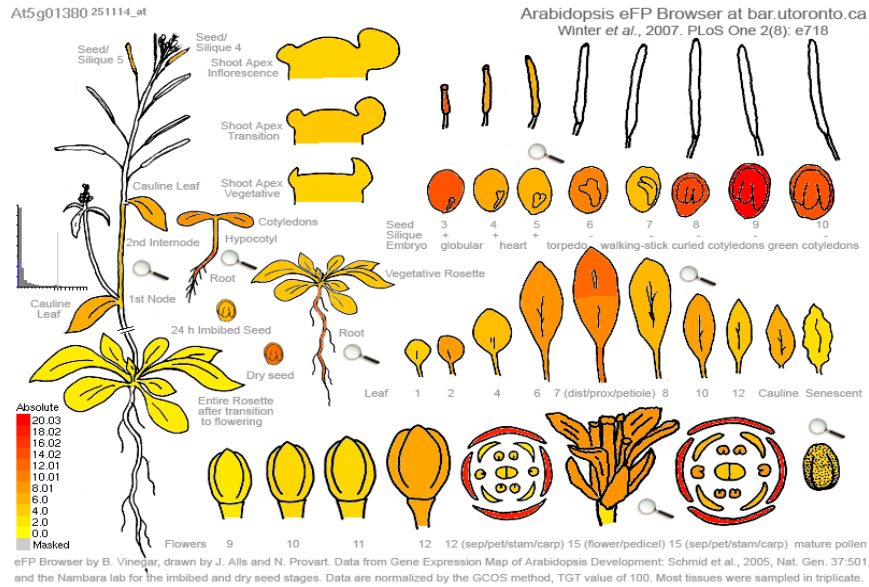
F: Expression analysis for *AtWRKY57*



G: Expression analysis for *AtWRKY53*

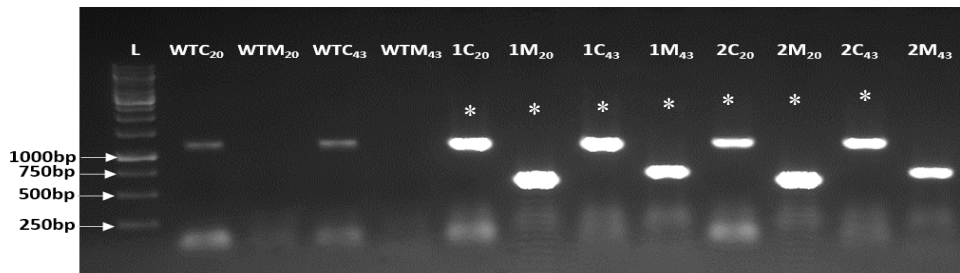


H: Expression analysis for *AtGT-3B*

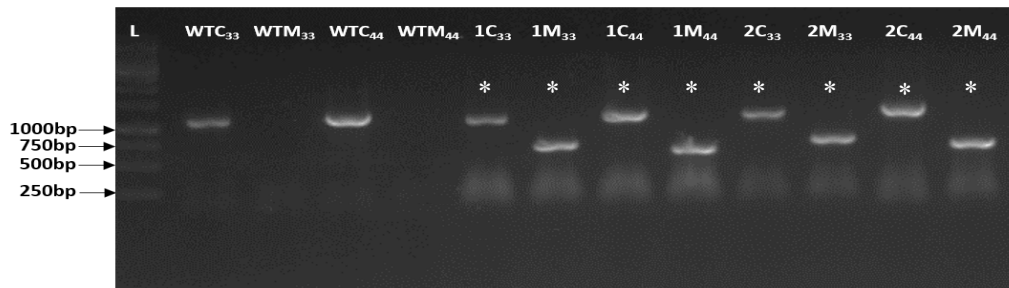


I: Expression analysis for *AtGT-3A*

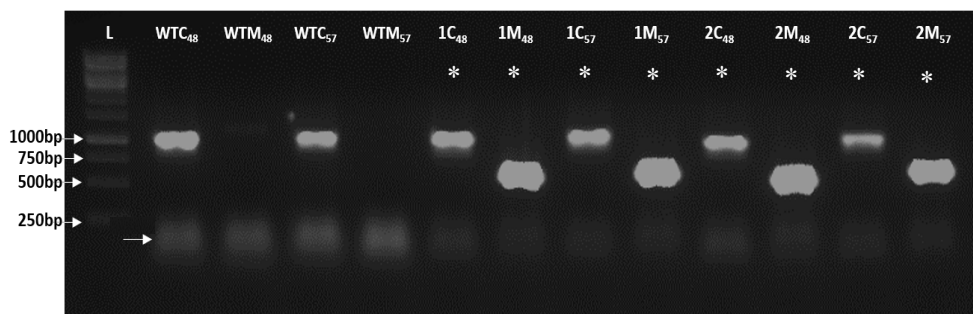
**Appendix 4F: Results of genotyping of T1 population of crossing between two T-DNA insertional mutants of different genes**



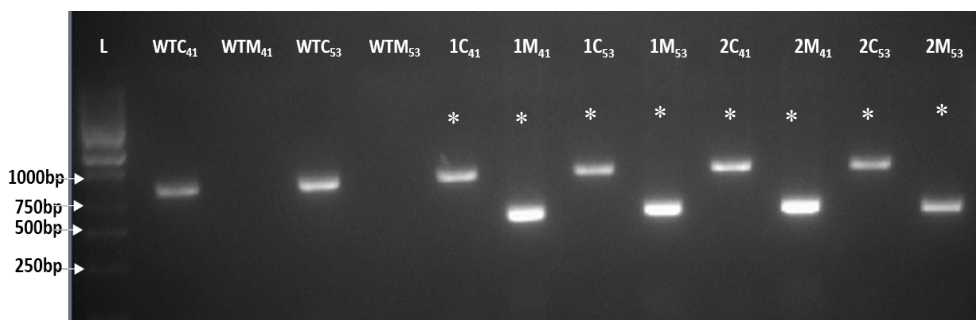
**A:** Genotyping results of *atmyb20* x *atmyb43* T1 plants



**B:** Genotyping results of *atwrky33* x *atwrky44* T1 plants



**C:** Genotyping results of *atwrky48* x *atwrky57* T1 plants



**D:** Genotyping results of *atwrky41* x *atwrky53* T1 plants

Individual gels for genotyping lines as indicated are shown. Heterozygous individuals for each seed line are indicated by asterisks.

## Appendix 4G: Additional investigations of the *atmyb20/atmyb43* double mutant

### 4G.1 Introduction

Secondary wall deposition in xylem is an example of localised wall deposition in plants similar in some respects to wall ingrowth deposition in TCs. MYB and NAC-domain family transcription factors act as master switches in regulating gene expression cascades resulting in secondary wall deposition in xylem (Zhong et al, 2008; Nakano et al., 2015). *AtMYB20* and its paralog *AtMYB43* are two members of the MYB family of transcription factors which are amongst a small cohort of other MYBs such as *MYB42*, *MYB69* and *MYB52/54*, which function as second-tier regulators of the hierarchical cascade of gene expression required for secondary wall deposition (Zhong et al, 2008, 2010; Zhong and Ye, 2014). Furthermore, *AtMYB20* and *AtMYB43* have been assigned to the component of this cascade that regulates gene expression responsible for biosynthesis of cellulose and hemicellulose constituents of the secondary wall (Zhong and Ye, 2014).

The *V. faba* ortholog of *AtMYB20*, namely *VfMYB20* (contig 9668; Table 1, Chapter 3) showed a log<sub>2</sub> fold-change of 7.1 specifically in epidermal cells within 3 h of cotyledon culture (Table 1 – Chapter 3), a response consistent with a role in regulating the rapid burst of wall ingrowth deposition occurring in epidermal TCs across this period. This result pointed to the possibility of conserved pathways regulating cellulose/hemicellulose biosynthesis in the deposition of both secondary walls and wall ingrowths. This possibility was tested by examining the effect of wall ingrowth deposition in PP TCs in the *atmyb20/atmyb43* double mutant, but as shown in Figure 4.4, no visible wall ingrowth phenotype was observed. Surprisingly, however, analysis of xylem elements in vascular bundles adjacent to PP TCs in this double mutant also showed no apparent difference between WT and the double mutant (see below). This result could be interpreted as evidence that *AtMYB20* and/or *AtMYB43* have no role in regulating secondary wall deposition, since no studies have been reported using a *atmyb20/atmyb43* double mutant to genetically test this assumption.

Given the value of the *atmyb20/atmyb43* double mutant generated in this study as novel germplasm to investigate secondary wall biology, additional analysis of this mutant was undertaken. In addition to providing a more detailed analysis of xylem production in vascular bundles as detected by mPS-PI staining and confocal microscopy, FTIR

spectroscopy and fluorogenic staining of inflorescence stem tissue were performed to assess the properties of the double mutant compared to WT.

## **4G.2 Materials and Methods**

### **4G.2.1 Analysis of xylem secondary wall deposition in leaves using mPS-PI staining**

Juvenile leaves (leaf 1 and leaf 2) of 21 day-old plants were harvested from the *atmyb20/atmyb43* double mutant and WT. Leaves from three replicate plants of each germplasm were collected and stained with propidium iodide. The leaves were processed and examined as described in section 4.2.8. The images from *atmyb20/atmyb43* were then compared with WT for any visible changes in secondary wall deposition in tracheary elements of xylem. In addition, ImageJ was used to quantify the intensity of propidium iodide staining in mutants and WT by measuring pixel intensity of labelled secondary wall deposition in xylem elements. For this analysis, the area of each xylem bundle in a given Z-stack image was defined as a region of interest and average pixel intensity was quantified using ImageJ. Sampling was conducted from at least 20 different xylem bundles in total from juvenile leaves 1 or 2 derived from three separate plants of each germplasm (i.e., WT or *atmyb20/atmyb43* double mutant).

### **4G.2.2 Cell wall compositional analysis by FTIR spectroscopy**

Inflorescence stem and fully expanded adult leaves from 3-week-old plants were harvested from three replicate plants and snap frozen in liquid nitrogen. The samples were then dried in an oven at 40°C for 6-7 days, and then transferred to 5 mL tubes with 3 mm ball bearings and washers and ground to a fine powder in a Qiagen TissueLyser II machine. The ground tissue was then washed three times with MQ water, followed by three washes with 70% ethanol. The samples were then dried in a vacuum concentrator and stored over molecular sieve until analysed. For analysis, approximately 20 mg of dried tissue was placed on the surface of an ATR crystal and FTIR spectra were generated using a Perkin Elmer Spectrum Two FTIR spectrometer with ATR two sampling attachment, as reported by Martin et al. (2013). A baseline correction and area normalisation were applied and the mean spectra for each '*line*' was plotted for chemical interpretation of FTIR absorption peaks (Figure 4G.2).

### **4G.2.3 Histological assessment of cellulose and lignin**

Calcofluor white and phloroglucinol-HCL staining were used for detecting cellulose and lignin respectively. Hand-cut sections were prepared from the base of inflorescence stems that had reached 5 cm in height. At least 5-10 sections per stem were prepared. Some sections were stained in phloroglucinol stain (0.5% (w/v) in 95% (v/v) ethanol) for one minute, followed by transfer to 20% (v/v) hydrochloric acid and washed for two minutes. The sections were then carefully mounted onto a glass slide with mounting solution (glycerol, lactic acid, 20 % hydrochloric acid and 0.5 % phloroglucinol in ethanol in a ratio of 50:40:7:3). Other sections were stained for 1 minute in 0.01% (w/v) calcofluor white and mounted onto a glass slide with 50% glycerol as mounting medium. The phloroglucinol-stained sections were examined under bright field and the calcofluor white-stained section examined under DAPI filter using a Zeiss AxioScope II fluorescence microscope, with images recorded using a Zeiss AxioCam HRc camera driven by Axiovision 4.6.3 SP1 software.

## **4G. 3 Results and Discussion**

### **4G.3.1 Analysis of xylem secondary cell wall in leaves of the *atmyb20/atmyb43* double mutant**

To examine secondary wall deposition in tracheary elements of xylem, juvenile leaves from WT and the *atmyb20/atmyb43* double mutant were stained using the mPS-PI procedure as described in section 4.2.8 and examined by confocal microscopy. A survey of replicate juvenile leaves showed no apparent differences in secondary cell wall deposition in xylem from the double mutant compared to WT. Representative images of this result are shown in Figure 4G.1A-F. The characteristic banding of localized secondary wall deposition was not appreciably different between the two genotypes, either in apparent density of banding per unit length along xylem, or intensity of staining by propidium iodide (Figure 4G1.A-F). To verify this conclusion quantitatively, analysis of propidium iodide-stained xylem elements was undertaken as described in section 4G.2.1. This analysis

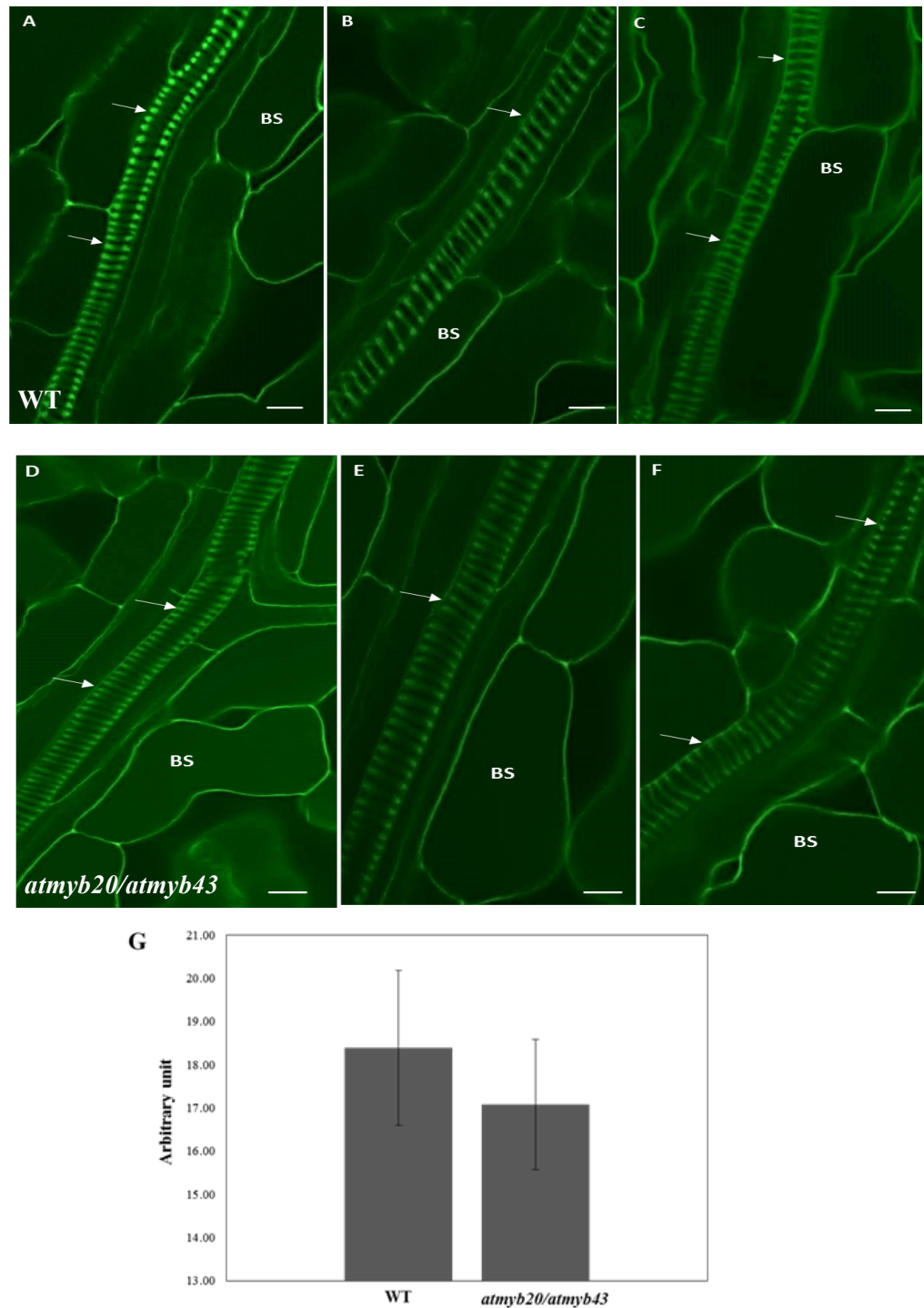


**Figure 4G.1: Analysis of xylem secondary cell wall in leaves of the *atmyb20/atmyb43* double mutant using mPS-PI staining.**

(A-F) mPS-PI staining showing xylem tracheary elements in minor veins of juvenile leaves. (A-C) WT. (D-F) *atmyb20/atmyb43* double mutant. Arrows indicate the tracheary elements of xylem. BS, bundle sheath cells. Scale bar = 5 $\mu$ m. (G) Quantification of mPS-PI staining of xylem elements by ImageJ software. The intensity of propidium iodide staining (expressed in arbitrary units) of xylem for both WT and the *atmyb20/atmyb43* double mutant is shown. Data was derived

from a minimum of 20 individual tracheary elements derived from three replicate leaves. No significant difference was observed between the two germplasms.

showed that while staining intensity was reduced in the double mutant compared to WT, this reduction was not significant, confirming the conclusion from the confocal imaging that no difference in secondary wall deposition in xylem in either WT or the *atmyb20/atmyb43* double mutant could be detected (Figure 4G.1G).

#### **4G.3.2 Cell wall compositional analysis FTIR spectroscopy of WT and *atmyb20/atmyb43* double mutant**

While the confocal microscopy analysis in juvenile leaves suggested no substantial differences in secondary wall deposition was observed in xylem between WT and the *atmyb20/atmyb43* double mutant, FTIR spectroscopy was used to assess if any compositional differences of cell walls from inflorescence stems or leaves could be detected between WT and the double mutant. Relative amounts of major classes of cell wall components can be determined from FTIR spectral analysis of dried plant material (Mouille et al., 2003; Largo-Gosens et al., 2014 ; Martin et al, 2013). The infrared spectra shown in Figure 4G.2 represents the mean spectral output from three independent replicate samples from both inflorescence stem and leaves, for both WT and the double mutant. A broad peak was observed from wavenumber 1162 – 946  $\text{cm}^{-1}$  with a maximum at 1028  $\text{cm}^{-1}$  that corresponds to polysaccharides like cellulose and hemicellulose (Largo-Gosens et al., 2014; Figure 4G.2). A second broad peak was observed in the range 1671 – 1510  $\text{cm}^{-1}$  that includes phenolic compounds, phenolic rings and lignin (Largo-Gosens et al., 2014; Figure 4G.2).

In leaf tissue there is a clear reduction in abundance of polysaccharides including cellulose/hemicellulose in the *atmyb20/atmyb43* double mutant compared to WT (peak at 1028  $\text{cm}^{-1}$ ; Figure 4G.2A), whereas phenolic compounds including lignin were more abundant in the *atmyb20/atmyb43* double mutant (1671-1510  $\text{cm}^{-1}$ ; Figure 4G.2A). By comparison, differences between the two lines were not as obvious in inflorescence stem tissue, with minor reductions in polysaccharides in the double mutant and a smaller increase in the abundance of phenolic compounds in the double mutant compared to WT (Figure 4G.2B). A reduction in polysaccharide composition would be expected in the *atmyb20/atmyb43* double mutant given the high hierarchical position of these genes in the secondary wall transcriptional cascade (Zhong et al., 2010), but why this reduction is

more apparent in leaves compared to inflorescence stem is unclear. A detailed chemical analyses using “wet” biochemistry or mass spectroscopy procedures (Zablackis et al., 1995; Roessner et al., 2006) would be required to further establish the chemical differences in wall composition between these two genotypes.

#### **4G.3.3 Histological analysis of cellulose and lignin in *atmyb20/atmyb43***

To further assess possible differences in secondary wall deposition between WT and the *atmyb20/atmyb43* double mutant, cellulose and lignin content in inflorescence stems were stained by calcofluor white and phloroglycinol-HCl, respectively, in hand cut sections of immature inflorescence stems. Autofluorescence of these sections under UV light showed no substantial differences in tissue organisation between WT and the double mutant (Figure 4G.3A-F). Blue autofluorescence indicative of aromatic compounds including lignin was comparable in xylem and interfascicular fibres in both lines (Figure 4G.3A-F). Staining of lignin using phloroglycinol-HCl indicated possibly reduced levels in the double mutant compared to WT (Figure 4G.3G-L). The purple colour resulting from lignin staining was localized to xylem and interfascicular fibres, and this appeared to be marginally more prominent in WT sections compared to the double mutant, however variations in section thickness might account for these apparent differences. Calcofluor white staining was used to analyse predominantly cellulose, and in this case the pale blue colouration was localized predominantly to phloem tissue and pith, with again no clear differences observed between WT and the *atmyb20/atmyb43* double mutant (Figure 4G.3M-R). Surprisingly, secondary walls in xylem and interfascicular fibres were not stained by calcofluor white. In summary, this histological analysis revealed no obvious differences in cellulose and lignin synthesis in inflorescence stems between WT and the *atmyb20/atmyb43* double mutant.

Collectively, the preliminary analysis of cell wall composition undertaken by FTIR and histological staining in the *atmyb20/atmyb43* double mutant indicated relatively minor differences compared to WT. In particular, the FTIR spectra detected reduced levels of polysaccharide components, which include cellulose and hemicelluloses, in the double mutant, with this reduction being more apparent in leaf tissue compared to inflorescence

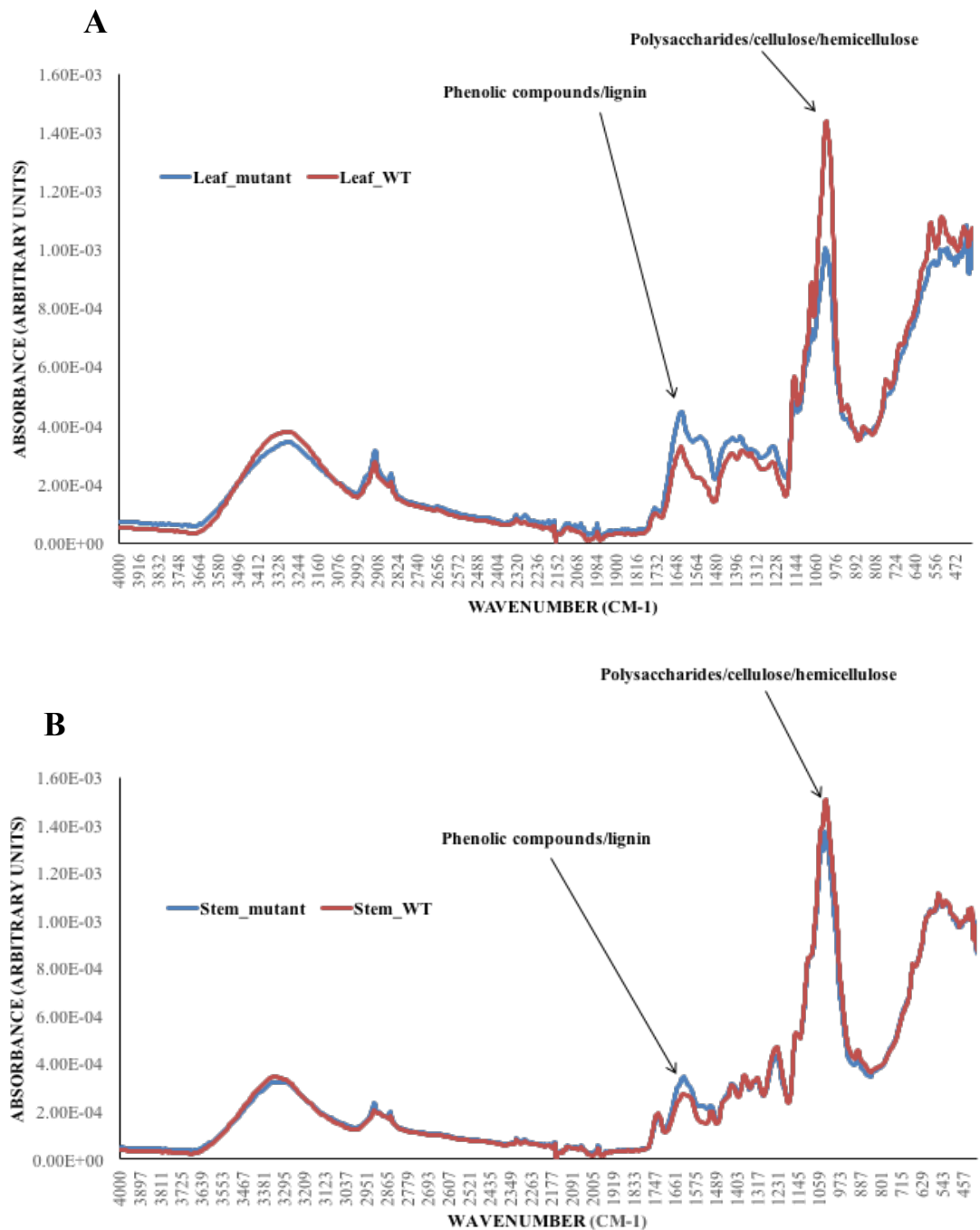


**Figure 4G.2: FTIR spectra of cell wall composition in leaf and inflorescence stem of WT and the *atmyb20/atmyb43* double mutant.**

(A) Leaf tissue - phenolic compounds were more abundant in the *atmyb20/atmyb43* double mutant compared to WT, however, polysaccharides including cellulose/hemicelluloses were clearly less abundant in the double mutant. (B) Inflorescence stems – phenolic compounds were only marginally more abundant in the mutant while the difference in polysaccharides in stem tissue was only marginal, with polysaccharides being slightly less abundant in the mutant compared to WT. FTIR spectroscopy and data interpretation was performed with the assistance of Christopher Brown and Antony Martin, Centre for Plant Science, University of Newcastle.

stems. The histological staining was undertaken to assess if any major anatomical differences could be detected in secondary walls in stem sections, but none were clearly evident. This approach, however, is not definitive as a means to detect structural and compositional differences in secondary wall formation (Mitra and Loque, 2014). The reduction, however, in cellulose/hemicellulose components of the cell wall as revealed by FTIR is consistent with *AtMYB20* and *AtMYB43* functioning as transcriptional regulators of gene pathways directing synthesis of these polysaccharides in secondary wall formation (Zhong et al, 2010). This reduction in cellulose/hemicelluloses, however, is not consistent with the apparent absence of an effect on xylogenesis in minor veins of the double mutant. In this case, either the mPS-PI staining of cell wall polysaccharides and imaging by confocal microscopy was not capable of detecting possibly subtle phenotypic differences in the double mutant compared to WT, or alternatively, xylogenesis in minor veins, which is an example of localized secondary wall deposition, does not involve *AtMYB20/AtMYB43*. Clearly, a more thorough analysis of the *atmyb20/atmyb43* double mutant is required to verify this possibility. However, the *atmyb20/atmyb43* double mutant remains a valuable line for analysis of secondary wall deposition, given the prominent position given to both *AtMYB20* and *AtMYB43* in the regulatory cascade controlling secondary wall formation. Despite the claim for these two genes acting as second tier regulators of secondary wall formation, no studies have been reported using single or double mutants to assess these claims, therefore future studies of this double mutant, including transcriptional profiling and detailed compositional analysis in different tissues would be useful to demonstrate direct effects on secondary wall formation.

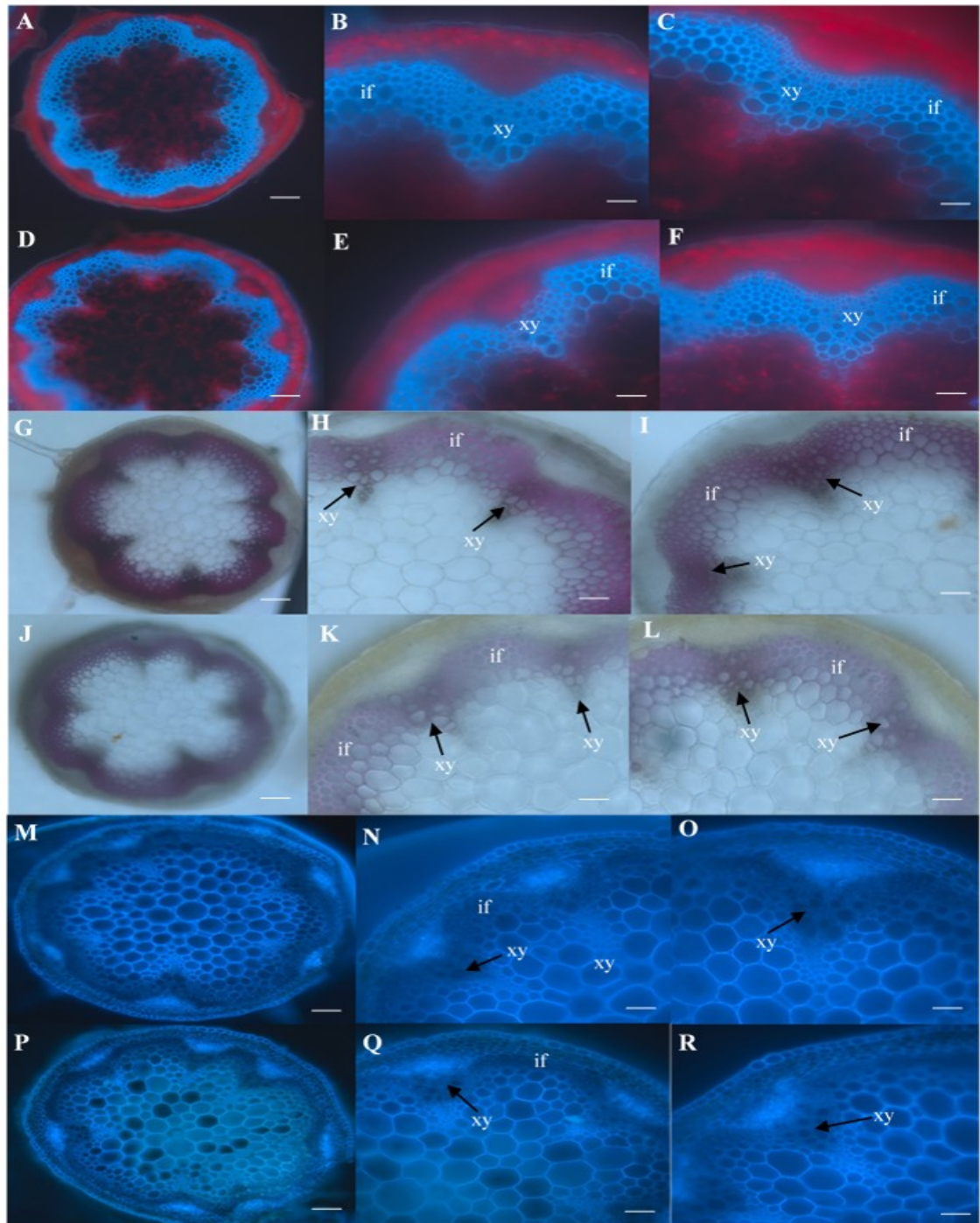


**Figure 4G.3** Histological assessment of xylem cell wall components in WT and *atmyb20/atmyb43*.

(A-F) Auto fluorescence of inflorescence stem sections observed under UV illumination. (A-C) WT stem sections. Scale bar on A 100  $\mu$ m, B,C 10  $\mu$ m. (D-F) *atmyb20/atmyb43* stem sections. Scale bar on D 100  $\mu$ m, E, F 10  $\mu$ m. (G-L) Phloroglucinol-HCL staining of lignin in the inflorescence stem sections observed under fluorescence microscope. (G-I) WT stem sections. Scale bar on G 100  $\mu$ m, H, I 10  $\mu$ m. (J-L) *atmyb20/atmyb43* stem sections. Scale bar on J 100  $\mu$ m, K, L 10  $\mu$ m (M-R) Calcofluor white staining of cellulose in the inflorescence stem sections observed under fluorescence microscope. (M-O) WT stem sections Scale bar on M 100  $\mu$ m, N, O 10  $\mu$ m. (P-R) *atmyb20/atmyb43* inflorescence stem sections. Scale bar on P 100  $\mu$ m, Q,R 10  $\mu$ m. xy-xylem, if-interfascicular fibres.

## REFERENCES

- Afzal, A.J., Wood, A.J. and Lightfoot, D.A. (2008). Plant receptor-like serine threonine kinases: roles in signaling and plant defense. *Molecular Plant-Microbe Interactions* **21**: 507–517.
- Allaway, W.G., Carpenter, J.L., and Ashford, A.E. (1985). Amplification of inter-symbiont surface by root epidermal transfer cells in the pisonia mycorrhiza. *Protoplasma* **128**: 227–231.
- Alves, M.S., Dadalto, S.P., Gonçalves, A.B., De Souza, G.B., Barros, V.A., and Fietto, L.G. (2014). Transcription factor functional protein-protein interactions in plant defense response. *Proteomes* **2**: 85–106.
- Ambawat, S., Sharma, P., Yadav, N.R., and Yadav, R.C. (2013). MYB transcription factor genes as regulators for plant responses: an overview. *Physiology and Molecular Biology of Plants* **19**: 307–321.
- Amiard, V., Demmig-Adams, B., Mueh, K.E., Turgeon, R., Combs, A.F., and Adams, W.W. III. (2007). Role of light and jasmonic acid signaling in regulating foliar phloem cell wall ingrowth development. *New Phytologist* **173**: 722–731.
- Amiard, V., Mueh, K.E., Demmig-Adams, B., Ebbert, V., Turgeon, R., and Adams, W.W. (2005). Anatomical and photosynthetic acclimation to the light environment in species with differing mechanisms of phloem loading. *Proceedings of the National Academy of Sciences of the United States of America* **102**: 12968–12973.
- Andriunas, F.A., Zhang, H.M., Weber, H., McCurdy, D.W., Offler, C.E., and Patrick, J.W. (2011). Glucose and ethylene signalling pathways converge to regulate *trans*-differentiation of epidermal cells in *Vicia narbonensis* cotyledons. *Plant Journal* **68**: 987–998.
- Andriunas, F.A. (2011). Transfer cell *trans*-differentiation in *Vicia faba* cotyledons: Regulatory roles of ethylene, glucose and reactive oxygen species. PhD thesis. University of Newcastle, Australia.
- Andriunas, F.A., Zhang, H.M., Xia, X., Offler, C.E., McCurdy, D.W., and Patrick, J.W. (2012). Reactive oxygen species form part of a regulatory pathway initiating *trans*-differentiation of epidermal transfer cells in *Vicia faba* cotyledons. *Journal of Experimental Botany* **63**: 3617–3629.
- Andriunas, F.A., Zhang, H.M., Xia, X., Patrick, J.W and Offler, C.E. (2013). Intersection of transfer cells with phloem biology-broad evolutionary trends, function and induction. *Frontiers in Plant Science* **4**: 221.
- Annadurai, R.S., Jayakumar, V., Mugasimangalam, R.C., Katta, M.A., Anand, S., Gopinathan, S., et al. (2012). Next generation sequencing and de novo

- transcriptome analysis of *Costus pictus* D. Don, a non-model plant with potent anti-diabetic properties. *BMC Genomics* **13**: 663.
- Arabidopsis Genome I. (2000). Analysis of the genome sequence of the flowering plant *Arabidopsis thaliana*. *Nature* **408**: 796–815.
- Ariel, F.D., Manavella, P.A., Dezar, C.A., and Chan, R.L. (2007). The true story of the HD-Zip family. *Trends in Plant Science* **12**: 419–426.
- Arun-Chinnappa, K.S., and McCurdy, D.W. (2015). *De novo* assembly of a genome-wide transcriptome map of *Vicia faba* (L.) for transfer cell research. *Frontiers in Plant Science* **6**: 217. doi: 10.3389/fpls.2015.00217.
- Arun-Chinnappa, K.S., Nguyen, T.T., Hou, J., Wu, Y., and McCurdy, D.W. (2013). Phloem parenchyma transfer cells in *Arabidopsis* – an experimental system to identify transcriptional regulators of wall ingrowth formation. *Frontiers in Plant Science* **4**: 102. doi: 10.3389/fpls.2013.00102.
- Austin, R.S., Vidaurre, D., Stamatiou, G., Breit, R., Provart, N.J., Bonetta, D., et al. (2011). Next-generation mapping of *Arabidopsis* genes. *Plant Journal* **67**: 715–725.
- Ayadi, A., David, P., Arrighi, J.F., Chiarenza, S., Thibaud, M.C., Nussaume, L. et al. (2015). Reducing the genetic redundancy of *Arabidopsis* PHT1 transporters to study phosphate uptake and signaling. *Plant Physiology* **172**: 1511–1526.
- Ayadi, M., Delaporte, V., Li, Y.F., and Zhou, D.X. (2004). Analysis of GT-3a identifies a distinct subgroup of trihelix DNA-binding transcription factors in *Arabidopsis*. *FEBS Letter* **562**: 147–154.
- Bahgat, S., Shabban, O.A., El-Shihy, O., Lightfoot, D.A., and El-Shemy, H.A. (2009). Establishment of the regeneration system for *Vicia faba* L. *Current Issues in Molecular Biology* **11**: (Suppl. 1) i47– 54.
- Bakshi, M., and Oelmüller, R. (2014). WRKY transcription factors: Jack of many trades in plants. *Plant Signal Behaviour* **9**: e27700.
- Barrero, C., Royo, J., Grijota-Martinez, C., Faye, C., Paul, W., Sanz, S., et al. (2009). The promoter of *ZmMRP-1*, a maize transfer cell-specific transcriptional activator, is induced at solute exchange surfaces and responds to transport demands. *Planta* **229**: 235–247.
- Becraft, P.W. (2002). Receptor kinase signaling in plant development. *Annual review of cell and developmental biology* **18**: 163–192.
- Beebe, D.U., and Russin, W.A. (1999). Plasmodesmata in the phloem-loading pathway. In *Plasmodesmata. Structure, Function, Role in Cell Communication*. (van Bel, A. J. E. and van Kesteren, W. J. P. eds), 261–294, Springer-Verlag, Berlin, Germany.

- Beebe, D.U., and Turgeon, R. (1992). Localization of galactinol, raffinose, and stachyose synthesis in cucurbita-pepo leaves. *Planta* **188**: 354–361.
- Berendzen, K.W., Weiste, C., Wanke, D., Kilian, J., Harter, K., and Dröge-Laser, W. (2012). Bioinformatic *cis*-element analyses performed in *Arabidopsis* and rice disclose bZIP- and MYB-related binding sites as potential AuxRE-coupling elements in auxin-mediated transcription. *BMC Plant Biology* **12**: 125. doi: 10.1186/1471-2229-12-125.
- Berthet, S., Demont-Caulet, N., Pollet, B., Bidzinski, P., Cézard, L., Le Bris, P., et al. (2011). Disruption of *LACCASE4* and *17* results in tissue-specific alterations to lignification of *Arabidopsis thaliana* stems. *Plant Cell* **23**: 1124–1137.
- Birkenbihl, R.P., Diezel, C., and Somssich, I.E. (2012). *Arabidopsis* WRKY33 is a key transcriptional regulator of hormonal and metabolic responses towards *Botrytis cinerea* infection. *Plant Physiology* **159**: 266–285.
- Booker, J., Chatfield, S., and Leyser, O. (2003). Auxin acts in xylem-associated or medullary cells to mediate apical dominance. *Plant Cell* **15**: 495–507.
- Borisjuk, L., Wang, T., Rolletschek, H., Wobus, U., and Weber, H. (2002). A pea seed mutant affected in the differentiation of the embryonic epidermis leads to deregulated seed maturation and impaired embryo growth. *Development* **129**: 1595–607.
- Borisjuk, L., Weber, H., Panitz, R., Manteuffel, R., and Wobus, U. (1995). Embryogenesis of *Vicia faba* L.: histodifferentiation in relation to starch and storage protein synthesis. *Journal of Plant Physiology* **147** : 203 – 21.
- Böttinger, P., Steinmetz, A., Schieder, O., and Pickardt, T. (2001). Agrobacterium-mediated transformation of *Vicia faba*. *Molecular Breeding* **8**: 243–254.
- Braun, D.M., and Slewinski, T.L. (2009). Genetic control of carbon partitioning in grasses: roles of sucrose transporters and tie-dyed loci in phloem loading. *Plant Physiology* **149**: 71–81.
- Bräutigam, A., Mullick, T., Schliesky, S., and Weber, A.P.M. (2011). Critical assessment of assembly strategies for non-model species mRNA-Seq data and application of next-generation sequencing to the comparison of C3 and C4 species. *Journal of Experimental Botany* **62**: 3093–3102. 10.1093/jxb/err029.
- Brewin, N.J. (2004). Plant cell wall remodelling in the rhizobium-legume symbiosis. *Critical Reviews in Plant Sciences* **23**: 293 – 316.
- Buchi, R., Bachmann, M., and Keller, F. (1998). Carbohydrate metabolism in source leaves of sweet basil (*Ocimum basilicum* L.), a starch-storing and stachyose-translocating labiate. *Journal of Plant Physiology* **153**: 308–315.

- Bush, D.R. (1993). Proton-coupled sugar and amino-acid transporters in plants. *Annual Review of Plant Physiology and Plant Molecular Biology* **44**: 513–542.
- Cabrera, J., Barcala, M., Fenoll, C., and Escobar, C. (2014). Transcriptomic signatures of transfer cells in early developing nematode feeding cells of *Arabidopsis* focused on auxin and ethylene signaling. *Frontiers in Plant Science* **5**: 107. doi: 10.3389/fpls.2014.00107
- Cao, S., Jiang, S., and Zhang, R. (2006). The role of GIGANTEA gene in mediating the oxidative stress response and in *Arabidopsis*. *Plant Growth Regulation* **48**: 261–270.
- Capella, M., Ribone, P.A., Arce, A.L., and Chan, R.L. (2015). *Arabidopsis thaliana* HomeoBox 1 (AtHB1), a Homeodomain-Leucine Zipper I (HD-Zip I) transcription factor, is regulated by PHYTOCHROME-INTERACTING FACTOR 1 to promote hypocotyl elongation. *New Phytology* **207**: 669–682.
- Chandrasekhar, T., Thangavel, K., and Elayaraja, E. (2011). Effective clustering algorithms for gene expression data. *International Journal of Computer Applications* **32**: 0975–8887.
- Charlton, W.L., Keen, C.L., Merriman, C., Lynch, P., Greenland, A.J., and Dickinson, H.J. (1995). Endosperm development in *Zea mays*: implication of gametic imprinting and paternal excess in regulation of transfer layer development. *Development* **121**: 3089–3097.
- Chen, H., Lai, Z., Shi, J., Xiao, Y., Chen, Z. and Xu, X. (2010). Roles of *Arabidopsis* WRKY18, WRKY40 and WRKY60 transcription factors in plant responses to abscisic acid and abiotic stress. *BMC Plant Biology* **10**: 281.
- Chen, J., Pei, Z., Dai, L., Wang, B., Liu, L., An, X., et al. (2014). Transcriptome profiling using pyrosequencing shows genes associated with bast fiber development in ramie (*Boehmeria nivea* L.). *BMC Genomics* **15**: 919. doi:10.1186/1471-2164-15-919.
- Chen, L-Q., Qu, X-Q., Hou, B-H., Sosso, D., Osorio, S., Fernie, A.R., et al. (2012). Sucrose efflux mediated by Sweet proteins as a key step for phloem transport. *Science* **335**: 207–210.
- Chepyshko, H., Lai, C.P., Huang, L.M., Liu, J.H., and Shaw, J.F. (2012). Multifunctionality and diversity of GDSL esterase/lipase gene family in rice (*Oryza sativa* L. japonica) genome: new insights from bioinformatics analysis. *BMC Genomics* **13**: 309. doi: 10.1186/1471-2164-13-309.
- Cho, H-T., and Cosgrove, D.J. (2002). Regulation of root hair initiation and expansin gene expression in *Arabidopsis*. *Plant Cell* **14**: 3237–3253.
- Clough, S.J., and Bent, A.F. (1998). Floral dip: A simplified method for *Agrobacterium*-mediated transformation of *Arabidopsis thaliana*. *Plant Journal* **16**: 735–743.

- Cochrane, M.P., and Duffus, C.M. (1980). The nucellar projection and modified aleurone in the crease region of developing caryopses of barley. *Protoplasma* **103**: 361–375.
- Conesa, A., Gotz, S., Garca-Gómez, J. M., Terol, J., Talon, M., and Robles, M. (2005). Blast2GO: a universal tool for annotation, visualization and analysis in functional genomics research. *Bioinformatics* **18**: 3674–3676.
- Cui, X.H., Hao, F.S., Chen, H., Chen, J., and Wang, X.C. (2008). Expression of the *Vicia faba* VfPIP1 gene in *Arabidopsis thaliana* plants improves their drought resistance. *Journal of Plant Research* **121**: 207–214.
- Czechowski, T., Bari, R.P., Stitt, M., Scheible, W-R., and Udvardi, M.K. (2004). Real-time RT-PCR profiling of over 1400 *Arabidopsis* transcription factors: unprecedented sensitivity reveals novel root- and shoot-specific genes. *Plant Journal* **38**: 366–379.
- Dahiya, P., and Brewin, N.J., (2000). Immunogold localization of callose and other cell wall components in pea nodule transfer cells. *Protoplasma* **214**: 210–218.
- De Hoon, M.J., Imoto, S., Nolan, J., and Miyano, S. (2004). Open source clustering software. *Bioinformatics* **20**: 1453–1454.
- Demmig-Adams, B., Cohu, C.M., Amiard, V., Zadelhoff, G., Veldink, G. A., Muller, O., et al. (2013). Emerging trade-offs - impact of photoprotectants (PsbS, xanthophylls, and vitamin E) on oxylipins as regulators of development and defense. *New Phytologist* **197**: 720–729.
- Desprez, T., Juraniec, M., Crowell, E.F., Jouy, H., Pochylova, Z., Parcy, F., et al. (2007). Organization of cellulose synthase complexes involved in primary cell wall synthesis in *Arabidopsis thaliana*. *Proceedings of the National Academy of Sciences of the United States of America* **104**: 15572–15577.
- DeWitt, G., Richards, J., Mohnen, D., and Jones, A.M. (1999). Comparative compositional analysis of walls with two different morphologies: archetypical versus transfer cell like. *Protoplasma* **209**: 238–245.
- Dibley, S.J., Zhou, Y., Andriunas, F.A., Talbot, M.J., Offler, C.E., Patrick, J.W., et al. (2009). Early gene expression programs accompanying trans-differentiation of epidermal cells of *V. faba* cotyledons into transfer cells. *New Phytologist* **182**: 863–877.
- Dietz, K.J., Vogel, M.O., and Viehhauser, A. (2010). AP2/EREBP transcription factors are part of gene regulatory networks and integrate metabolic, hormonal and environmental signals in stress acclimation and retrograde signalling. *Protoplasma* **245**: 3-14.

- Doblin, M.S., Pettolino, F., and Bacic, A. (2010). Plant cell walls: the skeleton of the plant world. *Functional Plant Biology* **37**: 357–381.
- Doblin, M.S., Johnson, K.L., Humphries, J., Newbigin, E.J., and Bacic, A. (2014). Are designer plant cell walls a realistic aspiration or will the plasticity of the plant's metabolism win out? *Current Opinion in Biotechnology* **26**: 108–114. 10.1016/j.copbio.2013.11.012.
- Dorn, K.M., Fankhauser, J.D., and Marks, M.D. (2013). *De novo* assembly of the pennycress (*Thalaspis arvense*) transcriptome provides tools for the development of a winter cover crop and biodiesel feedstock. *Plant Journal* **75**: 1028–1038.
- Doyle, J.J., Doyle, J.L., Ballenger, J.A., and Palmer, J.D. (1996). The distribution and phylogenetic significance of a 50 kb chloroplast DNA inversion in the flowering plant family Leguminosae. *Molecular Phylogenetics and Evolution* **5**: 429–438.
- Duan, J., Xia, C., Zhao, G., Jia, J., and Kong, X. (2012). Optimizing *de novo* common wheat transcriptome assembly using short-read RNA-Seq data. *BMC Genomics* **13**: 392. doi: 10.1186/1471-2164-13-392.
- Dubos, C., Stracke, R., Grotewold, E., Weisshaar, B., Martin, C., and Lepiniec, L. (2010). MYB transcription factors in Arabidopsis. *Trends in Plant Science* **15**: 573–581.
- Duc, G. (1997). Faba bean (*Vicia faba* L.). *Field Crops Research* **53**: 99–109.
- Eamens, A., Wang, M.B., Smith, N.A., and Waterhouse P.M. (2008). RNA silencing in plants: yesterday, today, and tomorrow. *Plant Physiology* **147**: 456–68.
- Eamens, A.L., and Waterhouse, P.M. (2011). Vectors and methods for hairpin RNA and artificial microRNA-mediated gene silencing in plants. *Methods in Molecular Biology* **701**: 179–197.
- Eamens, A.L., McHale, M., and Waterhouse, P.M. (2014). The use of artificial micro RNA technology to control gene expression in *Arabidopsis thaliana*. *Methods in Molecular Biology* **1062**: 211–24. e
- Edwards, J., Martin, A.P., Andriunas, F., Offler, C.E., Patrick, J.W., and McCurdy, D.W. (2010). GIGANTEA is a component of a regulatory pathway determining wall ingrowth deposition in phloem parenchyma transfer cells of *Arabidopsis thaliana*. *The Plant Journal* **63**: 651–661.
- Egan, A.N., Schlueter, J., and Spooner, D.M. (2012). Application of next generation sequencing in plant biology. *American Journal of Botany* **99**: 175–185.
- Ellwood, S.R., Phan, H.T.T., Jordan, M., Hane, J., Torres, A.M., Avila, C.M., et al. (2008). Construction of a comparative genetic map in faba bean (*Vicia faba* L.); conservation of genome structure with *Lens culinaris*. *BMC Genomics* **9**: 380. 10.1186/1471-2164-9-380.

- El-Rodeny, W., Kimura, M., Hirakawa, H., Sabah, A., Shirasawa, K., Sato, S., et al. (2014). Development of EST-SSR markers and construction of a linkage map in faba bean (*Vicia faba*). *Breeding Science* **64**: 252–263. doi: 10.1270/jsbbs.64.252
- Esch, J.J., Chen, M.A., Hillestad, M., and Marks, M.D. (2004). Comparison of TRY and the closely related At1g01380 gene in controlling *Arabidopsis* trichome patterning. *Plant Journal* **40**: 860–869.
- Farley, S.J., Patrick, J.W., and Offler, C.E. (2000). Functional transfer cells differentiate in cultured cotyledons of *V. faba* L. seeds. *Protoplasma* **214**: 102–117.
- Fellè, H.H., Hanstein, S., Steinmeyer, R., and Hedrich, R. (2000). Dynamics of ionic activities in the apoplast of the sub-stomatal cavity of intact *Vicia faba* leaves during stomatal closure evoked by ABA and darkness. *Plant Journal* **24**: 297–304. doi: 10.1046/j.1365-313x.2000.00878.x.
- Fowler, S., Lee, K., Onouchi, H., Samach, A., Richardson, K., Coupland, G., and Putterill, J. (1999). GIGANTEA: a circadian clock-controlled gene that regulates photoperiodic flowering in *Arabidopsis* and encodes a protein with several possible membrane-spanning domains. *EMBO Journal* **18**: 4679–4688.
- Franssen, S.U., Shrestha, R.P., Brautigam, A., Bornberg-Bauer, E., and Weber A.P.M. (2011). Comprehensive transcriptome analysis of the highly complex *Pisum sativum* genome using next generation sequencing. *BMC Genomics* **12**: 227. doi: 10.1186/1471-2164-12-227.
- Fry, S.C. (1992). Oxidative scission of plant cell wall polysaccharides by ascorbate-induced hydroxyl radicals. *Biochemical Journal* **332**: 507–515.
- Fukuda, M., Hasezawa, S., Asai, N., Nakajima, N., and Kondo, N. (1998). Dynamic organization of microtubules in guard cells of *Vicia faba* L. with diurnal cycle. *Plant and Cell Physiology* **39**: 80–86.
- Gamalei, Y.V. (1989). Structure and function of leaf minor veins in trees and herbs. A Taxonomic review. *Trees* **3**: 96–110.
- Gamalei, Y.V. (2007). The role of mesophyll cell tonoplast in determining the route of phloem loading. Thirty years of the studies of phloem loading. *Russian Journal of Plant Physiology* **54**: 1–9.
- Garg, R., Patel, R. K., Jhanwar, S., Priya, P., Bhattacharjee, A., Yadav, G., et al. (2011b). Gene discovery and tissue-specific transcriptome analysis in chickpea with massively parallel pyrosequencing and web resource development. *Plant Physiology* **156**: 1661–1678. doi: 10.1104/pp.111.17861.
- Garg, R., Patel, R.K., Tyagi, A.K., and Jain, M. (2011a). *De novo* assembly of chickpea transcriptome using short reads for gene discovery and marker identification. *DNA Research* **18**: 53–63.

- Gayral, P., Weinert, L., Chiari, Y., Tsagkogeorga, G., Ballenghien, M., and Galtier N (2011). Next-generation sequencing of transcriptomes: a guide to RNA isolation in non-model animals. *Molecular Ecology Resources* **11**: 650–661. 10.1111/j.1755-0998.2011.03010.x.
- Gheysen, G. and Fenoll, C. (2002). Gene expression in nematode feeding sites. *Annual Review of Phytopathology* **40**: 191–219.
- Ghosh, J.S., Chaudhuri, S., Dey, N.M and Pal, A. (2013). Functional characterization of a serine-threonine protein kinase from *Bambusa balcooa* that implicates in cellulose overproduction and superior quality fiber formation. *BMC Plant Biology* **13**: 128; doi:10.1186/1471-2229-13-128.
- Golinowski, W., Grundler, F.M.W., and Sobczak, M. (1996). Changes in the structure of *Arabidopsis thaliana* during female development of the plant-parasitic nematode *Heterodera schachtii*. *Protoplasma* **194**: 103–116.
- Gómez, E., Royo, J., Guo, Y., Thompson, R., and Hueros, G. (2002). Establishment of cereal endosperm expression domains: Identification and properties of a maize transfer cell-specific transcription factor, ZmMRP-1. *Plant Cell* **14**: 599–610.
- Gómez, E., Royo, J., Muñiz, L.M., Sellam, O., Paul, W., Gerentes, D., et al. (2009). The maize transcription factor myb-related protein-1 is a key regulator of the differentiation of transfer cells. *Plant Cell* **21**: 2022–2035.
- Gottwald, J.R., Krysan, P.J., Young, J.C., Evert, R.F., and Sussman, M.R. (2000). Genetic evidence for the in planta role of phloem-specific plasma membrane sucrose transporters. *Proceedings of the National Academy of Sciences of the United States of America* **97**: 13979–13984.
- Gotz, S., Garcia-Gómez, J.M., Terol, J., Williams, T.D., Nagaraj, S.H., Nueda, M.J., et al. (2008). High-throughput functional annotation and data mining with the Blast2GO suite. *Nucleic Acids Research* **36**: 3420–3435. doi: 10.1093/nar/gkn176.
- Grunewald, W., De Smet, I., Lewis, D.R., Lofke, C., Jansen, L., Goeminne, G. et al. (2012). Transcription factor WRKY23 assists auxin distribution patterns during *Arabidopsis* root development through local control on flavonol biosynthesis. *Proceedings of the National Academy of Sciences of the United States of America* **109**: 1554–1559.
- Grunewald, W., Karimi, M., Wieczorek, K., Van de Cappelle, E., Wischnitzki, E., Grundler, F., et al. (2008). A role for AtWRKY23 in feeding site establishment of plant-parasitic nematodes. *Plant Physiology* **148**: 358–368.
- Gunning, B.E.S., and Pate, J.S. (1974). “Transfer cells”, in *Dynamic Aspects of Plant Ultrastructure*, ed. A.W. Robards (London: McGraw-Hill), 441–479.

- Gunning, B., Pate, J., and Briarty, L. (1968). Specialized “transfer cells” in minor veins of leaves and their possible significance in phloem translocation. *The Journal of Cell Biology* **37**: C7–12.
- Gunning, B., Pate, J., Minchin, F., and Marks, I. (1974). Quantitative aspects of transfer cell structure in relation to vein loading in leaves and solute transport in legume nodules. *Symposia of the Society for Experimental Biology Journal* **28**: 87–126.
- Gunning, B.E.S. (1977). Transfer cells and their roles in transport of solutes in plants. *Science Progress* **64**: 539–568.
- Gunning, B.E.S., and Pate, J.S. (1969). Transfer cells: plant cells with wall ingrowths, specialized in relation to short distance transport of solutes - their occurrence, structure, and development. *Protoplasma* **68**: 107–33.
- Guo, S.G., Zheng, Y., Joung, J.G., Liu, S.Q., Zhang, Z.H., Crasta, O.R., et al. (2010). Transcriptome sequencing and comparative analysis of cucumber flowers with different sex types. *BMC Genomics* **11**: 384. doi: 10.1186/1471-2164-11-384.
- Gutierrez-Marcos, J.F., Costa, L.M., Biderre-Petit, C., Khbaya, B., O'Sullivan, D.M., Wormald, M., et al. (2004). Maternally expressed gene1 is a novel maize endosperm transfer cell-specific gene with a maternal parent-of- origin pattern of expression. *Plant Cell* **16**: 1288–1301.
- Hackel, A., Schauer, N., Carrari, F., Fernie, A.R., Grimm, B., and Kühn, C. (2006). Sucrose transporter LeSUT1 and LeSUT2 inhibition affects tomato fruit development in different ways. *The Plant Journal* **45**: 180–192.
- Hafke, J.B., Höll, S., Kühn, C., and van Bel, A. (2013). Electrophysiological approach to determine kinetic parameters of sucrose uptake by single sieve elements or phloem parenchyma cells in intact *Vicia faba* plants. *Frontiers in Plant Science* **4**: 274. doi: 10.3389/fpls.2013.00274.
- Hardham, A.R. (1976). Structural aspects of the pathway of nutrient flow to the developing embryo and cotyledons of *Pisum sativum* L. *Australian Journal of Botany* **24**: 711–721.
- Hardie, D.G. (1999). Plant protein serine/threonine kinases: Classification and function. *Annual Review of Plant Physiology and Plant Molecular Biology*. **50**: 97-131.
- Haritatos, E., Medville, R., and Turgeon, R. (2000). Minor vein structure and sugar transport in *Arabidopsis thaliana*. *Planta* **211**: 105–111.
- Harrington, G.N., Dibley, K.E., Ritchie, R.J., Offler, C.E., and Patrick, J.W. (2005). Hexose uptake by developing cotyledons of *Vicia faba*: Physiological evidence for transporters of differing affinities and specificities. *Functional Plant Biology* **32**: 987–995.

- Harrington, G.N., Nussbaumer, Y., Wang, X-D., Tegeder, M., Franceschi, V.R., Frommer, W.B., et al. (1997). Spatial and temporal expression of sucrose transport-related genes in developing cotyledons of *Vicia faba* L. *Protoplasma* **200**: 35–50.
- Henkel, C.V., Dirks, R.P., and De Wijze, D.L. (2012). First draft genome sequence of the Japanese eel, *Anguilla japonica*. *Gene* **511**: 195–201. doi: 10.1016/j.gene.2012.09.064.
- Henry, Y., and Steer, M.W. (1980). A re-examination of the induction of phloem transfer cell development in pea leaves (*Pisum sativum*). *Plant, Cell & Environment* **3**: 377–380.
- Holthaus, U., and Schmitz, K. (1991). Distribution and immunolocalization of stachyose synthase in *Cucumis melo* L. *Planta* **185**: 479–486.
- Hu, Y., Chen, L., Wang, H., Zhang, L., Wang, F. and Yu, D. (2013) Arabidopsis transcription factor WRKY8 functions antagonistically with its interacting partner VQ9 to modulate salinity stress tolerance. *Plant Journal* **74**: 730–745.
- Hueros, C., Gómez, E., Cheikh, N., Edwards, J., Weldon, M., Salamini, F., et al. (1999). Identification of a promoter sequence from the BETL1 gene cluster able to confer transfer-cell-specific expression in transgenic maize. *Plant Physiology* **121**: 1143–1152.
- Hueros, G., Varotto, S., Salamini, F., and Thompson, R.D. (1995). Molecular characterization of bet1, a gene expressed in the endosperm transfer cells of maize. *Plant Cell* **7**: 747–757.
- Inzé, A., Vanderauwera, S., Hoerberichts, F.A., Vandorpe, M., Van Gaever, T., and Van Breusegem, F. (2012). A subcellular localization compendium of hydrogen peroxide-induced proteins. *Plant Cell Environment* **35**: 308–320.
- Ishida, T., Adachi, S., Yoshimura, M., Shimizu, K., Umeda, M., and Sugimoto, K. (2010). Auxin modulates the transition from the mitotic cycle to the endocycle in Arabidopsis. *Development* **137**: 63–71.
- Iwase, A., Mitsuda, N., Koyama, T., Hiratsu, K., Kojima, M., Arai, T., et al. (2011). The AP2/ERF transcription factor WIND1 controls cell dedifferentiation in Arabidopsis. *Current Biology* **21**: 508–514.
- Ji, H., Gheysen, G., Denil, S., Lindsey, K., Topping, J.F., Nahar, K., et al. (2013). Transcriptional analysis through RNA sequencing of giant cells induced by *Meloidogyne graminicola* in rice roots. *Journal of Experimental Botany* **64**: 3885–98.
- Jiang, L., Schlesinger, F., Davis, C.A., Zhang, Y., Li, R., et al. (2011). Synthetic spike-in standards for RNA-seq experiments. *Genome Research* **21**: 1543–1551.

- Jones, M.G.K., and Gunning, B.E.S. (1976). Transfer cells and nematode-induced giant-cells in *Helianthemum*. *Protoplasma* **87**: 273–279.
- Joshi, P.A., Caetano-Anolles, G., Graham, E.T., and Gresshoff, P.M. (1993). Ultrastructure of transfer cells in spontaneous nodules of alfalfa (*Medicago sativa*). *Protoplasma* **172**: 64–76.
- Juge, N., Payan, F., and Williamson, G. (2004). XIP-I, a xylanase inhibitor protein from wheat: a novel protein function *Biochimica et Biophysica Acta* **1696**: 203–211.
- Kaiser, B.N., Rawat, S.R., Siddiqi, M.Y., Masle, J., and Glass, A.D.M. (2002). Functional analysis of an Arabidopsis T-DNA “knockout” of the high-affinity NH<sub>4</sub><sup>+</sup> transporter AtAMT1;1. *Plant Physiology* **130**: 1263–1275.
- Kang, J., Mizukami, Y., Wang, H., Fowke, L., and Dengler, N.G. (2007). Modification of cell proliferation patterns alters leaf vein architecture in *Arabidopsis thaliana*. *Planta* **226**: 1207–1218.
- Kaplan-Levy, R.N., Brewer, P.B., Quon, T., and Smyth, D.R. (2012). The trihelix family of transcription factors – light, stress and development. *Trends in Plant Science* **17**: 163–171.
- Kaur, S., Pembleton, L.W., Cogan, N.O., Savin, K.W., Leonforte, T., and Paull, J. (2012). Transcriptome sequencing of field pea and faba bean for discovery and validation of SSR genetic markers. *BMC Genomics* **13**: 104. doi: 10.1186/1471-2164-13-104.
- Kirik, V., Schnittger, A., Radchuk, V., Adler, K., Hulskamp, M. and Baumlein, H. (2001). Ectopic expression of the *Arabidopsis* AtMYB23 gene induces differentiation of trichome cells. *Developmental Biology* **235**: 366–377.
- Kondou, Y., Higuchi, M., and Matsui, M. (2010). High-throughput characterization of plant gene functions by using gain-of-function technology. *Annual Review of Plant Biology* **61**: 373–393.
- Koornneef, M., and Meinke, D. (2010). The development of Arabidopsis as a model plant. *Plant Journal* **61**: 909–921.
- Koryachko, A., Matthiadis, A., Ducoste, J.J., Tuck, J., Long, T.A., and Williams, C. (2015). Computational approaches to identify regulators of plant stress response using high-throughput gene expression data. *Current Plant Biology* **3-4**: 20–29.
- Krysan, P.J., Young, J.C., and Sussman, M.R. (1999). T-DNA as an insertional mutagen in Arabidopsis. *Plant Cell* **11**: 2283 – 2290.
- Kubo, M., Udagawa, M., Nishikubo, N., Horiguchi, G., Yamaguchi, M., Ito, J., et al. (2005). Transcription switches for protoxylem and metaxylem vessel formation. *Genes & Development* **19**: 1855–1860.

- Kühn, C., and Grof, C.P.L. (2010). Sucrose transporters of higher plants. *Current Opinion in Plant Biology* **13**: 287–297.
- Lalonde, S., Tegeder, M., Throne-Holst, M., Frommer, W.B., and Patrick, J.W. (2003). Phloem loading and unloading of sugars and amino acids. *Plant Cell and Environment* **26**: 37–56.
- Lalonde, S., Wipf, D., and Frommer, W.B. (2004). Transport mechanisms for organic forms of carbon and nitrogen between source and sink. *Annual Review of Plant Biology* **55**: 341–372.
- Largo-Gosens, A., Hernández-Altamirano, M., García-Calvo, L., Alonso-Simón, A., Álvarez, J., and Acebes, J.L. (2014). Fourier transform mid infrared spectroscopy applications for monitoring the structural plasticity of plant cell walls. *Frontiers in Plant Science* **5**: 303. doi: 10.3389/fpls.2014.00303.
- Lehnert, E.M., and Walbot, V. (2014). Sequencing and *de novo* assembly of a *Dahlia* hybrid cultivar transcriptome. *Frontiers in Plant Science* **5**: 340. doi:10.3389/fpls.2014.00340.
- Li, J. (2014). Role of WRKY transcription factors in Arabidopsis development and stress responses. PhD Thesis. University of Helsinki, Finland.
- Liang, X., and Joshi, C.P. (2004). Molecular cloning of ten distinct hypervariable regions from cellulose synthase gene superfamily in aspen trees. *Tree Physiology* **24**: 543–550.
- Libault, M., Joshi, T., Benedito, V. A., Xu, D., Udvardi, M. K., and Stacy, G. (2009). Legume transcription factor genes: what makes legumes so special. *Plant Physiology* **151**: 991-1001. doi: 10.1104/pp.109.144105.
- Liepmann, A.H., Wightman, R., Geshi, N., Turner, S.R., and Scheller, H.V. (2010). Arabidopsis: a powerful model system for plant cell wall research. *Plant Journal* **6**: 1107–1121.
- Ligrone, R., and Gambardella, R. (1988). The sporophyte-gametophyte junction in bryophytes. *Advanced Bryology* **3**: 225–274.
- Lin Z-J.D., Liebrand T.W.H., Yadeta, K.A., and Coaker, G.L. (2015). PBL13 is a serine/threonine protein kinase that negatively regulates Arabidopsis immune response. *Plant Physiology* **169**: 2950–62.
- Liu Q., Wen C., Zhao H., Zhang L., Wang J., Wang Y. (2014). RNA-Seq reveals leaf cuticular wax-related genes in welsh onion. *PLoS ONE* **9**: e113290. doi:10.1371/journal.pone.0113290.
- Liu, T., Zhu, S., Tand, Q., Chen, P., Yu, Y., and Tang, S. (2013). *De novo* assembly and characterization of transcriptome using Illumina paired-end sequencing and

- identification of CesaA gene in ramie (*Boehmeria nivea* L. Gaud). *BMC Genomics* **14**: 125. DOI: 10.1186/1471-2164-14-125
- Lucas W.J., Groover A., Lichtenberger R., Furuta K., Yadav S.R., Helariutta Y., et al. (2013). The plant vascular system: evolution, development and functions. *Journal of Integrative Plant Biology* **55**: 294–388.
- Maeda, H., Sage, T.L., Isaac, G., Welti, R., and DellaPenna, D. (2008). Tocopherols modulate extraplastidic polyunsaturated fatty acid metabolism in *Arabidopsis* at low temperature. *Plant Cell* **20**: 452–470.
- Maeda, H., Song, W., Sage, T., and DellaPenna, D. (2014). Role of callose synthases in TC wall development in tocopherol deficient mutants. *Frontiers in Plant Science* **5**: 46.
- Maeda, H., Song, W., Sage, T.L., and DellaPenna, D. (2006). Tocopherols play a crucial role in low-temperature adaptation and phloem loading in *Arabidopsis*. *Plant Cell* **18**: 2710–2732.
- Mantello, C. C., Cardoso-Silva, C.B., Da Silva, C.C., De Souza, L.M., Scaloppi Junior, E. J., Goncalves, P. S., et al. (2014). *De novo* assembly and transcriptome analysis of the rubber tree (*Hevea brasiliensis*) and SNP markers development for rubber biosynthesis pathways. *PLoS ONE* **9**: e102665. doi: 10.1371/journal.pone.0102665.
- Martin, A.P., Palmer, W.M., Byrt, C.S., Furbank, R.T., and Grof, C.P.L. (2013). A holistic high-throughput screening framework for biofuel feedstock assessment that characterizes variations in soluble sugars and cell wall composition in *Sorghum bicolor*. *Biotechnology for Biofuels* **6**: 186.
- Martin, L.B.B., Fei, Z., Giovannoni, J.J. and Rose, J.K.C. (2013). Catalyzing plant science research with RNA-seq. *Frontiers in Plant Science* **4**: 66. doi: 10.3389/fpls.2013.00066.
- McCarthy, D.J., and Smyth, G.K. (2009). Testing significance relative to a fold-change threshold is a TREAT. *Bioinformatics* **25**: 765–771.
- McCarthy, R. L., Zhong, R., and Ye, Z. H. (2009). MYB83 is a direct target of SND1 and acts redundantly with MYB46 in the regulation of secondary cell wall biosynthesis in *Arabidopsis*. *Plant and Cell Physiology* **50**: 1950–1964.
- McCurdy, D.W. (2015). “Transfer cells: novel cell types with unique wall ingrowth architecture designed for optimal nutrient transport” in *Plant Cell Wall Patterning and Cell Shape*, ed. H. Fukuda (Hoboken, New Jersey: Wiley-Blackwell), 287–317.
- McCurdy, D.W., Patrick, J.W., and Offler, C.E. (2008). Wall ingrowth formation in transfer cells: novel examples of localized wall deposition in plant cells. *Current Opinion in Plant Biology* **11**: 653–661.

- McDonald, R., Fieuw, S., and Patrick, J.W. (1996). Sugar uptake by the dermal transfer cells of the developing cotyledons of *V. faba* L.: mechanism of energy coupling. *Planta* **198**: 502–509.
- Mehrnia, M., Balazadeh, S., Zanon, M-I., and Mueller-Roeber, B. (2013). EBE, an AP2/ERF transcription factor highly expressed in proliferating cells, affects shoot architecture in Arabidopsis. *Plant Physiology* **162**: 842–857.
- Meinke, D.W., Cherry, J.M., Dean, C., Rounsley, S.D., and Koornneef, M. (1998). *Arabidopsis thaliana*: A model plant for genome analysis. *Science* **282**: 662.
- Meyer, E., Logan, T.L., and Juenger, T.E. (2012). Transcriptome analysis and gene expression atlas for *Panicum hallii* var. *filipes*, a diploid model for biofuel research. *Plant Journal* **70**: 879–890. doi: 10.1111/j.1365-313X.2012.04938.x.
- Meyer, S., Melzer, M., Truernit, E., Hümmer, C., Besenbeck, R., Stadler, R., et al. (2000). *AtSUC3*, a gene encoding a new *Arabidopsis* sucrose transporter, is expressed in cells adjacent to the vascular tissue and in a carpel cell layer. *Plant Journal* **24**: 869–882.
- Mims, C.W., Rodriguez-Lothar, C., and Richardson, E.A. (2001). Ultrastructure of the host-parasite interaction in leaves of *Duchesnea indica* infected by the rust fungus *Frommeela mexicana* var. *indicae* as revealed by high pressure freezing. *Canadian Journal of Botany-Revue Canadienne De Botanique* **79**: 49–57.
- Mitra, P.P, and Loqué, D. (2014). Histological staining of Arabidopsis thaliana secondary cell wall elements. *Journal of Visualized Experiments* **87**: e51381.
- Mitsuda, N., and Ohme-Takagi, M. (2009). Functional analysis of transcription factors in Arabidopsis. *Plant and Cell Physiology* **50**: 1232–1248.
- Mitsuda, N., Iwase, A., Yamamoto, H., Yoshida, M., Seki, M., Shinozaki, K., et al. (2007). NAC transcription factors, NST1 and NST3, are key regulators of the formation of secondary walls in woody tissues of Arabidopsis. *Plant Cell* **19**: 270–280.
- Mitsuda, N., Seki, M., Shinozaki, K., and Ohme-Takagi, M. (2005). The NAC transcription factors NST1 and NST2 of *Arabidopsis* regulate secondary wall thickenings and are required for anther dehiscence. *Plant Cell* **17**: 2993–3006.
- Mizrachi, E., Hefer, C.A., Ranik, M., Joubert, F., and Myburg, A.A. (2010). *De novo* assembled expressed gene catalog of a fast-growing Eucalyptus tree produced by Illumina mRNA-Seq. *BMC Genomics* **11**: 681. doi: 10.1186/1471-2164-11-681.
- Moreton, J., Dunham, S.P., and Emes, R.D. (2014). A consensus approach to vertebrate *de novo* transcriptome assembly from RNA-Seq data: assembly of the duck (*Anas platyrhynchos*) transcriptome. *Frontiers in Genetics* **5**: 190.

- Mortazavi, A., Williams, B.A., McCue, K., Schaeffer, L., and Wold, B. (2008). Mapping and quantifying mam-malian transcriptomes by RNA-Seq. *Nature Methods* **5**: 621–628.
- Motose, H., Fukuda, H., and Sugiyama, M. (2001). Involvement of local intercellular communication in the differentiation of zinnia mesophyll cells into tracheary elements. *Planta* **213**: 121–31.
- Mouille, G., Robin, S., Lecomte, M., Pagant, S., and Hofte, H. (2003). Classification and identification of Arabidopsis cell wall mutants using Fourier-transform infrared (FT-IR) microspectroscopy. *Plant Journal*. **35**: 393–404.
- Mukherjee, K., and Brocchieri, L. (2010). Evolution of Plant Homeobox Genes. *eLS*.
- Mullineaux, P.M., Karpinski, S., and Baker, N.R. (2006). Spatial dependence for hydrogen peroxide-directed signaling in light-stressed plants. *Plant Physiology* **141**: 346-350.
- Muniz, L.M., Royo, J., Gómez, E., Barrero, C., Bergareche, D., and Hueros, G. (2006). The maize transfer cell-specific type-A response regulator ZmTCRR-1 appears to be involved in intercellular signaling. *Plant Journal* **48**: 17–27.
- Muñiz, L.M., Royo, J., Gómez, E., Baudot, G., Paul, W., Hueros G., et al. (2010). Atypical response regulators expressed in the maize endosperm transfer cells link canonical two component system and seed biology. *BMC Plant Biology* **10**: 84 10.1186/1471-2229-10-84.
- Mustilli, A-C., Merlot, S., Vavasseur, A., Fenzi, F., and Giraudat, J. (2002). Arabidopsis OST1 protein kinase mediates the regulation of stomatal aperture by abscisic acid and acts upstream of reactive oxygen species production. *Plant Cell* **14**: 3089–99.
- Nakano, Y., Nishikubo, N., Goué, N., Ohtani, M., Yamaguchi, M., Katayama, Y., et al. (2010). MYB transcription factors orchestrating the developmental program of xylem vessels in Arabidopsis roots. *Plant Biotechnology Journal* **27**: 267–272.
- Nakano, Y., Yamaguchi, M., Endo, H., Rejab, N.A., and Ohtani M. (2015). NAC-MYB-based transcriptional regulation of secondary cell wall biosynthesis in land plants. *Frontiers in Plant Science* **6**: 288. 10.3389/fpls.2015.00288.
- Nelson, D.L., and Cox, M.M. (2005). *Lehninger Principles of Biochemistry* (4th ed.). W. H. Freeman. ISBN 978-0-7167-4339-2.
- Nguyen, S.T. and McCurdy, D. (2015). High-resolution confocal imaging of wall ingrowth deposition in plant transfer cells: Semi-quantitative analysis of phloem parenchyma transfer cell development in leaf minor veins of Arabidopsis. *BMC Plant Biology* **15**: 1–14.
- Nguyen, T.T.S., and McCurdy, D.W. (2016). “Transdifferentiation – a plant perspective” in *Molecular Cell Biology of the Growth and Differentiation of Plant Cells*, ed. R.J.

- Rose (Boca Raton: CRC Press), in press.
- O'Rourke, J.A., Yang, S.S., Miller, S.S., Bucciarelli, B., Liu, J., Rydeen, A., et al. (2013). An RNA-Seq transcriptome analysis of orthophosphate-deficient white lupin reveals novel insights into phosphorus acclimation in plants. *Plant Physiology* **161**: 705–724.
- Offler, C.E., Liet, E., and Sutton, E.G. (1997). Transfer cell induction in cotyledons of *Vicia faba* L. *Protoplasma* **200**: 51–64.
- Offler, C.E., McCurdy, D.W., Patrick, J.W., and Talbot, M.J. (2003). Transfer cells: Cells specialized for a special purpose. *Annual Review of Plant Biology* **54**: 431–454.
- Offler, C.E., Nerlich., and Patrick, J.W. (1989). Pathway of photosynthate transfer in the developing seed of *V. faba* L. transfer in relation to seed anatomy. *Journal of Experimental Botany*, **40**: 769–780.
- Oparka, K.J. (1990). What is phloem unloading. *Plant Physiology* **94**: 393–396.
- Oparka, K.J., and Turgeon, R. (1999). Sieve elements and companion cells-traffic control centers of the phloem. *Plant Cell* **11**: 739–50.
- Osorio, M.B., Bucker-Neto, L., Castilhos, G., Turchetto-Zolet, A.C., Wiebke-Strohm, B., Bodanese-Zanettini, M.H., et al. (2012). Identification and in silico characterization of soybean trihelix-GT and bHLH transcription factors involved in stress responses. *Genetics and Molecular Biology* **35**: 233-246.
- Park, C., Kim, M.L., Kang, Y.H., Jeon, J.M., Yoo, J.H., Kim, M.C., et al. (2004). Pathogen- and NaCl-induced expression of the SCaM-4 promoter is mediated in part by a GT-1 box that interacts with a GT-1-like transcription factor. *Plant Physiology* **135**: 2150–2161.
- Parra-González, L., Aravena-Abarzúa, G., Navarro-Navarro, C., Udall, J., Maughan, J., Peterson, L. M., et al. (2012). Yellow lupin (*Lupinus luteus* L.) transcriptome sequencing: molecular marker development and comparative studies. *BMC Genomics* **13**: 425. doi: 10.1186/1471-2164-13-425.
- Pate, J.S., and Gunning, B.E.S. (1969). Vascular transfer cells in angiosperm leaves. A taxonomic and morphological survey. *Protoplasma* **68**: 135–156.
- Pate, J.S., and Gunning B.E.S. (1972). Transfer cells. *Annual Review of Plant Physiology* **23**: 173.
- Patrick, J.W. (1997). Phloem unloading: Sieve element unloading and post-sieve element transport. *Annual Review of Plant Physiology and Plant Molecular Biology* **48**: 191–222.
- Patrick, J.W., and Offler, C.E. (2001). Compartmentation of transport and transfer events in developing seeds. *Journal of Experimental Botany* **52**: 551–564.

- Pearson, W.R. (2013). An introduction to sequence similarity (“homology”) searching. *Current Protocols in Bioinformatics* **42**: 3.1.1–3.1.8. doi: 10.1002/0471250953.bi0301s42.
- Peremyslov, V.V., Cole, R.A., Fowler, J.E., and Dolja, V.V. (2015). Myosin-powered membrane compartment drives cytoplasmic streaming, cell expansion and plant development. *PLoS One* **10**: e0139331. doi: 10.1371/journal.pone.0139331. eCollection 2015.
- Perez-Rodriguez, P., Riano-Pachon, D.M., Correa L.G.G., Stefan A., Rensing S.A., Kersten, B., et al. (2009). PlnTFDB: updated content and new features of the plant transcription factor database. *Nucleic Acids Research* **38**: 822. doi: 10.1093/nar/gkp805.
- Persson, S., Paredez, A., Carroll, A., Palsdottir, H., Doblin, M., Poindexter, P., et al. (2007). Genetic evidence for three unique components in primary cell-wall cellulose synthase complexes in Arabidopsis. *Proceedings of the National Academy of Sciences of the United States of America* **104**: 15566–15571.
- Pigeaire, A., Abernethy, D., Smith, P.M., Simpson, K., Fletcher, N., Lu, C-Y., et al., (1997). Transformation of a grain legume (*Lupinus angustifolius* L.) via *Agrobacterium tumefaciens*-mediated gene transfer to shoot apices. *Molecular Breeding* **3**: 341–349.
- Pires, D.N., and Dolan, L. (2012). Morphological evolution in land plants: new designs with old genes. *Philosophical Transactions of the Royal Society B* **367**: 508–518;
- Portillo, M., Cabrera, J., Lindsey, K., Topping, J., Andres, M.F., Emiliozzi, M et al. (2013). Distinct and conserved transcriptomic changes during nematode-induced giant cell development in tomato compared with Arabidopsis: a functional role for gene repression. *New Phytologist* **197**: 1276–1290.
- Prigge, M.J., Otsuga, D., Alonso, J.M., Ecker, J.R., Drews, G.N., and Clark, S.E. (2005). Class III homeodomain-leucine zipper gene family members have overlapping, antagonistic, and distinct roles in Arabidopsis development. *Plant Cell* **17**: 61–76.
- Pugh, D.A., Offler, C.E., Talbot, M.J., and Ruan, Y-L. (2010). Evidence for the role of TCs in the evolutionary increase in seed and fiber biomass yield in cotton. *Molecular Plant* **3**: 1075–1086.
- Rae, A.L., Perroux, J.M., and Grof, C.P.L. (2005). Sucrose partitioning between vascular bundles and storage parenchyma in the sugarcane stem: A potential role for the ShSUT1 sucrose transporter. *Planta* **220**: 817–825.
- Raven, P.H., Evert, R.F., and Eichhorn, S.E. (1999). Biology of Plants. In, Ed 6. New York: W.H. Freeman and Company.

- Remy E., and Duque, P. (2014). Beyond cellular detoxification: A plethora of physiological roles for MDR transporter homologs in plants. *Frontiers in Physiology* **5**: 201.
- Robert, P., Jamme, F., Barron, C., Bouchet, B., Saulnier, L., Dumas, P., et al. (2011). Change in wall composition of transfer and aleurone cells during wheat grain development. *Planta* **233**: 393–406 10.1007/s00425-010-1306-1307
- Roberts, A.G., and Oparka, K.J. (2003). Plasmodesmata and the control of symplastic transport. *Plant Cell and Environment* **26**: 103–124.
- Roberts, A.W., Frost, A.O., Roberts, E.M., and Haigler, C.H. (2004). Roles of microtubules and cellulose microfibril assembly in the localization of secondary-cell-wall deposition in developing tracheary elements. *Protoplasma* **224**: 217–229.
- Rocha, S., Monjardino, P., Mendonça, D., Machado, A.C., Fernandes, R., Sampaio, P., et al. (2014). Lignification of developing maize (*Zea mays* L.) endosperm transfer cells and starchy endosperm cells. *Frontiers in Plant Science* **5**: 102. doi: 10.3389/fpls.2014.00102.
- Roessner, U., Patterson, J.H., Forbes, M.G., Fincher, G.B., Langridge, P., and Bacic, A. (2006). An investigation of boron toxicity in barley using metabolomics. *Plant Physiology* **142**: 1087–1101. 10.1104/pp.106.084053.
- Royo J., Gómez E., Barrero C., Muniz L.M., Sanz Y., and Hueros G. (2009). Transcriptional activation of the maize endosperm transfer cell-specific gene BETL1 by ZmMRP-1 is enhanced by two C2H2 zinc finger-containing proteins. *Planta* **230**: 807–818. 10.1007/s00425-009-0987-2.
- Rushton, P.J., Somssich, I.E., Ringler, P., and Shen, Q.J. (2010). WRKY transcription factors. *Trends in Plant Science* **15**: 247-258. doi: 10.1016/j.tplants.2010.02.006.
- Sauer, N. (2007). Molecular physiology of higher plant sucrose transporters. *FEBS Letters* **581**: 2309–2317.
- Schaller, G.E., Kieber, J.J., and Shiu, S-H. (2008). Two-component signaling element and histidyl-aspartyl phosphorelays. *The Arabidopsis Book* doi: 10.1199/tab.0012.
- Scheres, B., van Engelen, F., van der Knaap, E., van de Wiel, C., van Ab, K., and Bisseling, T. (1990). Sequential induction of nodulin gene expression in the developing pea nodule. *Plant Cell* **2**: 687–700.
- Schikora, A., and Schmidt, W. (2001). Acclimative changes in root epidermal cell fate in response to Fe and P deficiency: a specific role for auxin? *Protoplasma* **218**: 67–75.
- Schikora, A., and Schmidt, W. (2002). Formation of transfer cells and H<sup>+</sup>-ATPase expression in tomato roots under P and Fe deficiency. *Planta* **215**: 304–311.

- Schmid, M., Davison, T.S., Henz, S.R., Pape, U.J., Demar, M., et al. (2005). A gene expression map of *Arabidopsis thaliana* development. *Nature Genetics* **37**: 501–506.
- Schmutz, J., Cannon, S.B., and Schlueter, J. (2010). Genome sequence of the palaeopolyploid soybean. *Nature* **463**: 178–183. doi: 10.1038/nature08670.
- Schopfer, P. (2002). Hydroxyl radical-induced cell-wall loosening in vitro and in vivo: implications for the control of elongation growth. *Plant Journal* **28**: 679–688.
- Schroeder, J.I., Raschke K., and Neher, E. (1987). Voltage dependence of K<sup>+</sup> channels in guard-cell protoplasts. *Proceedings of the National Academy of Sciences of the United States of America* **84**: 4108–4112.
- Schulz, A., and Thompson, G.A. (2009). Phloem structure and function. *Encyclopedia of Life Sciences*. 10.1002/9780470015902.a9780470001290.pub9780470015902.
- Shen, Q.H., Saijo, Y., Mauch, S., Biskup, C., Bieri, S., Keller, B., et al. (2007). Nuclear activity of MLA immune receptors links isolate-specific and basal disease-resistance responses. *Science* **315**: 1098–1103.
- Simon, P. (2003). Q-Gene: processing quantitative real-time RT-PCR data. *Bioinformatics* **19**: 1439–1440.
- Simon, S.A., Zhai, J., Nandety, R.S., McCormick, K.P., Zeng, J., Mejia, D., et al. (2009). Short-read sequencing technologies for transcriptional analyses. *Annual Review of Plant Biology* **60**: 305–333.
- Sjolund, R.D. (1997). The phloem sieve element: A river runs through it. *Plant Cell* **9**: 1137–1146.
- Slewinski, T.L., and Braun, D.M. (2010). Current perspectives on the regulation of whole-plant carbohydrate partitioning. *Plant Science* **178**: 341–349.
- Smita, S., Katiyar, A., Chinnusamy, V., Pandey, D.M., and Bansal, K.C. (2015). Transcriptional regulatory network analysis of MYB transcription factor family genes in rice. *Frontiers in Plant Science* **6**: 1157.
- Song, X., She, X., He, J., Huang, C., and Song, T. (2006). Cytokinin- and auxin-induced stomatal opening involves a decrease in levels of hydrogen peroxide in guard cells of *Vicia faba*. *Functional Plant Biology* **33**: 573–583 10.1071/FP05232.
- Srivastava, A.C., Ganesan, S., Ismail, I.O., and Ayre, B.G. (2009). Effective carbon partitioning driven by exotic phloem-specific regulatory elements fused to the *Arabidopsis thaliana* *AtSUC2* sucrose–proton symporter gene. *BMC Plant Biology* **9**: 7.
- Steinwand, B., and Kieber, J. (2010). The role of receptor-like kinases in regulating cell wall function. *Plant Physiology* **2010**: 479–484.

- Sun, W-Q., and Bassuk, N.L. (1993). Auxin-induced ethylene synthesis during rooting and inhibition of budbreak of ‘Royalty’ rose cuttings. *Journal of the American Society for Horticultural Science* **118**: 638–43.
- Sun, Y.G., Wang, B., Jin, S.H., Qu, X.X., Li, Y.J., and Hou, B.K. (2013) Ectopic expression of Arabidopsis glycosyltransferase UGT85A5 enhances salt stress tolerance in tobacco. *PLoS One* **8**: e59924.
- Sweetman, C, Wong, D.C., Ford, C.M., and Drew, D.P. (2012). Transcriptome analysis at four developmental stages of grape berry (*Vitis vinifera* cv. Shiraz) provides insights into regulated and coordinated gene expression. *BMC Genomics* **13**: 691.
- Taiz, L., and Zeiger, E. (2002). *Plant Physiology* (3<sup>rd</sup> edition). Sinauer associates, Inc. Sunderland, USA.
- Talbot, M.J., Franceschi, V.R., McCurdy, D.W., and Offler, C.E. (2001). Wall ingrowth architecture in epidermal transfer cells of *V. faba* cotyledons. *Protoplasma* **215**: 191–203.
- Talbot, M.J., Offler, C.E., and McCurdy, D.W. (2002). Transfer cell wall architecture: a contribution towards understanding localized wall deposition. *Protoplasma* **219**: 197–209.
- Talbot, M.J., Wasteneys, G., McCurdy, D.W., and Offler, C.E. (2007a). Deposition patterns of cellulose microfibrils in flange wall ingrowths of transfer cells indicate clear parallels with those of secondary wall thickenings. *Functional Plant Biology* **34**: 307–313.
- Talbot, M.J., Wasteneys, G.O., Offler, C.E., and McCurdy, D.W. (2007b). Cellulose synthesis is required for deposition of reticulate wall ingrowths in transfer cells. *Plant and Cell Physiology* **48**: 147–158.
- Taylor-Teeple, M., Lin, L., de Lucas, M., Turco, G., Toal, T. W., and Gaudinier, A. (2015). An *Arabidopsis* gene regulatory network for secondary cell wall synthesis. *Nature* **517**: 571–575. 10.1038/nature14099.
- Tegeder, M., Wang, X.D., Frommer, W.B., Offler, C.E., and Patrick, J.W. (1999). Sucrose transport into developing seeds of *Pisum sativum* L. *Plant Journal* **18**: 151–61.
- Thiel, J., Weier, D., Sreenivasulu, N., Strickert, M., Weichert, N., Melzer, M., Czauderna, T., Wobus, U., Weber, H., and Weschke, W. (2008). Different hormonal regulation of cellular differentiation and function in nucellar projection and endosperm transfer cells: a microdissection-based transcriptome study of young barley grains. *Plant Physiology* **148**: 1436–1452.
- Thiel, J. (2014). Development of endosperm transfer cells in barley. *Frontiers in Plant Science* **5**: 108. doi: 10.3389/fpls.2014.00108.

- Thiel, J., Hollmann, J., Rutten, T., Weber, H., Scholz, U., and Weschke, W. (2012a). 454 transcriptome sequencing suggests a role for two-component signaling in cellularization and differentiation of barley endosperm TCs. *PloS One* **7**: e41867-e41867.
- Thiel, J., Riewe, D., Rutten, T., Melzer, M., Friedel, S., Bollenbeck, F., Weschke, W., and Weber, H. (2012b). Differentiation of endosperm transfer cells of barley: a comprehensive analysis at the micro-scale. *Plant Journal* **71**: 639–655.
- Thompson, R.D., Hueros, D., Becker, H.A., and Maitz, M. (2001). Development and functions of seed transfer cells. *Plant Science* **160**: 775–783.
- Thorpe, M.R., Furch, A.C.U., Minchin, P.E.H., Föllner, J., van Bel, A.J.E., and Hafke, J.B. (2010). Rapid cooling triggers forisome dispersion just before phloem transport stops. *Plant Cell & Environment* **33**: 259–271. doi: 10.1111/j.1365-3040.2009.02079.x.
- Torres, A.M., Weeden, N.F., and Martin, A. (1993). Linkage among isozyme, RFLP and RAPD markers in *Vicia faba*. *Theoretical Applied Genetics* **85**: 937–945. doi: 10.1007/BF00215032.
- Truernit, E., and Sauer, N. (1995). The promoter of the *Arabidopsis thaliana* SUC2 sucrose-H<sup>+</sup> symporter gene directs expression of beta-glucuronidase to the phloem: evidence for phloem loading and unloading by SUC2. *Planta* **196**: 564-570.
- Truernit, E., Bauby, H., Dubreucq, B., Grandjean, O., Runions, J., Barthelemy, J., et al. (2008). High-resolution whole-mount imaging of three-dimensional tissue organization and gene expression enables the study of phloem development and structure in *Arabidopsis*. *Plant Cell* **20**: 1494–1503.
- Turchi, L., Carabelli, M., Ruzza, V., Possenti, M., Sassi, M., and Peñalosa, A. et al. (2013). *Arabidopsis* HD-Zip II transcription factors control apical embryo development and meristem function. *Development* **140**: 2118–2129.
- Turgeon, R., and Hepler, P.K. (1989). Symplastic continuity between mesophyll and companion cells in minor veins of mature *Cucurbita pepo* L. leaves. *Planta* **179**: 24–31.
- Turgeon, R., and Wolf, S. (2009). Phloem Transport: Cellular pathways and molecular trafficking. *Annual Review Plant Biology* **60**: 207–221.
- Turgeon, R., Beebe, D.U., and Gowan, E. (1993). The intermediary cell - minor-vein anatomy and raffinose oligosaccharide synthesis in the *Scrophulariaceae*. *Planta* **191**: 446–456.
- Tzafrir, I., Pena-Muralla, R., Dickerman, A., Berg, M., Rogers, R., Hutchens, S., et al. (2004). Identification of genes required for embryo development in *Arabidopsis*. *Plant Physiology* **135**: 1206–1220.

- Ueki, S., Magori, S., Lacroix, B., and Citovsky, V. (2013). Transient gene expression in epidermal cells of plant leaves by Biolistic DNA delivery. *Methods in Molecular Biology* **940**: 17–26.
- Unamba, C.I.N., Nag, A., and Sharma, R.K. (2015). Next generation sequencing technologies: the doorway to the unexplored genomics of non-model plants. *Frontiers in Plant Science* **6**: 1074.
- Van Bel, A.J.E. (1996) Interaction between sieve element and companion cell and the consequences for photoassimilate distribution: two structural hardware frames with associated physiological software packages in dicotyledons. *Journal of Experimental Botany* **47**: 1129–1140.
- Van-Bel, A.J.E. (2003). The phloem, a miracle of ingenuity. *Plant Cell and Environment* **26**: 125–149.
- Vaughn, K.C., Talbot, M.J., Offler, C.E., and McCurdy, D.W. (2007). Wall ingrowths in epidermal transfer cells of *Vicia faba* cotyledons are modified primary walls marked by localized accumulations of arabinogalactan proteins. *Plant Cell Physiology* **48**: 159–168.
- Verma, P., Shah, N., and Bhatia, S. (2013). Development of an expressed gene catalogue and molecular markers from the de novo assembly of short sequence reads of the lentil (*Lens culinaris* Medik.) transcriptome. *Plant Biotechnology Journal* **11**: 894–905. doi: 10.1111/pbi.12082.
- Vision, T.J., Brown, D.G., and Tanksley, S.D. (2000). The origins of genomic duplications in *Arabidopsis*. *Science* **290**: 2114–2117.
- Wang, H-L., Offler, C.E., and Patrick, J.W. (1995). Cellular pathway of photosynthate transfer in the developing wheat grain. II. A structural analysis and histochemical studies of the transfer pathway from the crease phloem to the endosperm cavity. *Plant Cell and Environment* **18**: 373–388.
- Wang, Y.H. (2008). How effective is T-DNA insertional mutagenesis in *Arabidopsis*? *Journal of Biochemical Technology* **1**: 11–20.
- Wang, Z., Fang, B., Chen, J., Zhang, X., and Luo, Z. (2010). *De novo* assembly and characterization of root transcriptome using Illumina paired-end sequencing and development of cSSR markers in sweet potato (*Ipomoea batatas*). *BMC Genomics* **11**: 726. doi: 10.1186/1471-2164-11-726.
- Wardini, T., Talbot, M.J., Offler, C.E., and Patrick, J.W. (2007a). Role of sugars in regulating transfer cell development in cotyledons of developing *Vicia faba* seeds. *Protoplasma* **230**: 75–88. doi: 10.1007/s00709-006-0194-y.
- Wardini, T., Wang, X.D., Offler, C.E., and Patrick, J.W. (2007b). Induction of wall ingrowths of transfer cells occurs rapidly and depends upon gene expression in cotyledons of developing *V. faba* seeds. *Protoplasma* **231**: 15–23.

- Weber, A.P.M. (2015). Discovering new biology through sequencing of RNA. *Plant Physiology* **169**: 1524-1531.
- Weber, H., Rolletschek, H., Heim, U., Golombek, S., Gubatz, S., and Wobus, U. (2000). Antisense-inhibition of ADP-glucose pyrophosphorylase in developing seeds of *Vicia narbonensis* moderately decreases starch but increases protein content and affects seed maturation. *Plant Journal* **24**: 33–43.
- Weeks, J.T., Ye, J., and Rommens, C.M. (2008). Development of an in planta method for transformation of alfalfa (*Medicago sativa*). *Transgenic Research* **17**: 587-97.
- Wei, W., Qi, X., Wang, L., Zhang, Y., Hua, W., Li, D., et al. (2011). Characterization of the sesame (*Sesamum indicum* L.) global transcriptome using Illumina paired-end sequencing and development of EST-SSR markers. *BMC Genomics* **12**: 451
- Weschke, W., Panitz, R., Gubatz, S., Wang, Q., Radchuk, R., Weber, H., et al. (2003). The role of invertases and hexose transporters in controlling sugar ratios in maternal and filial tissues of barley caryopses during early development. *Plant Journal* **33**: 395–411. doi: 10.1046/j.1365-313X.2003.01633.x.
- Williams, R. (1998). Plant homeobox genes: many functions stem from a common motif. *BioEssays* **20**: 280–282.
- Wimmers, L.W., and Turgeon, R. (1991). Transfer cells and solute uptake in minor veins of *Pisum sativum* leaves. *Planta* **186**: 2–12.
- Wu, G., Zhang, L., Yin, Y., Wu, J., Yu, L., Zhou, Y., et al., (2015). Sequencing, *de novo* assembly and comparative analysis of *Raphanus sativus* transcriptome . *Frontiers in Plant Science* **6**: 198. <http://dx.doi.org/10.3389/fpls.2015.00198>.
- Wu, K.L., Guo, Z.J., Wang, H.H., and Li, J. (2005). The WRKY family of transcription factors in rice and Arabidopsis and their origins. *DNA Research* **12**: 9–26.
- Wuyts, N., Palauqui, J.C., Conejero, G., Verdeil, J.L., Granier, C., and Massonnet, C. (2010). High-contrast three-dimensional imaging of the Arabidopsis leaf enables the analysis of cell dimensions in the epidermis and mesophyll. *Plant Methods* **6**: 17.
- Xia, X., Zhang, H-M., Andriunas, F.A., Offler, C.E., and Patrick J.W. (2012). Extracellular hydrogen peroxide, produced through a respiratory burst oxidase/superoxidedismutase pathway, directs ingrowth wall formation in epidermal transfer cells of *Vicia faba* cotyledons. *Plant Signaling and Behaviour* **7**: 1–4 10.4161/psb.21320.
- Xia, Z.H., Xu, H.M., Zhai, J.L., Li, D.J., He, C.Z., and Huang X (2011). RNA-Seq analysis and *de novo* transcriptome assembly of *Hevea brasiliensis*. *Plant Molecular Biology*. **77**: 299-308.

- Xianjun, P., Linhong, T., Xiaoman, W., Yucheng, W., and Shihua, S. (2014). *De novo* assembly of expressed transcripts and global transcriptomic analysis from seedlings of the paper mulberry (*Broussonetia kazinoki* x *Broussonetia papyifera*). *PLoS ONE* **9**: e97487. doi: 10.1371/journal.pone.0097487.
- Xiong, Y., Li, Q-B., Kang, B-H., and Chourey, P. (2011). Discovery of genes expressed in basal endosperm transfer cells in maize using 454 transcriptome sequencing. *Plant Molecular Biology Reporter*. **29**: 835–47.
- Xu, S.L., Rahman, A., Baskin, T.I., and Kieber, J.J. (2008) Two leucine-rich repeat receptor kinases mediate signaling linking cell wall biosynthesis and ACC synthase in Arabidopsis. *Plant Cell* **20**: 3065–3079.
- Xu, X., Chen, C., Fan, B., and Chen Z. (2006). Physical and functional interactions between pathogen-induced Arabidopsis WRKY18, WRKY40, and WRKY60 transcription factors *Plant Cell* **18**: 1310–1326.
- Yang, C.Y., Xu, Z.Y., Song, J., Conner, K., Barrena, G.V., and Wilson, Z.A. (2007). Arabidopsis MYB26/MALE STERILE35 regulates secondary thickening in the endothecium and is essential for anther dehiscence. *Plant Cell* **19**: 534–548.
- Zabackis, E., Huang, J., Müller, B., Darvill, A.G., and Albersheim, P. (1995). Structure of plant-cell walls: characterization of the cell-wall polysaccharides of *Arabidopsis thaliana* leaves. *Plant Physiology* **107**: 1129–38.
- Zhang, H., Imtiaz, M.S., Laver, D.R., McCurdy, D.W., Offler, C.E., van Helden, D.F., et al. (2015c). Polarized and persistent Ca<sup>2+</sup> plumes define loci for formation of wall ingrowth papillate in transfer cells. *Journal of Experimental Botany* **66**: 1179–90.
- Zhang, H-M., Talbot, M.J., McCurdy, D.W., Patrick, J.W., and Offler, T.E. (2015d). Calcium-dependent depletion zones in the cortical microtubule array coincide with sites of, but do not regulate, wall ingrowth papillae deposition in epidermal transfer cells. *Journal of Experimental Botany* **66**: 6021–6033.
- Zhang, H-M., van Helden, D.F., McCurdy, D.W., Offler, C.E., and Patrick, J.W. (2015a). Plasma membrane Ca<sup>2+</sup>-permeable channels are differentially regulated by ethylene and hydrogen peroxide to generate persistent plumes of elevated cytosolic Ca<sup>2+</sup> during transfer cell *trans*-differentiation. *Plant and Cell Physiology* **56**: 1711–1720.
- Zhang, H-M., Wheeler, S., Xia, X., Radchuk, R., Weber, H., Offler, C.E., et al. (2015b). Differential transcriptional networks associated with key phases of ingrowth wall construction in *trans*-differentiating epidermal transfer cells of *Vicia faba* cotyledons. *BMC Plant Biology* **15**: 103. doi: 10.1186/s12870-015-0486-5.
- Zhang, J.A., Liang, S., Duan, J.L., Wang, J., Chen, S.L., Cheng, Z.S., et al. (2012). *De novo* assembly and characterisation of the transcriptome during seed development,

- and generation of genetic-SSR markers in peanut (*Arachis hypogaea* L.). *BMC Genomics* **13**: 90. doi: 10.1186/1471-2164-13-90.
- Zhang, L., Garneau M.G., Majumdar, R., Grant, J., and Tegeder, M. (2015) Improvement of pea biomass and seed productivity by simultaneous increase of phloem and embryo loading with amino acids. *Plant Journal* **81**: 134–46.
- Zhang, Z., Wang, J., Zhang, R., and Huang, R. (2012). ERF protein AtERF98 enhances tolerance to salt through the transcriptional activation of ascorbic acid synthesis in *Arabidopsis*. *Plant Journal* **71**: 273–287.
- Zhao, S., Fung-Leung, W.P., Bittner, A., Ngo, K., and Liu, X. (2014). Comparison of RNA-Seq and microarray in transcriptome profiling of activated T cells. *PLoS ONE* **9**: e78644. 10.1371/journal.pone.0078644.
- Zhong, R., and Ye, Z-H. (2014). Complexity of the transcriptional network controlling secondary wall biosynthesis. *Plant Science* **229**: 193–207.
- Zhong, R., Lee, C., and Ye, Z.H. (2010). Evolutionary conservation of the transcriptional network regulating secondary cell wall biosynthesis. *Trends in Plant Science* **15**: 625-632.
- Zhong, R., Peña, M.J., Zhou, G.K., Nairn, C.J., Wood-Jones, A., Richardson, E.A., et al. (2005). *Arabidopsis Fragile Fiber8*, which encodes a putative glucuronyltransferase, is essential for normal secondary wall synthesis. *Plant Cell* **17**: 3390–3408. 10.1105/tpc.105.035501.
- Zhong, R., Richardson, E.A., and Ye, Z-H. (2007). The MYB46 transcription factor is a direct target of SND1 and regulates secondary wall biosynthesis in *Arabidopsis*. *Plant Cell* **19**: 2776–2792.
- Zhong, R.Q., Demura, T., and Ye, Z.H. (2006). SND1, a NAC domain transcription factor, is a key regulator of secondary wall synthesis in fibers of *Arabidopsis*. *Plant Cell* **18**: 3158–3170.
- Zhong, R.Q., Lee, C.H., Zhou, J.L., McCarthy, R.L., and Ye, Z.H. (2008). A battery of transcription factors involved in the regulation of secondary cell wall biosynthesis in *Arabidopsis*. *Plant Cell* **20**: 2763–2782.
- Zhong, R.Q., Richardson, E.A., and Ye, Z.H. (2007). Two NAC domain transcription factors, SND1 and NST1, function redundantly in regulation of secondary wall synthesis in fibers of *Arabidopsis*. *Planta* **225**: 1603–1611.
- Zhou, J., Lee, C., Zhong, R., and Ye, Z.H. (2009). MYB58 and MYB63 are transcriptional activators of the lignin biosynthetic pathway during secondary cell wall formation in *Arabidopsis*. *Plant Cell* **21**: 248–266.

- Zhou, Y., Qu, H., Dibley, K.E., Offler, C.E., and Patrick, J.W. (2007). A suite of sucrose transporters expressed in coats of developing legume seeds includes novel pH-independent facilitators. *The Plant Journal* **49**: 750–764.
- Zhou, Y.C., Andriunas, F., Offler, C.E., McCurdy, D.W., and Patrick, J.W. (2010). An epidermal-specific ethylene signal cascade regulates trans-differentiation of transfer cells in *V. faba* cotyledons. *New Phytologist* **185**: 931–943.
- Zhu, H., Kim, D-J., Baek, J-M., Choi, H-K., Ellis, L.C., Kuester, H., et al. (2003). Syntenic relationships between *Medicago truncatula* and Arabidopsis reveal extensive divergence of genome organization. *Plant Physiology* **131**: 1018–1026.